The origins of iron ores in the middleback ranges, South Australia

kean Lnton Ashworth

THE ORIGINS OF IRON ORES IN THE MIDDLEBACK RANGES, SOUTH AUSTRALIA

Thesis submitted for the degree of Doctor of Philosophy in the University of Durham

by

Kevan Lynton Ashworth

University College August 1973

The genesis of an orebody is a fundamental problem of more than academic importance.

K.R.Miles, 1954.

ACKNOWLEDGEMENTS

The background work on this project was carried out whilst working as a geologist for The Broken Hill Proprietary Company Limited. I wish to acknowledge the extensive assistance and encouragement given by company personnel, in particular Mr. I.W. Reid, and including at various stages Messrs. D.E. Catley, D. Burger, A. Vezis and D.V. Furber. The company transported several hundred samples and thin sections from Australia to the United Kingdom, and permitted full use of company records and reports. This assistance made the project possible and is appreciated by the author.

In Durham, Mr. R. Phillips supervised and critically reviewed the project work, providing lucid comment and continued encouragement, for which the author is grateful. Acknowledgements are also due to the following staff and research students for assistance in specialised fields:

Dr. A. Peckett - electron microprobe analysis

Dr. J.G. Holland - XRF analysis

Dr. A.J. Hall - X-ray diffraction procedures

Mr. R.G. Hardy - X-ray diffraction data

Mr. F.W. Smith - fluid inclusion procedures

Mrs. C.L. Mines - typing

Professor G.M. Brown and Professor M.H.P. Bott are acknowledged for permission to carry out the project within the

department and to use department equipment.

The author is also grateful to Dr. B.L. Hodge for repeated stimulus during the later stages of the project, and to Mrs. K.L. Ashworth for providing financial support during the last two years.

ABSTRACT

The Middleback Ranges consist of tightly folded Precambrian iron-formations flanked by granite-gneisses and feldspathic metasediments. Hematite orebodies occur within the iron-formations and are confined to pitching synforms and steeply dipping fold limbs. At Iron Duke, a large hematite orebody extends down the pitch of a synform into a hidden body of magnetite-hematite-carbonate rock which is surrounded by talcose zones. Various theories including granitisation, primary sedimentation, and supergene leaching have been proposed previously to account for the origin of the hematite orebodies. The magnetite-hematite-carbonate and talcose rocks of Iron Duke have been attributed to carbonate metasomatism affecting the iron-formation.

The mineralogy and microtextures of the iron-formation units are described. Mineral assemblages indicate that regional metamorphism reached lower amphibolite facies grade at temperatures and pressures in the order of 450°C to 550°C and 2kb to 6kb. Microtextures suggest that mineral layers within the iron-formations remained as essentially closed systems during metamorphism and there was negligible movement of components other than water and carbon dioxide.

The geology of Iron Duke is described in detail, with emphasis on the mineralogy and geochemistry of the magnetite-hematite-carbonate and associated rocks. The ores occur in a tight,

pitching synform terminated on the east side by a high angle reverse fault. There is considerable evidence to show that hydrothermal activity has played an important role in the formation of the magnetite-hematite-carbonate ore. Fluid inclusion studies suggest that the hydrothermal solutions were brines at temperatures in the order of 120°C to 250°C and a maximum possible pressure of 2-3 kb.

The origin of the magnetite-hematite-carbonate ore is discussed. It is proposed that the ore formed by hydrothermal fluid action on an iron-formation unit near the base of the iron-formation sequence, which contained interlayered iron oxides, carbonates, tremolite and quartz. The silicate minerals were replaced by carbonates in a complex process of carbonate metasomatism and silica removal. Ore controls include the pre-existing rock mineralogy, the tight synformal structure, and the coincidence of a thick basal carbonate unit with the major reverse fault.

Theories of hematite ore genesis in the Middleback Ranges are discussed. It is concluded that the ores formed by supergene leaching and enrichment, and that ore controls include favourable structures, pre-existing rock mineralogy, and the presence of underlying impermeable layers.

CONTENTS

SECTION II: THE GEOLOGY OF IRON DUKE

SECTION III: ORIGIN OF THE ORES

FIGURES

TABLES

INTRODUCTION

Location

The Middleback Ranges lie 30 miles west of Whyalla on the east side of Eyre Peninsula, South Australia (Fig. 1). They rise 600' - 800' above the surrounding plain and extend for 22 miles along a north-south line, broken in the middle by the Kimba Gap. A line of low ridges, the Camel Hill line, extends from the northern tip of the Middleback Ranges to the Katunga Hills and Iron Monarch, 15 miles to the north.

In this thesis, location names beginning with "Iron" denote a hematite orebody as, for example, Iron Monarch or Iron Duke.

Definitions and general geology

There is considerable confusion in world literature over terms used to describe iron-formations. For example, Trendall and Blockley (1970) define jaspilite as a rock with alternating thin bands of jasper (red chert) and iron oxides or chert of another colour. In the Middleback Ranges, the term has been used in a wider sense and includes rock types which Trendall and Blockley would define as "banded iron formation (BIF)". Similar discrepancies occur throughout world literature and until there is agreement on the use of certain terms, they must be defined for each particular area. Definitions for the Middleback Range area are:

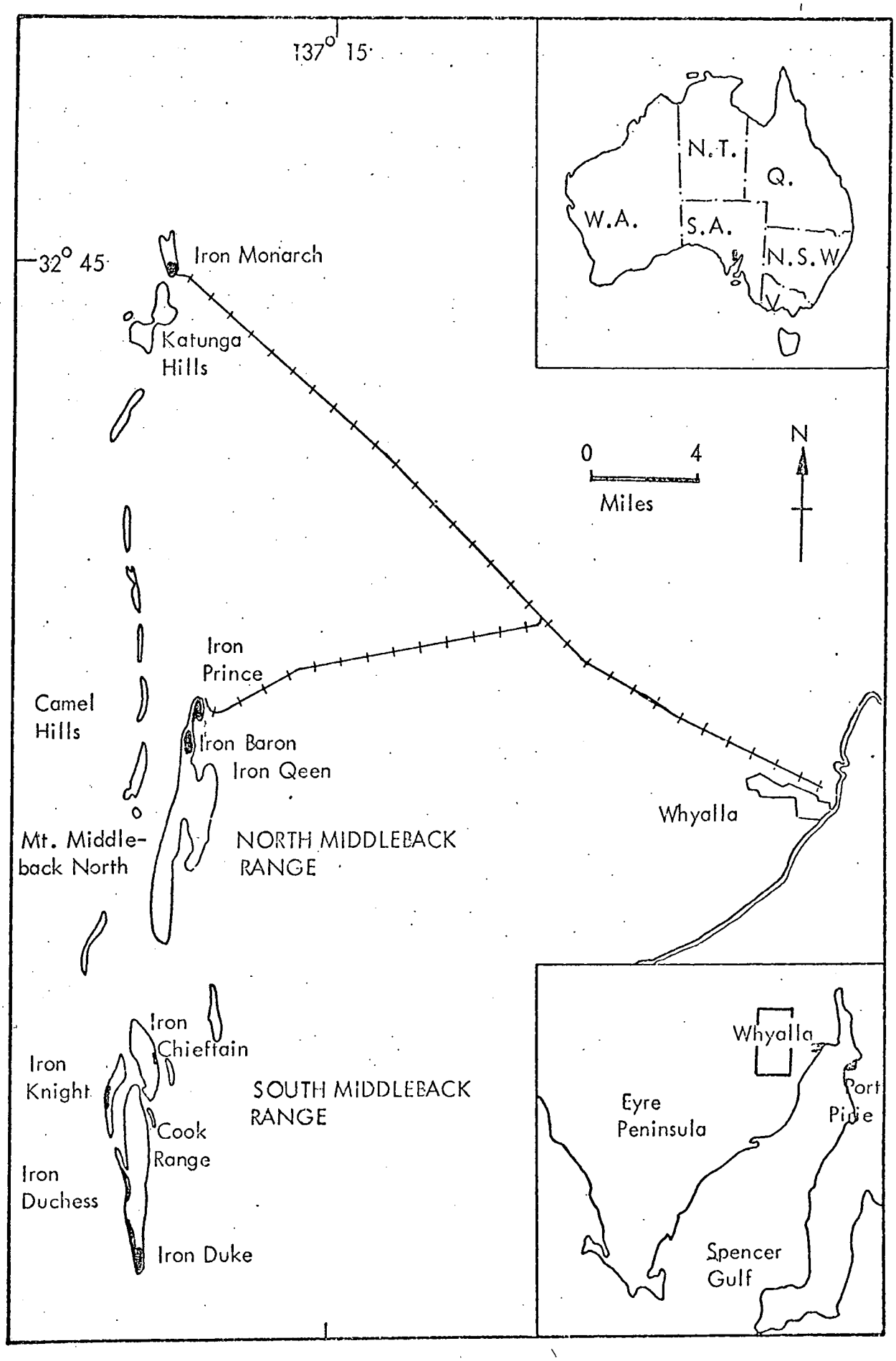

Fig. 1. Locality plan of the Middleback Range area. Major hematite orebodies shown in black.

Iron-formation - fine-grained rock consisting of quartz and iron oxides with lesser amounts of amphibole and occasionally carbonate. The proportions of each mineral can vary considerably and there is complete gradation to quartzite, iron ore, amphibole schist and massive carbonate. An arbitrary value of 10% - 15% Fe defines the lower limit of the term. The rocks are normally banded.

This definition conforms with James's (1966) detailed description of world wide iron-formations and his use of the term.

Jaspilite - the term is not used in this thesis but is deeply entrenched in company work and has been used in all publications describing Middleback Range geology in the last 10 years. It is synonymous with iron-formation as defined above and is discarded only to conform more closely to world wide usage.

The Middleback Ranges and hills to the north are formed of strongly folded iron-formations with interlayered schists, carbonate units and amphibolites. Numerous amphibolites also cut across the strike of the layered rocks. Fold axes are aligned north-south and the lenticular outcrop pattern of the iron-formations is caused by cross-warping, with topographic gaps marking broad east-west anticlinal axes (Fig. 2). The broad

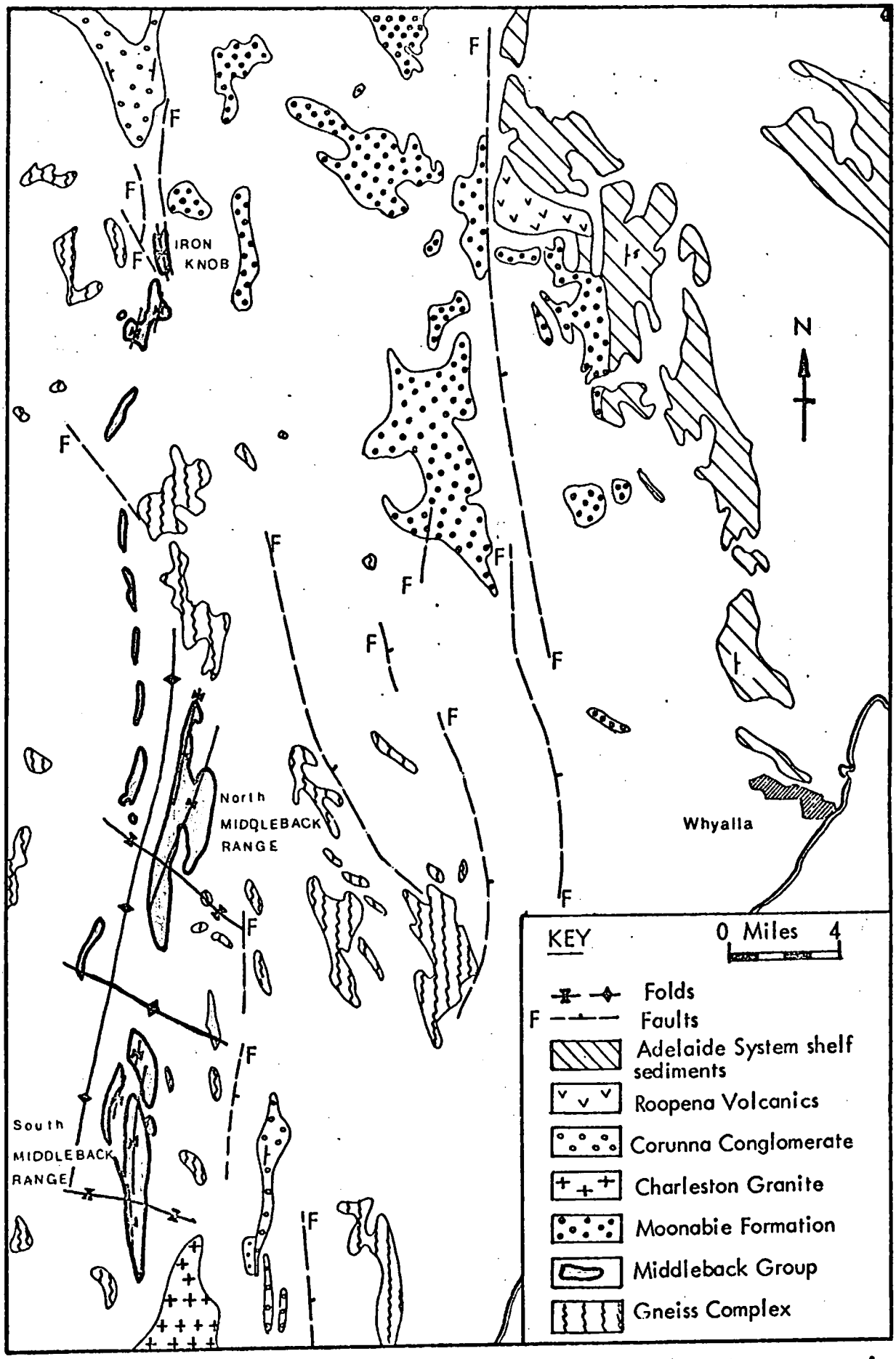

Fig. 2. Regional geology of the Middleback Range area, showing the main exposures of different rock types.
Based on South Australia Geological Survey Port Augusta 4 miles sheet 1969, and Miles, 1954.

structures of both the north and south ranges are canoe shaped as shown in Fig.3 (Rudd 1940, Miles 1954).

Flanking the ranges and underlying the surrounding level plain is a gneissic complex with varied rock types including migmatite, granite-gneiss, mica schists, dolomites and felspathic quartzites. These are cut by basic intrusives and by several large granite masses. Foliation and fold axes in the gneiss complex strike broadly parallel to the iron-formations.

Hematite orebodies occur within the iron-formations in pitching synclines or steeply dipping fold limbs. Major orebodies are Iron Monarch, Iron Prince, Iron Baron and Iron Duke (Fig.1). All known orebodies outcrop and the major orebodies form hills or ridges which merge into the iron-formation ridges. At Iron Duke, hematite ore in the hinge zone of a pitching syncline passes down pitch into a large body of magnetite-hematite-carbonate rock which is hidden below 300' - 400' of siliceous iron-formation. The magnetite-hematite-carbonate is brecciated and contains considerable coarse grained carbonate. No other large bodies are known in the Middleback Range area, although small amounts of similar material occur below the hematite ores at Iron Baron, Iron Queen and Iron Monarch.

The term "ore" is used in this thesis in the sense defined by King (1966); ".....any metallic or mineral deposit which is of sufficient economic interest to require estimation of tonnage and grade". This includes the hematite bodies, large

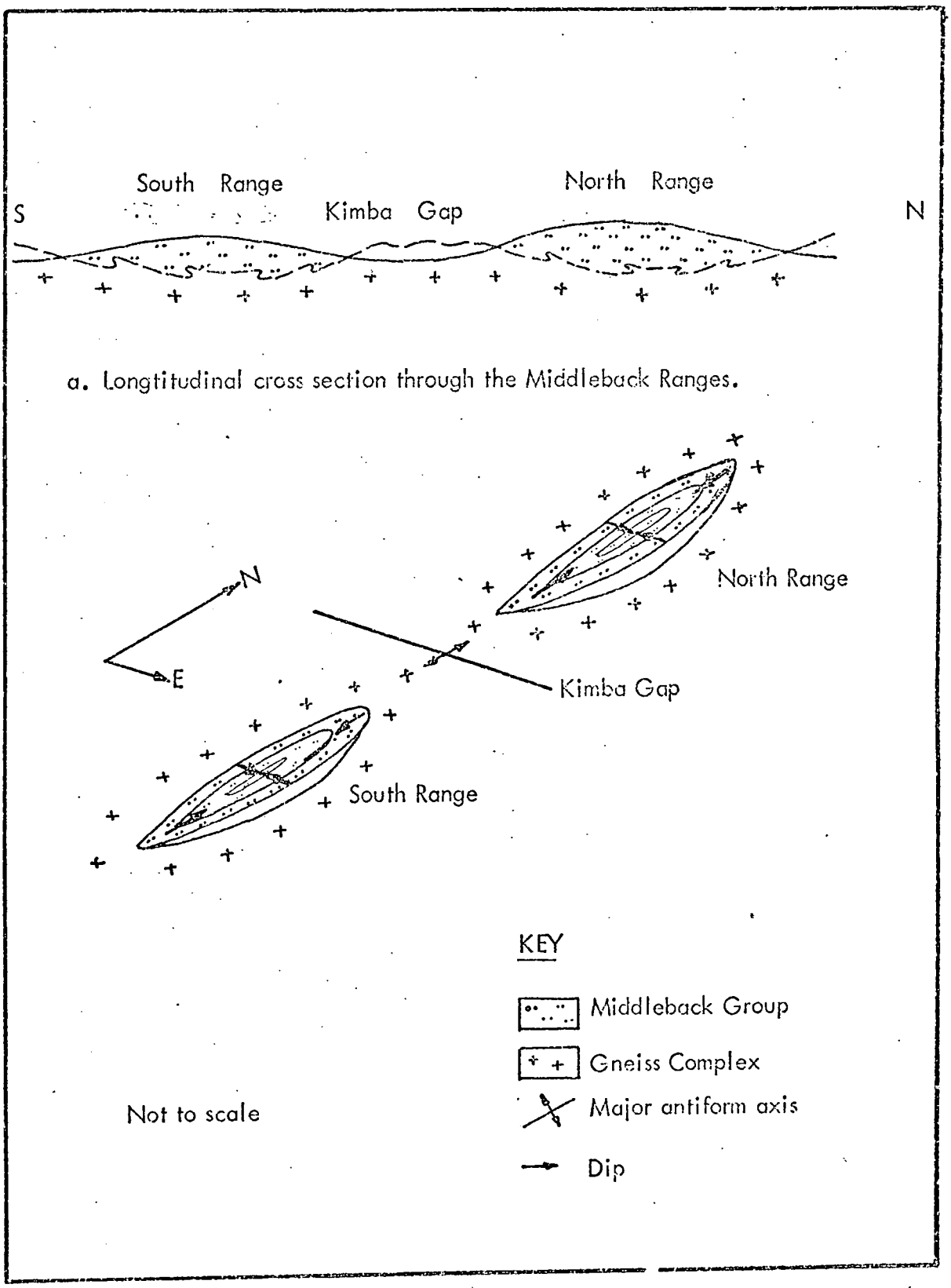

Fig. 3. Diagram to illustrate the broad structural forms of the Middleback Ranges. Based on diagrams by Rudd (1944) and Miles (1954).

or small, and the magnetite-hematite-carbonate body but does not include the iron-formations.

Previous work

The hematite ores were first worked in the 1890's as flux for smelting Broken Hill silver-lead-zinc ores. The ore at Iron Knob was hand loaded into horse-drawn drays and carried the 30 miles to Whyalla, where it was transferred to barges and shipped to Port Pirie on the east side of Spencer Gulf (Fig. 1). In the early 1900's, a steel works was built on the east coast of Australia and the increased demand for iron ore resulted in the Broken Hill Proprietary Company Ltd. building a railway between Iron Knob and Whyalla. For the next 70 years the Middleback Range deposits formed the basis of the Australian iron and steel industry and two deposits, Iron Monarch and Iron Prince, are currently in production with a combined annual output of approximately 7.5 million long tons of direct feed ore and fines for pelletizing.

The economic interest in the Middleback Ranges has resulted in a great deal of geological work by both the B.H.P. Company Ltd. and the Geological Survey of South Australia. Most of the company work is unpublished but all the data was available to the author.

Company work has concentrated on the iron-formations and includes geophysical surveys, geological mapping at 1"=200' throughout the ranges, drilling and tunneling within the hematite

orebodies, petrological examination of drill core samples and many thousands of chemical analyses. Six papers have been published by company geologists in the last twenty years; four on Iron Duke (Whitehead 1962, Catley 1963, Burger 1963, Ashworth 1965), one on Iron Monarch, (Owen 1963) and one summarizing the geology of the iron-formations (Owen and Whitehead 1965). The papers summarize the individual authors' ideas of ore genesis but some additional ideas and observations are found in unpublished company reports, particularly in the case of Whitehead, who was the first petrologist to work on the magnetite-hematite-carbonate. These are acknowledged at appropriate points in the text of this thesis.

Geological Survey work includes geophysical surveys, detailed mapping of the hematite orebodies, regional mapping of the gneiss complex, petrological work and limited drilling in the Middleback Ranges. Most of the results are summarized in Bulletin No.33, "The Geology and Iron Ore Resources of the Middleback Range Area" (1954) by K.R. Miles, which remains the classic text on regional geology for this area. Some drilling was carried out subsequent to this report and the results were available to the author. The Geological Survey 1"= 4 miles sheet covering the area north of Iron Baron was issued in 1968 and shows some changes from Miles's 1954 map. These will be discussed as relevant in the text.

Theories of hematite ore genesis are many and varied and the main proposals, in chronological order, are:

Jack (1922) - the iron-formations and hematite ores are due to hydrothermal replacement of schists.

Edwards (1936) - the iron-formations and hematite ores are of sedimentary origin and represent an ancient coastal deposit. The essentially sedimentary character of the iron-formations has been accepted by all later authors, although ideas on the sedimentary environment have been modified. Subsequent debate has centred upon the origin of the hematite ores.

Rudd (1940) - hematite ore developed by groundwater leaching silica and concentrating iron within siliceous iron-formation.

Ward (1949) - hematite ore was deposited from hydrothermal solutions.

Miles (1954) - iron was concentrated by fluids moving before a granitising front.

Whitehead (1962) - some hematite is formed by groundwater leaching of magnetite-hematite-carbonate. The latter had been discovered, by drilling, in 1957.

Catley (1963) - the hematite ore at Iron Duke is sedimentary.

Owen and Whitehead (1965) - hematite formed by groundwater removing carbonates and silica from magnetite-hematite-carbonate and siliceous iron-formation.

Ashworth (1965, 1970) - as Owen and Whitehead (1965), with emphasis on the role played by carbonates and on structural control.

The three main theories are that the ore is sedimentary (Catley 1963), that it is due to granitising fluids (Miles 1954)

and that it is due to groundwater leaching and enrichment (Rudd 1940, Whitehead 1962, Owen and Whitehead 1965, Ashworth 1965, 1970). In the last theory, the main point of debate is the original rock type from which the ore was derived.

There are fewer ideas on the origin of the magnetite-hematite-carbonate, probably because it was not discovered until 1957. The two main theories are:

(a) Carbonate metasomatism of iron-formation, involving large scale replacement of quartz or amphiboles by carbonates. (Whitehead 1962, Catley 1963, Owen and Whitehead 1965, Ashworth 1965).

(b) Removal of silica from a carbonate rich unit of the iron-formation by hydrothermal solutions, leaving carbonate and iron oxides. (Ashworth 1970).

Aims of the thesis

Although there has been considerable discussion on the origins of the hematite and magnetite-hematite-carbonate ores during the past 10 years, there has been no rigorous examination of the available evidence and the mechanisms of ore genesis have rarely been defined in any detail. The first aim of this thesis is to define the processes of ore formation.

Iron Duke is critical to theories of ore genesis because it is the only area in which large bodies of hematite and magnetite-hematite-carbonate occur together. No detailed account of Iron Duke geology and petrology has been published,

yet these are fundamental to concepts of ore genesis. The second aim of this thesis is to describe, and present an interpretation of, Iron Duke geology.

The thesis is divided into three sections:
Section I describes the tectonic setting of the Middleback Ranges, the petrology of the main rock types in the iron-formations and the mineral assemblages which indicate regional metamorphic grade.
Section II describes the geology and petrology of Iron Duke.
Section III discusses the origins of the hematite and magnetite-hematite-carbonate ores.

Analytical data and operating conditions are given in Appendices I-V. The main techniques used were electron microprobe (190 analyses), XRF (138 analyses), fluid inclusion homogenisation and X-ray diffraction. Approximately 500 thin sections and 50 polished sections were examined. Analyses used in the text were carried out by the author unless it is stated otherwise; 20 quantitative analyses of different rock types were carried out by the Chemical Laboratory, B.H.P., Whyalla, at the author's request and these, together with a number of drillcore assays are acknowledged as appropriate.

SECTION I: REGIONAL GEOLOGY

REGIONAL GEOLOGY

A. REGIONAL SETTING AND STRATIGRAPHY

1. Setting

Eyre Peninsula is part of the South Australian Precambrian shield known as the Gawler Block (Fig.4). It contains a wide variety of rock types including gneisses, schists, carbonate units, iron-formations and large, intrusive granite masses. Relationships between the different rock types are often inconclusive due to poor exposure but the general impression is of long, sinuous metasedimentary units surrounded by a wide expanse of augen gneiss and migmatite.

The shield rocks are strongly folded on a regional scale with fold amplitudes in the order of several miles and the gneiss foliation remains approximately parallel to the strike of the metasediments (Johns 1961). Fold axes are broadly aligned north-east to south-west but this trend is modified by flexuring, as in the Middleback Range area where the strike is predominantly north-south.

All the shield rocks are metamorphosed, the grade varying from greenschist to granulite facies (Tilley 1920a, b, 1921a, b; Thomson 1969, Ashworth 1970). The augen gneisses and migmatites appear to be products of granitisation or partial melting and whichever process is invoked, the effects are very widespread, covering many thousands of square miles (Miles, 1954,

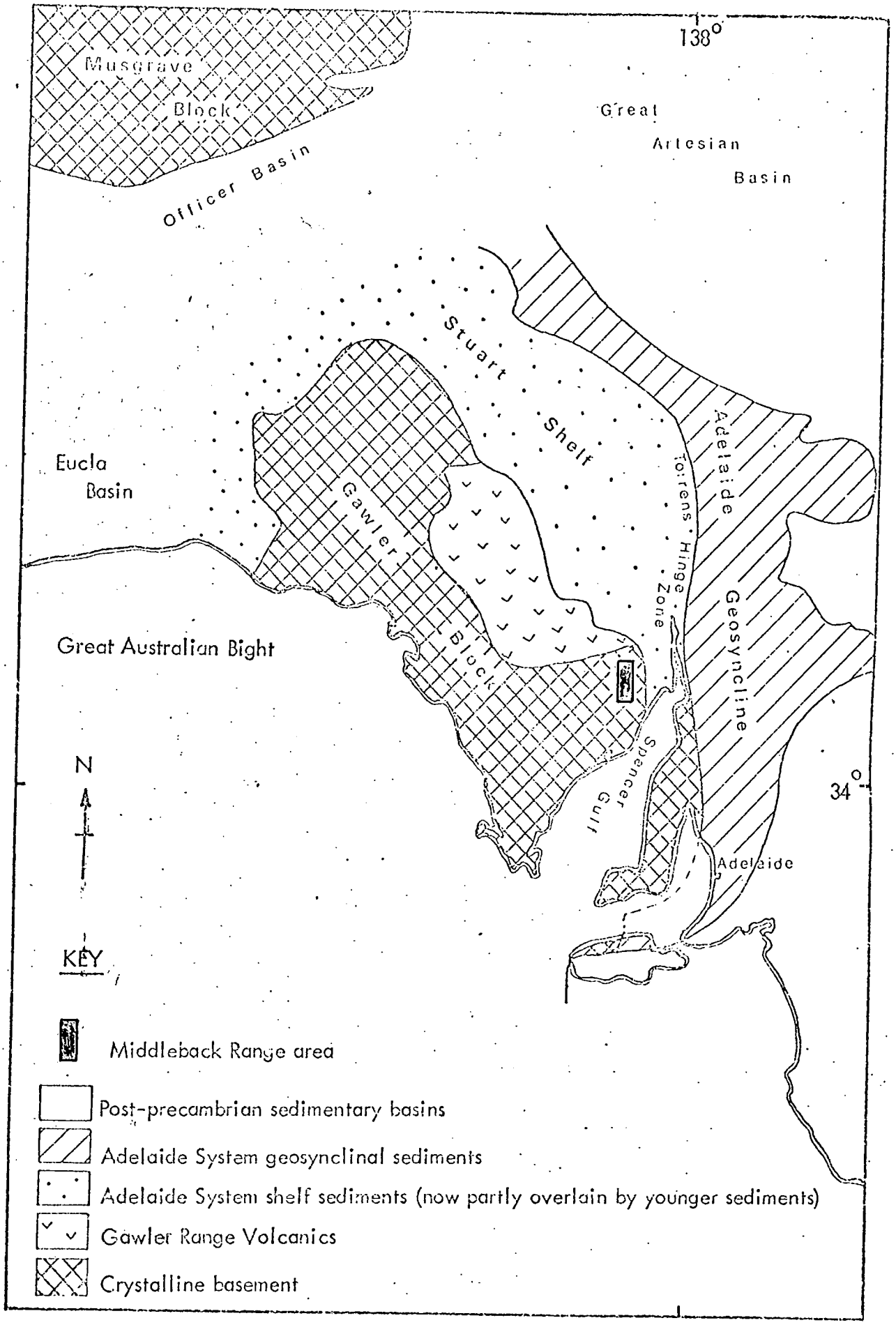

Fig. 4. Tectonic setting of the Middleback Range area (based on Thomson 1966, 1969)

Johns 1961). Radiometric age determinations on the gneisses indicate an age of about 1780 million years (Compston and Arriens 1968).

The Middleback Ranges are near the eastern margin of the Gawler Block which is defined by an ancient north-south lineament named the Torrens Hinge Zone (Thomson 1969). East of the hinge zone, younger sediments thicken rapidly and form part of the late Proterozoic to Palaeozoic Adelaide Geosyncline. West of the hinge zone, the shield rocks are covered by flat-lying shelf sediments which are typically exposed to the north of Whyalla. Gentle folding in the shelf sediments shows the lack of strong tectonic disturbance in this area since the late Proterozoic.

Graben faulting occurred during the Tertiary and resulted in Spencer Gulf, Gulf St. Vincent and the long meridional step faults between the Middleback Ranges and the coast (Fig.2). These movements had little affect on the shelf sediments, and it is clear that the shield has remained essentially stable since the late Proteozoic. Long periods of erosion have produced a mature landscape with virtually complete peneplanation.

2. Stratigraphy

Stratigraphy within the block is complicated by a lack of distinct marker units and the complex history of the rocks. It is preferable, therefore, to concentrate on a limited area and an interpretation of the stratigraphy of the north-east Eyre

Peninsula is shown in Table 1.

The iron-formations and interlayered schists of the Middleback Ranges form a distinct lithological group named the Middleback Group by Miles (1954). Their relationship to the surrounding gneissic rocks is uncertain. Miles (1954) considered that the iron-formations are remnants of an almost totally granitised sedimentary sequence, and are completely enclosed by gneissic rocks. By contrast, Owen and Whitehead (1965) record an unconformity between the lowest unit of the iron-formations and the underlying gneisses. Until the relationships are clarified, the iron-formations and schists are best grouped together as the Cleve Metamorphics, a general term including most of the shield rocks of the Eyre Peninsula (Thomson 1969). In Table 1, the iron-formations are placed above the gneisses because this is the dominant apparent relationship in this area.

The Moonabie Formation is a mildly metamorphosed sedimentary sequence dated by cross-cutting intrusives at pre-1590 million years (Thomson 1966). It unconformably overlies the gneisses but is strongly folded and may be considered a true member of the shield. The main rock types are quartzites and conglomerates, the latter sometimes containing pebbles of iron-formation. All the main exposures are in the plains east of the Middleback Ranges and the Formation does not come into contact with the iron-formations. Recent Geological Survey mapping to the north-east of the Middleback Ranges has reclassified as Moonabie Formation large areas of weathered exposure which were

Table 1. Stratigraphy of North-East Eyre Peninsula

Compiled from Miles 1954, Thomson 1966, 1969, Geological Survey Port Augusta 4 miles sheet 1969, Compston and Arriens 1968, and slightly modified by the author.

Age	Sedimentary	Metamorphic	Igneous
Recent-Quart.	Sand, kunkar, soil		
Tertiary	Laterite, sandstone, limestone		
550 m.y.	Tent Hill Formation (sandstone and shale)		
Adelaide System	Pandurra Formation (sandstone)		
	Backy Point Formation (sandstone)		Roopena Volcanics (1345 m.y.) Cultana Granite.
1400 m.y.	Corunna Conglomerate		Gawler Range Volcanics. (1535 m.y.)
			Charleston Granite (1590 m.y.)
			Burkitt Granite (1590 m.y.)
1600 m.y.			Moonabie Porphyry
		Moonabie Formation	
		Middleback Group	
	Cleve Metamorphics	Gneiss Complex	

Note: (a) —— —— = unconformity
(b) Basic intrusives have not been included in the table as there are several sets and their age is uncertain.

previously mapped as gneisses (Geol. Surv. Port Augusta 1"=4 miles sheet, 1968). The Moonabie Formation is clearly much more extensive than was previously thought and it seems likely that further re-classification will be necessary as the Survey mapping progresses southwards.

The Corunna Conglomerate unconformably overlies the Moonabie Formation and is dated at about 1550 million years by Rb-Sr determinations on whole rock and illite samples (Compston, Crawford and Bofinger 1966). It is unmetamorphosed and occupies a unique stratigraphic position, being neither part of the shield nor of the overlying Adelaide Geosyncline shelf sediments, and separated from both by major unconformities. The beds are normally gently folded. The main rock types are conglomerates, sandstones and shales and iron-formation pebbles are present in some conglomerates. Pebbles of hematite are present in one exposure to the east of Iron Duke (Rudd 1940).

The Adelaide System sequence of sandstones and shales, which unconformably overlie the Corrunna Conglomerate in the north-east of the area, are geosynclinal shelf sediments. They dip gently eastwards towards the main part of the Adelaide Geosyncline but no trace of these beds or their continental equivalents are found further west. This suggests that the Middleback Range area was on the margin of the continental mass during geosynclinal sedimentation.

Intrusives of various ages and compositions cut the shield rocks of north-east Eyre Peninsula. They may be summarised as follows:

Granites - (a) Foliated granites which merge into the surrounding gneiss and are either earlier than or contemporaneous with the gneiss.

(b) Large, clearly discordant granite masses, dated at 1600-1500 million years (Compston and Arriens 1968). Two of these masses occur quite close to the Middleback Ranges, one about 6 miles north-east of Iron Knob and the other within 1 mile of Iron Duke.

Porphyries - (a) Small feldspar porphyry intrusives which were emplaced at about the same time as the younger granites.

(b) A volcanic province of porphyritic acid extrusives which covers several thousand square miles to the north-west of Iron Knob. This is known as the Gawler Range Volcanic Province and the rocks have been radiometrically dated at about 1535 million years (Compston, Crawford and Bofinger 1966).

Basics - Basic intrusives of at least three periods cut both the gneisses and the iron-formations. The earliest of these may be contemporaneous with the iron-formation sediments (Miles 1954). Two sets of younger, cross-cutting dykes can be identified and these are younger than the metamorphism, often following fault planes.

B. PETROLOGY OF THE MIDDLEBACK GROUP

The Middleback Group consists of two iron-formation units, each in the order of 500' - 800' thick, separated and underlain by argillaceous schists and carbonate bands. The schist unit which separates the iron-formations reaches 700' in thickness and is named the Cook Gap Schists (Miles 1954).

Lithologies in the Middleback Group are similar to those of iron-formation sequences in other parts of the world (Miles 1954, James 1966). The schists were originally normal argillaceous sediments whereas the iron-formations represent long periods of chemical or biochemical precipitation of iron and silica which produced ferruginous cherts (James,1954, 1966, Borchert 1960, Trendall and Blockley 1970). There is no doubt that the major lithological units are of sedimentary origin.

The petrology of the Middleback Group has been described in a number of papers (Edwards 1936, 1954, Whittle 1954, Miles 1954, Whitehead 1962) and in company reports by Whitehead and Burger. These define the main rock and mineral types but have little comment on the conditions of metamorphism or the mobility of components during metamorphism.

Iron-formations, carbonate units and schists are the three rock types which definitely pre-date the metamorphism. They therefore offer most information on the metamorphic conditions and the mobility of components. Mineral compositions in each of these three groups were determined by electron microprobe and the iron-

formation microtextures were examined in some detail. The results are described in the following pages and the implications are discussed.

1. Iron-formations

Iron-formation outcrops as a hard, brittle rock, varying in colour from uniform blue-black to clearly banded light and dark brown (Fig.5a). The latter varieties generally have light brown flecks aligned parallel to the banding and these are limonitised amphiboles. In drill core from below the zone of weathering, the rock is light grey to black, distinctly banded and usually with more amphibole than is seen at the surface (Fig.5b).

Typical iron-formation is composed of fine-grained quartz and iron oxides with amphiboles dispersed as single crystals or grouped into thin bands (Fig. 6). The proportion of amphibole varies and there is every gradation between a pure quartz-iron oxide rock and an amphibole schist.

The simple and uniform whole-rock geochemistry is shown in Table 2, and 28 additional whole-rock analyses are given in Appendix I. There is no sodium or potassium present in the rocks and virtually no alumina. The three main components are silica, iron, magnesium and to a lesser degree calcium, and this is typical of iron-formations throughout the world (James 1966). Trace element content is low.

(a) Mineralogy

Iron oxides - hematite is the predominant iron oxide in the weathered zone, which normally extends 250' - 350' below the surface. It has mainly replaced magnetite, often retaining a cubic form, and remnant magnetite frequently occurs in small

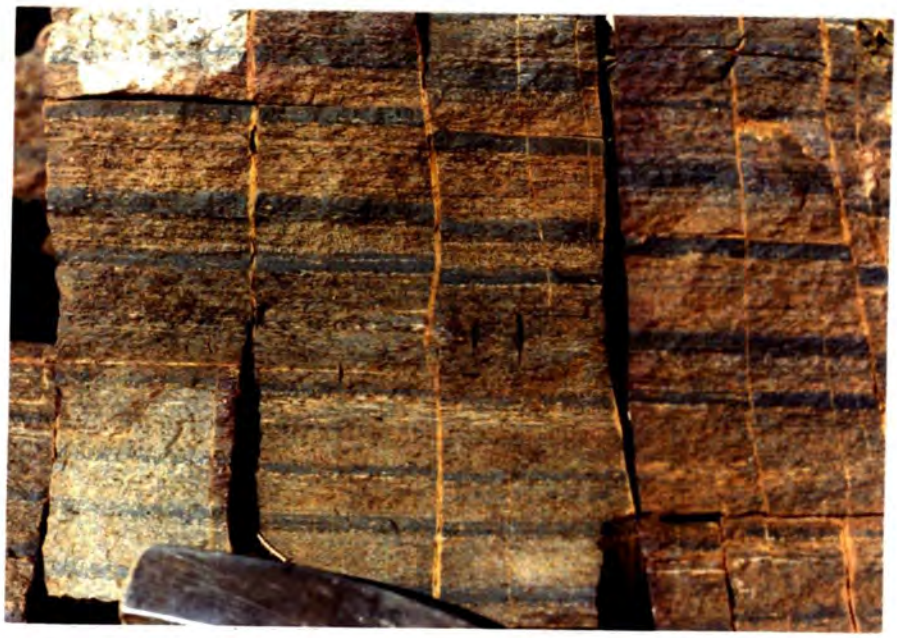

Fig. 5a. Iron-formation outcrops on the West side of Iron Duke. The darker layers are hematite-magnetite rich, the lighter layers quartz rich. Limonitised amphiboles show as light brown flecks. Scale given by hammer head at base of photograph.

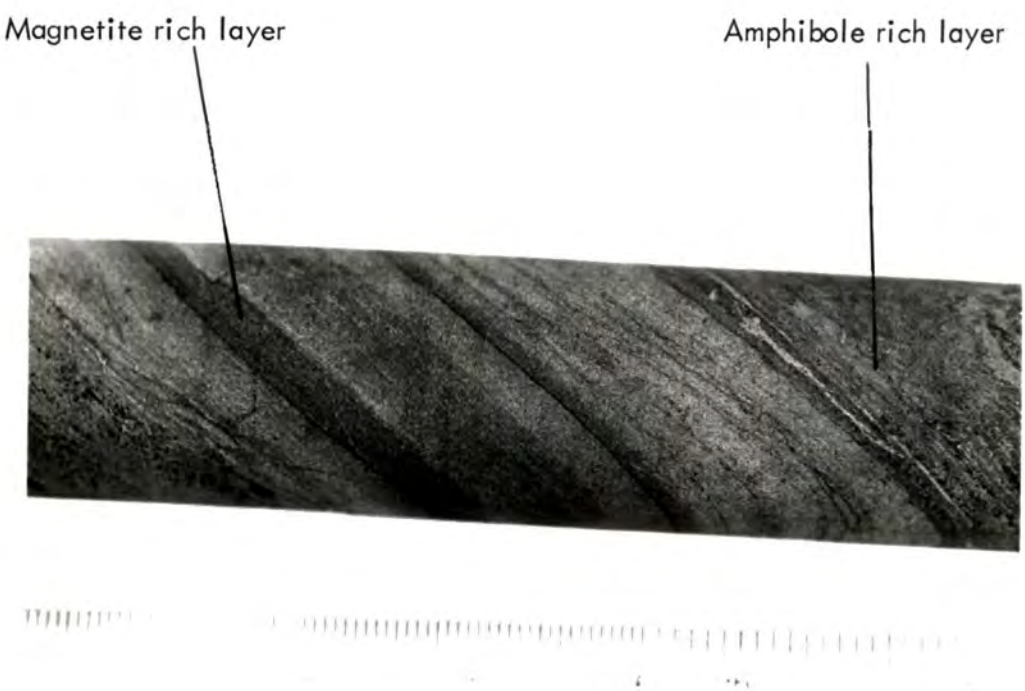

Fig. 5b. Iron - formation from below the zone of oxidation. The darker layers are magnetite rich and the fibrous layers are amphibole rich. Note the impression of graded bedding in the magnetite rich layers. Cook Range, DDH82, approx. 1,000'.

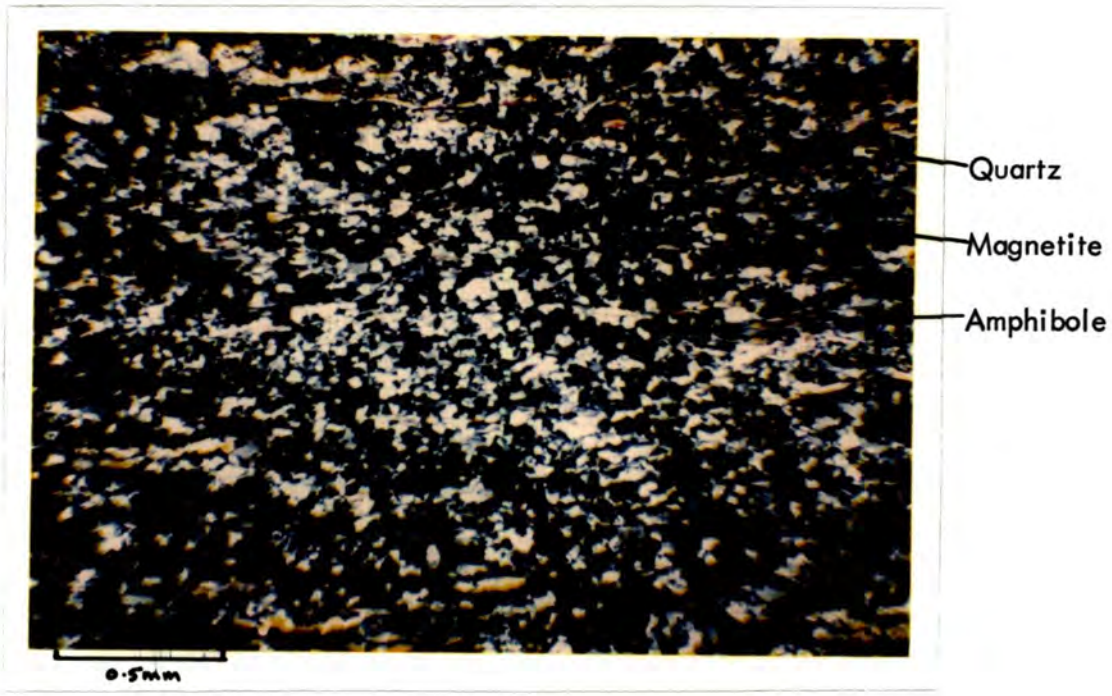

Fig. 6. Typical iron-formation microtexture from below the zone of oxidation. Composed of quartz and magnetite with dispersed amphiboles.
Sample 63-307, crossed polars.

Table 2. Whole-rock analyses of Middleback Range iron-formations

A. Major element analyses, by Chemical Laboratory, B.H.P., Whyalla

per cent	62-606	57-2426 (assay)
SiO_2	55.1	49.0
Al_2O_3	0.1	0.5
Fe_2O_3	40.0	45.3
MgO	3.8	2.5
CaO	0.3	2.8
Na_2O	0.0	N.D.
K_2O	0.0	N.D.
TiO_2	0.1	0.2
MnO	0.3	0.2
S	0.1	0.0
P_2O_5	0.1	0.1
Ig. Loss	0.2	0.1
	100.1	100.7

Table 2 (ctd.)

B. Trace element analyses, XRF by author

ppm	Grunerite rich 62-606	Tremolite rich 62-1085
Zn	29	13
Cu	0	27
Ni	6	17
Ba	0	0
Nb	Approx. 1-4	Approx. 1-4
Zr	1	4
Y	0	0
Sr	0	0
Rb	0	0

patches within the hematite grains. A little limonite is present in the weathered zone due to the breakdown of amphiboles. At depth, magnetite is the predominant iron oxide and hematite is rare, occurring as small elongate blade forms confined to particular bands and quite distinct from the accompanying magnetite.

Carbonates - carbonates are rare within the bulk iron-formation. Whitehead (1962) records calcite associated with tremolite in some bands and in one microprobe sample examined by the author, calcite was identified in a tremolite layer (62-1316). In the lower part of the iron-formation sequence there is some interlayering of siliceous and carbonate units. The carbonate mineral in these layers is a low-iron ankerite, identical in composition to the ankerites of the thicker carbonate units which will be discussed later (analyses 1 to 3, Appendix II sample 83-575).

Amphiboles - the amphiboles have been optically identified as grunerite-cummingtonite and tremolite-actinolite by Whittle (1954) and Whitehead (1962 and company reports). Whittle also records glaucophane from beneficiation concentrates.

The amphiboles frequently occur in discrete layers and Whitehead (1962) observed that only one amphibole is present in any particular band. Catley (1964), records rapid alternation of clearly defined tremolite schist and grunerite schist bands in bore DDH 62, Iron Duchess. This segregation is not complete, because Whittle (1954) records grunerite, cummingtonite and

actinolite coexisting in amphibole schist in the Katunga Hills.

Amphiboles in eleven samples were analysed by electron microprobe and 34 analyses are plotted in Fig.7. The complete data is given in Appendix II.

The analyses show that two amphiboles dominate the silicate layers and have the following approximate compositions:

$Ca_2Mg_{4.3}Fe_{0.8}Si_8O_{22}(OH)_2$ - Tremolite, average of 11 analyses.

$Mg_{2.3}Fe_{4.5}Si_8O_{22}(OH)_2$ - Grunerite, average of 21 analyses.
(Water content assumed)

A third amphibole was identified in two samples (57-2081, 1627) and this is an iron rich actinolite with the approximate composition $Ca_2Mg_{3.2}Fe_{1.9}Si_8O_{22}(OH)_2$ (average of 2 analyses).

In ten of the eleven thin sections only one amphibole was present and in the one outstanding section, a single lathe of actinolite was identified amongst grunerite (57-2081). Within any one section, the amphibole composition remained essentially constant and no zoning or exsolution was detected.

The samples were chosen from widely separated drill-holes in the south Middleback Range and the results,

(i) confirmed that particular bands are characterised by one amphibole composition,

(ii) show that the segregation is not complete,

(iii) show that the precise amphibole compositions have very limited ranges throughout a wide area.

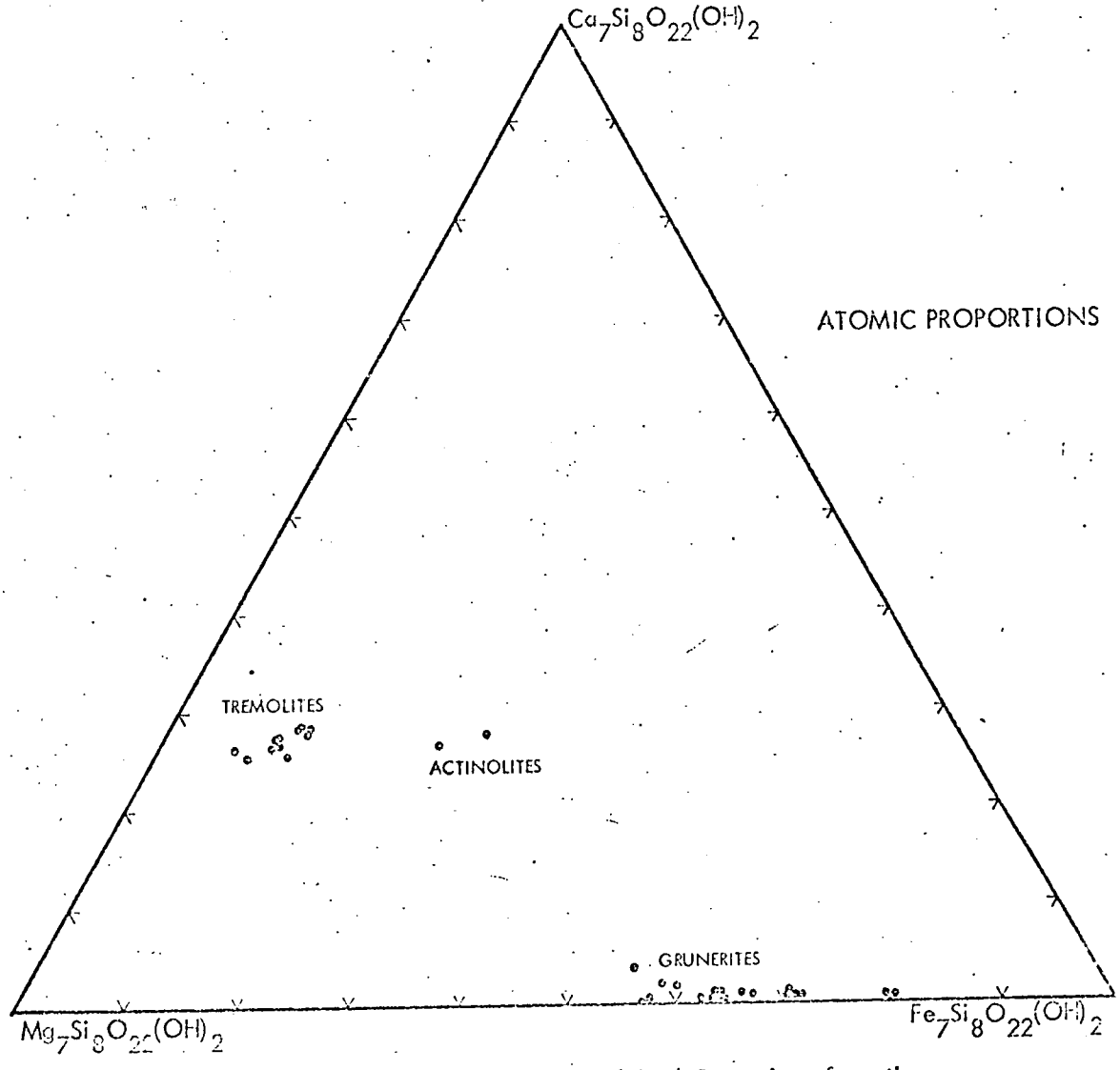

Fig.7. Compositions of amphiboles in Middleback Range iron-formations.

(b) Microtextures:

Thin sections show evenly sized, interlocking quartz grains with frequent triple point junctions and an average diameter of 0.1mm - 0.2mm (Fig.6). Magnetite grains, of similar size or rather smaller, are grouped into trains and bands or dispersed throughout the quartz. Amphiboles occur as well formed bladed crystals sometimes growing from the magnetite and often concentrated in specific bands.

The iron-formation banding is of two types; a regular, broad layering generally between 1cm and 3cm wide which is commonly visible in outcrop, and a fine scale, often microscopic layering which occurs within and parallel to the broader bands. Both are due to varying proportions of quartz, magnetite and amphibole.

The fine scale layering shows striking variations of texture both in hand specimen and thin section. Five microtextures can be distinguished and these are illustrated in Figs. 8a to 8e and described in Table 3. The most important factors are the amount of amphibole present and the quantity and size of the magnetite grains. Amphibole bands become markedly schistose and the quartz grains are frequently elongate parallel to the amphiboles. If large magnetite crystals are present in an amphibole rich band, quartz grows from the crystal faces in distinct tails (Fig.8e). In layers with large, closely packed magnetite grains, the interstitial quartz is more coarsely crystalline than normal and has undulose extinction.

Table 3. Microtextures in iron-formations

Predominant mineral	Additional minerals	Fig.	
1.Quartz	magnetite (amphibole)	8a	An even, fine-grained texture with very small magnetite grains evenly dispersed throughout larger quartz grains.
2.Amphibole	magnetite quartz	8b	Distinctly schistose with coarse grained magnetite. Quartz often in bladed forms parallel to the amphibole.
3.Magnetite	quartz (amphibole)	8c	(i) an even, sieve-like texture with magnetite aggregates forming the mesh and fine grained quartz in the interstices.
		8d	(ii) a coarse granular texture with large magnetite grains forming an irregular network and coarsely crystalline interstitial quartz with undulose extinction.
4.Magnetite	amphibole quartz	8e	Coarse and granular, similar to 8d but with larger magnetite grains and pronounced elongation of the magnetite grain clusters and the interstitial amphibole.

Brackets indicate that a mineral is present in minor quantity and may be absent.

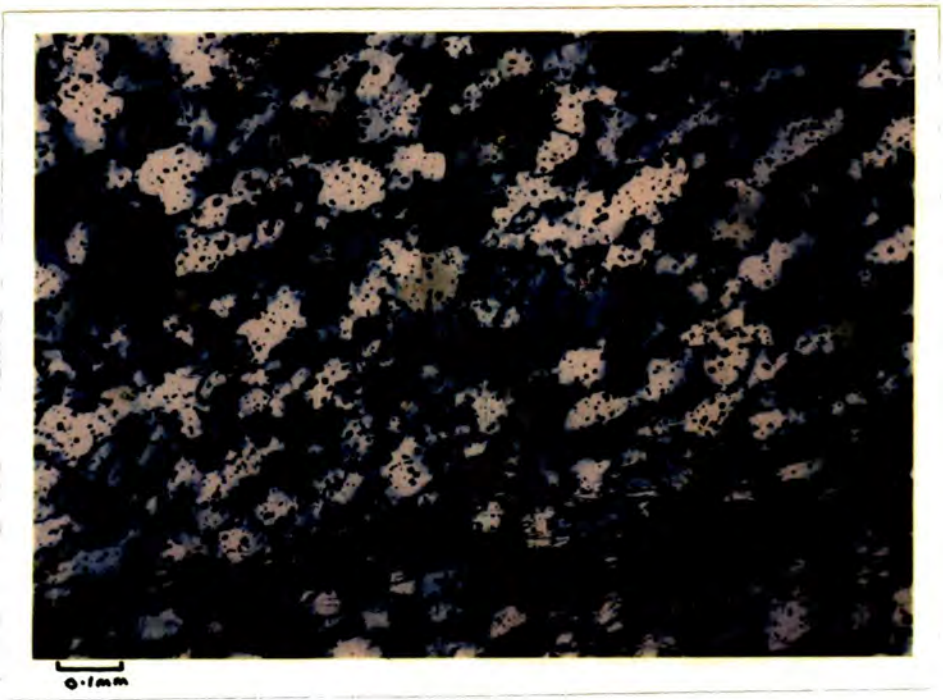

Fig. 8a. Iron-formation - microtexture type 1.
Quartz predominant, magnetite evenly distributed, amphibole minor. Note small size of magnetite grains.
Sample 63-307.

Fig. 8b. Iron-formation - microtexture type 2.
Amphibole rich, with less quartz and iron oxide. Quartz tends to be elongate parallel to the amphibole lineation.
Sample 63-307, crossed polars.

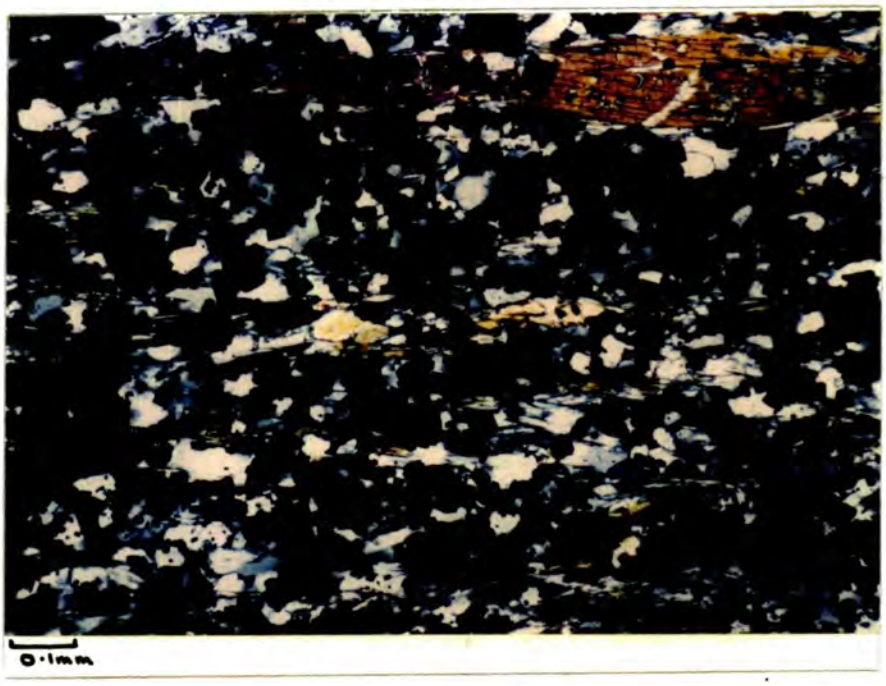

Fig. 8c. Iron-formation-microtexture type 3(i).
Iron oxides, mainly magnetite, in about equal quantity with quartz. Minor amphibole. Note the fine grain and regular distribution of components.
Sample 63-307, crossed polars.

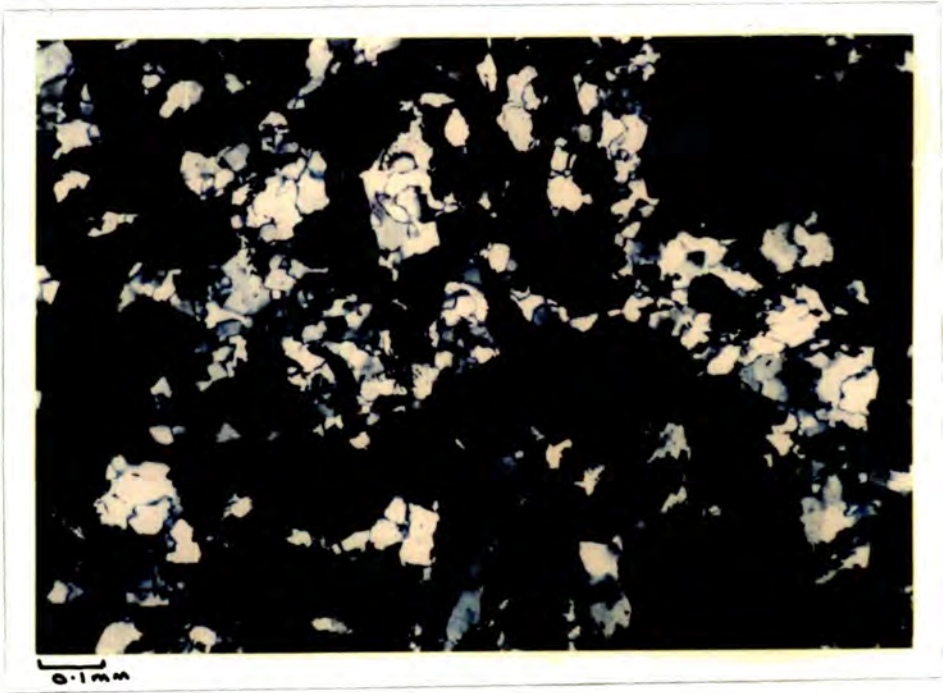

Fig. 8d. Iron formation - microtexture type 3(ii). Iron oxides and quartz. Note large quartz grains with undulose extinction.
Sample 76-690, crossed polars.

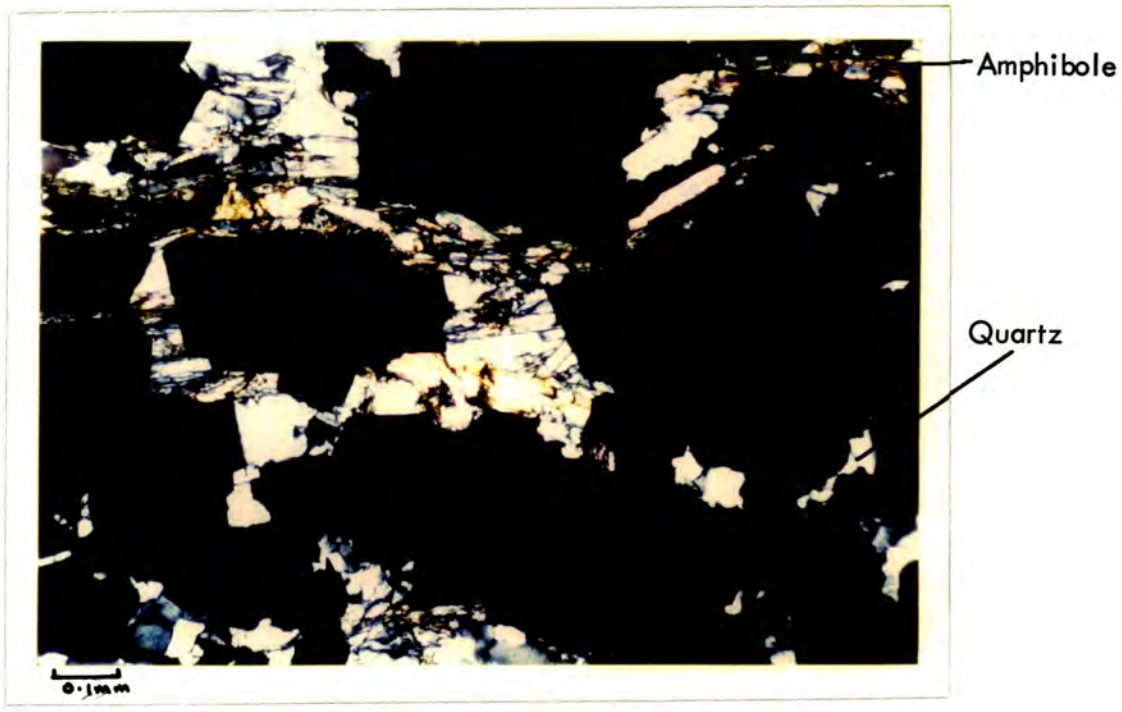

Fig. 8e. Iron-formation - microtexture type 4.
Iron oxides predominant with interstitial quartz and amphibole.
Note tendency for quartz to grow as tails behind iron oxides.
Sample 63-213, crossed polars.

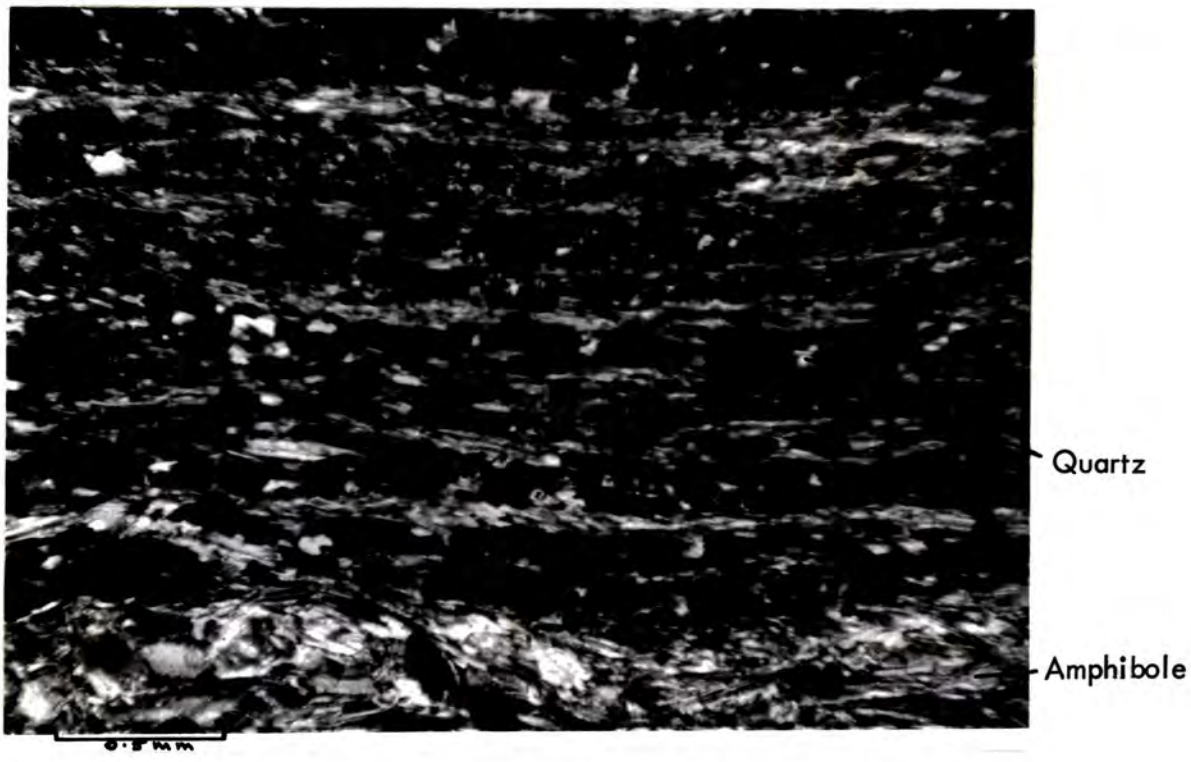

Fig. 8f. Iron-formation - Alternating bands of quartz-magnetite and amphibole-magnetite which result in a fine but distinctly layered iron-formation.
Sample 2746, crossed polars.

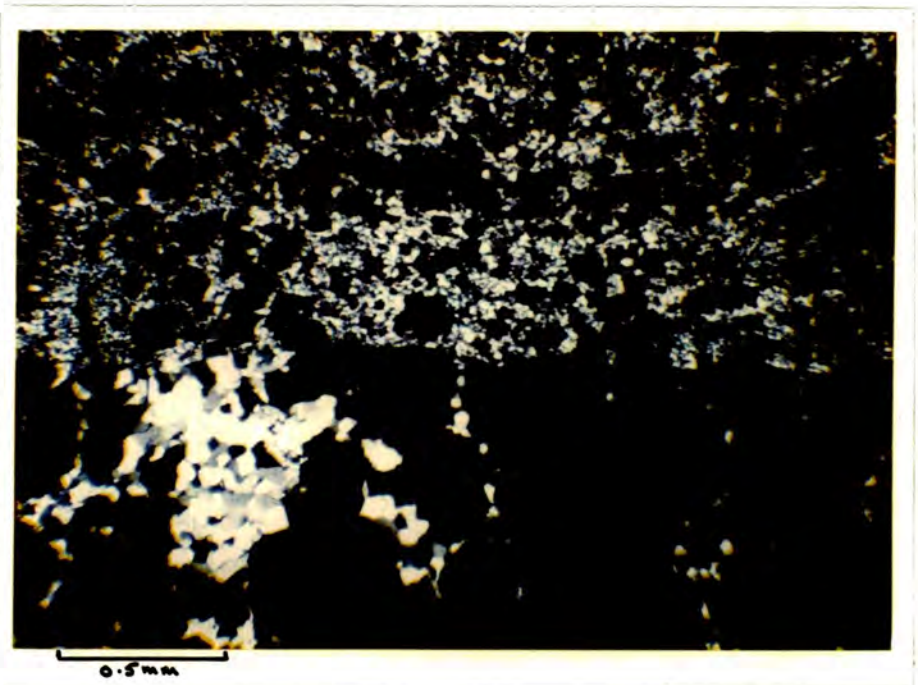

Fig. 8g. Hamersley range iron-formation. Iron oxides and quartz. Note the variation in quartz grain size.

Bands showing different microtextures can alternate on a very small scale, as in section 2746 which has up to 30 distinct bands within 1mm (Fig.8f). In addition to the main microtextures, some sections show a very fine grained magnetite layering parallel to the wider layers. In these, the magnetite grains are frequently enclosed by the quartz grains.

The microtextures show that during regional metamorphism, components within the iron-formations behaved in an orderly manner. Magnetite crystallised early, followed by quartz and amphiboles. Any migration of iron must therefore have taken place at an early stage of metamorphism. The very fine, evenly dispersed magnetite in some layers has clearly not migrated and there is no evidence that iron has moved into the magnetite rich layers. Contacts between magnetite rich and magnetite poor layers are often sharp, with no enriched or deficient zones between the two, as may be expected with migration. It appears likely, therefore, that iron remained immobile during metamorphism and the magnetite contents of individual layers reflect differences in iron content of the original rock.

2. Carbonate units

A carbonate unit occurs towards the base of the iron-formation sequence, outcropping intermittently on the flanks of the ranges. It is of variable thickness, reaching several hundred feet in places and was named the Middleback North Dolomite by Miles (1954). In outcrop, the rock is dark brown to buff coloured and the upper part contains siliceous bands which stand out as sharp ridges. When fresh, the rock is light to dark grey, compact and fine or medium grained with an even, crystalline texture. A second, 50' to 100' thick carbonate unit occurs within the schists separating the two iron-formation units at Cook Gap in the South Middleback Range.

(a) Mineralogy

Carbonates - Edwards (1954) describes the exposure at Mount Middleback North (Fig.1) as a recrystallised dolomite-marble. The same unit was intersected by Geological Survey drilling at Katunga Hills, 15 miles to the north, and is described by Whittle (1954) as a mixture of calcite and lesser dolomite with considerable tremolite and diopside.

At Iron Duke, the carbonate unit was intersected in several drillholes and whole-rock analyses of 9 samples (Appendix I) show it to be a dolomite containing between 4.0% and 9.4% iron expressed as Fe_2O_3 and approximately 0.9% MnO. Electron microprobe analyses on mineral grains in one sample (47-1041) confirm this general composition (Appendix II). Representative whole-rock and

electron microprobe analyses are shown in Table 4.

Deer, Howie and Zussman (1963) divide dolomite from ankerite on the arbitrary ratio of Mg:Fe = 4:1 and the carbonate described above has an element weight percent ratio of 1.6:1. By this definition, the mineral is a low-iron ankerite and will be referred to as ankerite in this thesis.

Information on carbonate mineralogy in other parts of the Middleback Range area is more limited than for Iron Duke. Miles (1954) records five whole-rock analyses of carbonates from widely separated localities and they are similar to the Iron Duke analyses except that they contain up to 4% MnO. Two of these analyses are shown in Table 4, together with analyses of a typical Iron Duke sample. The similarity between all the analyses suggests that a good deal of the carbonate mapped as dolomite is a low-iron ankerite.

Reconnaissance electron microprobe analysis was carried out on one sample (CN1) from the thin carbonate unit amongst the schists which separate the iron-formation units at Cook Gap. This showed a composition very similar to the Iron Duke carbonate.

Silicates - tremolite and diopside are reported by Whittle (1954) from the basal carbonate unit at Katunga Hills and Whitehead (1962 and company reports) has recorded diopside at Iron Duke.

The diopside at Iron Duke occurs as large crystals, up to 1cm in length, and grouped in random orientation. Electron micro-

Table 4. Whole-rock and electron microprobe analyses of Middleback Range carbonate units

Per cent	(Miles 1955)	(Miles 1955)	47-104(XRF)	47-1041 (Probe)
SiO_2	2.20	2.07	1.0	
Al_2O_3	0.52	N.D.	0.2	
Fe_2O_3	4.76	5.61	7.5	8.6
FeO	2.75			
MgO	15.04	17.05	13.7	16.0
CaO	29.65	28.33	26.3	29.5
Na_2O	0.16	N.D.	0.0	
K_2O	0.08	N.D.	0.1	
TiO_2	Nil	Nil	0.1	
MnO	1.25	4.16	1.0	0.7
S	N.D.	N.D.	0.0	
FeS_2	0.07	N.D.	N.D.	
P_2O_5	0.01	0.01	0.1	
CO	42.56	N.D.	N.D.	
H_2O (Tot.)	0.88	0.35	N.D.	
Cl	0.02	N.D.	N.D.	
Diff.	-	42.42	50.0	45.2
	99.95	100.00	100.0	100.0

Location: 1. West flank of Iron Knight
2. South-east corner of South Middleback Range
3. } Iron Duke, analyses by author, with Fe expressed
4. } as Fe_2O_3.

probe analyses of crystals in one sample (SA1, Appendix II) show a uniform composition of $Ca_1Mg_{0.8}Fe_{0.3}Si_2O_6$ with no detectable zoning in the crystals.

Quartz - interlayered quartz and carbonate bands are recorded by Rudd (1940) and Miles (1954) from the upper part of the carbonate unit. Drillhole DDH 83 at Iron Duke intersected similar interlayered material at the same stratigraphic level.

Iron oxides - magnetite occurs in thin layers in the upper part of the carbonate unit at Iron Duke. It is present as well formed, often cubic grains. Hematite is commonly found within the carbonate near to hematite orebodies and occurs as a fine red dust along carbonate grain boundaries and cleavages.

(b) Microtextures:

Thin sections were available of the Cook Gap carbonate band and the thick basal carbonate at Iron Duke.

The former is an equigranular mosaic of carbonate grains with numerous triple point junctions (Fig.9). The crystals often show well developed cleavage. At Iron Duke, the microtexture is very similar but the grains tend to be less defined, with diffuse boundaries. In the upper part of the Iron Duke unit, thin layers of magnetite produce a fine layering almost identical, in hand specimen to that of the iron-formations. Thin sections show that the layering is due entirely to varying proportions of magnetite which occurs in subhedral, blocky grains.

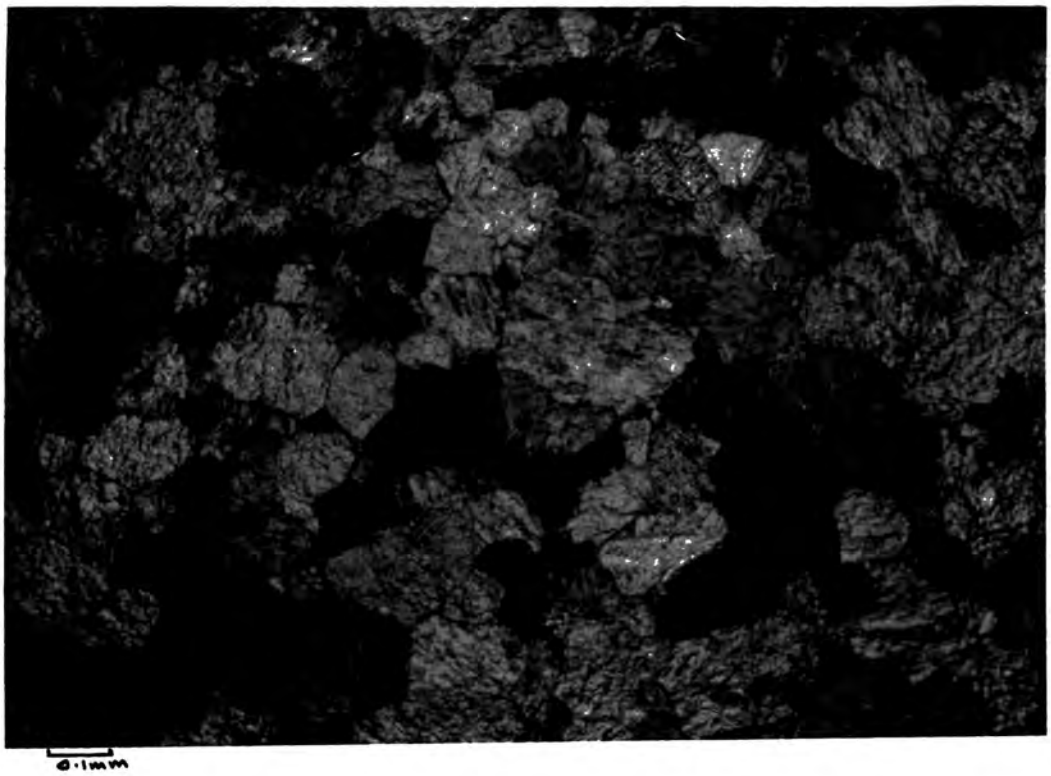

Fig. 9. Microtexture of carbonate unit at Cook Gap. Note the fairly regular crystal size and shape, and the triple point junctions. Sample CG1, crossed polars.

No samples were available from other parts of the ranges but Taylor (1954), describes the Iron Prince exposure as fine to medium grained granular dolomite and Whittle (1954) describes the Katunga Hills drillhole intersections as an equigranular mosaic of carbonates.

Two important points have been established by the above descriptions:

(a) the general composition of the carbonate units is that of an ankerite with about 5%-9% iron plus manganese,
(b) the regional microtexture is a medium grained equigranular mosaic which is a typical regional metamorphic texture (Spry (1969).

3. Schists

Thin bands of schist occur below and within the iron-formations. These are mainly quartz-chlorite and quartz-biotite schists but chloritoid is recorded from one band in the south range (Edwards 1954).

The main schist unit separates the iron-formations and is up to 700' thick (Miles 1954, Owen and Whitehead 1965). It consists of quartz-chlorite and quartz-biotite-hornblende schists which contain variable amounts of feldspar and garnet. Quartz lenticles are common and stretched pebbles are recorded by Rudd (1940) and Miles (1954).

(a) Mineralogy

Minerals in four thin sections were examined by electron microprobe. The complete analyses are given in Appendix II and the results are summarised below:

Biotite $K_{1.8}(Mg_{2.1}Fe_{3.0}Ti_{0.1}Al_{1.2})(Si_{5.4}Al_{2.6})O_{20}(OH)_4$

This composition is the average of two analyses in two thin sections (1958, 5-157). The range of total atomic Al is 3.4 to 4.3 and of Si is 5.1 to 5.7.

Hornblende $Ca_{1.8}Na_{0.9}(Mn_{0.1}Fe_{2.4}Mg_{1.5}Al_{1.2})(Al_{1.7}Si_{6.3})O_{22}(OH)_2$

The composition is from one analysis on section 5-157. Reconnaissance analysis showed that other crystals in the section were of similar composition. The amphibole basic formula name is Pargasite (Phillips 1965).

Plagioclase Ab 62, An 32, Or 6.

The composition is the average of two analyses in one thin section (1961).

Chlorite $(K_{0.6}Mg_{3.0}Fe_{5.8}Al_{2.7})(Si_{5.4}Al_{2.6})O_{20}(OH)_{16}$

The composition is from one analysis in thin section 5-1952. Reconnaissance analysis showed the chlorite to have a uniform composition. The chlorite composition is that of a Ripidolite (Hey 1954).

Garnet Almandine (Fe-garnet).

Garnets were analysed in three thin sections (1961, 5-1952, 5-157) and all were basically almandines but showed considerable variation in Fe, Mn and to a lesser extent Ca. This may be illustrated by the two compositions below from different thin sections:

	Fe	Mn	Ca	Mg
5-1952	Alm.83	Spess.4	Gross.8	Pyr.5
5-157	Alm.57	Spess.22	Gross.15	Pyr.6

Two of the thin sections (5-157, 1961) were quartz rich schists with amphibole, biotite, plagioclase and a little chlorite. The garnets in these were very small and conformed to the composition shown for 5-157 above. The third thin section (5-1952) was a chlorite schist with larger garnets which had Mn deficient rims (Fig.10).

(b) Microtextures

Eleven thin sections of the schist were available, all from a deep Geological Survey drillhole (MSDD5). The majority

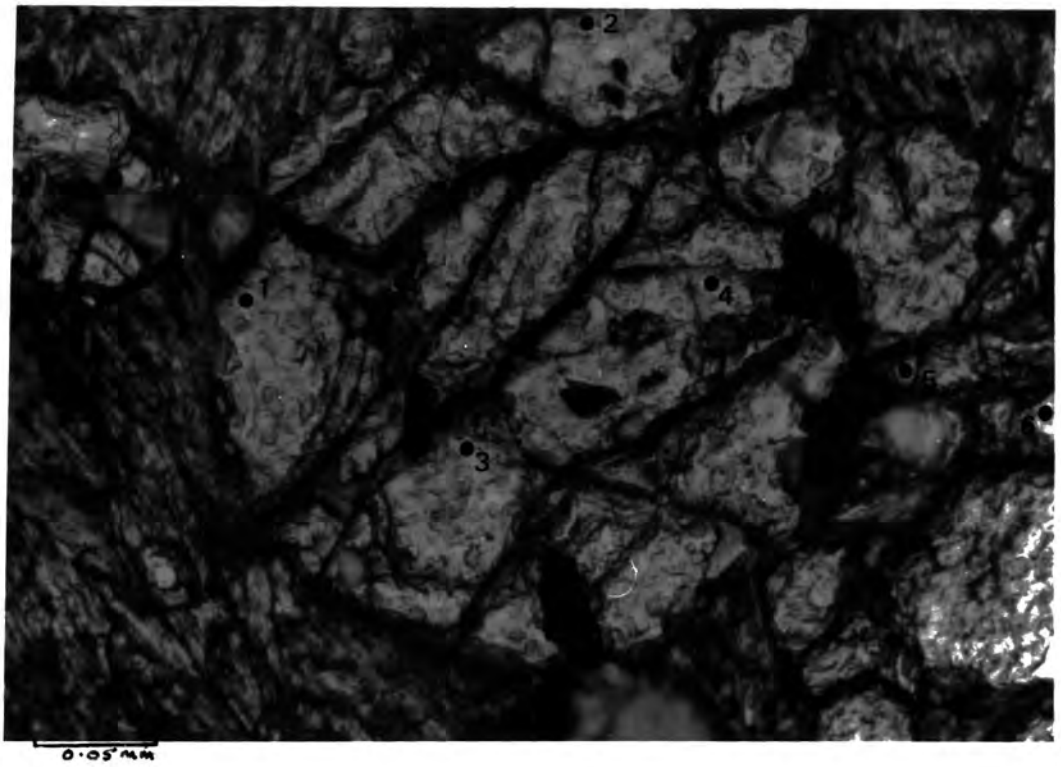

Fig. 10. Photomicrograph of garnet crystal in chlorite schist, part of the Cook Gap schists, sample No. S-1952. Uncorrected Mn and Al determinations at the points marked on the photograph are:

	Mn	Al
1.	0.9	10.1
2.	1.0	10.0
3.	1.4	10.0
4.	2.1	10.1
5.	2.7	10.9
6.	2.3	10.4

contain fine-grained quartz and amphibole, with varied amounts of biotite, plagioclase, garnet and chlorite. Fine grained sericite appears to be present in some samples. The bladed and fibrous minerals are generally aligned parallel producing a strong lineation in thin section. Quartz eyes are common and are elongate parallel to the lineation. The garnets, when present, do not affect the orientation of the amphiboles or biotites and appear to be contemporaneous with them.

Chlorite occurs in some sections, as small, irregular green patches with no clear crystal form. These merge with the biotite and hornblende and sometimes appear to replace them but no definite replacement textures were found.

4. Discussion

The iron-formation banding has been regarded as sedimentary by most authors. Whitehead (1962) and Catley (1965), for example, suggested that the alternating layers of different amphiboles reflect variations in composition within the original sediment. However, Jones (1968), in an undergraduate study of Iron Duke structures, detected small scale isolated fold closures within the plane of the iron-formation banding and suggested that these may be remnants of an earlier layering. This raises the possibility that the iron-formation layering is due to metamorphic differentiation, as suggested also by Talbot (pers. comm.) who has worked on metamorphic layering of a broadly similar type in the south-east of South Australia (Talbot and Hobbs 1968). The main factors which suggest that the banding is sedimentary rather than metamorphic are as follows:

(i) As would be expected of sedimentary layering, the banding is generally parallel to the margins of the main units and to the thin, interlayered argillaceous schists.

(ii) Iron-formations throughout the world are characterised by alternating layers rich in quartz, iron oxides, silicates and carbonates (James 1966). In unmetamorphosed areas, the typical minerals are quartz, magnetite, hematite, greenalite, minnesotaite, stilpnomelane, dolomite and siderite. Metamorphism produces assemblages identical to those of the Middleback Ranges, and in areas with metamorphic zoning, the new assemblages reflect the pre-existing mineralogy (James 1955, Gross 1967).

(iii) The finely layered Middleback Range banding is similar in scale and appearance to the unmetamorphosed Hamersley Group iron-formations of north-west Australia. Thirteen Hamersley specimens were examined of which eight were much finer grained than the Middleback Range material but five had similar microtextures as illustrated in Fig. 8 . This suggests that metamorphism has not greatly changed the iron-formation layering, the main affects being a slight increase in grain size and the development of amphiboles.

For these reasons, the iron-formation layering is considered to be sedimentary and the different amphiboles to reflect differences in the original mineralogy. In this context, the intrafolial microfolds recorded by Jones (1968) may be sedimentary slump structures.

The interpretation of the fine-scale layering as sedimentary in origin implies that there was negligible movement of the main components during metamorphism. Whitehead (1962) reached a similar conclusion from the close proximity of separate quartz-magnetite-tremolite and magnetite-tremolite-calcite layers. Each band acted as an essentially closed system resulting in the systematic variation in microtextures. The main visible effects of metamorphism are recrystallisation of quartz and iron oxides and the development of amphiboles.

The original sediments of the Middleback Group were chemically or biochemically precipitated cherts, iron oxides,

carbonates and Fe,Mg-silicates forming the iron-formation and carbonate units together with normal argillaceous clastic sedimentation forming the present schist units. In common with iron-formations throughout the world, the iron-formation units represent long, stable periods of chemical or biochemical deposition with uniform conditions over the whole area (James 1966). The proportions of the main components varied gradually from place to place and with time.

In the lower part of the sequence, carbonate sedimentation was dominant, producing thin interlayered carbonate-chert-iron oxide layers at the base of the sequence, followed by the thick basal carbonate unit. Above the basal carbonate, iron and silica precipitation increased, at first subsidiary to carbonate forming a transition zone and then becoming dominant to form the main iron-formation units. The iron-formations consisted of chert, iron oxides and thin bands of carbonates and Fe,Mg-silicates.

Metamorphism of these layered iron-formations produced tremolite and grunerite from the chert-carbonates and chert-Fe,Mg-silicates assemblages and recrystallised the chert and iron-oxides. Thick carbonate units such as the basal carbonate were recrystallised and the normal clastic sediments were converted to schists.

C. METAMORPHISM OF THE MIDDLEBACK GROUP

Mineral assemblages in the iron-formations and schists of the Middleback Ranges are strikingly similar to those recorded by James (1955) from Michigan iron-formations in the garnet zone of regional metamorphism (Fig.11). In a more general classification this is equivalent to the upper greenschist and lower part of the amphibolite facies (Turner 1968).

It is important to establish the regional metamorphic grade with reasonable certainty as a basis for discussing ore genesis for both the hematite and the magnetite-hematite-carbonate ores. The regional metamorphism will therefore be discussed in more detail in the following pages.

The simple but widespread mineralogy and the regular microtextures in iron-formation and carbonate units suggests that regional metamorphism was uniform throughout the area and that equilibrium was generally attained. All the assemblages satisfy the Phase rule in that $F \geqslant 2$, where $F=C-P+2$ (F=variance, C=components and P=phases), with H_2O considered as a mobile component throughout and CO_2 considered as an inert component in carbonate bands and as a mobile component in other assemblages. This is consistent with their having attained equilibrium (Klein 1966).

In the Middleback Ranges, no minerals clearly define the metamorphic grade but a number of assemblages contribute

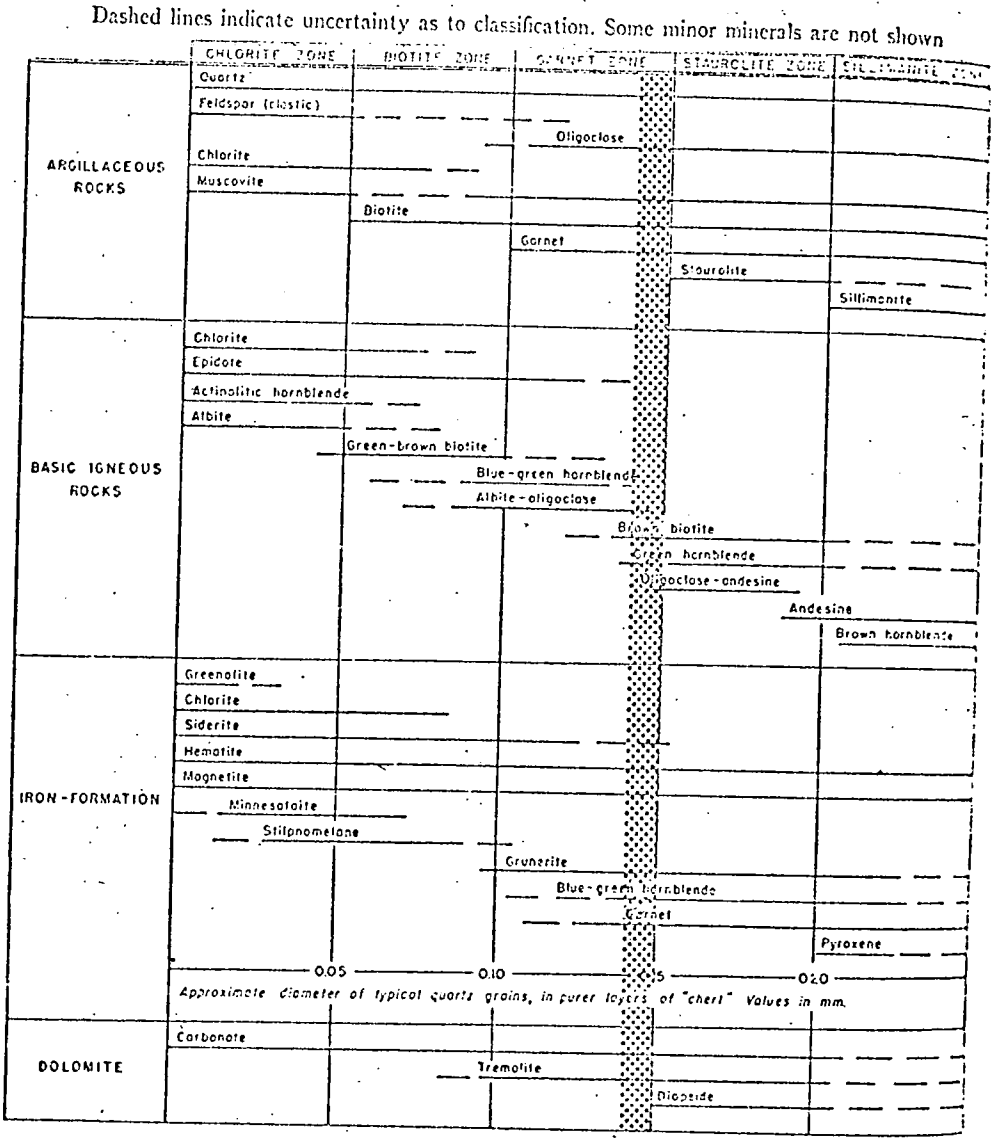

Fig. 11. Mineral assemblages in the metamorphic zones of Northern Michigan, from James 1955. The approximate position of the Middleback Group in terms of mineral assemblages and estimated metamorphic grade is shown on the diagram by the stippled area.

information which, when accumulated, enables an estimate of pressure-temperature conditions. As the assemblages themselves are a function of chemical components, it is convenient to group them for description into chemical systems (Klein 1966). The mineral assemblages present are illustrated in Fig.12.

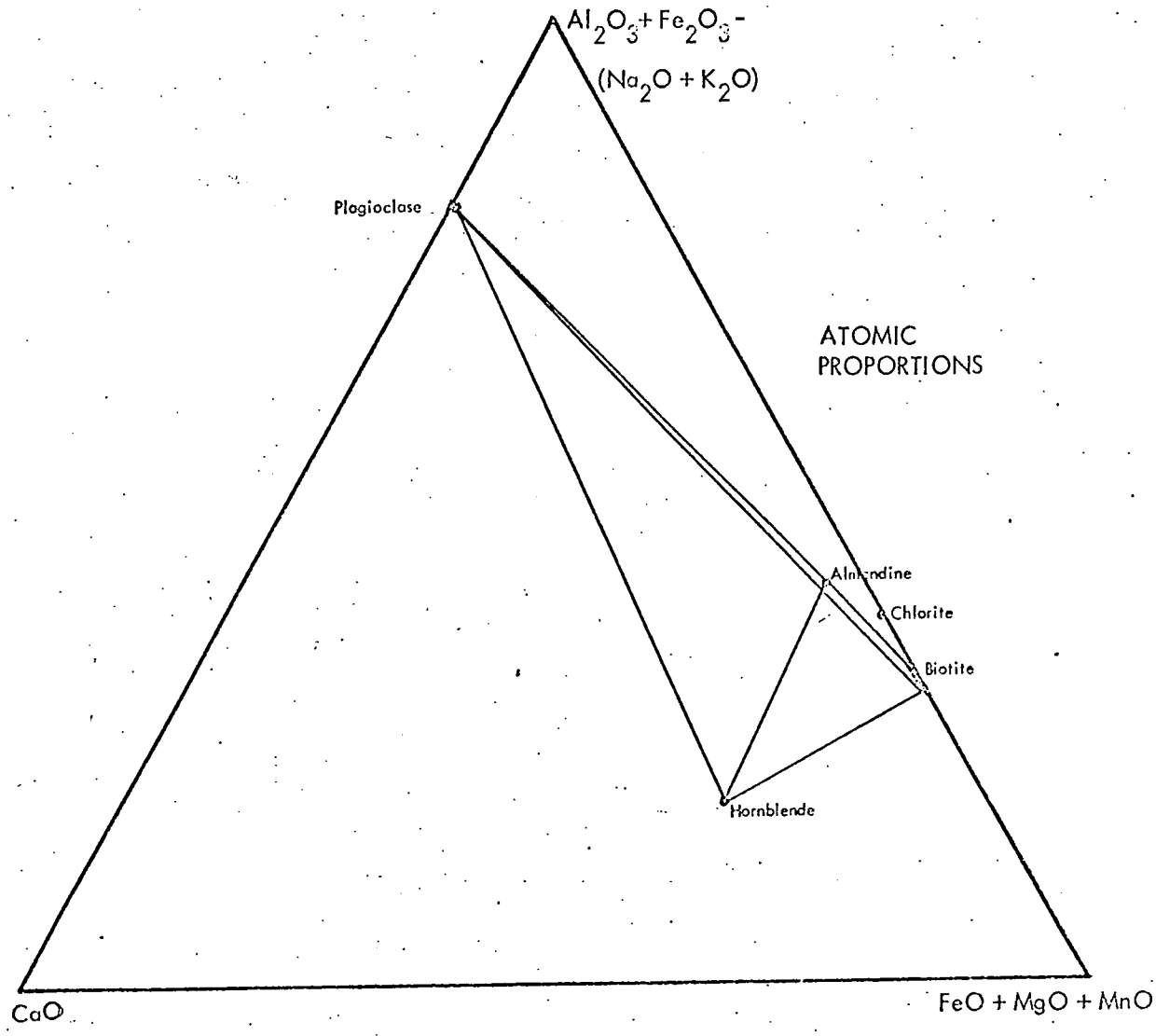

Fig. 12a. Main pelitic assemblages in the Cook Gap schists.
Excess SiO_2. ACF diagram, mineral compositions from electron microprobe analyses.

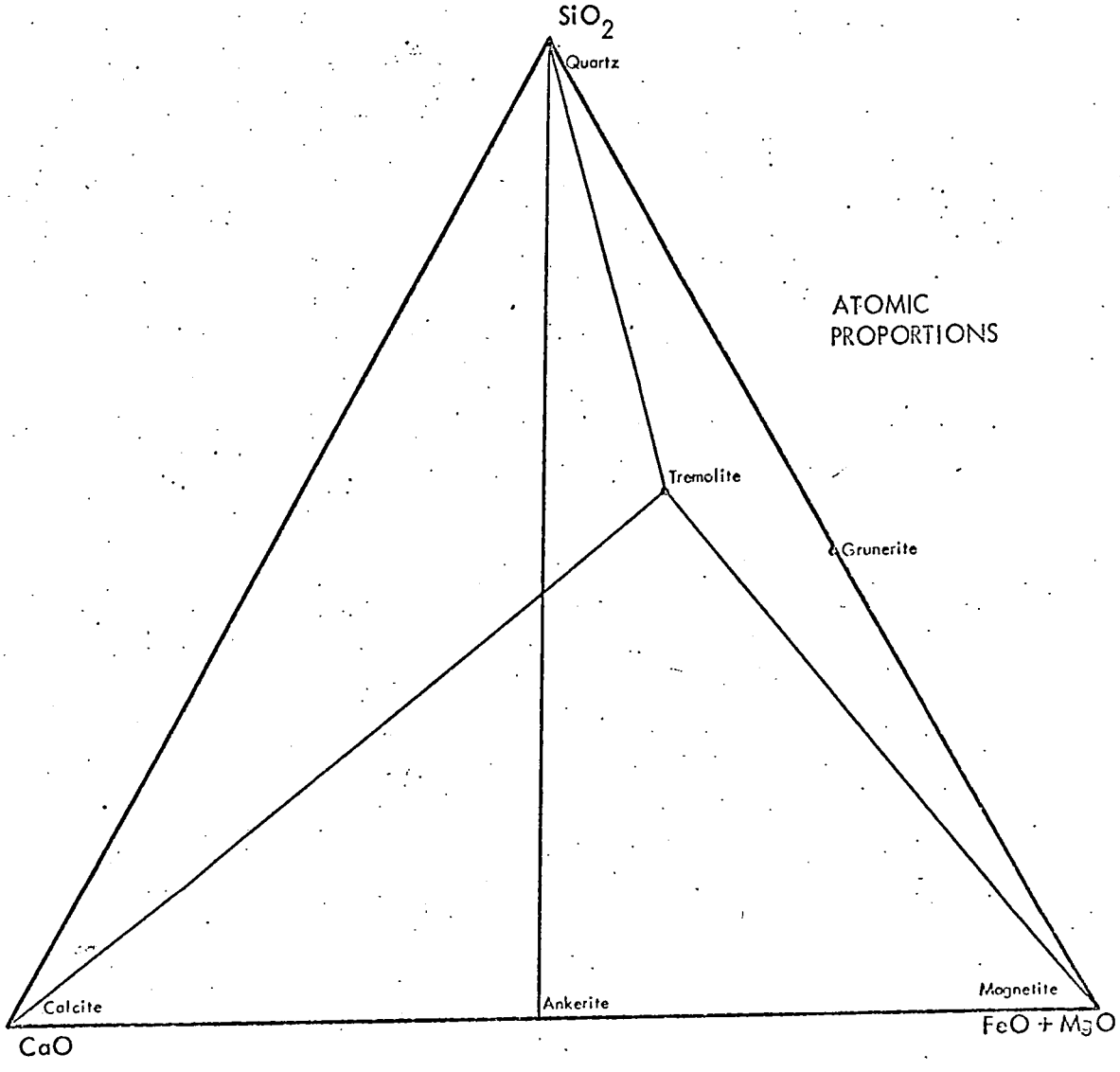

Fig. 12b. Iron-formation assemblages. Excess SiO_2. ACF diagram, mineral compositions from electron microprobe analyses.

1. SiO_2-FeO-Fe_2O_3-MgO-H_2O

Quartz-magnetite
Quartz-magnetite-grunerite } Iron-formations

Grunerite with the approximate composition of Middleback material has been synthesised at 570°C with P_{H2O}=1000 bars and P_{CO2}=80 ± 10 bars (Schürmann 1968). This conforms to a broadly intermediate grade of regional metamorphism.

In nature, grunerite is normally formed by one of the following three reactions:

7 Magnetite + 24 Quartz + 3 H_2O ⟶ 3 Grunerite + 7/2 O_2 (1)

7 Siderite + 8 Quartz + 1 H_2O ⟶ 1 Grunerite + 7 CO_2 (2)

7(FeMg-silicates) + 10 Quartz ⟶ 3 Grunerite + 11 H_2O (3)

Equation (1) from French, 1971.
Equations (2) and (3) from Deer, Howie and Zussman 1963, with equation (3) slightly modified.

In the Middleback Ranges, reaction (1) is unlikely because magnetite-quartz mixtures are common and show no sign of reaction. Furthermore, the Middleback grunerites contain a minimum of about 6% by weight MgO which is not accounted for in the quartz-magnetite reaction. Amphiboles do grow from magnetite crystal faces in some cases but this applies to tremolite as well as grunerite and appears to be due to the dynamics of crystallisation rather than to chemical control.

Reactions (2) and (3) are both possible and will be discussed separately:

(2) $7(Fe,Mg)CO_3 + 8SiO_2 + 1H_2O \longrightarrow 1(Fe,Mg)_7Si_8O_{22}(OH)_2 + 7CO_2$

Siderite Quartz Grunerite

French (1971), from laboratory work and thermodynamic calculations, estimates that grunerite forms from pure $FeCO_3$ and quartz at 300°C to 400°C. The presence of Mg in the siderite extends its stability field and raises the minimum temperature of reaction. Grunerites in the Middleback Ranges all contain appreciable Mg and the original siderite must have been Mg rich unless other minerals also took part in the reaction. Assuming an Mg rich siderite, temperatures of 350°C to 450°C are reasonable for the first appearance of grunerite.

In the North Michigan area of North America, grunerite first appears in the upper part of the biotite zone at estimated temperatures in the order of 300°C to 350°C in the pressure range 1000 b. to 4000 b. (James 1954). The estimates agree with those of French described above and suggest a minimum possible grade of upper biotite facies for the Middleback Range rocks.

If the quartz-siderite reaction did take place in the Middleback Ranges, it was carried to completion because siderite is now completely absent. In the North Michigan area this occurred within the garnet zone, remnant pockets of siderite co-existing with quartz and grunerite in the main part of the zone

but siderite being completely absent in the higher grade, staurolite zone. By analogy, the Middleback rocks must have reached middle to upper garnet zone (upper greenschist) metamorphic grade.

(3) $7(Fe,Mg)_3Si_2O_5 + 10SiO_2 \longrightarrow 3(Fe,Mg)_7Si_8O_{22} + 11H_2O$

FeMg-silicates Quartz Grunerite

The silicate composition shown above is greenalite but similar FeMg-silicates such as minnesotaite and stilpnomelane are common in mildly metamorphosed iron-formations and are suitable in composition to form grunerite (Blake 1965, James 1966).

French (1971) suggests on the basis of synthetic work that the upper stability limit of minnesotaite is in the order of 300°C at 2000 bars pressure.

In the North Michigan area, minnesotaite and stilpnomelane are eliminated, presumably converting to grunerite, in the upper biotite zone at estimated temperatures in the order of 300°C to 350°C (James 1955). The actual change is not seen, but grunerite commences as the other silicates disappear and the temperature estimates fit well with those of French.

In the Middleback Range iron-formations, no metamorphic silicates other than amphiboles are present and the conversion must have carried to completion. This indicates

a minimum possible grade of biotite-garnet transition facies (upper greenschist) at temperatures of 300°C - 350°C.

2. SiO_2-FeO-Fe_2O_3-MgO-CaO-H_2O-CO_2

Ankerite-quartz Ankerite-(diopside)	Carbonate units
Tremolite-magnetite^{+}-quartz^{+}-calcite Tremolite-magnetite-hematite-quartz	Iron-formations

These assemblages are of particular interest because the presence of tremolite enables an estimate of the lowest possible metamorphic grade and coexisting tremolite and calcite in iron-formation bands suggests an upper limit. In addition, the presence of unreacted ankerite-quartz and tremolite in the Middleback Group provides some interesting information on the conditions prevailing in different layers during metamorphism.

There is no experimental evidence for reactions in ankerite-quartz mixtures but there is abundant data concerning the metamorphism of siliceous dolomites and, as the Middleback Group ankerites have low iron contents, it is reasonable to consider the available information on dolomite-quartz reactions.

At intermediate grades of regional metamorphism, tremolite forms from quartz and dolomite in two main ways (Winkler 1967, Turner 1968):

(4) 3 Dolomite + 4 Quartz + 1 H_2O ⟶ 1 Talc + 3 Calcite + 3CO_2

followed by

2 Talc + 3 Calcite ⟶ 1 Tremolite + 1 Dolomite + 1 H_2O + 1 CO_2

(5) 5 Dolomite + 8 Quartz + 1 H_2O ⟶ 1 Tremolite + 3 Calcite + 7 CO_2

No metamorphic talc occurs in the Middleback Ranges so that the second stage of reaction (4) must have carried to completion if the tremolite formed in this way.

Both reactions are pressure dependent and Turner (1968) estimates the first appearance of tremolite from thermodynamic calculations as follows:

$PH_2O=PCO_2$ in bars	500	1000	1400
Temperature °C	400°	450°	480°

These temperatures may be somewhat reduced if the carbonate is ankerite rather than dolomite (Turner 1968) and a minimum temperature in the order of 350°C to 400°C appears reasonable for the Middleback Group.

In the North Michigan area, tremolite first occurs in the upper part of the biotite zone at approximately the same time as grunerite in the iron-formations (Fig.11). This suggests rather lower temperatures than are indicated by Turner's calculations and by analogy with the North Michigan area, the lowest grade that could have been attained in the Middleback Group carbonate is upper biotite zone (upper greenschist facies) at temperatures of about 300°C.

An upper temperature limit is indicated by the presence

of coexisting quartz-tremolite-calcite. At high temperatures, tremolite reacts with quartz and calcite to form diopside in the following way (Winkler 1967):

(6) 1 Tremolite + 3 Calcite + 2 Quartz $\rightleftharpoons$ 5 Diopside + $3CO_2$ + $1H_2O$

The precise temperature of this reaction is dependant on the partial pressures of CO_2 and H_2O in the interstitial pore fluid. Turner (1968) estimates from thermodynamic calculations that the reaction takes place at about 100°C above the tremolite and calcite forming reaction (5) for pressures up to 1750 bars. Fig. 15 shows Turner's calculated curve for stable equilibrium in the reaction, extrapolated linearly to the pressure range of 2kb. to 6kb., and this indicates a maximum possible temperature for the Middleback Group in the order of 650°C.

This estimate is supported, to some extent, by the presence of unreacted ankerite-quartz. If water is absent from the interstitial pore fluid, tremolite development is inhibited and at high temperatures diopside is formed by the following reaction (Turner 1968):

(7) 1 Dolomite + 2 Quartz $\longrightarrow$ 1 Diopside + 2 CO_2

The estimated equilibrium curve for this reaction is plotted on Fig.15 and shows that metamorphism of the Middleback Group could not have proceeded to temperatures beyond about 650°C for pressures up to 4 kb.

Diopside does occur within the thick carbonate unit towards the base of the Middleback Group. However, it occurs as large crystals up to 1 cm in length with a random orientation, and these form a texture strikingly different from the fine-grained even or schistose textures characteristic of all the clearly regional metamorphic assemblages. All the known diopside is from drillholes at over 1000' below the surface and geological interpretation at these depths is uncertain but it is possible that the diopside is a product of contact metamorphism due to basic intrusives or to the action of hydrothermal solutions. It is therefore regarded as an unreliable indicator of regional metamorphic grade.

The presence of both tremolite and unreacted ankerite-quartz in the same sequence can be explained by differences of P_{CO2} in the interstitial pore fluid. The two tremolite forming reactions (4) and (5) both depend upon the P_{CO2}/P_{H2O} ratio of the interstitial fluid, requiring higher temperatures for reaction as the P_{CO2} rises. The ankerite-quartz bands therefore represent layers with high P_{CO2}/P_{H2O} ratios and the tremolite rich bands represent layers with a higher water content in the pore fluid. The possible reasons for variations in the P_{CO2}/P_{H2O} ratio are discussed below.

As pore water is driven out by progressive metamorphism, the P_{CO2}/P_{H2O} ratio in any particular layer will depend primarily on the carbonate content of the layer. With increasing grade, the thicker carbonate layers build up a high P_{CO2} and prevent

the inward diffusion of water from adjacent layers (Turner 1968). Thinner carbonate layers will be affected in two ways:

(1) Water may penetrate the layer, lowering the P_{CO2}/P_{H2O} ratio and promoting the tremolite forming reactions.

(2) When hydrous silicates are present in a carbonate rich layer, the loss of structural water will ensure a low P_{CO2}/P_{H2O} ratio, facilitating the tremolite forming reactions.

These two factors combined would explain the lack of carbonate in the main part of the iron-formation sequence where original carbonate layers were thin, and the fact that the unreacted ankerite-quartz mixtures are all from the upper part of the main carbonate unit.

Reactions (4) and (5) both produce a carbonate in addition to tremolite but tremolite bands in the Middleback Ranges rarely contain carbonates. This indicates that CO_2 has been lost from the system (Mueller 1960). CO_2 and presumably H_2O must therefore have been mobile in some parts of the sequence during metamorphism. On the other hand, the preservation of the ankerite-quartz assemblage requires a very high P_{CO2} which suggests that CO_2 remained immobile in these bands. Klein (1966), faced with an identical situation in the Wabush Lake area of Canada concluded that in parts of the area CO_2 was inert whilst in others it was able to diffuse out resulting in strong P_{CO2} gradients. It may, perhaps be more satisfactorily explained as

limited penetration of H_2O into the carbonate units which had developed high partial pressures of CO_2.

3. SiO_2-Al_2O_3-MgO-FeO-K_2O-Na_2O-CaO-H_2O

Quartz-hornblende^{+}-Biotite^{+}-plagioclase^{+}-garnet^{+}-chlorite
Quartz-chlorite-chloritoid
Quartz-chlorite-muscovite
} Schists

The Middleback Range schist assemblages are similar to those at intermediate grades of metamorphism in the Barrovian zones of Scotland (Turner 1968) and the iron-formations of North Michigan (James 1955). Detailed comparison is difficult because of differences in metamorphic conditions and whole-rock starting compositions. Individual mineral compositions give some information on the precise grade attained during metamorphism and these are discussed below.

Hornblende

The term hornblende is a general term used by metamorphic petrologists for green or brown amphiboles containing some Na, K or Al in the structure in addition to Ca, Fe and Mg. The amphiboles in argillaceous schist units in the Middleback Ranges conform to this description.

The change of amphibole composition from actinolite to hornblende marks the onset of amphibolite grade conditions (Leake 1964).

Harry (1950), suggested that with increasing metamorphic grade Al substitutes for Si in the Z site. The Middleback Range hornblendes contain about 1.3 atoms of Al in the Z site

which conforms to the amphibolite facies group.

Harry's suggestion was supported to some extent by data from southern Japan (Banno 1964) but was refuted by Shido (1958), also working in southern Japan, who maintained that Al variation is not systematic with grade but that the alkali content increases with increasing grade. Engel and Engel (1962) report definite increases in Na, K and TiO_2 with increasing grade but no increase in Al.

Whole-rock composition is a major chemical control and may influence the precise composition of hornblende more than subsequent pressure-temperature changes (Engel and Engel 1962). The titanium content of an amphibole, for example, may reflect the abundance or paucity of titanium in the original rock.

The presence of other ferromagnesian minerals may also strongly influence hornblende compositions. Elements, such as Ti, may be partitioned between several ferromagnesium minerals and a hornblende in this situation will contain less of these particular elements than if it were the only ferromagnesian mineral present (Leake 1964).

The use of hornblende compositions to indicate metamorphic grade is therefore fraught with difficulty. The presence of hornblende indicates a minimum grade of lower amphibolite facies but the mineral composition cannot be used to estimate the final grade attained.

Biotite

Biotite forms in the upper part of the greenschist facies by complex dehydration reactions involving chlorites and muscovites (McNamara 1965, Turner 1968). The precise temperature at which biotite forms depends upon the Mg content of the pre-existing chlorite, the required temperature increasing with higher Mg contents (Atherton 1964). It is therefore not possible to define a precise lower temperature of biotite formation in the Middleback Ranges as the pre-existing chlorite compositions are not known. Experimental work is consistent with the development of biotites at 300°C to 400°C under water pressures of a few bars (Turner 1968), and this agrees well with estimated temperatures for the upper greenschist facies of the Scottish Barrovian zones (McNamara 1965). The presence of considerable biotite therefore establishes a minimum metamorphic grade of upper greenschist facies at temperatures not less than 300°C for the Middleback Range rocks.

Engel and Engel (1960) showed that the biotite composition changes systematically with increasing metamorphic grade, Mg and Ti increasing, Mn and Fe decreasing. However, the biotite composition is strongly influenced by the whole-rock composition and by the coexisting mineral phases (Atherton 1964). Each area may therefore have its own suite of biotite compositions and it is invalid to compare data from different areas without full knowledge of the whole rock and all phase compositions. This evidence is not fully available for the Middleback Ranges.

Plagioclase

Plagioclase grains were examined in one thin section by electron microprobe and had a uniform composition of approximately An32. The grains were small, rounded and are presumed to be of sedimentary origin.

At the first stages of low grade metamorphism, clastic plagioclases of up to 1 cm in size are made over into pure albite (Leake 1964). Within the greenschist facies the plagioclases are normally albites with An0 - An5 and the anorthite molecule content increases slightly with increasing grade. In the transition zone between the greenschist and amphibolite facies there is a sudden composition change from about An7 to An15-20 (Waard 1959, Engel and Engel 1960). This marked compositional break was used by Turner (1958) to define the boundary between greenschist and amphibolite facies and, whilst this may not be strictly applicable in all situations, it is generally accepted that plagioclase with An15 denotes a minimum grade of greenschist-amphibolite facies transition.

Within the amphibolite facies there is a general increase of anorthite content with increasing grade but the precise composition depends upon other phases present in the rock. The Middleback Range plagioclase, with an anorthite molecule content of An32 clearly indicates a minimum grade of lower amphibolite facies.

Garnets

Almandine garnet is a characteristic mineral of amphibolite facies grade metamorphism but may occur in the upper part of the greenschist facies (Turner 1968). In Scotland and North Michigan, the almandine starts sharply at the base of the garnet zone (James 1955, Atherton 1964). This is equivalent to the greenschist-amphibolite transition of more general classifications and the presence of garnet in the Middleback Group schists clearly establishes a minimum grade of upper greenschist facies.

Variations in garnet composition with increasing metamorphic grade have been investigated by a large number of authors. It is firmly established that there is systematic variation of the main components, but the relation between these variations and metamorphic grade is complex.

The general variation with grade was well illustrated by Atherton (1964) who summarised data from four well known areas; Stavanger, Perthshire, the Adirondacks and southern Japan. The data was presented in a series of diagrams, one of which is shown in Fig.13. In all four cases, with increasing grade FeO and MgO increase, MnO decreases rapidly and CaO decreases slightly. The curves are different for each area and may cross in different places. The Middleback Range garnets from quartz-hornblende-biotite schists fit well onto the Stavanger area data as shown in Fig.13 and their composition suggests lower, rather than higher grades of metamorphism.

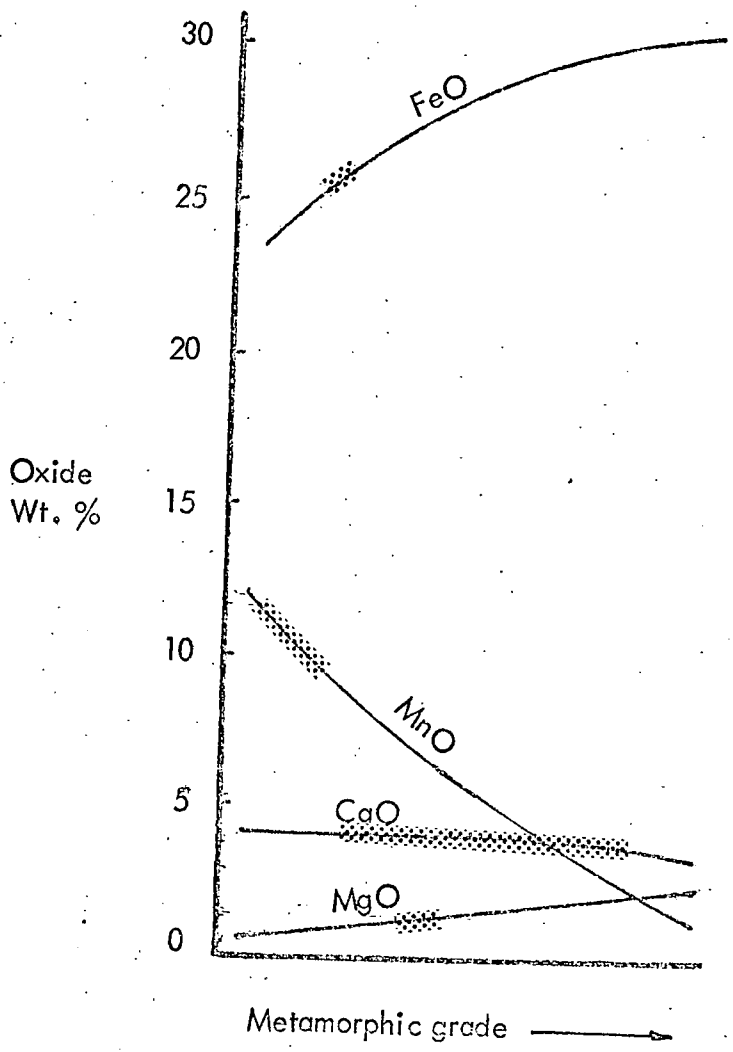

Fig. 13. Plot of variation of garnet composition with grade in the Stavanger area. From Atherton 1965, with the approximate composition of the Cook Gap schist garnets shown on the diagram as stippled areas.

A number of authors have studied garnet Mn content and shown that it decreases as grade increases (Miyashiro 1953, Engel and Engel 1960). The initial garnet composition depends upon the whole-rock composition and oxidation state but with subsequent increases in temperature, there is a gradual reduction in Mn (Chinner 1960, Atherton 1964).

The Middleback Range garnets show considerable variation in Mn. In the three thin sections examined by electron microprobe, two (1961, 5-157) contained garnets with approximately 10% Mn whereas the third (5-1952) contained garnets with 2% Mn (analyses G1 to G5, Appendix II). This may be due to differences in Mn content of the parent rocks. No whole-rock analyses are available for these samples but the parent rock mineralogy is strikingly different. The high manganese garnets occurred in quartz-hornblende-biotite schists with quartz the predominant mineral and the ferromagnesian minerals other than biotite contained up to 0.5% Mn. By contrast, the low manganese garnets occurred in massive chlorite schist, and the chlorite mineral contained no detectable Mn. The low Mn content of this garnet may therefore be due to an inherently low content of Mn in the parent rock.

In most papers concerned with garnet compositions, the data is from typical amphibolite facies schist and gneiss assemblages. The high Mn garnets described above are in rocks which fit this description and may be compared with the results from other areas. The low Mn garnets are in a massive chlorite

schist of unknown origin and the chlorite has a high FeO content (32%) which is anomalous for garnet grade metamorphism. These low Mn garnets are therefore not included in the following comparison with compositions in other areas.

Several authors have collected garnet analyses from different areas and plotted various combinations of the chemical components against estimated grade. The results, as they may apply to the Middleback Range rocks are summarised in Table 5. There are obvious difficulties in this sort of comparison when the garnet composition is influenced by variables such as whole-rock composition which are not represented in the plots. The results are, however, a general indication of grade and all agree that the Middleback Range garnets represent an upper greenschist to lower amphibolite facies.

Miyashiro (1953) suggested that the Mn content of almandine may depend partly on pressure. This was refuted by Müller and Schneider (1971), who compared garnet compositions from Norway, North America and Japan and can find no correlation between Mn content and pressure. It seems likely that host rock composition plays a far greater part in controlling the Mn content than does pressure.

Muscovite

Muscovite is typical of greenschist facies metamorphism but can exist at much higher grades (Winkler 1967, Turner 1968). There are considerable changes in composition with

Table 5. Comparison of Middleback Range high Mn garnets with plotted data from other areas.

Author	Plot against estimates of regional metamorphic grade	Grade indicated for Middleback Ranges
Myashiro 1954	Atomic props. Fe^{++}, Mg^{++}, Mn^{++}	Upper greenschist
Sturt 1962	CaO + MnO/FeO + MgO wt.%	Upper greenschist (biotite zone)
Nandi 1967	CaO + MnO/FeO + MgO wt.%	Greenschist-amphibolite transition (garnet zone)
Müller and Schneider 1971	wt.% MnO	Lower Amphibolite (420°C to 460°C compared with Stavanger phyllites)

All the plots contain data from various parts of the world, mainly from pelitic assemblages.

metamorphic grade and fractionation of Fe and Mg between co-existing muscovite and biotite has possibilities as a geo-thermometer (Butler 1968), but no thin sections of Middleback Range material were suitable for microprobe analysis and no analyses are recorded in the literature.

Chloritoid and Staurolite

No chloritoid was observed in the sections available but the mineral is recorded from schists below iron-formations by Edwards (1954).

Chloritoid is typical of the greenschist facies and does not occur beyond the lowermost amphibolite facies grade. Its presence therefore suggests that the Middleback Range rocks did not progress beyond a lower amphibolite facies grade.

Staurolite is not recorded from the Middleback Range rocks. It forms in the lower amphibolite facies by reactions between chlorite, chloritoid and muscovite and its absence, together with the recorded presence of chloritoid, suggest that the grade did not surpass lower amphibolite facies (Winkler 1967).

Chlorite

Electron microprobe analysis was carried out on chlorite in one sample of chlorite-garnet schist from the Cook Gap area (5-1952, page 44 and Appendix II). The chlorite has a molecular Fe:Mg ratio of 1:9 and contains over 10% Al_2O_3 which indicates a

typical low grade metamorphic chlorite (Atherton 1964).

With increasing metamorphism, chlorites become richer in Mg at the expense of Fe (Green 1963). This increases the chlorite stability and Mg-rich chlorites can remain stable into the amphibolite facies, but chlorites with a high Fe:Mg ratio become unstable towards the top of the greenschist facies (Atherton 1964).

The atomic proportions of Fe and Mg in the analysed Middleback Range chlorite are plotted in Fig. 14, together with chlorite analyses from southern Japan (Banno 1964) and west-central Vermont (Zen 1960). The Japanese chlorites are from the glaucophane schist-epidote amphibolite transition facies and the epidote amphibolite facies and their variable FeMg contents demonstrate the difficulty of direct comparison. There is, however, a tendency for the higher grade chlorites to have lower Fe:Mg ratios and this is emphasised by the Vermont data which is for lower greenschist facies material. The Middleback Range analysis plots on precisely the same point as one of the low grade Vermont analyses and has a higher Fe:Mg ratio than any of the Japanese chlorites.

This strongly suggests that the Middleback Range chlorite would be unstable at grades higher than the upper greenschist facies.

The coexistence of high Fe chlorite and typical amphibolite grade minerals such as garnet and hornblende is therefore anomalous and the chlorite may be due to a retrograde phase of metamorphism.

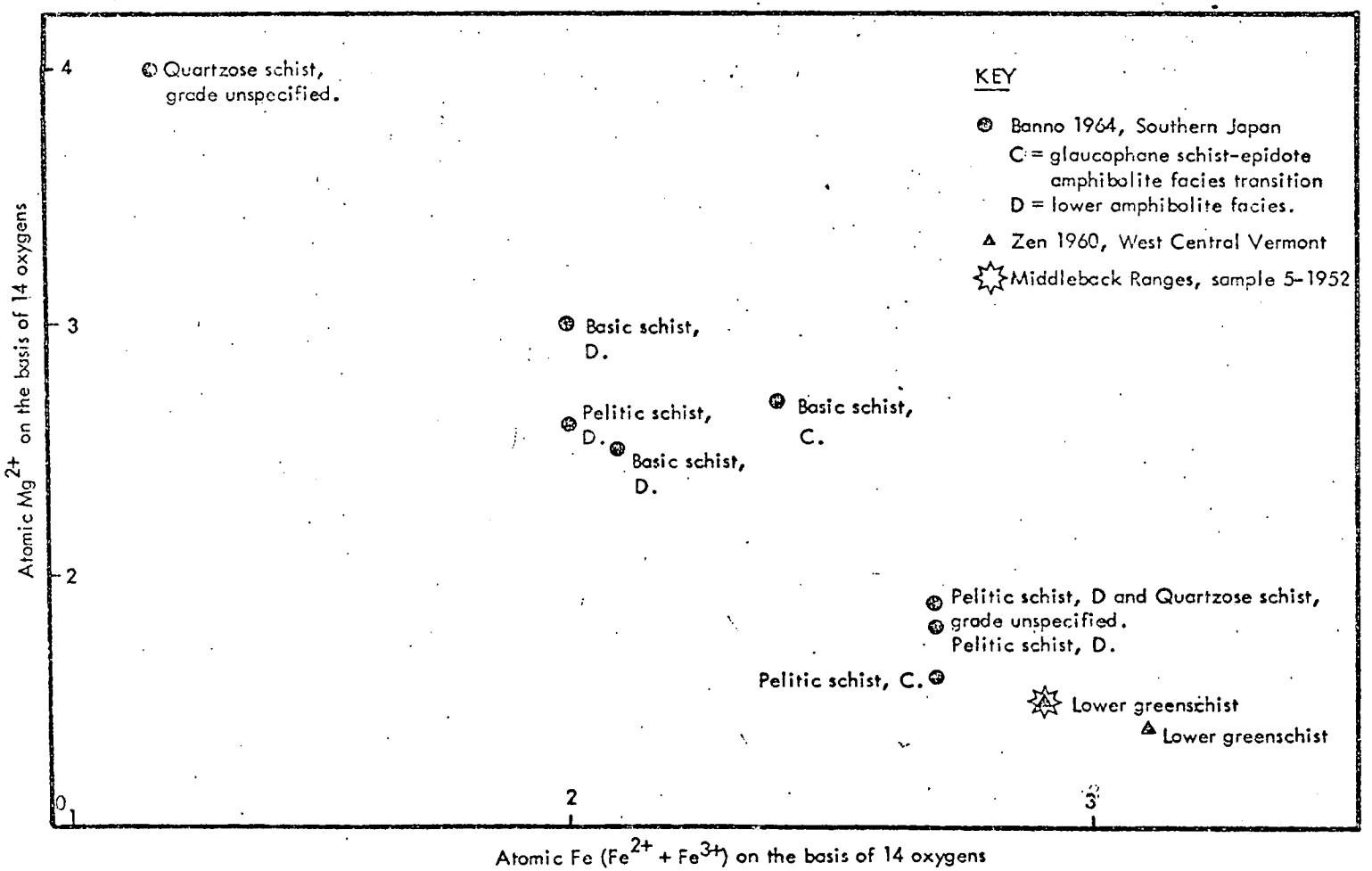

Fig. 14. Composition of chlorite in one sample of Cook Gap schist compared with chlorite compositions from Southern Japan and West Central Vermont.

There is limited support for this in the microtextures, where small chlorite patches appear in places to replace other ferromagnesian minerals. Furthermore, in the Iron Duke area, where there has definitely been low temperature hydrothermal activity, the schists are completely chloritised. Electron microprobe analyses from one sample of quartz-chlorite schist at Iron Duke (60-995, Appendix II) show that the chlorite has a variable Fe:Mg ratio and that some is iron rich and similar in composition to the Cook Gap chlorite discussed above.

4. Amphibolites

No detailed work was carried out on the amphibolites because it is impossible to tell which pre-date and which post-date the metamorphism without more extensive field work and careful sampling.

They are composed of hornblende, intermediate plagioclase, quartz and chlorite with minor ilmenite, sphene and magnetite. Optical determinations on the plagioclases, using Carlsbad and Albite twin extinction angles, indicate that they are andesines (Ab50-Ab60).

In the large intrusive basic mass at Iron Duke, the feldspar and hornblende crystals are in random orientation and appear to be igneous. The mineralogy of this mass conforms to that of a diorite as defined by Hatch, Wells and Wells (1961). Smaller bodies with the same mineral composition are found in other parts of the ranges and in places are definitely cross-cutting the iron-formations.

5. Summary of metamorphic grade

Comparison with the North Michigan metamorphic assemblages indicates that the Middleback Group rocks reached the garnet zone of regional metamorphism. This is equivalent to the upper part of the greenschist facies and the lower part of the amphibolite facies.

Grades indicated by mineral assemblages and individual minerals support this as shown in Table 6. The minimum grade indicated for the rocks, excluding the chlorite assemblages, is upper greenschist facies, and the maximum possible grade is middle to upper amphibolite facies.

An indication of the pressure-temperature conditions is shown in Fig. 15. The possible field for the Middleback Group covers a wide area because of the difficulty in estimating pressure. Turner's (1968) boundaries of the greenschist and amphibolite facies are also shown and it is clear that over the most likely pressure range, from 2 kb to 6 kb, the Middleback Groups may be classified as lower amphibolite facies.

The presence of iron rich chlorite indicates that there has been a period of retrograde metamorphism, resulting in chloritisation in the schist bands.

Table 6. Summary of metamorphic grades indicated by mineral assemblages and individual minerals

Assemblage or mineral	Minimum grade indicated	Maximum grade indicated	Comments
Grunerite	Upper greenschist 300°C		
Tremolite	Upper greenschist 300°C		
Quartz-tremolite-calcite		Middle to upper amphibolite 600°C	
Hornblende	Lower amphibolite		Composition suggests amphibolite facies.
Biotite	Upper greenschist 300°C		
Plagioclase	Lower amphibolite		
Garnet	Upper greenschist		Composition suggests upper greenschist to lower amphibolite facies
Chloritoid		Lower amphibolite	
Staurolite (absence)		Lower amphibolite	
Chlorite (Fe rich)		Upper greenschist	Probably retrograde

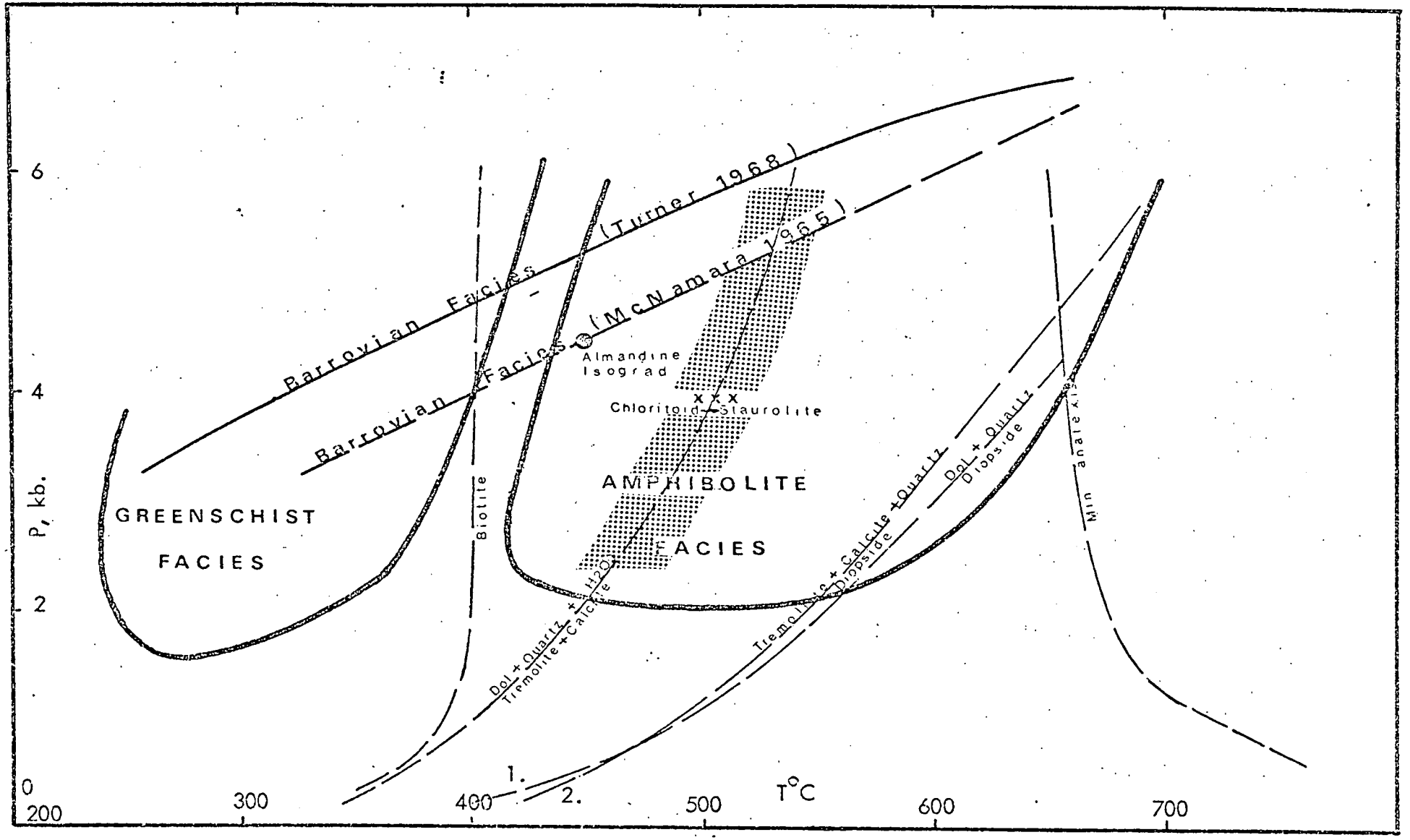

Fig. 15. Estimated pressure-temperature conditions for regional metamorphism of the Middleback Group, shown by stippled area. Constructed from diagrams and data in Turner 1968, curve 1 extrapolated linearly beyond 1.75 kb by the author. Curve for minimum anatexis from Winkler 1967. For curve 1, $P = P_{H_2O} = P_{CO_2}$, for curve 2, $P = P_{CO_2}$, and for all other curves, $P = P_{H_2O}$.

D. CONCLUSIONS FOR SECTION I

1. The Middleback Ranges are part of the South Australian Precambrian shield and occur on the north-east margin of the Gawler Block.

2. The Middleback Range area has remained essentially stable since the late Proterozoic and there has been almost complete peneplanation.

3. The Middleback Group have undergone regional metamorphism to lower amphibolite facies, at temperatures in the order of 450°C to 550°C and pressures between 2 kb and 6 kb. Regional metamorphism has affected the rock types in the following ways:

   (a) All the rock types have developed fine-grained, even microtextures, becoming schistose when acicular or platy minerals are present.

   (b) Amphiboles have formed within the iron-formations and garnets, amphiboles and micas developed in the schist units. Massive carbonate units simply recrystallised.

4. During regional metamorphism, components within the iron-formations were essentially immobile, except for H_2O and CO_2, and individual layers behaved as closed chemical systems.

5. The present iron-formation layering reflects the original sedimentary layering.

6. The main period of regional metamorphism was followed by a phase of retrograde metamorphism which produced chlorite in the schists.

SECTION II: THE GEOLOGY OF IRON DUKE

A. GENERAL GEOLOGY

1. South Middleback Range

Iron Duke is at the extreme southern tip of the South Middleback Range (Fig.16). The southern half of the range consists of two narrow iron-formation ridges; on the west the Iron Duke - Iron Duchess ridge and on the east the Cook Range. These are separated by a steep sided valley known as Death Adder Gully. In the northern half of the range the valley swings eastwards into Cook Gap which separates Cook Range from the hill mass of Iron Chieftain.

The ridges and hills are formed of iron-formations whereas Death Adder Gully and Cook Gap are deep cuttings into schists. Granitic schists and gneisses outcrop below the iron-formations on the east and west flanks of the range.

The iron-formations are strongly folded about north-south axes, which are frequently arranged en echelon and fade along the axis length, so that synforms may pass along strike into antiforms. A gentle cross fold causes a south pitch in the northern two thirds of the range and a north pitch in the southern one third (Fig. 16). Cook Range has an overall synformal structure, as does the Iron Duke - Iron Duchess ridge. The Iron Knight iron-formations dip eastwards and the Iron Chieftain mass is strongly folded with a steady south pitch of 15° - 20°.

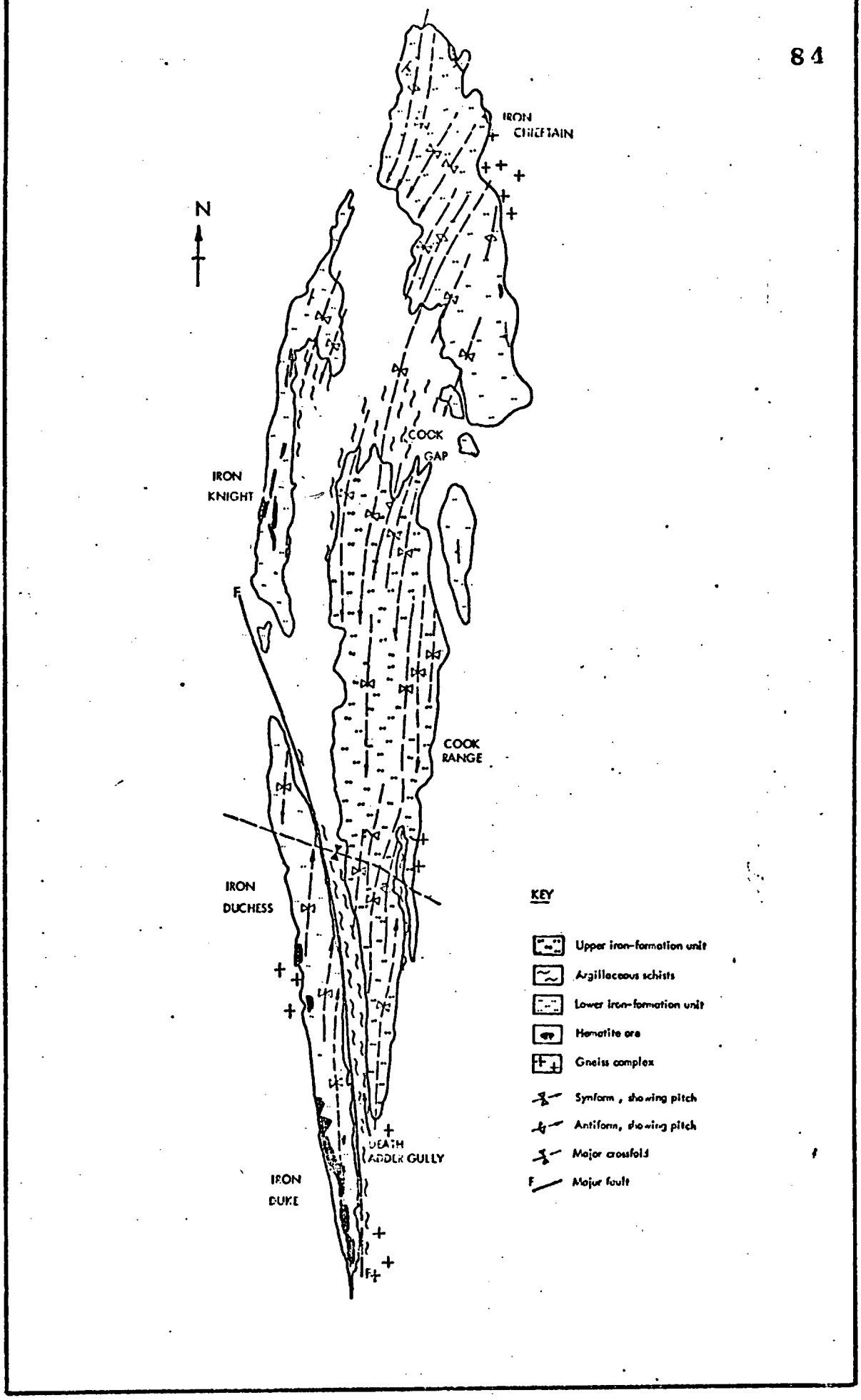

Fig. 16. Geological plan of the South Middleback Range.
From Miles 1954, modified by the author.

Miles (1954) interpreted the stratigraphy as two iron-formation units separated by the Cook Gap schists. The lower iron-formation forms Iron Duke, Iron Duchess, Iron Knight and Iron Chieftain and the upper iron-formation forms Cook Range. These are folded into a canoe shape with part of the east limb missing (Fig. 17A). This is supported by the broad outcrop pattern and by two drillholes put down by the Geological Survey, one in Cook Gap and the other in Death Adder Gully on the east side of Iron Knight (Fig. 16). Both drillholes were collared in Cook Gap schist but intersected iron-formations below the schists at depths indicated by the regional dip and pitch.

The southern half of the range does not clearly conform to the interpretation of two iron-formation units. Iron Duke-Duchess and Cook Range are both basically synformal structures and the few exposures of schist in Death Adder Gully dip west below Iron Duke and east below Cook Range in an antiformal structure. Miles (1954) proposed a tight antiform on the east side of Iron Duke (Fig. 17B) to bring the iron-formations below the schists but this is not supported by recent exposures in drill roads and tunnels at Iron Duke. Catley (pers. Comm.) proposed that there is only one iron-formation unit which is underlain by the Cook Gap schists. This concept applies more satisfactorily to the Iron Duke area but less well in the northern half of the range.

The authors' interpretation of the stratigraphy and structure is shown in Figs. 17b and 21. A major high angle

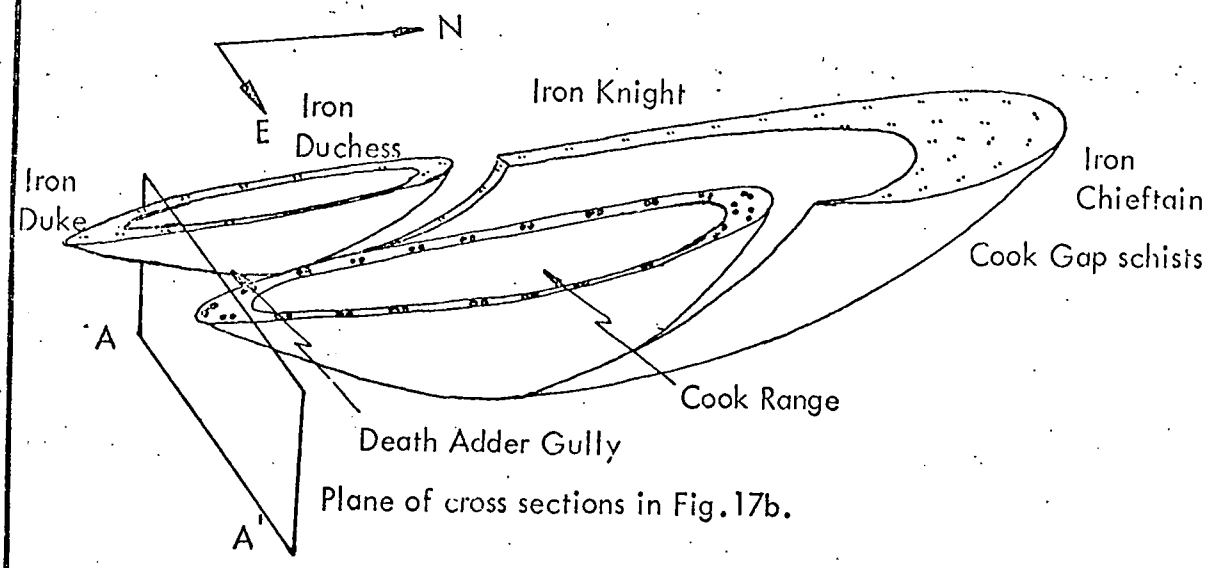

a. Simplified structure of the South Middleback Range, showing the canoe shape. Note that part of the east limb of the lower iron-formation is missing, as shown in the diagram. Author's interpretation, based on Miles (1954). Not to scale.

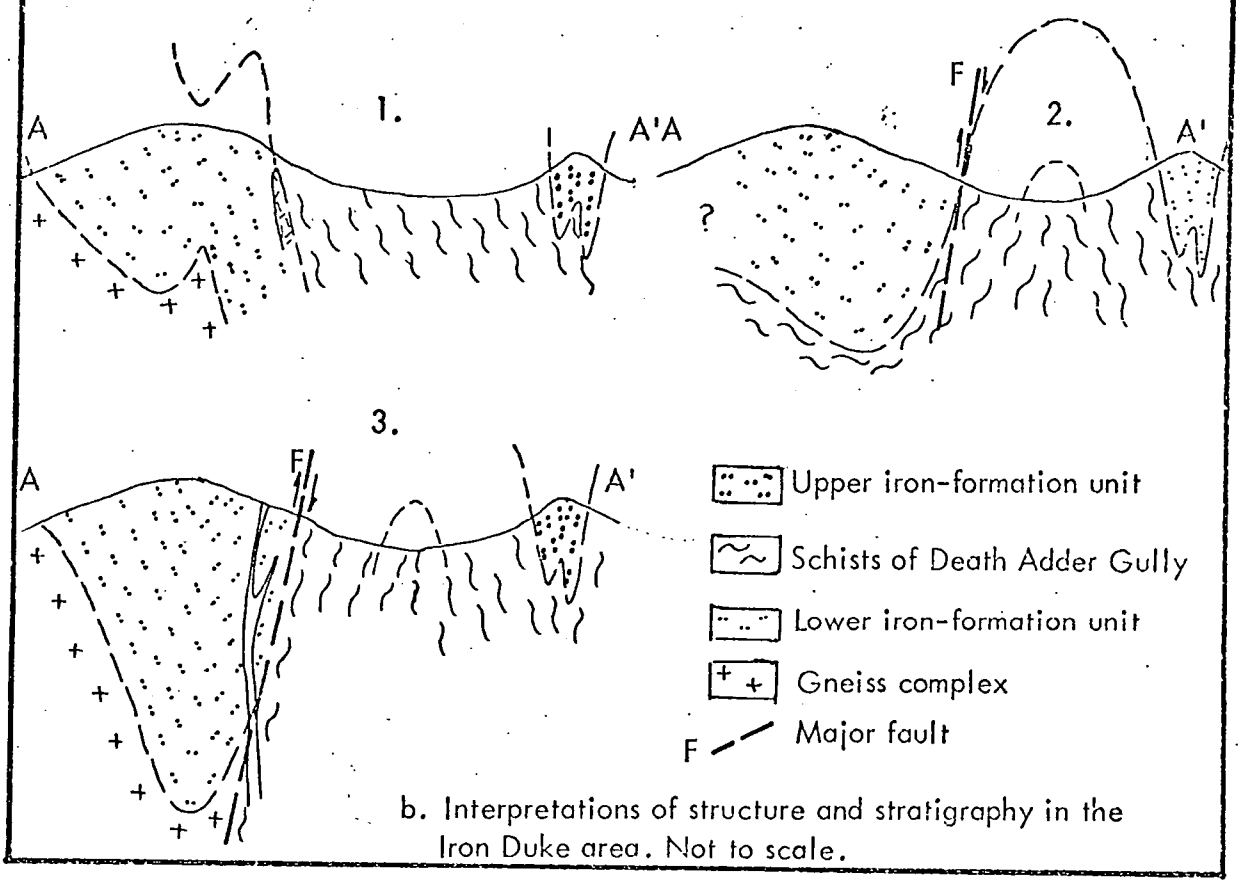

b. Interpretations of structure and stratigraphy in the Iron Duke area. Not to scale.

Fig. 17. Interpretations of the structure and stratigraphy of the South Middleback Range.

In b, Interpretation 1- based on Miles(1954), with two iron-formation units separated by the schists of Death Adder Gully.

Interpretation 2- based on a suggestion by Catley (pers. comm.), with a single iron-formation unit underlain by the schists of Death Adder Gully

Interpretation 3- author's interpretation, with two iron-formation units separated by the schists of Death Adder Gully.

reverse fault extends along the east side of Iron Duke and Iron Duchess, moving the Iron Duke-Duchess iron-formations upwards and to the south. This explains the juxtaposition of a synform in the lower iron-formation against an antiform in the stratigraphically higher schists. The concept of two iron-formation units separated by the Cook Gap schist is retained. The evidence for this fault is discussed in the section on Iron Duke structures.

2. Iron Duke

Iron Duke is the southern one third of the Iron Duke-Duchess ridge (Fig.18). The division between Iron Duke and Iron Duchess is arbitrary and is taken in company work as an east-west mapping grid line to the north of the main hematite orebody, designated 00 for reference coordinates. The main vegetation is low, stunted scrub with occasional trees but exposure is moderate to poor because of extensive surface rubble and deep weathering in the schists and amphibolites.

Hematite outcrops along the ridge crest south of 4000S (Fig.18). North of this, iron-formation occupies the centre of the ridge and hematite outcrops on the western flanks. Below the hematite and iron-formations on both sides are scattered outcrops of schist and weathered amphibolite. Granitic schists outcrop on each side of the ridge in the extreme south-east and south-west.

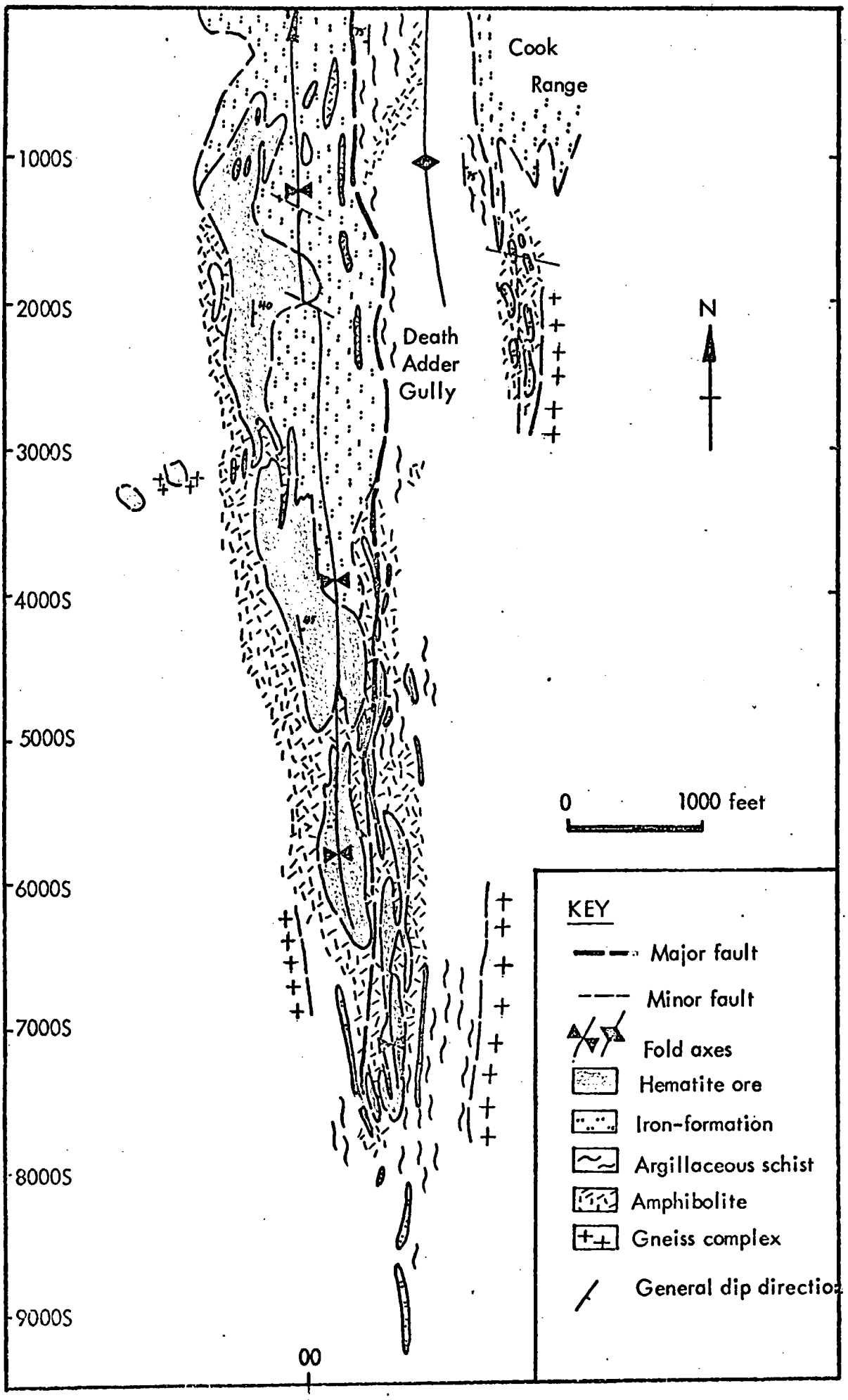

Fig. 18. Generalised plan of the geology of Iron Duke, based on field mapping by Catley, with some data from Miles (1954), and modified in places by the author on the basis of field observation and interpretation.

A well marked synformal axis extends along the full length of Iron Duke, coinciding with the ridge crest. It pitches steadily to the north at 10° - 15° and is dislocated in several places by small cross faults. Drilling and tunnelling on the east side have established the presence of a major strike fault separating the iron-formations from the schists in Death Adder Gully.

Drilling has shown that the hematite passes down pitch and down dip into magnetite-hematite-carbonate ore. This occurs as a long, torpedo shaped body which extends along almost the full length of Iron Duke and at no point is less than 300 feet below the surface. It is surrounded by a zone rich in talc.

The magnetite-hematite-carbonate has brecciated and coarsely crystalline carbonate structures which are strikingly different from the even, fine grained metamorphic structures characteristic of other Middleback Group rocks. It is believed to have been affected by, or produced by, hydrothermal activity subsequent to the regional metamorphism.

B. PREVIOUS WORK

Owing to the economic interest of the orebodies, extensive work has been carried out in the area by The Broken Hill Proprietary Company Ltd. and, to a much lesser extent, by the Geological Survey of South Australia. The ores are now penetrated by over 100,000' of drilling and nearly 2000' of exploratory tunnelling and winzing. Most of the company work is unpublished but all the data was made available to the author. In the following summary of previous work, B.H.P. refers to The Broken Hill Proprietary Company Ltd.:

1935-1936 Two tunnels were driven into the hematite ore by the company.

1938-1940 One additional tunnel was driven into the hematite ore. A B.H.P. geological field party mapped the area at a scale of 1" = 100' and established that the hematite ore occurs in the hinge area and west limb of a north pitching syncline. The results were included in an unpublished company report which covered the whole Middleback Range area (Rudd 1940).

1948-1954 A Geological Survey field party mapped the area at scales of 1" = 100' and 1" = 200' and the results were included in Bulletin No.33 by K.R. Miles. The structure was interpreted as a fairly open syncline passing into a tighter anticline on the eastern side (Fig. 17b). The hematite ore was considered to pass down dip and down pitch into iron-formation.

1955-1964 Extensive drilling by B.H.P. broadly outlined the hematite orebody and in 1957, the magnetite-hematite-carbonate ore was discovered below 300' of iron-formation a little way to the north of the hematite orebody.

The area was re-mapped at a scale of 1" = 100' and the geology re-interpreted by D.E. Catley, who published the main conclusions in 1963. The structure was considered to be open syncline, partly cut through on the east side by a major fault (Fig. 17b). Hematite ore was interpreted as passing down dip into iron-formation, mostly overlying the magnetite-hematite-carbonate ore which is treated as a sedimentary unit. The amphibolites were regarded as conformable sheets and the interpreted sequence included thick interlayered argillaceous schist bands.

Considerable petrological work was carried out during this period by S. Whitehead and D. Burger, with particular emphasis on the magnetite-hematite-carbonate and associated talcose rocks. The results are summarised in two papers, Whitehead (1962) and Burger (1963) but a wealth of detail is available in unpublished company petrological reports. These are acknowledged as necessary in the text. The most important conclusion was that the magnetite-hematite-carbonate was formed by carbonate metasomatism of siliceous iron-formation.

Reports during this period were fragmentary and no comprehensive report on the geology or petrology was written.

1964-1967 Further deep drilling and tunnelling were carried out to outline the magnetite-hematite-carbonate and talcose rocks. The author was in charge of these programmes and re-interpreted the geology, with a tighter, deep and somewhat asymmetrical synform, terminated on the east side by a high angle reverse fault (Fig. 17b). The hematite ore is regarded as passing directly down pitch and down dip into magnetite-hematite-carbonate and the main amphibolites are interpreted as cross cutting dykes.

The author also carried out extensive thin section, carbonate staining and X-ray diffraction work in an attempt to correlate the different rock types and to elucidate the origins of the ores. The results were used to interprete the geology as drilling and tunnelling progressed.

Two papers concerning Iron Duke were published during this period. Owen and Whitehead (1965), in a summary of Middleback Range geology, described the geology of Iron Duke and included a cross section showing a deep synform with cross cutting basic intrusives. Ashworth (1965) described the Iron Duke geology in rather more detail and the cross section included is very similar to Fig. 20g of this thesis.

1969-1972 The author continued work on the Iron Duke rocks at Durham and a comprehensive account of Iron Duke geology was submitted to the company in 1970.

The work at Durham includes re-examination of all

available thin sections and additional polished sections, major and trace element analysis by XRF on 138 whole-rock samples, X-ray diffraction, fluid inclusion studies and use of the electron microprobe to determine the precise ore mineralogy.

C. STRATIGRAPHY AND STRUCTURE

1. Stratigraphy

Drilling has established the sequence of lithologies shown in Table 7. There is no evidence to show whether this is the true stratigraphic sequence or whether the rocks are inverted and use of terms such as basal carbonate expresses the relative position within the lithological sequence.

The hematite ore and magnetite-hematite-carbonate are not strictly stratigraphic in the sense of proven sedimentary origin but they appear, to the author, to occur at a particular stratigraphic position and are therefore included in Table 7.

The lowest unit is a relatively thin band of quartz-biotite and quartz-chlorite schists with a little lean iron-formation and carbonate layers in the upper part. The unit does not outcrop but was intersected in drillholes on the west side of Iron Duke (DP 30, Fig. 20g). Its relationship to the underlying granitic schists is not known.

Tremolite rich iron-formations occur above the schists. They are thinly bedded, with some interlayered schist bands, and they do not outcrop but were intersected by drillhole DDH 57 (Fig. 20g).

A carbonate unit of variable thickness occurs above

Table 7. Stratigraphy of Iron Duke

Unit	Thickness	Major components	Comments
Iron-formation	400'+	Si, Fe	
Talc-quartz schist= grunerite-quartz schist	150'	Si, Fe, Mg	
Hematite ore=magnetite-hematite-carbonate	200' to 400'	Fe, Ca, Mg	ORES occur at this level
Chloritised basic intrusive	Nil to 100'		
Thin chlorite schist, talc schist, carbonate	20' to 100'	Si, Fe, Mg, Ca, Al, S	
Carbonate unit	50' to 200'	Ca, Mg	BASAL CARBONATE
Iron-formation	100'	Si, Fe, Ca, Mg	Thickness uncertain
Quartz-biotite schist	Unknown possibly 100'		

GNEISSIC BASEMENT

Note: (a) The relationship of the gneissic basement to the iron-formation sequence is not known.

(b) The iron-formation sequence shown above is part of the lower of the two major iron-formation units in the South Middleback Range.

these iron-formations. It outcrops only once, at 7700S/400E (Fig. 18), in outcrops too small to be shown on the plan, but it is consistently intersected in drillholes and is the most useful marker unit in the sequence. The unit appears to thicken in the centre of the synform and to thin on the limbs. It has been given various names in the past but is most conveniently referred to as the basal carbonate unit.

Thin layers of chlorite schist, and talc schist with irregular carbonate patches are present above the basal carbonate. These include bands rich in pyrite and other, thin bands with graphite. Iron sulphides are found at this stratigraphic level throughout Iron Duke and in drillholes at Iron Queen in the North Middleback Range. They are probably sedimentary in origin.

A chlorite schist or chloritised basic intrusive consistently occurs at the base of the magnetite-hematite-carbonate. It appears to be interlayered with the main units and is probably a concordant sill.

Hematite ore and magnetite-hematite-carbonate occur above the chloritised intrusive, passing laterally into each other. In other parts of the Middleback Range, this stratigraphic level is occupied by iron-formation and it may be regarded as the lower part of the main iron-formation sequence. Neither the hematite ore nor the magnetite-hematite-carbonate are strictly confined to one band but they broadly occupy a

specific stratigraphic level at the base of the main iron-formation sequence.

Above the ores is a band of siliceous talc schist. The talc is due to hydrothermal alteration but the original rock type is thought to be a band of grunerite schist which was intersected by drillholes in iron-formations to the north (DDH 62, Iron Duchess). This is regarded as a stratigraphic unit.

The main iron-formation sequence occurs above the talc schists and consists of a thick sequence of amphibole rich iron-formations with thin layers of argillaceous schist.

The most significant feature of the stratigraphy is the marked change of lithology above the basal carbonate. Below this level the sedimentary types are varied, with interlayered schists, carbonates and thin iron-formations and overlying these is the thick basal carbonate. This part of the sequence is characterised by carbonate and argillaceous sedimentary units. Above the basal carbonate, and disregarding the ores, the sequence is predominantly siliceous with thin argillaceous bands and negligible carbonate.

2. Structure

(a) Folding

Surface mapping shows a clearly defined synform axis extending the full length of the Iron Duke ridge, coincident

with the ridge crest. Outcrops and tunnel intersections on either side of the ridge show a steady inward dip. Small scale folds and rodding on the surfaces of iron-formation layers both have a uniform pitch to the north of 10° - 20°. The major structure is therefore well established as a north pitching syncline.

Rudd (1940) and Miles (1954) both interpreted the syncline as a fairly open fold and Miles included a tight anticline on the east side. Field evidence does not support the presence of the anticline; the great majority of dips on the eastern slope are steeply to the west, as are the dips in Tunnels Nos. 3 and 4 (Figs. 20c, 20g). Tunnel No.4 was driven subsequent to Miles's work and his interpretation did not include this information.

Catley (1963), on the basis of detailed field mapping and considerable drilling, retained a fairly open fold style which became tighter in places throughout its length.

Jones (1968) recognised three fold groups:

F1 Rare, isoclinal microfolds with axes aligned north-south. These are considered by Jones to be remnants of pre-existing sedimentary layering but by the author to be sedimentary slump structures.

F2 Major and minor folds, varying in scale from micro-structures to the main synformal structure. The fold axes are aligned north-south with a gentle pitch to

the north and the axial planes are approximately vertical.

F3 Conjugate folds and kink bands with axial planes near vertical and striking at 60° or 120° from true north.

Minor folding has played an important part in interpretations of the major structure, particularly prior to drilling when minor structures were the only indications of fold style. The best exposures are not on Iron Duke but to the north and east on Iron Duchess and Cook Range, where outcrops show small folds varying in scale from a few millimetres to 10 or 15 metres across. There is considerable variety in style as shown by Figs. 19a, b, and the more open, concentric folds often outcrop giving the impression that they are the dominant fold style. The minor folds have generally been regarded as small scale replicas of the major structure and Miles's interpretation of the main Iron Duke synform is strikingly similar to the fold shown in Fig. 19a.

Drilling has shown that this direct comparison is deceptive; the main synform is tighter and more lobate in form, with thickening in the axial region. Minor folds of this type are rarely seen at the surface, but Fig. 19b shows a small fold exposed in Tunnel No.1 which has a form similar to that of the main structure.

The major synform is best described in three parts, south of 4200S, north of 4200S and section 1000S:

Fig. 19a. Open concentric syncline in siliceous iron-formation seen on a cross cutting joint.
Iron Duke, 00/190W.

Fig. 19b. Syncline in weathered iron-formation in the south wall of Tunnel No. 1 (approx. 530'). Note the pronounced thickening of beds in the nose of the fold.

South of 4200S (Figs. 18, 20a, 20b)

Hematite ore outcrops in the hinge area of the synform. The structure pitches northwards at 10° - 20° and this controls the disposition of the outcrops. Surface dips in hematite near the fold axis suggest that the fold is symmetrical but the outcrop pattern of a thin band of iron-formation below the hematite suggests a slight degree of asymmetry with the east limb steeper than the west. The basal carbonate unit was consistently intersected in drillholes with the depth of intersection increasing to the north, and a small outcrop at the very southern tip of the range confirms that the fold closes to the south.

Between 5400S and 4000S a large intrusive mass of diorite penetrates the synform and obscures the structure.

4200S-1000S (Figs. 20e to 20f)

Hematite ore outcrops on the western flank of the ridge and iron-formation occupies the crest and outcrops sporadically on the eastern slopes. Drilling shows that the synform deepens steadily due to the north pitch and becomes increasingly asymmetric.

The west limb has a uniform dip of about 55°, increasing slightly in steepness to the north. This is well established by consistent drillhole intersections in the basal carbonate unit, as for example DP 14 and DDH 47 in Fig. 20e.

Fig. 20a - 20g. Geological cross-sections of Iron Duke

KEY


Siliceous iron-formations


Hematite ore


Talc zone rocks


Magnetite-hematite-carbonate ore


Basal carbonate unit


Amphibolite


Argillaceous schists of Death Adder Gully


Pyrite


Fault, with direction of movement shown by arrows


Drillhole

SCALE approximately 1 inch equals 300 feet.

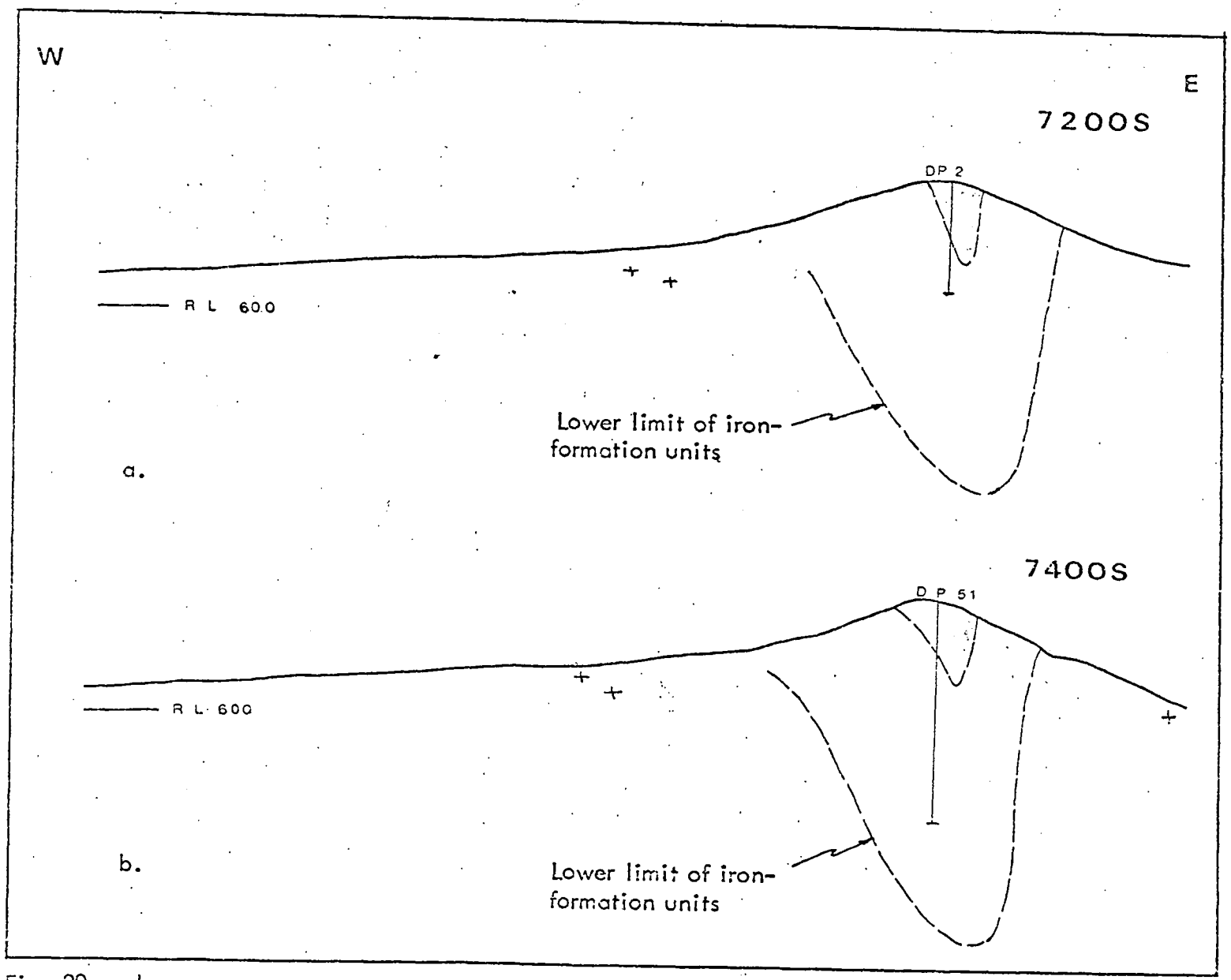
W
E
7200S
DP 2
R L 600
Lower limit of iron-formation units
a.
7400S
D P 51
R L 600
b.
Lower limit of iron-formation units

Fig. 20. a, b.

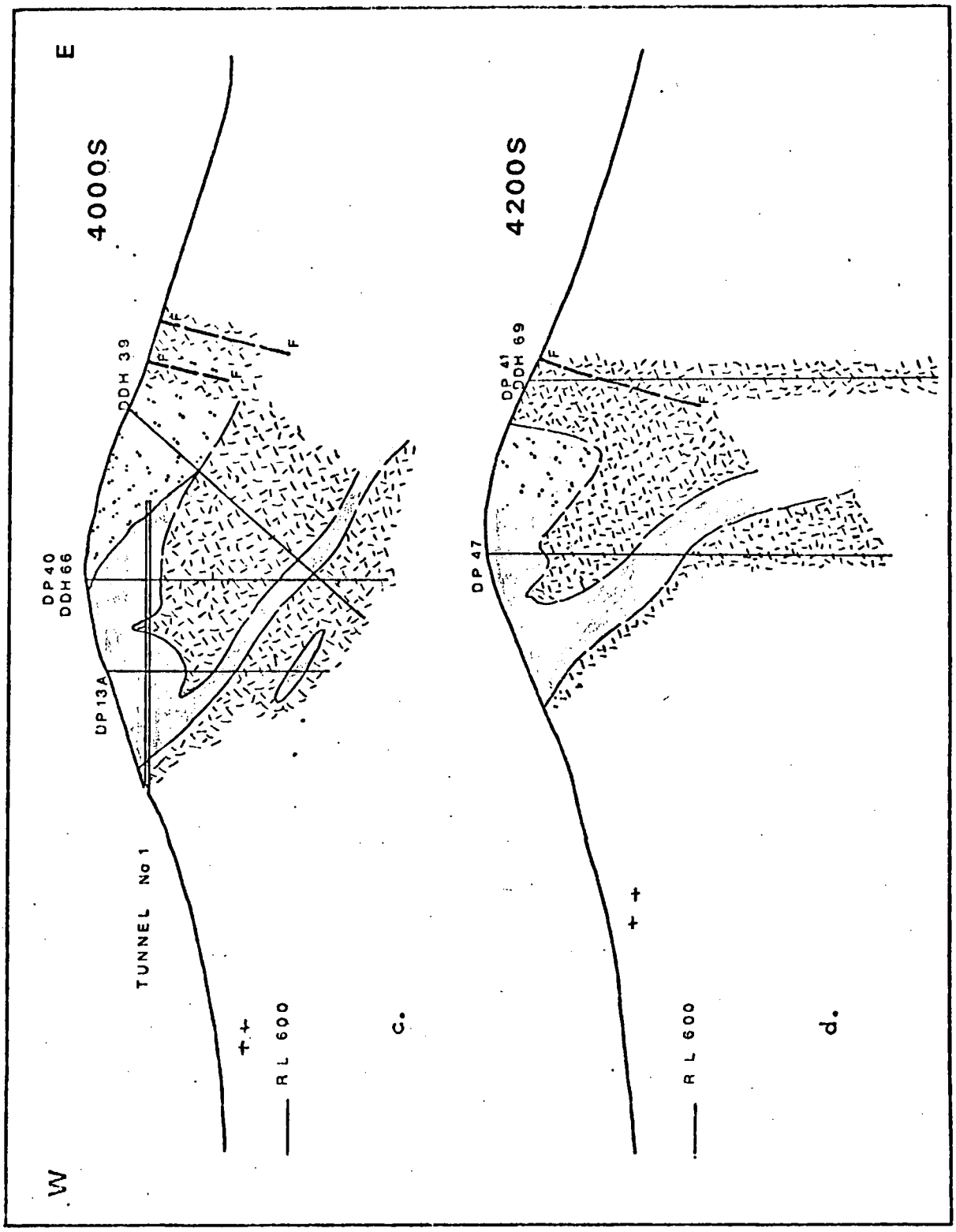
W
E
4000S
4200S
DDH 39
DP40
DDH 66
DP13A
TUNNEL No 1
DP 41
DDH 69
DP 47
F
R L 600
c.
d.

Fig. 20. c,d.

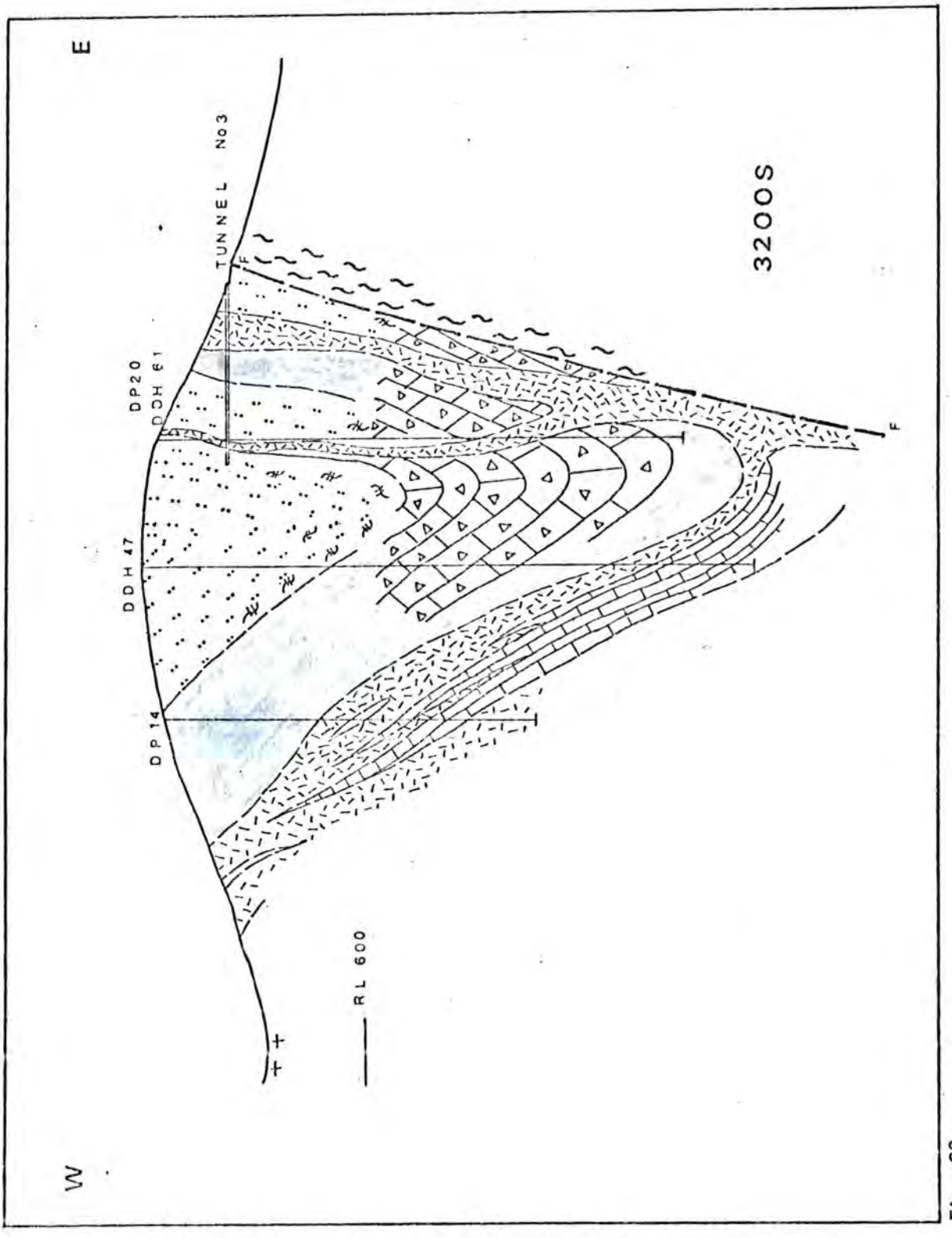

Fig. 20e.

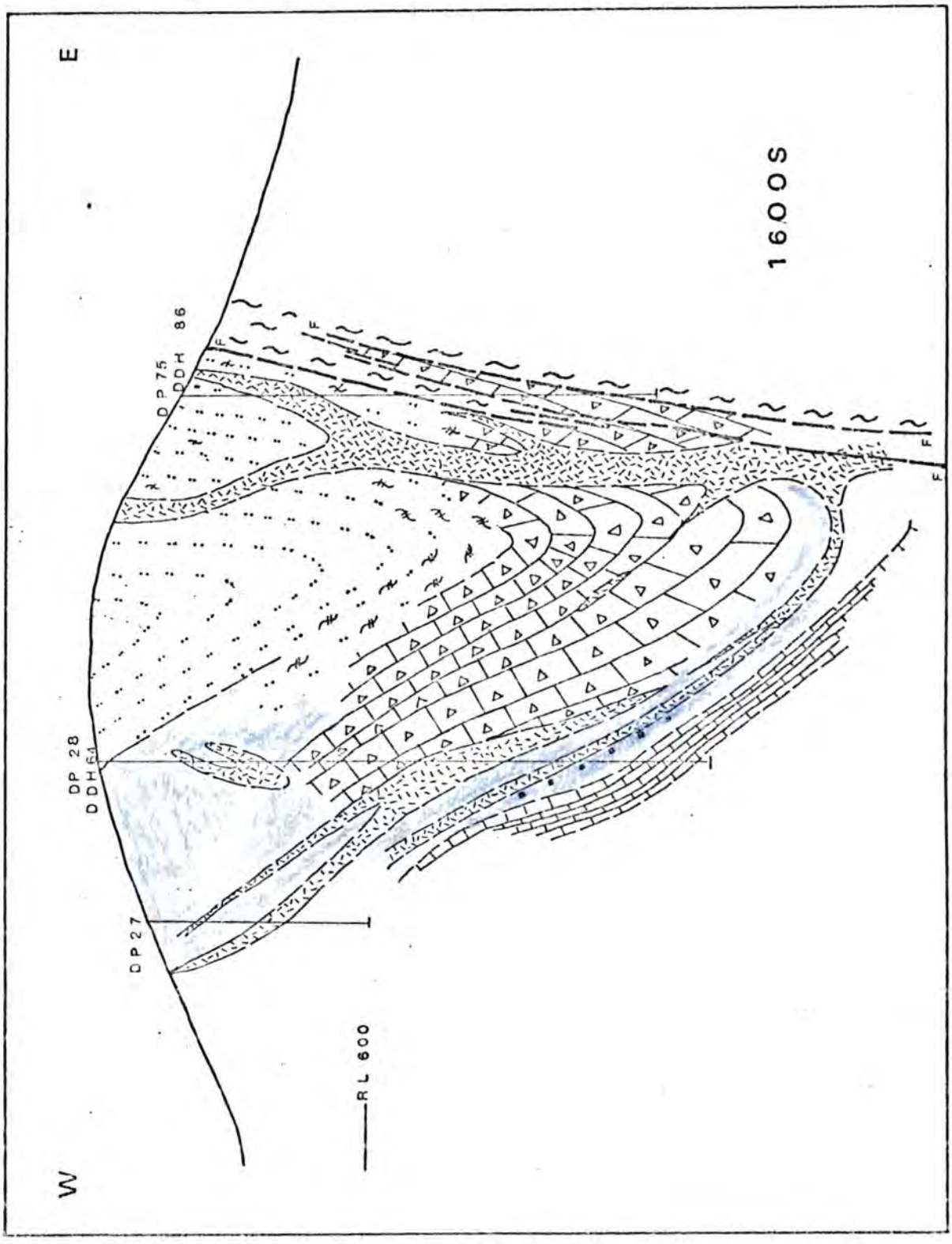

Fig. 20f.

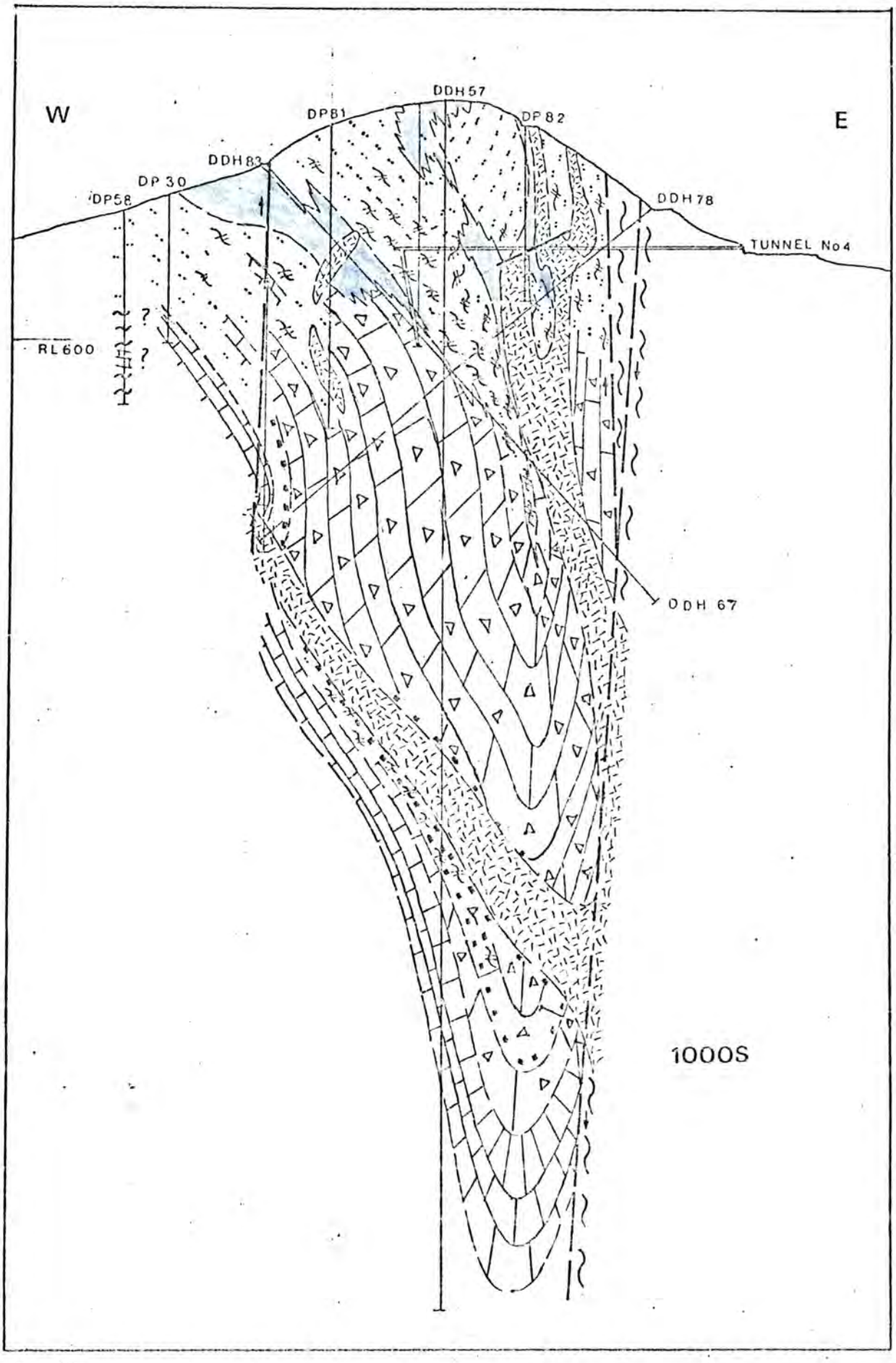
W
E
DDH57
DP81
DP82
DDH83
DP 30
DP58
DDH78
TUNNEL No4
RL600
DDH 67
1000S

Fig. 20g.

The east limb is more complex and the very presence of an east limb is open to question because the basal carbonate unit does not outcrop, nor does it appear in any drillholes or tunnels. The strongest support for an east limb is on section 3200S (Fig. 20e), where exposures on the east side of the ridge dip steeply to the west and these dips are confirmed in Tunnel No.3. The absence of the basal carbonate shows, therefore, that part of the east limb is missing.

1000S (Fig. 20g)

1000S is the best drilled section at Iron Duke and, partly for this reason, is the most difficult to interpret.

Iron-formation occupies most of the ridge and the hematite outcrop on the west flank is considerably reduced. This elimination of the hematite is quite sudden, taking place about 100' south of the section and the ore passes along strike into iron-formation. Immediately to the north of the section the ridge narrows into a low saddle which suggests that there may be faulting in the area.

The general inclination of the west limb is established by three drillhole intersections, DDH83, DDH78 and DDH57. The limb dips rather more steeply than to the south and is faulted as shown by brecciation in DDH83 and at the surface. The inclination and full affect of this faulting is not clear.

The east limb is shown to be present by westerly dips in outcrop and in Tunnel No.4. There is no sign of the basal carbonate unit and, again, part of the east limb is missing.

The synform axis passes approximately through the collar of DDH57 at the surface, and in Tunnel No.4 is within 100' of the western end. It therefore has a steep western dip in this upper part which conflicts with the general interpretation to the south and with the information at lower levels. DDH 78 and DDH57 suggest that the basal carbonate is inclined to the east and extrapolation from drillholes further south supports this, making it very unlikely that the fold closes to the west of DDH57 at depth. The axis must therefore shift from the west side of DDH57 in the upper levels to the east side at depth. Dips in the basal carbonate intersection of DDH57 vary from 20° to 70° and this could indicate the proximity of the main fold axis or simply be due to minor folding.

Movement of the synform axis is also indicated by the disposition of a talc-magnetite schist layer which overlies the magnetite-hematite-carbonate ore and is considered to be a stratigraphic unit. It is intersected by four drillholes, DDH's 67, 57, 78, DP83, and Tunnel No.4 and is unusually thick in the area around the western end of Tunnel No.4. Below Tunnel No.4, it extends down dip to the east, indicating that the synform axis is to the east of DDH57.

This movement of the fold axis could be due to faulting or flexuring. The change of direction must take place fairly suddenly, within 100' below Tunnel No.4, if the interpretation of the schist as a stratigraphic unit is correct. The thickening of the talc schist could be explained by tight isoclinal folding in the axial region of the main synform but there is no evidence for this in Tunnel No.4, where the dip is to the west throughout most of the tunnel. Small scale folds in the talc have steeply dipping axial planes which strike north-south, parallel to the main synform axis, and there are no indications of complex folding although this could, to some extent be obscured by the effects of hydrothermal activity. There is a good deal of faulting in Tunnel No.4, one large fault being inclined at 30° to the west. Movement along a plane of this orientation would shift the fault axis at a point about 60' below Tunnel No.4 and the fault would pass through Winze No.4. There is intense deformation in Winze No.4 but no clear major fault plane.

It is clear from the above discussion that the structure in the centre of the synform at 1000S is complex and cannot, as yet, be adequately explained.

Future drilling to the north of 1000S may clarify the structure.

The magnetite-hematite-carbonate on section 1000S appears to pass up the western limb into interlayered carbonates

and talcose iron-formations intersected by DP81 and DDH83. The uncertainty of the structure and the fact that DP81 is projected 30' from the south in a faulted area makes the precise relationship uncertain.

The eastern contact with the schists of Death Adder Gully is established as essentially vertical by drillholes DDH67, DDH78 and Tunnel No.4.

North of 1000S there is relatively little information. A deep drillhole in the centre of the ridge at 00 penetrated iron-formations to about 250' followed by 1000' of siliceous magnetite-talc schists with two thick layers of magnetite-hematite-carbonate. The synform axis continues to the north and the basic structure appears to be similar to Iron Duke.

(b) Strike-faulting

It has already been shown that part of the east limb of the synform is missing. This is interpreted as due to a high angle reverse fault extending along the east side of Iron Duke between the iron-formations and the schists in Death Adder Gully. The evidence for such a fault is discussed below.

A strike fault was mapped by Catley (1964) on the east side of Iron Duke in the contact area between iron-formation and schist. It is marked in part by a line of broken iron-formation

outcrops. Catley regarded it as a reverse fault but placed it within the iron-formations rather than at the contact with schist.

The lack of basal carbonate in the east limb must be due to flowage or faulting. Drilling in the east limb has established that the contact between the iron-formations and the schists of Death Adder Gully is steeply west dipping to vertical and is sharp. In Tunnel No.4, the contact is obscured by a thick chloritised basic intrusive but at approximately 300' from the portal there is a 100' wide zone of chloritic quartzite which looks conglomeratic with quartzite fragments cemented by chlorite and quartz. The fragments tend to be elongate and aligned north-south. The structure of the rock is difficult to ascertain but it appears to be crushed and breaks easily in hand specimen. There is a well developed lineation due to the chlorite, which is aligned north-south and inclined gently to the north, parallel to the regional trend. On the west side of this zone the rock is intermixed with lean iron-formation and there is a 7' wide strip of massive green chlorite rock which dips vertically. The whole zone is interpreted as a crush belt between the iron-formations and the schists.

This is supported by numerous narrow fault zones in the first 500' of Tunnel No.4 (Fig. 20g). Most of these are vertical to steeply west dipping but the sense of movement is obscured by the lack of distinct marker units and the presence

of hydrothermal magnetite and sometimes carbonate.

A faulted contact is also supported by drillhole DDH86 (Fig. 20f) which intersected alternating slivers of quartz-chlorite schist and magnetite-hematite-carbonate with brecciation in both rock types.

A fault bringing together the iron-formations of Iron Duke and the schists of Death Adder Gully could not be a normal fault as the schists are stratigraphically higher than the iron-formations. A reverse fault would satisfy the geometric requirements, at a high angle as indicated by the drilling, and would result in the iron-formations moving upwards, overriding the schists to the east. There is a little support for this in Winze No.4, where a low angled thrust in chlorite-hematite strikes north-east and is inclined at 10° to 20° to the north-west. This is at a much shallower angle than the main fault zone but the sense of movement, with overthrusting to the south-east, is similar to that envisaged for the main fault.

There is no change in strike along the east side of Iron Duke nor is any observed in the tunnels. Even in the crush zone of Tunnel No.4, the strike is maintained at roughly north-south and the lineation is inclined to the north parallel to the pitch of the main fold axis. This suggests that the planes of movement were parallel to the strike and that movement was essentially vertical. There may, however, be a sense of lateral movement, with the iron-formations moving south relatively

to the schists, as indicated by the small thrust in Winze No.4 which was described above.

Further north along the east side of Iron Duchess, scattered outcrops of schist below the iron-formation show that the basal carbonate unit is missing and the fault probably continues. There is a marked topographic gap between the Iron Duchess and the Iron Knight iron-formations to the north and the projected fault line would extend through this gap as suggested by Reid (pers. comm.).

An interpretation of the faulting is shown in Fig.21.

(c) Cross-faults

A number of small cross-faults shift the synform axis with lateral movements generally not greater than about 100'. The movement is consistently sinistral.

This movement of the fold axis is reflected by sharp sideways movement of the ridge crest and the line of faulting is generally marked by a small saddle. The sense of movement is therefore plain but the actual direction of the fault plane is difficult to establish because the saddles have little exposure. Occasional smaller scale faulting seen in outcrop, and slight flexuring in the fold axis near to some cross-faults, suggest that the fault planes are striking north-east.

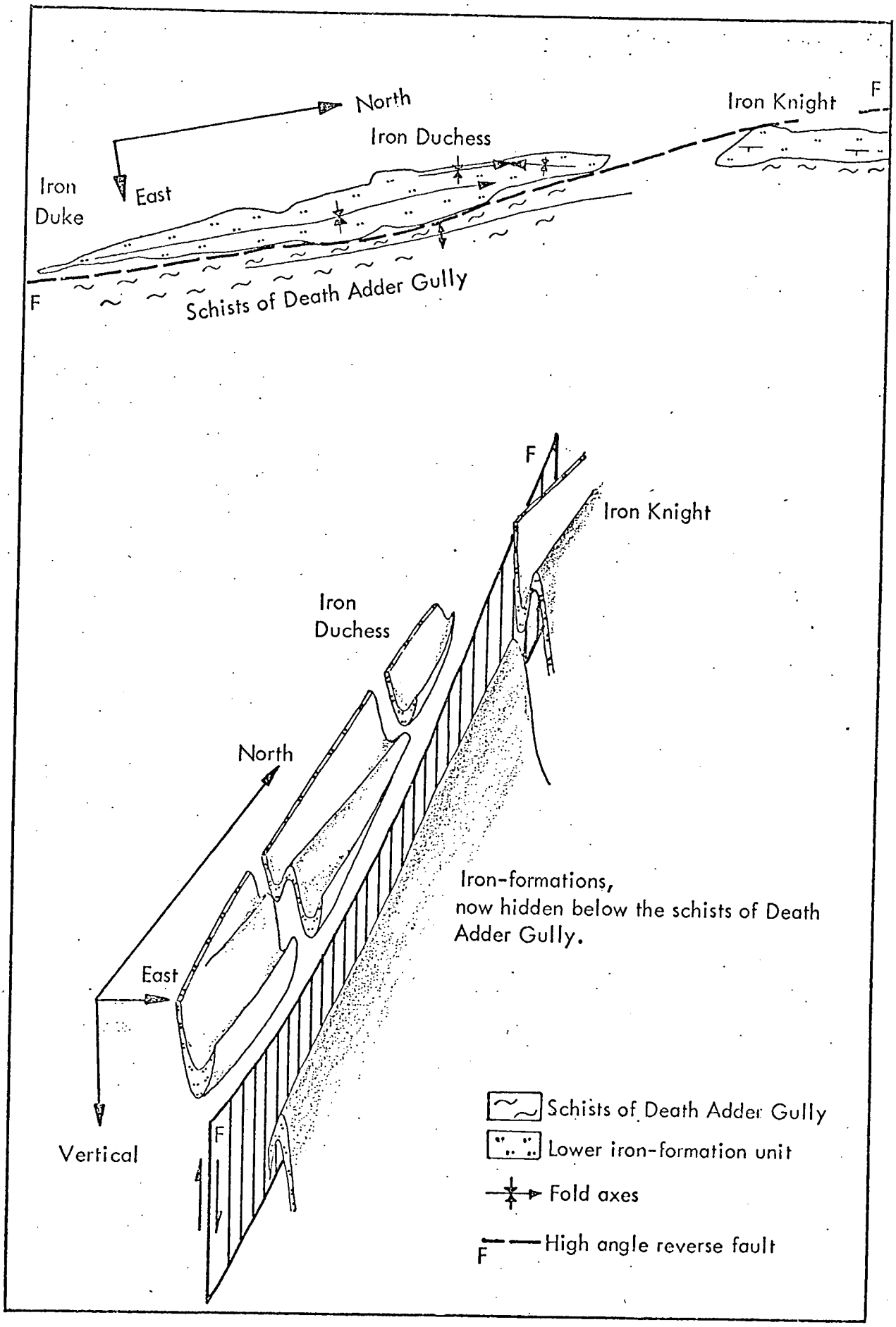

Fig.21. Diagram to show the effects of the strike fault on the east side of Iron Duke. Not to scale.

(d) Lineations

Amphibole rich iron-formations show a strong lineation on surfaces broken parallel to the banding due to parallel orientation of the fibrous minerals. Talcose rocks have a similar lineation and in both cases the lineation strike is approximately north-south with a gentle inclination to the north parallel to the fold axes.

Rodding is often well developed on iron-formation outcrops where the layering plane surfaces are exposed (Figs. 22a,b). It is primarily due to quartz grains forming small elongate knots and is consistently parallel to the fold axes (Jones 1968). Rodding of identical appearance is also formed by very small scale tight folding within the iron-formation and is also parallel to the main fold axes.

Fig. 22a. Rodding on layer surface parallel to axis of a broad concentric fold. Probably due to strong small scale folding. Iron Duchess, approx. 220N/130W. Siliceous iron-formation outcrops.

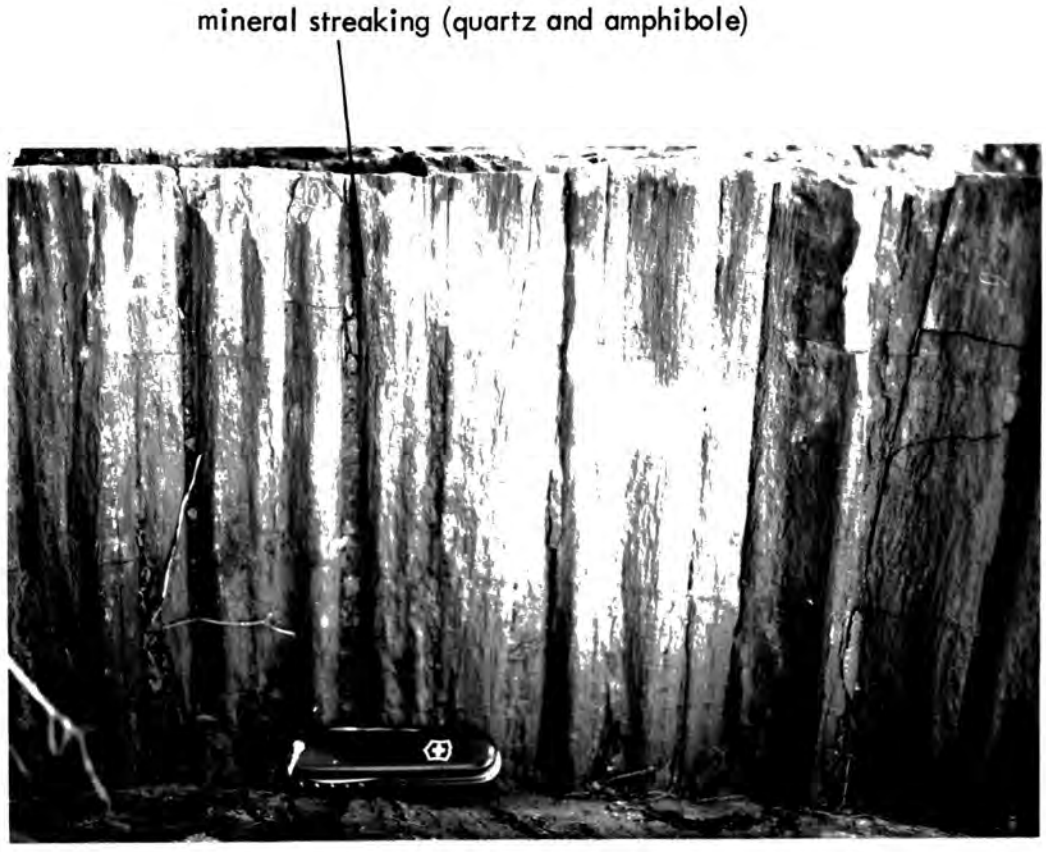

Fig. 22b. Closer view of rodding in 22a. Note smaller scale lineation due to mineral streaking.

D. DISPOSITION OF ORES, TALC ZONES AND AMPHIBOLITES

1. Magnetite-hematite-carbonate

The magnetite-hematite-carbonate occurs as a long, cylindrical body which extends along the length of the ridge at depth. It occupies the hinge area of the synform and is thickest at the northern end of Iron Duke, becoming progressively thinner up pitch to the south (Figs. 20a to 20g). The ore is not found above a depth of 300'.

The orebody is bounded on the east side by the steeply west dipping fault contact with chlorite schists of Death Adder Gully. Contacts between the two rock types are sharp.

Talcose rocks occur immediately above the ore and these pass gradually upwards into iron-formation. The contact between magnetite-hematite-carbonate and the talcose rocks is well exposed in Winze No.4 (Fig.20g), where the main contact is quite sharp but is overlain by a mixed zone of talc and chlorite schist with considerable carbonate veining and layers of massive banded hematite-carbonate (Figs.23a, b). The carbonate veins often occur in joints and fractures and taper upwards.

The orebody is underlain by a chloritised basic intrusive in the northern part of the area and contacts between the two rock types are sharp. To the south, hematite ore occurs in a thin layer along the base of the magnetite-hematite-carbonate body and contacts between the two ore types are gradational.

Fig. 23a. Upper contact of the magnetite-hematite-carbonate orebody.

The ore is overlain by hematite-chlorite-talc rocks which are highly disturbed, and the sharp contact may be due to faulting.
The width of the photograph covers about 5 feet.

Winze No. 4, approximately 185 feet.

Fig. 23b. Layered magnetite-hematite-carbonate surrounded by chloritic and talcose rocks immediately above the orebody. The chlorite-talc rocks are strongly deformed, and have flowed around the blockier magnetite-hematite-carbonate layers.

On the west side the orebody passes up dip into hematite ore. Drillholes in the northwest and north parts of the area suggest that the magnetite-hematite-carbonate ore gradually becomes divided into two thick layers separated by siliceous talc schists and iron-formations north of 1000S.

To the south, the orebody passes up pitch into hematite ore. The transition occurs rather sharply but is obscured by a large intrusive basic mass (Fig.20d).

2. Talc zones

The magnetite-hematite-carbonate body is overlain and underlain by zones of talc rich rocks. The main rock types are talc-magnetite schist and quartz-hematite-talc rock. In the lower zone there is often considerable pyrite.

The upper talc zone is thickest in the north where it has a stratigraphic thickness of about 200' (Fig.20g). It becomes progressively thinner to the south as shown in Figs. 20e and 20f.

There is a gradual transition from talcose rocks to the overlying iron-formations. The quantity of talc decreases, the quartz grain size decreases, amphiboles become the dominant silicate mineral and the whole character of the rock gradually becomes that of a typical iron-formation.

The lower talc zone is only seen clearly on section 1000S (Fig.20g), where it forms a narrow strip of 50' to 100' thick between the magnetite-hematite-carbonate and the underlying basal carbonate. It contains a good deal of carbonate and is heavily

packed with pyrite in places. Further south, this zone passes directly into hematite ore.

In the northern part of the area, both the talc zones thicken and a third zone appears within the magnetite-hematite-carbonate body, north of 1000S. The talc zones therefore form a partial envelope about the magnetite-hematite-carbonate body, occurring above the ore, below it and enclosing part of the ore at the northern end.

3. Hematite ore

In the southern half of the area, hematite ore occurs in the hinge area of the synform, resting upon argillaceous schists at the extreme southern end and upon a large basic intrusive further north.

In the northern half of the area, the ore is in two parts, the main body occupying the upper portion of the west limb and a smaller body extending along the base of the magnetite-hematite-carbonate into the hinge area of the synform (Figs. 20c to 20g). The main orebody is up to 300' thick in stratigraphic thickness and generally rests upon an amphibolite sill. It is overlain by iron-formations and there is a narrow transition zone of about 20' to 50' between the two.

Drilling has established that the hematite ore in the west limb passes down dip into both magnetite-hematite-carbonate and talc zone rocks. Part of the ore also appears to pass down dip into iron-formation.

The main hematite orebody terminates abruptly at about 500S (Fig.18), passing laterally into iron-formations. The precise nature of this transition is obscured by poor exposure and considerable faulting in the area.

The smaller orebody occurs as a thin layer, at its maximum about 150' thick, along the base of the magnetite-hematite-carbonate body (Figs. 20c to 20g). It extends down pitch from the main southern hematite orebody and down dip from the hematite ore in the west limb. To the north, it becomes progressively thinner and at 1000S (Fig.20g) is completely absent.

The bulk of the hematite ore at Iron Duke is within 500' of the surface.

4. Amphibolites

Miles (1954) used the term amphibolite to describe bodies of intrusive and interlayered basic igneous rocks which occur throughout the Middleback Ranges. The term, as used in this sense, includes a variety of rock types and does not imply that the bodies are premetamorphic. It is a convenient term and is retained in this thesis.

A large basic intrusive mass penetrates the synform between 4000S and 4600S (Figs. 20c,d). It is poorly exposed and is known mainly by drilling, which makes interpretation of the size and shape difficult, but it is definitely several hundred feet thick and can be interpreted as one or more massive intrusion penetrating the synform from depths to the east.

Dykes extend north and south from this mass. The southern dykes are thick and irregular in form and cut across the synform axis (Fig.18). They occur mainly within the hematite ore and also penetrate the schists of Death Adder Gully.

The northern dykes are thinner, generally not more than 150' thick and occur principally in the fold limbs (Figs. 20c to 20g). In the vicinity of the magnetite-hematite-carbonate and talcose zones they are completely chloritised. Their intrusive character may be demonstrated in Tunnel No.4 (Fig.20g) where one typical dyke shows a chilled margin against schist and another cuts irregularly across banded iron-formation.

A small intrusive body, different in form and texture from the other intrusives, occurs in the upper part of the west limb (Fig.20g). It is completely chloritised but the remnant texture is porphyritic and there is no obvious source for a feldspar porphyry in the area.

E. PETROLOGY

The iron-formations of the Middleback Ranges have already been described in Section I and, as those at Iron Duke represent the general type, they will not be described further.

The hematite-magnetite-carbonate, talcose rocks and chloritised intrusives are unusual rock types which are rarely mentioned in world literature. They will be described in detail, together with a brief description of the schists in Death Adder Gully which show significant differences in mineralogy from their stratigraphic equivalents to the north. *

1. Magnetite-hematite-carbonate

The rock is a mixture of magnetite, hematite and carbonate with oxides in about equal proportions to the carbonates. It is mixed blue-black and creamy white in colour and the carbonate is usually fairly coarse grained whereas the iron oxides are fine grained and granular. (Fig. 24)

(a) Structures

Most of the rock has an unusual structure consisting of fragments of finely banded magnetite-hematite-carbonate merging into and cemented by coarsely crystalline carbonate (Figs. 25 to 29). It often appears to be a mixture of brecciation and plastic flow.

DDH 57 (Fig.20g) intersected 800' of this material and drillholes to the south have shown it to be characteristic of the whole body. There is rather less brecciation and the banding is

* The petrology of these rock types is described in detail in Company reports by Whitehead and Burger using microscopic techniques. The reports were used by the author as a basis during the early part of this work, but the following descriptions are based on the author's own observations.

less disturbed at high levels on the east side of the orebody. Vein carbonate tends to increase towards the base of the orebody, particularly on the east side.

Structures observed in drill core can be categorised into three main types, banded, brecciated and veined:

Banded structures (Figs.25a,b) vary in scale from microscopic to layers several inches thick which are themselves finely banded. The banding is usually diffuse and frequently shows swelling, stretching and flowage structures, often accompanied by tight, small scale folding. Massive bands, with a higher proportion of oxide minerals, do not show such strong distortion. The carbonate is usually fairly coarsely crystalline, even in well banded samples, and carbonate rich bands tend to be still more coarsely crystalline and merge into vein carbonate. Rare specimens with undisturbed banding show a fine layering similar in scale and appearance to that of the iron-formations, each layer having a texture dependent on the proportion and grain size of its components, particularly the iron oxides*. The carbonate is finer grained in these bands.

Brecciated structures (Figs. 26a,b,) consist of angular fragments of magnetite-hematite-carbonate enclosed by vein carbonate and sometimes by magnetite. The fragments are usually banded but the carbonate of the fragment merges into the enclosing carbonate, the fragment boundaries are commonly indistinct, and the layering tends to become vague. The enclosing carbonate is fairly coarsely crystalline and sometimes has small vughs with euhedral crystals projecting into the cavities.

*as noted by Whitehead in Company reports.

Fig. 24. Hematite-magnetite-carbonate ore exposed in Winze No.4.
The white is carbonate and the mottled grey-black areas are hematite-magnetite-carbonate. Note the fine scale layering in some iron oxide rich patches.
Approximately half natural scale.

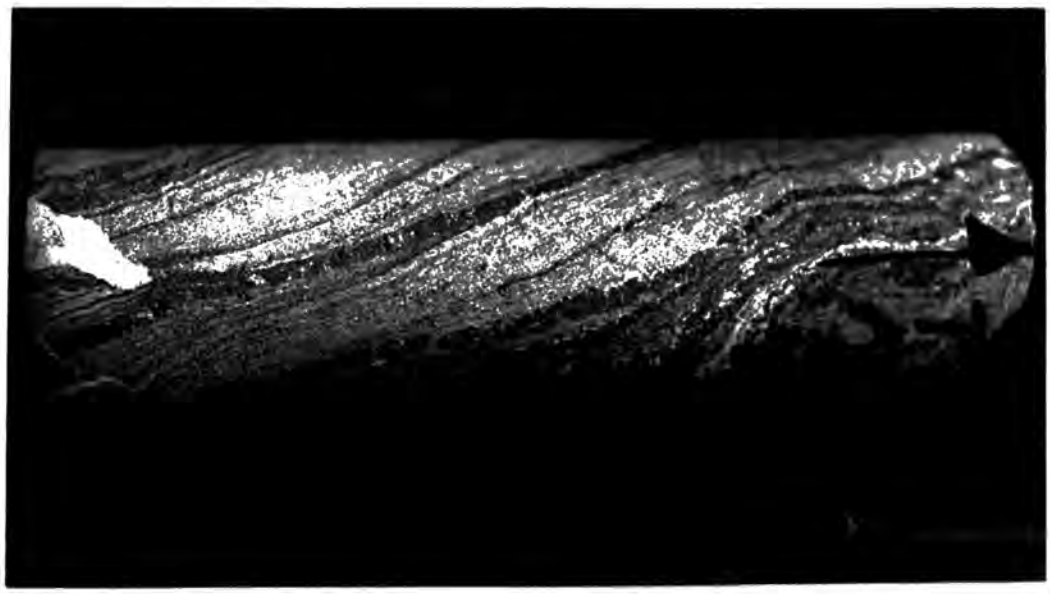

Fig. 25a. Layered magnetite-hematite-carbonate. Arrow points upwards in vertical core.
Sample no. 85-810. Scale on right is in tenths of an inch, drillcore is approximately $1\frac{1}{4}$ inches in diameter.

Fig. 25b. Layered magnetite-hematite-carbonate. Note the well developed fine layering of magnetite rich bands on the right, diffuse layering on the left and coarsely crystalline carbonate in the centre. Upper scale on the rule is in inches, lower in centimetres. Sample no. 2.

Fig. 26a. Brecciated hematite-magnetite-ankerite ore. Note distinct layering of iron oxides and carbonate in the breccia fragments. Sample No. 85-665. Drillcore is approxima tely $1\frac{1}{4}$ inches in diameter.

Fig. 26b. Brecciated hematite-magnetite-calcite. The fragments are in vein calcite. Scale in inches. Sample No. 7.

Fig. 27 . Veins of ankerite cutting layered hematite-magnetite-carbonate with chlorite-talc layers immediately above the orebody. Winze No. 4, north wall. Scale approximately one-third natural size.

Fig. 28. Folding in magnetite-hematite-carbonate ore. Winze No. 4. Approximately two-thirds natural size. Note the very fine scale layering within the light coloured carbonate rich layer.

Vein structures (Fig. .27) include clearly cross cutting veins of carbonate and, to a much lesser extent, magnetite. Patches of coarsely crystalline carbonate, several feet thick, are sometimes intersected by drilling and these are assumed to be parts of larger veins. The larger veins are found mainly towards the base of the orebody but may occur at any level. Small vughs with euhedral crystals projecting into the cavities are common.

The characteristic structure for the whole orebody is a mixture of the three types described above. Some kind of banding is almost always present but there is every gradation between banded and vein structures. It is frequently impossible to tell whether coarsely crystalline carbonate is a true vein in the sense that it has been introduced into the rock, or whether it is formed by carbonate rich bands flowing and merging to produce a vein type of structure.

Massive magnetite frequently occurs at the contacts with chloritised intrusives, often forming a layer several feet wide and passing gradually into the magnetite-hematite-carbonate. The contact between magnetite and the intrusive is, in all cases, knife sharp. The magnetite frequently encloses angular fragments of chloritised intrusive and, more rarely, fragments of banded magnetite-hematite-carbonate. It has a granular texture and there is frequently some intermixed coarsely crystalline carbonate present amongst the magnetite grains.

Folding is sometimes present in drill core varying in scale from broad, gentle flexuring to crenulations on a micro scale.

The styles vary from open concentric folds to tight similar folds with hinge area thickening and the typical style is intermediate between these two (Fig 28).

Other small scale structures observed in drill core are normal faults and a mineral lineation on surfaces broken parallel to the banding planes. The latter is mainly found in the upper part of the orebody where a little talc is present in the rock and is due to the alignment of talc crystals and sometimes magnetite trains, on the surfaces

It is impossible to precisely determine the orientation of small scale structures without fully oriented drill core and this is not available. The dip of the banding fluctuates widely relative to the drill core axis but conforms broadly to the main structure if the dip direction is assumed to be parallel to the fold limbs. Fold axes are generally gently inclined from the horizontal and small concentric folds exposed in Winze No.4 (Fig. 28) have axes striking due north and inclined to the north at about 10°, parallel to the regional trend. Lineations, when present in folded samples, are parallel to the fold axes.

(b) Microtextures

(1) Transmitted light

A typical thin section of magnetite-hematite-carbonate ore includes part of an iron oxide rich fragment and part of a coarsely crystalline carbonate band or vein.

The iron oxides occur as blocky grains, sometimes grouped into bands but more often forming an irregular sieve-like texture (Figs.29, 30). The carbonate which fills the interstices between iron oxide grains is in irregularly sized, interlocking crystals which enclose the smaller oxide grains. Sometimes this interstitial carbonate is in large crystals up to 4mm across which completely enclose the majority of the iron oxide grains. The carbonate is characteristically cloudy with blurred interlocking edges.

The carbonate rich portion consists of large, interlocking crystals with very ragged edges. The crystals are normally cloudy with dark areas, probably due to included fluid, and the crystals generally contain fluid inclusions. Some of the crystals may be well formed and clear of inclusions and these tend to occur in small groups which merge into the darker material. Cleavages are sometimes well developed but more often are poor and the crystals often show undulose extinction.

Two microtextures are not included in the above description, massive ore and well banded ore:

Massive ore (Figs.31a, b), probably represents iron oxide rich layers of a broad banding. It has even, granular microtextures with the iron oxides distributed evenly throughout the section. Magnetite is normally the predominant iron oxide and the grains are usually unoriented producing a regular, sieve-like texture (83-848) but may be grouped into elongate patches producing a weak orientation within the section (61-532, Fig.31a). In some samples, bladed

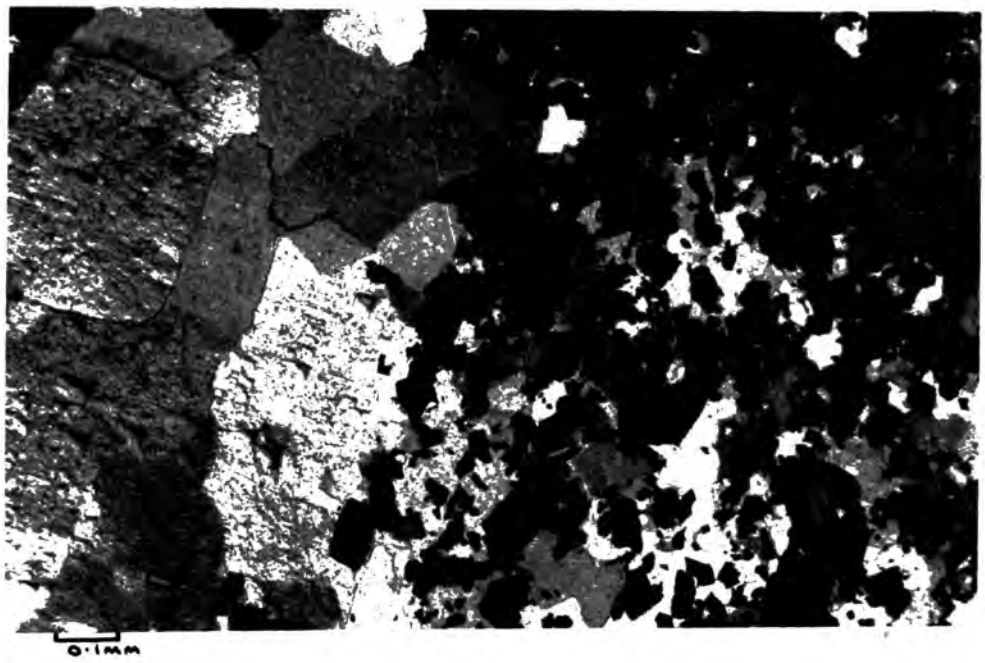

Fig. 29. Typical thin section of magnetite-hematite-carbonate ore. Note the coarsely crystalline vein carbonate on the left merging to more finely crystalline carbonate in the magnetite rich portion. 60-867, crossed polars.

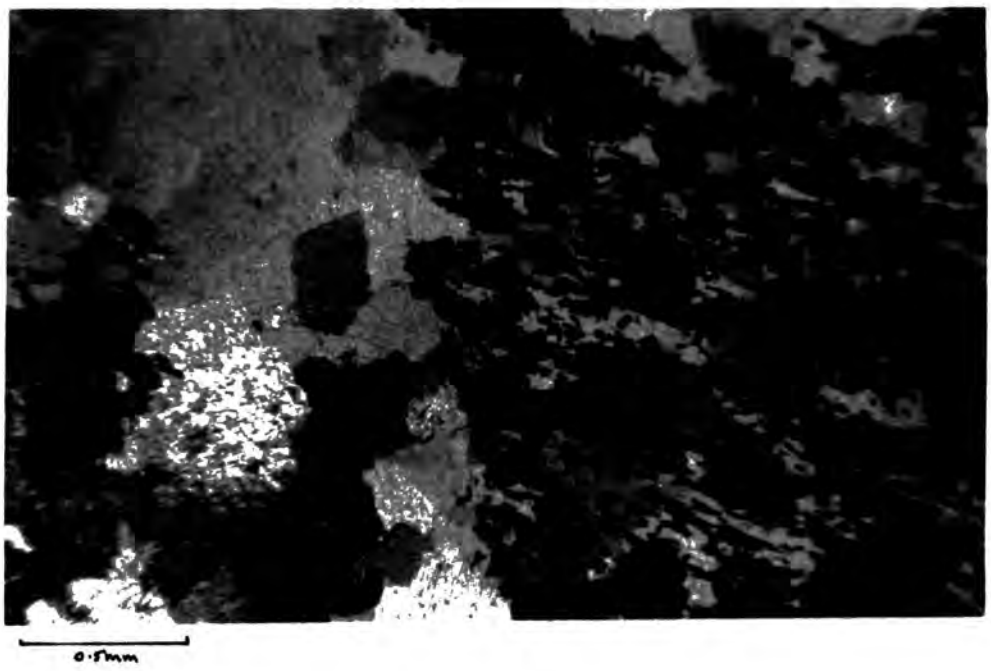

Fig. 30. Coarsely crystalline vein carbonate enclosing a fragment of hematite-magnetite-carbonate. Note the parallel orientation of hematite grains. 59-721, crossed polars.

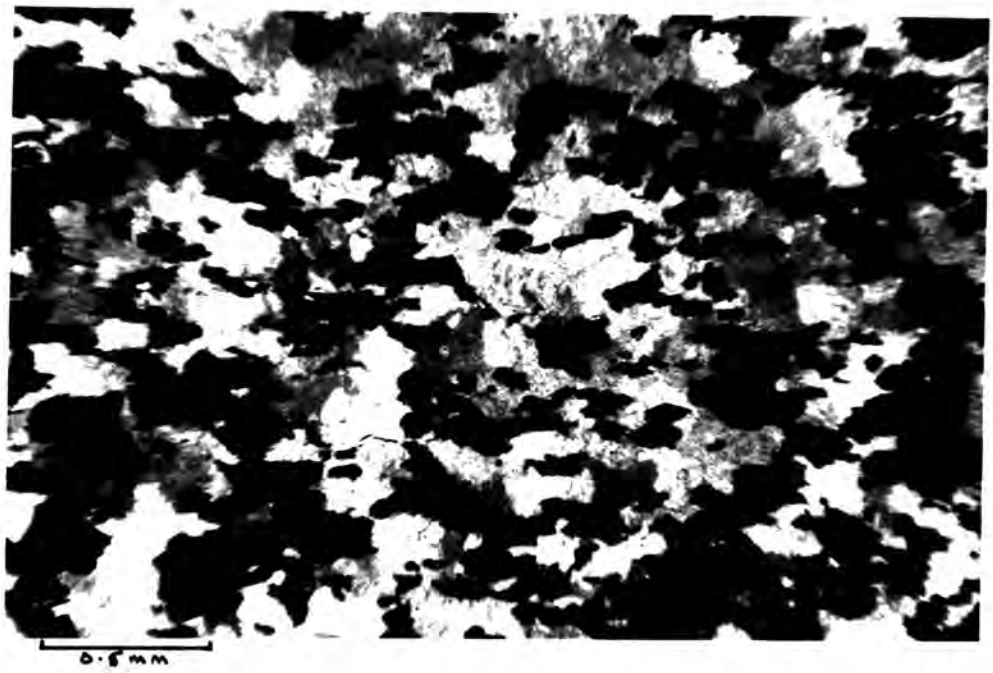

Fig. 31a. Microtexture of massive magnetite-hematite-carbonate ore. Note regular distribution of magnetite grains with parallel alignment and fairly even size of carbonate crystals. Probably part of larger scale layering.
61-532, crossed polars.

Fig. 31b. Massive hematite-carbonate ore. Specular hematite in coarsely crystalline carbonate.
78-990, crossed polars.

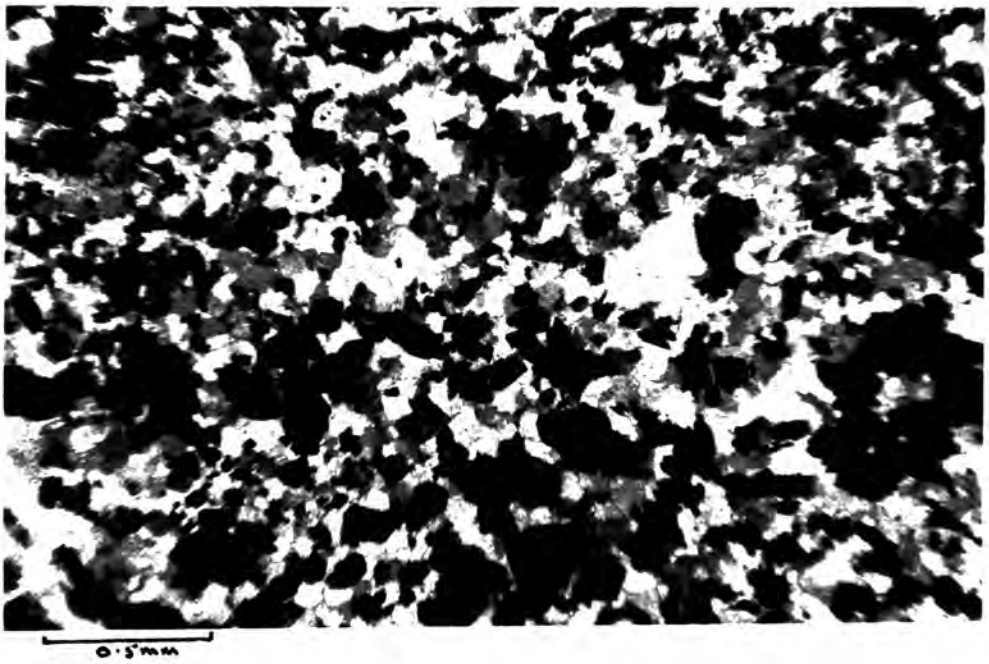

32. Microtexture of well banded magnetite-hematite-carbonate. Note the fine grained, fairly evenly sized carbonate crystals.
60-813, crossed nichols.

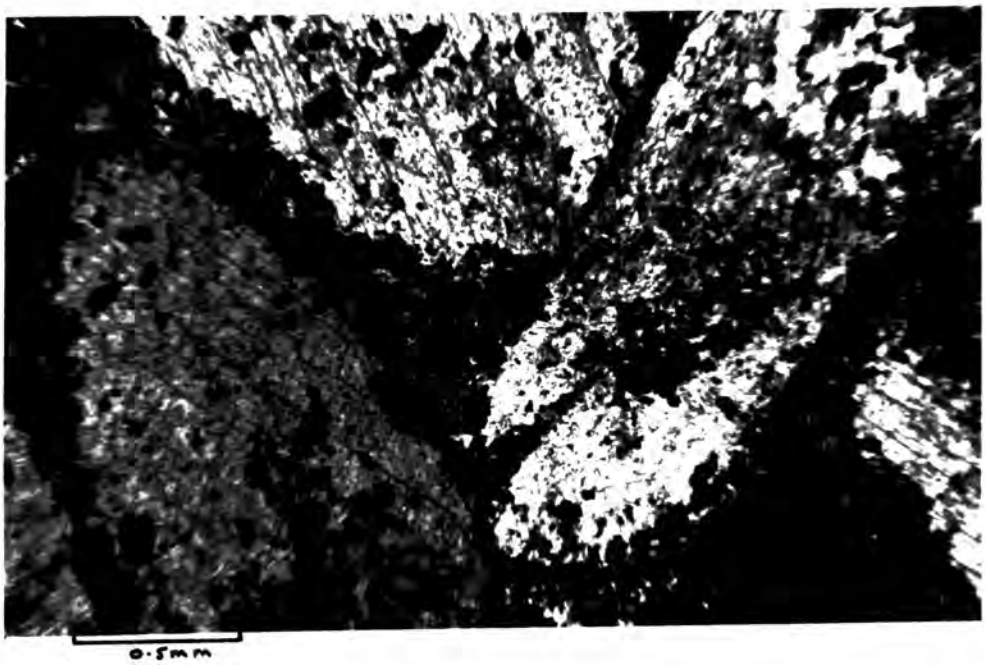

33. Siderite crystals with magnetite and hematite grains. The siderite crystals occur within coarsely crystalline ankerite, near the upper margin of the orebody.
67-352, crossed nichols.

hematite predominates, generally in crystals between 0.1mm and 0.5mm in length and these may be distributed at random (78-990, Fig.31b) or aligned in parallel orientation (59-722). The interstitial carbonate is generally evenly sized and similar in grain size to the iron oxides but it may merge to form areas up to 4mm across in optical continuity.

Well banded ore (Figs.32) is characterised by fine grained, even microtextures. The banding varies in scale from almost submicroscopic (78-853) to broad layers up to 5mm in width (60-813). Within any particular band, texture is controlled by the quantity and grain size of the iron oxides. This is well illustrated in sample No.2 which has distinct banding very similar to that of the iron-formations (Figs.25b, 32). The blockier bands in hand specimen have relatively large magnetite grains with a coarse, open microtexture. The interstitial carbonate is also relatively coarse in these bands and sometimes has an undulose extinction similar to that of quartz in coarser bands of the iron-formations. The finer grained bands may contain the same quantity of iron oxide but the grain size is much smaller, producing a closely packed, even microtexture. In these layers the carbonate is also finer grained. In some samples, the oxides occur in larger, interlocking patches that tend to be elongate parallel to the banding and produce a coarser, more oriented texture. Carbonate textures are generally a little coarser than those of sample No.2 and consist of evenly sized crystals in the size range 0.1mm to 0.4mm. They are irregular in shape and are very cloudy with numerous small fluid inclusions. The carbonate crystals sometimes merge to form larger crystals which contain shadows of smaller crystals.

At the upper margin of the orebody, quartz and carbonate occasionally occur together (85-498, 60-637). The quartz usually occurs as clear, irregular patches interlocked with carbonate crystals of similar size. It sometimes encloses trains and bands of iron oxide grains. Occasionally, the quartz occurs in small grains which appear to be partly replaced by carbonate. Thin talc layers are sometimes developed at the quartz-carbonate interfaces.

Also at the upper margin of the orebody, carbonate and talc occur together, the carbonate frequently appearing to replace the talc and sometimes having a finely fibrous appearance.

(2) Reflected light

Magnetite and hematite may occur alone or together in any particular sample regardless of the microtextures described above. In magnetite veins or concentrations adjacent to chloritised intrusives, only magnetite is present.

Magnetite is generally in blocky grains in the size range 0.02mm to 0.25mm and often has a roughly cubic form. The crystals tend to have concave edges and are frequently slightly elongated and aligned parallel to the banding. Bladed magnetite was observed in one sample (60-643,) projecting from a banded fragment into vein carbonate. The blade form is characteristic of hematite and the magnetite in this case must have completely replaced specular hematite.

Hematite occurs in two main forms:

(i) Partly or wholly replacing magnetite (57-1239) and

often enclosing remnants of magnetite (85-810).

(ii) As roughly bladed or elongate forms evenly distributed throughout carbonate (61-780). Magnetite accompanies this form of hematite in some samples (X).

(c) Whole-rock geochemistry

Forty-two whole-rock analyses are given in Appendix I and four representative analyses are shown in Table 8. The large number of samples covers all ore types but there is little chemical variation other than in those elements which constitute carbonates and iron oxides. The chosen four analyses are fair representatives of their respective ore types.

The major element analyses are semi-quantitative but give a good indication of the general levels for each element, as discussed in Appendix I.

In all the ore types, CaO, MgO and Fe (expressed as Fe_2O_3) show wide variation due to the differing proportions of iron oxides and carbonates in the rocks. There are negligible amounts of Al_2O_3, Na_2O, K_2O and TiO_2 and the low amounts shown in the analyses are at the limits of accuracy for the technique used. No S is detected by the analyses but a little pyrite is sometimes present in the ore. Results for the other major elements may be summarised as follows:

SiO_2 - generally less than 1%, the highest value within the main orebody being 2.3% and the average 0.6%. The source of silica is not immediately obvious in most samples and,

Table 8. Whole-rock analyses of magnetite-hematite-carbonate ore

86-734 Typical ore with mixed layered, vein and breccia structures.

57-979 Layered ore.

67-823 Vein ankerite with minor iron oxides.

57-1140 Calcite rich ore.

Per cent	86.734	57-791	67-823	57-1140
SiO_2	1.3	0.3	2.1	0.9
Al_2O_3	0.2	0.2	0.2	0.3
Fe_2O_3	56.2	47.9	15.7	37.5
MgO	8.6	12.1	18.7	9.4
CaO	13.7	17.1	21.1	19.7
Na_2O	0.2	0.0	0.1	0.2
K_2O	0.1	0.1	0.0	0.1
TiO_2	0.1	0.1	0.1	0.1
MnO	0.4	0.6	0.8	4.4
S	0.0	0.0	0.0	0.1
P_2O_5	0.3	0.2	0.1	0.1
Ig. Loss	19.2	(21.4 diff.)	40.6	27.7
	100.3	100.0	99.5	100.5
ppm				
Zn	12	0	2	5
Ni	5	7	0	12
Ba	<30	<30	0	<30
Nb	N.D.	N.D.	0	N.D.
Zr	<16	<16	2	<16
Y	1	4	20	14
Sr	7	5	29	14
Rb	0	0	4	0

Notes: 1. Major elements - analyses 86-734, 67-823 and 57-1140 by chemical Laboratory, B.H.P., Whyalla, analysis 57-791 semi-quantitative XRF by author.

2. Trace elements, XRF by author.

as the analyses are within the order of ± 0.6%, there is probably negligible silica in most of the rock. Some samples definitely contain a little silica and this is due to small amounts of talc or vein quartz.

MnO - over 0.4% MnO is present in all the samples, the highest value being 4.4%. The vein ankerite, calcite rich ore and siderite rich ore all tend to be rather higher in MnO than typical diffusely banded and brecciated ankerite ore, or than well banded ore. This is illustrated in Table 8.

P_2O_5 - the general level is in the order of 0.2% - 0.3% in all the ore types except the vein carbonates, which contain about 0.1%.

Trace element concentrations are low in all the ore types with erratic, relatively high values in some samples. The most significant variation is shown by Sr, which is markedly higher in some calcite rich ore samples.

(d) Mineralogy

Most of the magnetite-hematite-carbonate ore is a simple mixture of iron oxides and carbonates. Small amounts of intermixed quartz, talc and pyrite occur in the upper and lower contact areas with more siliceous rocks.

Iron oxides

Magnetite and hematite are finely intermixed within the

rock and it is difficult to visually estimate their relative proportions. However, using a hand magnet and the red streak of hematite as guides, examination of several thousand feet of drill core suggests that magnetite is most abundant in the northern, deeper parts of the orebody and along the eastern side by the fault zone. To the south and west, the hematite proportion progressively increases and the ore gradually passes into hematite ore.

Electron microprobe analyses were carried out on magnetite grains in three samples, each representing a different ore type. The results are shown in Table 9, together with two analyses of synthetic hematite which was used as a standard. Magnetite in the sample of banded ore (83-575) contained an average of 0.12% Mg and 0.16% Ti. These values are significantly higher than Mg and Ti values in the typical ore sample (74-575) and the vein magnetite (67-1029). The electron microprobe beam was finely focussed, the magnetite grains were relatively large and the Mg and Ti results for synthetic hematite were consistent, so the differences between samples must result from variations of Mg and Ti within the magnetite lattice. The results for Si and Mn must be treated with caution as there are marked differences between the two analyses of synthetic hematite and this suggests experimental variation.

Reconnaissance microprobe analyses in hematite of the banded ore sample (83-575) show concentrations of Si, Mg and Ti similar to those in magnetite from the same sample. Si is slightly higher in the hematite.

Table 9. Trace elements in magnetite grains within different types of magnetite-hematite-carbonate ore

		Si	Mn	Mg	Ti
Banded magnetite-ankerite (83-575)		0.36	0.04	0.18	0.16
	same grain	0.12	0.00	0.10	0.13
		0.12	0.00	0.05	0.10
	smaller grains	0.07	0.00	0.10	0.13
		0.07	0.00	0.18	0.27
Typical ore (74-579)	Banded portion	0.05	0.00	0.00	0.03
		0.26	0.06	0.00	0.00
		0.07	0.06	0.00	0.00
	vein portion	0.19	0.26	0.00	0.00
		0.19	0.18	0.00	0.00
Vein magnetite (67-1029)		0.19	0.18	0.00	0.03
		0.19	0.20	0.00	0.03
		0.19	2.12	0.00	0.10
Synthetic hematite (standard)		0.07	0.31	0.00	0.03
		0.20	0.20	0.00	0.03

Carbonates

Carbonate compositions throughout the orebody were investigated by staining 50 samples with Alizarin Red S and NaOH in the technique described by Ward (1962), checking the results by 35 X-ray powder diffraction films and analysing carbonate crystals by electron microprobe in eleven samples.

The full results are given in Appendices II and III and establish that the bulk of the carbonate is an intermediate ankerite as defined by Deer, Howie and Zussman (1962). Along the top of the orebody there is a thin layer of intermixed ankerite and siderite and at the base is a layer of ankerite and calcite (Fig.34). The carbonate minerals may be described as follows:

Ankerite is the only carbonate mineral present in most of the ore. It is normally cream to milky white and stains a distinct red-mauve. The staining tends to be blotchy, with slight gradational colour changes to reddish-brown and mauve-purple suggesting compositional variation. This was checked by X-ray powder diffraction and electron microprobe analysis and is not due to variations in composition.

X-ray diffraction patterns show that only one carbonate mineral is present and indicate that its composition is broadly uniform throughout the orebody. The X-ray diffraction data for a typical sample is shown in Table 10. Some samples show slight shifts in certain lines which suggest small variations in carbonate composition but all the patterns are similar and conform to that of an intermediate ankerite (ref. A.S.T.M. cards 12-88 and 11-78).

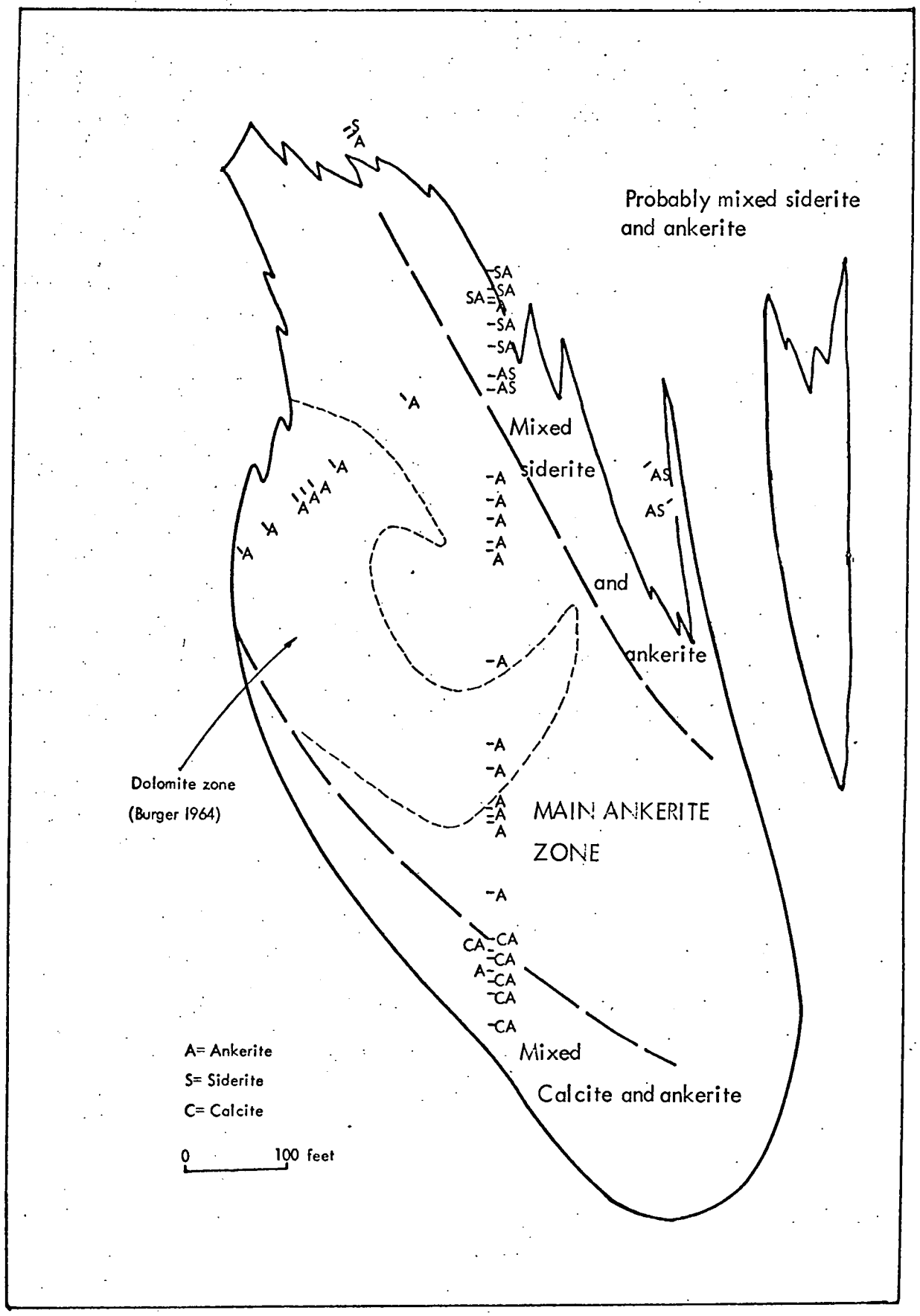

Fig. 34. Distribution of carbonate types within the magnetite-hematite-carbonate ore on section 1000S. Carbonate identification based on staining and X-ray diffraction techniques.

Table 10. X-ray diffraction data for Iron Duke ankerite

Ankerite $Ca_{1.0}$ $Mg_{0.7}$ $Fe_{0.3}$ $(CO_3)_2$ (Sample 78-800)

dÅ	I/I_1	hkl
3.69	40	012
2.904	100	104
2.676	20	006
2.535	20	015
2.399	50	015
2.399	50	110
2.190	70	113
2.060	20	021
2.014	50	202
1.845	30	024
1.804	70	018
1.788	70	116, 009
1.560	30	211
1.545	40	122
1.465	40	214
1.443	30	028
1.432	20	119
1.415	20	125
1.389	40	030
1.339	30	0.0.12
1.298	30	217
1.272	30	0.2.10
1.239	30	128
1.203	20	220
1.170	30	1.1.12
1.145	10	312
1.125	30	2.1.10
1.111	40	134
1.098	30	226, 309
1.009	40	404
1.003	30	318
0.978	30	1.0.16

Table 10 (ctd.)

0.9649	30	3.0.12
0.9310	10	3.2.14

hexagonal cell:

$a_o = 4.8176 \pm 0.0009$ Å

$c_o = 16.098 \pm 0.006$ Å

A hand picked ankerite sample from the centre of the orebody (57-749) gave the following chemical analysis:

SiO_2	Al_2O_3	Fe (as FeO)	MgO	CaO	MnO	S	P_2O_5	Ign. Loss
0.1	0.1	8.7	15.7	28.4	1.0	0.2	0.0	44.4

(Analysis by Chemical Laboratory, B.H.P., Whyalla).

Electron microprobe analyses on individual carbonate crystals support this general composition and are plotted in Fig.35 and presented in full in Appendix II.

The electron microprobe analyses provide a number of interesting items of information:

(i) All the samples from within the main part of the orebody contain one carbonate type which has a similar composition throughout the body. There is some variation in detail, as described in paragraphs (ii) and (iii).

(ii) Within any particular thin section, different carbonate crystals can vary by up to 7% Mg CO_3 and 9% Fe CO_3, and there is a converse relationship between these components. This indicates that Fe and Mg substitute easily for each other within a limited range, whilst Ca remains essentially constant.

(iii) In several samples there are broadly two carbonate compositions characterised by slightly different Mg/Fe+Mn ratios. This is illustrated by the following data:

61-780	$CaCO_3$	$MgCO_3$	$FeCO_3$	$MnCO_3$	$\frac{MgCO_3}{MgCO_3+FeCO_3+MnCO_3}$
Type 1	51.1	34.1	11.5	1.8	0.7
Type 2	52.5	39.8	5.0	0.9	0.9

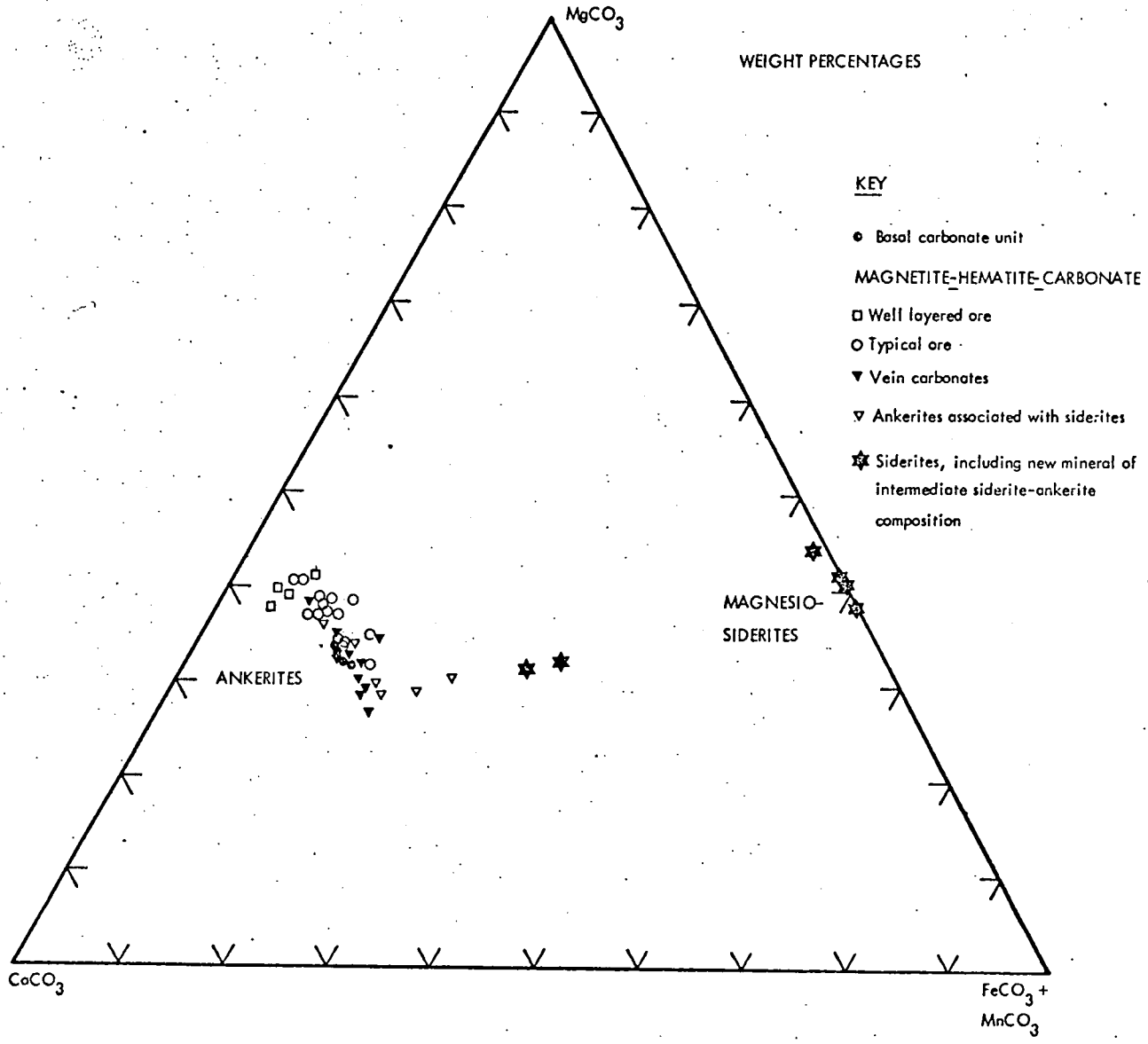

Fig. 35. Compositions of carbonates in the magnetite-hematite-carb and basal carbonate unit, Iron Duke.

The precise carbonate compositions are different for any particular sample, but when two compositions are present, as in 61-780, they occur together in both banded and vein carbonate.

(iv)Fine grained carbonate interstitial to iron oxides can merge into vein carbonate with no major change in composition. This may be illustrated by two analyses from 57-900:

	$CaCO_3$	$MgCO_3$	$FeCO_3$	$MnCO_3$	Total
Fine-grained interstitial carbonate	51.0	36.5	8.7	1.7	97.9
Vein carbonate	51.3	35.9	7.9	2.5	97.6

In both the vein and interstitial carbonate, well formed clear crystals are sometimes present amongst the normally cloudy material and these tend to be slightly enriched in Fe and Mn, although in some cases they are depleted in these elements. This general tendency for Fe and Mn enrichment in coarse carbonate of vein type is illustrated in its most extreme case in the two analyses shown below. These are from two electron microprobe sections cut in one core length which contains fine grained carbonate in banded layers (Sample 2) and coarsely crystalline carbonate in intervening layers (Sample 1).

	$CaCO_3$	$MgCO_3$	$FeCO_3$	$MnCO_3$	Total
Fine grained carbonate (2)	51.3	41.3	5.3	1.6	99.5
Vein type carbonate (1)	51.0	31.5	13.8	2.0	98.3

The $FeCO_3$ content of the coarsely crystalline carbonate in the above analysis (1) is higher than normal and in most samples

both the fine grained and coarse carbonate crystals have broadly similar compositions and similar variations.

(v) Within individual crystals, there is some variation in Mg, Fe and Mn but this is not systematic and no zoning was detected other than that in euhedral crystals projecting into cavities which is described in paragraph (vi) below. There is no change in carbonate composition near to iron oxide grains except in rare cases where a little cloudy material occurs around iron oxide grains and is rich in $FeCO_3$ (83-575).

(vi) Zoned crystals which project into cavities show no systematic differences in composition between the light and dark zones, as illustrated in Fig.36. There is a slight but steady decrease in $MnCO_3$ from the outer rims to the centres of the crystals but this is unrelated to colour variations. Analyses of the darker bands tend to have low totals, in the order of 96%-97%, which suggests that the cloudy character may be due to included fluid. These darker bands are packed with fluid inclusions.

In two traverses across adjacent crystals, the Mn decrease from rim to centre was complimented by fluctuations in Mg and Fe with a general increase in Fe, as shown in Fig.36. This indicates that during crystal growth, Mn could take the place of either Fe or Mg in the crystal structure.

The crystals project from a mass of finer grained carbonate which tends to contain less Fe and more Mg as illustrated by the following analyses:

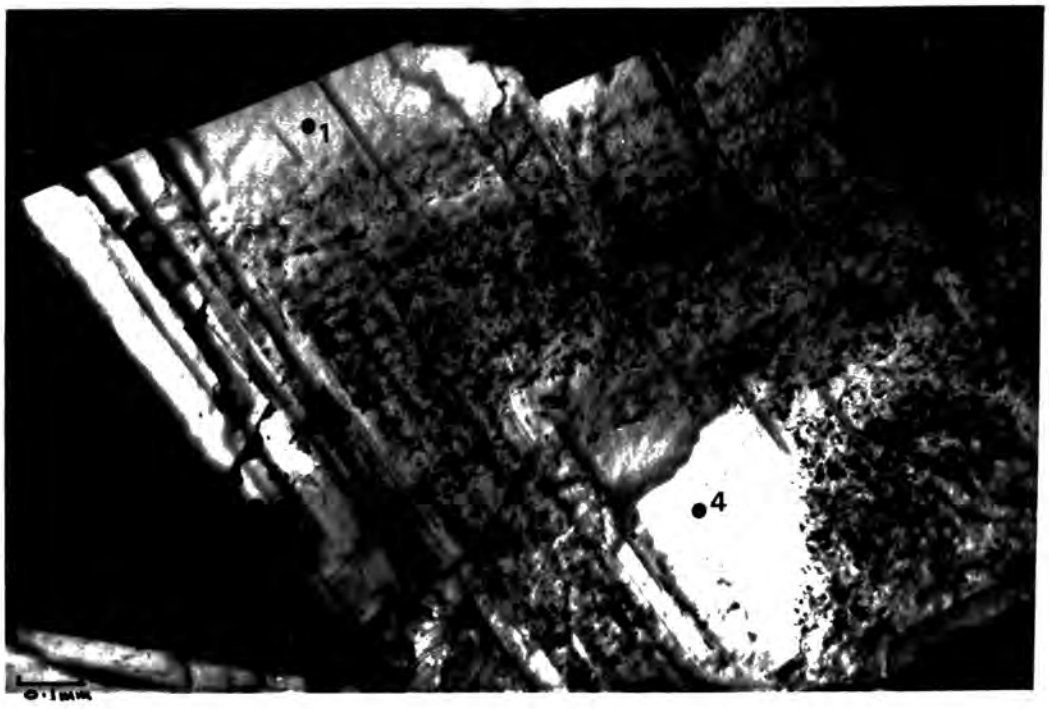

Fig. 36. Carbonate crystals projecting into a small cavity in magnetite-hematite-carbonate ore, 78-800. Electron microprobe analyses given below.

Sequence 1	$CaCO_3$	$MgCO_3$	$FeCO_3$	$MnCO_3$	Total
1	51.6	27.4	15.5	3.2	97.7
2	51.1	26.5	17.3	3.0	97.9
3	51.7	28.1	16.1	2.1	98.0
4	52.0	31.7	14.6	1.4	99.7
Sequence 2 (not shown on photograph but on adjacent crystal)					
5	51.9	29.2	16.0	2.2	99.3
6	52.1	31.5	12.7	1.9	98.2
7	52.2	32.9	11.3	1.6	98.0

78-800	$CaCO_3$	$MgCO_3$	$FeCO_3$	$MnCO_3$	Total
Groundmass	51.5	33.9	11.5	1.3	98.2
Euhedral crystal	51.9	29.2	16.0	2.2	99.3

The analytical results support Burger's (1963) study of carbonate refractive indices in which the bulk of the carbonate was classified as parankerite, a term used by Winchell (1951) to include the above compositions. Burger's central dolomite zone (Fig.34) was not detected but his refractive indices for this zone are a little higher than normal for dolomite and the carbonate mineral is probably ankerite with a lower iron content than the surrounding material.

Calcite occurs in both vein and banded structures at the base of the orebody, frequently intermixed with ankerite. It is normally milky white and indistinguishable from the ankerite in hand specimen but stains bright red in cold Alizarin Red S, whereas the ankerite remains white.

An analysis of hand picked material (57-1343) gave the following composition:

SiO_2	Al_2O_3	Fe (as FeO)	MgO	CaO	MnO	S	P_2O_5	Ign. Loss
0.3	0.1	0.2	0.3	52.8	1.9	0.0	0.0	42.2

(Analysis by Chemical Laboratory, B.H.P., Whyalla).

Electron microprobe analyses of crystals in one sample (57-1239) confirm this general analysis, but show up to 5.3% $MnCO_3$ The analyses are plotted together with the other carbonates in Fig.35. Sample 57-1239 consists of banded magnetite-hematite-calcite fragments enclosed by coarsely crystalline vein carbonate,

and the analyses show that there is no major difference in composition between calcite in the banded fragments and that of the vein. This is illustrated in Table 11, below:

Table 11. Calcite analyses in the banded and vein portions of sample 57-1239

	$CaCO_3$	$MgCO_3$	$FeCO_3$	$MnCO_3$	Total
Interstitial carbonate	92.4	0.0	0.3	4.2	96.9
Adjacent clear vein	92.5	0.3	0.4	3.7	96.9
Sequence from interstitial to vein carbonate:					
1.Interstitial	93.2	0.0	0.5	5.1	98.8
2.Edge of interstitial	92.1	0.0	0.1	5.3	97.5
3.Clear vein carbonate	94.7	0.0	0.3	2.6	97.6

Note: The first two analyses have rather low totals. The calcite was scanned by electron microprobe for all likely major and trace elements in addition to those listed above and no other components were detected. The $CaCO_3$ component of the first two analyses is slightly low and the deficiency is probably an analytical error in the Ca determination.

Siderite occurs in both vein and banded structures in a narrow layer along the top of the orebody. It is frequently intermixed with ankerite but is easily distinguished by its creamy brown colour. When treated with hot Alizarin Red S and NaOH, it stains a distinct deep brown which contrasts strongly with the ankerite red-mauve (Fig.37).

X-ray diffraction patterns give d-spacings similar to those of the A.S.T.M. siderite (Table 12).

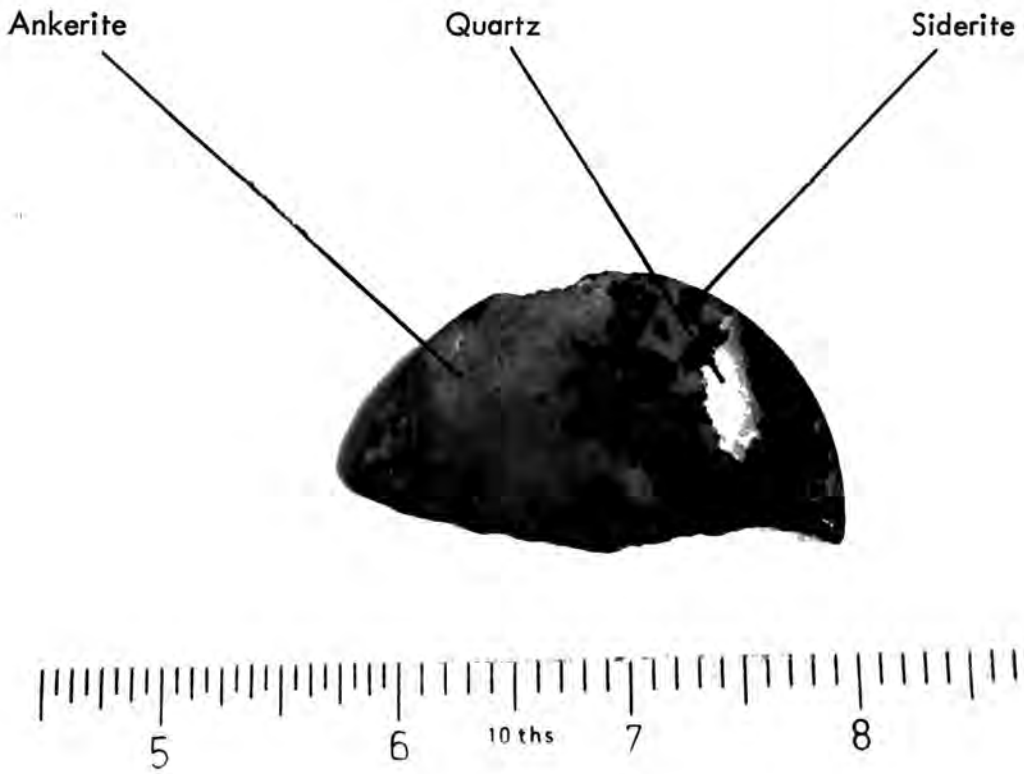

Fig. 37. Stained magnetite-hematite-carbonate ore. Euhedral crystals of siderite stained brown and quartz, unstained, in ankerite which is stained re-mauve. Scale in inches.

Table 12 X-ray diffraction data for Iron Duke magnesio-siderite

Magnesio-siderite $Fe_{0.5}Mg_{0.5}CO_3$ (Sample 60-643)

dA (Å)	I/I_1	hkl
3.59	50	012
2.781	100	104
2.331	70	110
2.120	80	113
1.953	70	202
1.783	60	024
1.718	90	018, 116
1.497	60	122
1.415	60	214
1.388	40	208
1.346	60	030
1.192	40	128
1.077	60	134
1.062	40	226
0.978	50	404
0.968	50	318
0.925	60	3.0.12

hexagonal cell:

$a_o = 4.680 \pm 0.002$ Å

$c_o = 15.254 \pm 0.009$ Å

Two samples of intermixed siderite and ankerite were examined by electron microprobe and the analyses are plotted in Fig.35. The siderite compositions were different in each sample, as shown by the two analyses in Table 13.

In sample 60-643, the siderite has an $MgCO_3$ component of about 40% by weight and is therefore not a true siderite but a member of the solid solution series between siderite and magnesite (Fig.38). The siderite crystals occur as well formed blades amongst ankerite and these bladed crystals are usually zoned with a clear outer rim, a mottled inner zone and a clear centre. A traverse across one of these zoned crystals is shown in Table 13 and it is clear that the outer rim is siderite but the inner core is ankerite. The intermediate cloudy zone contains a composition intermediate between the two, containing approximately 31% $CaCO_3$, 32% $MgCO_3$ and 32% $FeCO_3$. This composition has not previously been recorded in the literature and can result from one of two possibilities:

(i) The material is a mixture of ankerite and siderite intermixed so finely that the two could not be distinguished by an electron microprobe spot of about 10 microns.

(ii) Fe can substitute for Ca in the ankerite structure or Ca can substitute for Fe in some siderites. This suggests that there may be solid solution series between points on the dolomite-ferrodolomite join and points on the magnesite-siderite join (Fig.38).

The second possibility suggested above is supported by the analyses from sample 74-811 of coarsely crystalline siderite,

Table 13. Electron microprobe analyses of intermixed siderite and ankerite

60-643	$CaCO_3$	$MgCO_3$	$FeCO_3$	$MnCO_3$	Total
Intermixed siderite and ankerite:					
(a) Siderite	0.4	40.8	53.4	4.2	98.4
	0.4	38.4	55.7	4.6	98.7
	0.1	41.3	54.8	3.2	99.4
	0.3	40.6	52.3	5.3	98.5
	1.5	43.5	50.9	3.7	99.6
(b) Ankerite	51.1	35.1	8.9	1.2	96.3
	43.1	30.4	23.1	3.1	99.7
Zoned crystal:					
Clear, outer rim	0.6	38.3	57.5	3.5	99.9
Mottled zone	31.0	31.9	32.0	2.9	97.8
Clear centre	50.6	37.3	7.3	1.0	96.2
74-811					
Large, mottled crystals	35.2	31.1	30.7	1.7	98.7
Small, clear crystals	52.3	30.5	14.2	1.5	98.5

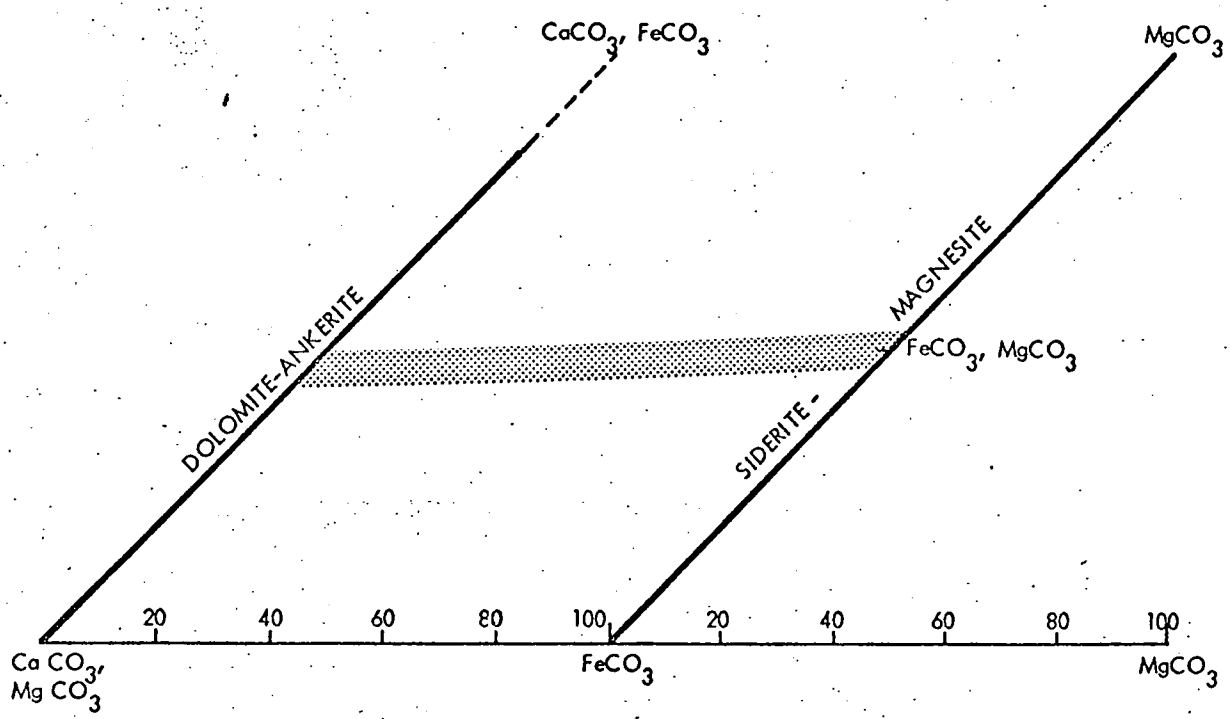

Fig. 38. Carbonate solid-solution series
Stippled area shows new solid solution series suggested by Iron Duke carbonate compositions.
Data from Deer Howie and Zussman 1963.

which is the main carbonate in the sample. The siderite analysis shown in Table 13 is similar to that of 60-643 and reconnaissance throughout sample 74-811 showed that this composition is fairly uniform. It is concluded, therefore, that a new magnesio-siderite composition has been identified, approximating to $Ca_{0.3}Mg_{0.4}Fe_{0.3}CO_3$.

(e) Carbonate relationships

(1) Ankerite-calcite

The usual relationship is of vein calcite enclosing fragments of banded iron-oxide rich fragments which contain both calcite and ankerite. Within the fragments, the two carbonates are intimately mixed and ankerite is normally predominant. Both are usually fairly coarse grained. Ankerite also occurs within the calcite as minute scattered grains and subhedral crystals. The general impression from examining the stained samples with a low power binocular microscope is that the calcite is replacing ankerite but the textures are ambiguous and some of the banded fragments have a finer grain suggesting original ankerite-calcite layers.

(2) Ankerite-siderite

Siderite is normally coarsely crystalline. In banded samples it occurs as large crystals enclosing iron oxide bands and ankerite, when present, is distributed through the siderite as small clear patches (77-811).

When mixed with ankerite in vein structures, the siderite often shows well developed crystal forms which are sometimes bladed (60-643) as can be seen in Fig.37 . However, staining and low power mignification show that these bladed crystals are riddled with small

patches of ankerite which concentrate in the centre of the crystal, whilst the rim is well formed. There is sometimes a zoning of light and dark bands parallel to the sides of siderite crystals. In hand specimens, the siderite crystal edges appear to have sharp, straight contacts with the surrounding ankerite but magnification shows frequent small, irregular embayments which are generally concave towards the siderite crystal. When ankerite is dominant in a vein, small irregular patches of siderite occur dispersed through it and frequently define faint crystal outlines.

Electron microprobe analyses (Table 13) show that the ankerite coexisting with siderite is similar in composition to the ankerite throughout the rest of the orebody.

The general impression conveyed by the textural relationships is that the ankerite is replacing siderite. However, this must be regarded with caution, as the textures are usually ambiguous.

2. Basal carbonate unit

The fresh rock is light grey in colour, and fine to medium grained. In the southern half of the area, where it is near to hematite ore, the rock becomes red due to finely dispersed hematite. When stained with hot Alizarin Red S and NaOH, it becomes a uniform red-mauve of a similar shade to the ankerite in the magnetite-hematite-carbonate body.

Nine whole-rock analyses are given in Appendix I and two representative analyses are shown in Table 14. The rock is characterised by its uniform composition and low trace element values.

Thin sections show a coarsely crystalline mass of interlocking crystals varying widely in size but with the range 0.2mm to 0.5mm predominant (Fig.39). Crystal edges are ragged and the crystal forms are generally irregular but are sometimes roughly rounded or elongate. Larger crystals often contain, and appear to be replacing, small crystals and are themselves surrounded by interstitial, very fine grained carbonate. All the crystals are cloudy and often contain fluid inclusions which may have small bubbles. Cleavages are well developed in some crystals and poorly developed in others.

Electron microprobe analyses of crystals in one sample (47-1041) show compositions very similar to the whole-rock analyses. Seven analyses are given in Appendix II and three of these are shown in Table 14b. The analyses confirm that the carbonate composition is uniform from crystal to crystal and there is no mineral zoning.

Table 14A. Whole-rock analyses of the Basal Carbonate unit Iron Duke

Analysis XRF by author

Per cent	47-1197	59-1352
SiO_2	0.1	0.4
Al_2O_3	0.2	0.2
Fe_2O_3	5.4	6.7
MgO	14.6	12.8
CaO	27.4	25.1
Na_2O	0.0	0.0
K_2O	0.1	0.1
TiO_2	0.1	0.1
MnO	0.9	1.1
S	0.0	0.0
P_2O_5	0.2	0.01
Diff.	51.0	52.4
	100.0	100.0
ppm		
Zn	11	1
Ni	5	3
Ba	0	0
Nb	0	0
Zr	3	3
Y	4	11
Sr	10	18
Rb	5	3

Table 14B Electron microprobe analyses of carbonates in the Basal Carbonate unit, Iron Duke

Element analyses recalculated as carbonates.

Sequence from a typical large, clear carbonate crystal to the surrounding granular, fine grained, cloudy matrix:

	$CaCO_3$	$MgCO_3$	$FeCO_3$	$MnCO_3$	Total
Large crystal centre	53.2	32.9	12.9	1.6	100.6
Large crystal rim	51.4	32.3	13.3	2.2	99.2
Fine-grained matrix	52.1	32.1	11.4	3.3	98.9

Fig. 39a. Core sample of the basal carbonate unit, Iron Duke, Note the fine, even grain. Sample no. 47-1041. Scale in inches.

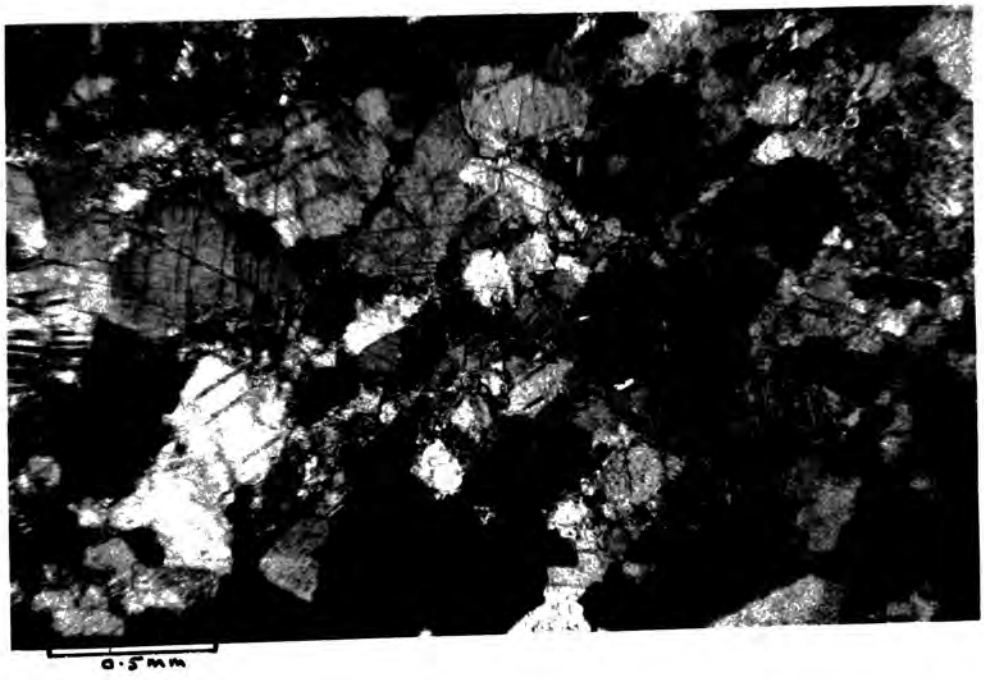

Fig. 39b. Thin section of the basal carbonate unit, Iron Duke. Sample No. 47-1038, crossed polars.

The fine grained interstitial material is essentially the same composition as the larger crystals.

In one drillhole (DDH83, 1000S Fig.20) bands of carbonate several feet thick were interlayered with quartzite and iron-formation bands of similar thickness. These carbonate bands often contain thin but distinct layers of magnetite forming a well defined banding. They have a microtexture similar to that described above except that the carbonate grains tend to be elongate and aligned approximately parallel to the banding. The magnetite is in fairly evenly sized blocky grains also aligned roughly parallel to the banding. At contacts with siliceous bands the quartz is coarsely crystalline and small patches occur amongst the carbonate grains.

A little talc occurs in thin layers in the upper part of the unit.

3. Talcose rocks

Rocks in the upper talc zone consist of talc schists and massive quartz-talc rock with variable amounts of magnetite and hematite. The proportions of talc, quartz and iron oxides vary rapidly and thin, 1"-2" layers of quartz rich rock can alternate with soft,green talc schist (Fig.40a,b). The talc occurs in small, fibrous crystals, generally aligned parallel to the major fold axis, producing a distinct schistosity.

Quartz rich material occurs either as layers parallel to softer magnetite-talc bands or as patches, often rounded and several feet across. These patches are surrounded by talc-magnetite which is often well banded and is folded around the harder block. The softer material has a well developed schistosity and traces of this appear in the siliceous patch. Within the siliceous patch, there is a tendency for the quartz to be concentrated into layers separated by very thin talc rich bands, and this layering is roughly parallel to that of the enclosing magnetite-talc schist. Hematite is the predominant iron oxide in siliceous parts although in some darker, glassy patches magnetite is also present. The hematite is often in spots 1mm to 2mm across and is usually silvery, bladed specularite (Fig.40b).

Talc-magnetite schists generally show a distinct layering due to the concentration of magnetite into bands. The magnetite bands are generally not more than 1"-6" thick and have a granular texture.

Fig. 40a. Talc zone exposure - layered magnetite-hematite-talc with siliceous patches. Tunnel No. 4, north wall. Scale given by magnet at bottom of photograph.

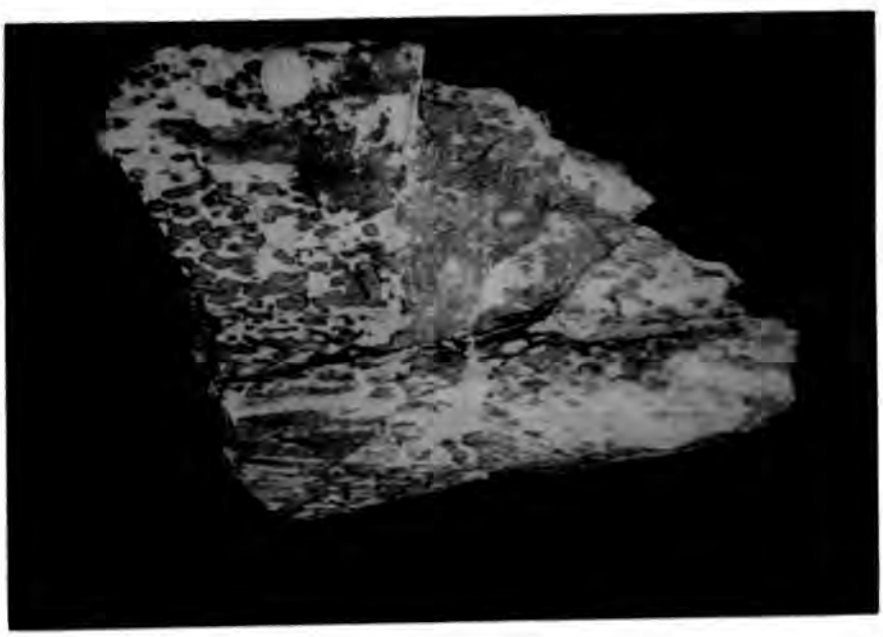

Fig. 40b. Talc zone sample - quartz-hematite-talc rock. Note the spots of bladed hematite. The sample is approximately one foot long at its base. Tunnel No. 4.

The lower talc zone is a thin layer underlying the magnetite-hematite-carbonate ore in the northern, deeper area and consists of talc-magnetite-hematite schists, chlorite schists and irregular carbonate patches. In parts, it contains considerable pyrite, often in small well developed crystals.

Whole-rock analyses of four samples from the talc zones are given in Appendix I and two of these are shown in Table 15. The analyses are not truly representative, as there is considerable variation in the proportions of quartz, talc and iron oxides but they give a fair impression of the simple chemistry. Trace element contents are low in all the analyses.

In thin section, the talc rich bands show a uniform texture of parallel talc fibres with occasional elongate quartz crystals aligned parallel to the schistosity. Small, blocky iron oxide grains are dispersed irregularly through the talc. In quartz rich bands, the quartz is densely packed and has an unusual elongate, bladed form with ragged crystal ends and undulose extinction (Fig. 57, Section III) Quartz crystals are generally evenly sized, between 0.1mm and 1.0mm long with some crystals reaching 5mm in length, and they are usually aligned with the long axes parallel. Extinction is oblique to the crystal axes. The crystals appear to have a well developed cleavage parallel to the long axis but high power magnification shows that the 'cleavages' are, in fact, long needle-like inclusions of talc or amphibole. Talc occurs as flakes and needles amongst the quartz and is broadly aligned parallel to the long axes of the quartz crystals. Iron oxides occur as patches up to 2mm across and often roughly oval

Table 15 Whole-rock analyses of talc zone rocks

Major element analyses by Chemical Laboratory, B.H.P., Whyalla.
Trace elements, XRF by author

Per cent	59-387	77-275
SiO_2	47.7	47.2
Al_2O_3	0.1	0.1
Fe_2O	47.3	42.0
MgO	3.0	8.6
CaO	0.1	0.1
Na_2O	0.0	0.1
K_2O	0.0	0.0
TiO_2	0.1	0.1
MnO	0.1	0.1
S	0.0	0.0
P_2O_5	0.1	0.1
Ig. Loss	+0.4	0.7
	98.1	99.0
ppm		
Zn	5	5
Cu	0	0
Ni	7	8
Ba	0	0
Zr	1	4
Y	0	0
Sr	0	1
Rb	0	0

Nb is in the order of 1 ppm to 4 ppm for both samples.

in shape with the long axis parallel to the schistosity.

Both magnetite and hematite are present in all the talc zone samples. Magnetite tends to occur in distinct layers (Fig.40) and is in small, regularly sized crystals which are often densely packed together. In the talc-iron oxide schist layers, magnetite is the predominant oxide.

Hematite frequently partly replaces magnetite and tends to form large flaky areas in optical continuity. This is particularly noticeable in the quartz rich patches, where the hematite occurs in spots (Fig.40b). Within the spots are densely packed magnetite crystals partly replaced by hematite which forms an irregular skeletal framework in the form of rudimentary specularite crystals. The replacement of magnetite grains is therefore not a simple pseudomorph mechanism but is part of the development of larger hematite crystals.

Twenty four electron microprobe analyses of talc from five samples are plotted on Fig.41. The results are given in full in Appendix II and three representative analyses are shown in Table 16.

The talc is unusual in its high iron content. No natural talcs of this composition have been previously recorded although work on synthetic talcs has shown that such compositions are stable (French 1971). The two talcs most commonly found are the Mg end member $Mg_3Si_4O_{10}(OH)_2$ which is common talc, and much more rarely, an iron rich member, which is minnesotaite. The Iron Duke talc is

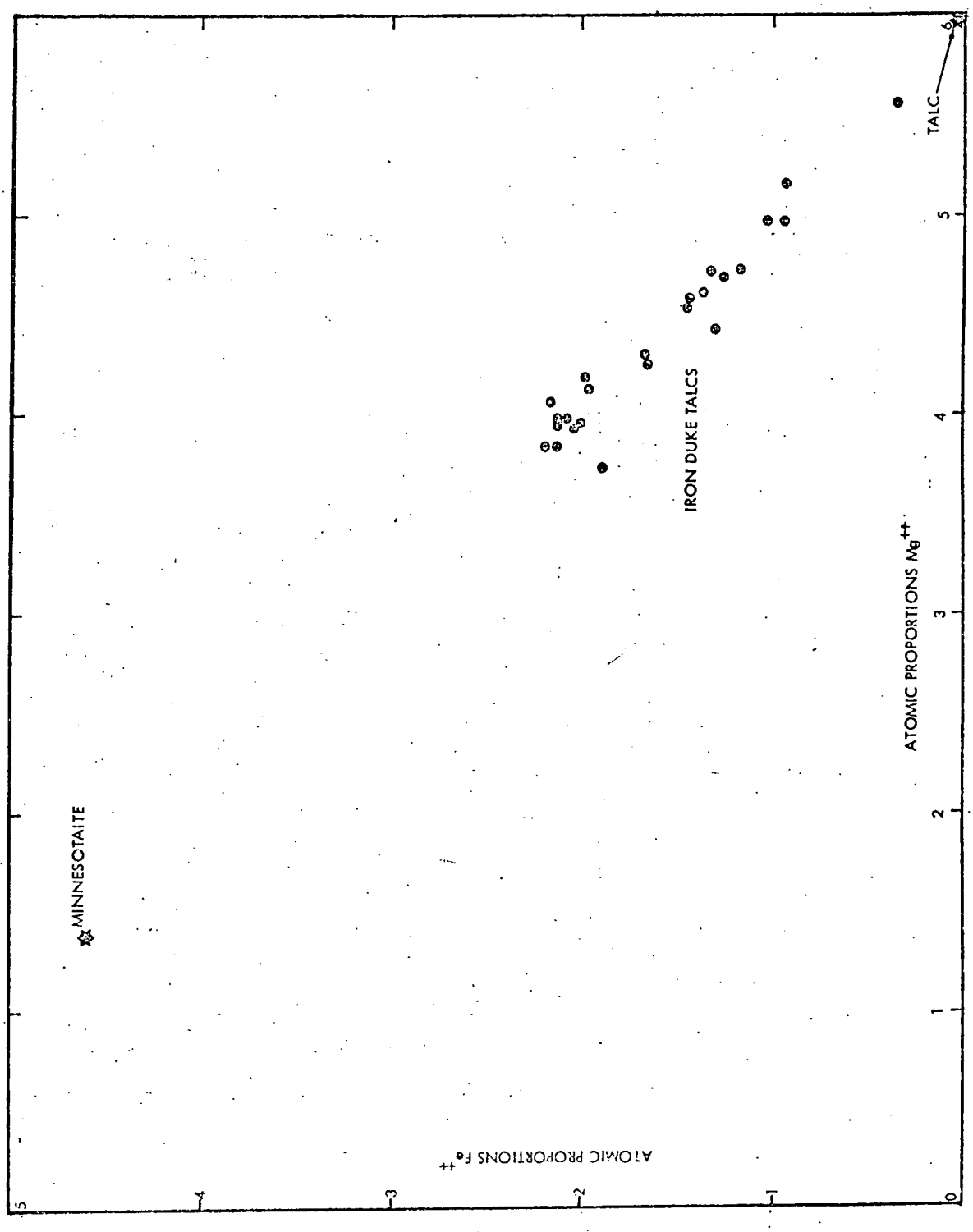

Fig. 41. Compositions of Iron Duke talcs compared with pure talc and minnesotaite.

Table 16. Electron microprobe analyses of talc from Iron Duke

	59-633	2159	74-453
SiO_2	61.8	61.0	56.4
Al_2O_3	N.D.	0.2	N.D.
FeO	3.1	10.5	18.4
MgO	28.7	24.1	18.2
CaO	0.1	0.0	0.1
Na_2O	N.D.	0.1	N.D.
TiO_2	N.D.	0.0	N.D.
MuO	N.D.	0.0	N.D.
Total	93.7	95.9	93.1

Atomic proportions on the basis of 22 oxygens.

Si	8.04	8.03	7.98
Al	-	0.03	-
Fe_2	0.34	1.16	2.18
Mg	5.56	4.73	3.84
Ca	0.01	0.00	0.02
Na	-	0.03	-
Ti	-	0.00	-
Ma	-	0.00	-

between the two and shows that members of the solid solution series other than the two previously recorded members can occur in nature.

4. Amphibolites

Rocks categorised as amphibolites are of two distinct types, unchloritised and chloritised. The former include the large basic intrusive which penetrates the southern part of the synform and some drillhole intersections of unaltered intrusive from below the basal carbonate unit. The chloritised intrusives include the northern dyke sheets and a small irregular intrusive in the west limb of the synform, all of which are within or near to the magnetite-hematite-carbonate orebody.

Unchloritised amphibolites are massive, dark green rocks, fine to medium grained with an equigranular igneous texture. There is sometimes a weak foliation due to the parallel orientation of dark minerals. Thin, cross cutting fractures filled by green chlorite are often present.

Whole-rock analyses for 27 samples are given in Appendix I and one of these is shown in Table 17. The compositions of all the samples are very similar and the most significant feature of the analyses is the high, and somewhat variable iron content which averages 14.3% Fe_2O_3 with a range between 12.0% and 16.4% Fe_2O_3. Trace element data are summarised in Fig.42 and are notable for the generally high Ba content and the occasional high Sr values.

Thin sections show the rock to consist of plagioclase (40% - 50%), hornblende (25% - 35%), chlorite (10% - 25%), and quartz (2% - 5%), with lesser amounts of sericite and ilmenite. The plagioclase was determined optically as andesine-labradorite using the albite twins and combined Carlsbad-albite twin extinction method. The typical texture is an interlocked mass of evenly

Table 17. Whole rock analyses of amphibolites from Iron Duke

Major element analyses by Chemical Laboratory, B.H.P., Whyalla.
Trace element analyses, XRF by author.

Per Cent	Unchloritised 66-584	Chloritised 67-908
SiO_2	51.2	29.6
Al_2O_3	13.4	13.7
Fe_2O_3	15.0	24.3
MgO	5.8	17.4
CaO	10.1	0.9
Na_2O	1.9	0.1
K_2O	0.6	0.0
TiO_2	1.4	2.9
MnO	0.3	1.2
S	0.1	0.1
P_2O_5	0.3	1.2
Ig. Loss	0.9	9.4
	100.1	100.8
ppm		
Zn	113	239
Cu	82	70
Ni	56	78
Ba	409	9
Nb	3	4
Zr	90	174
Y	29	27
Sr	115	4
Rb	20	0

sized felspar and hornblende crystals usually in random orientation (Fig.43), but sometimes with a well developed alignment. In the large intrusive mass, the amphibole crystals are well formed and sometimes appear to contain traces of pyroxene but in smaller bodies they tend to be flaky with ragged ends. The plagioclase is usually intensely sericitised but there are sometimes patches of clear material. Green chlorite appears to be replacing amphibole and, to a lesser extent, plagioclase. This chlorite is optically quite different from the chlorite in the cross cutting veins which shows anomalous blue interference colours and is similar to that in the chloritised intrusives. The mineral composition of the large basic mass in the south of the area is that of a diorite (Joplin 1964).

Chloritised amphibolites are massive, dark green and fine to medium grained rocks with an even, igneous texture. They are generally soft enough to be scratched by a finger nail, producing a white, slightly green-tinted streak.

Whole-rock analyses for seventeen samples are given in Appendix I and one typical analysis is shown in Table 17. The chloritised amphibolites are all similar in chemical composition and are markedly rich in iron and magnesia but low in silica, calcium and alkalis relative to the unchloritised amphibolites. Trace element contents, summarised in Fig.42, show that they have higher Zn, but lower Ba and Sr values than the unchloritised amphibolites.

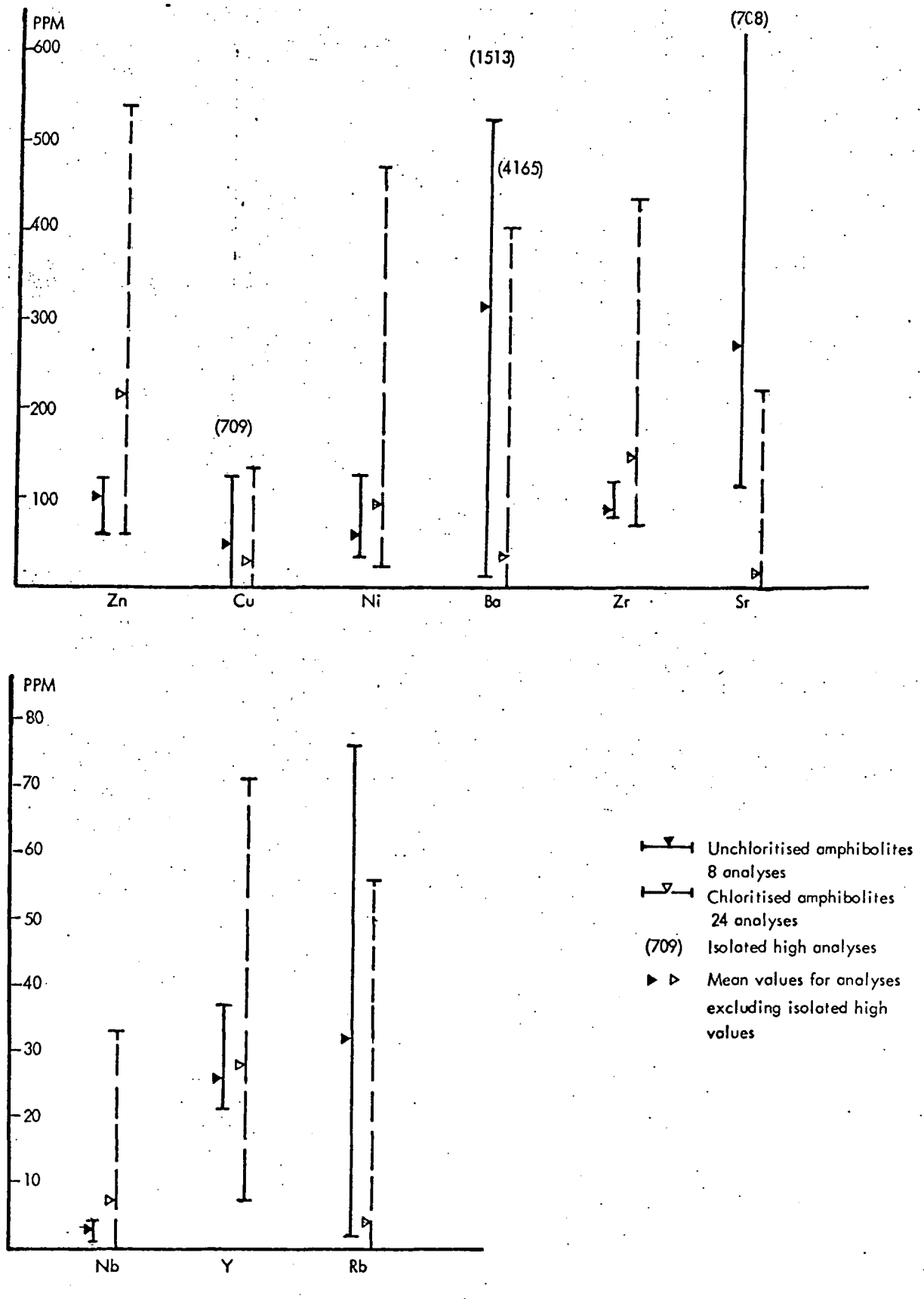

Fig. 42. Trace element data for chloritised and unchloritised amphibolites.

Fig. 43a. Thin section of unchloritised amphibolite, from the large mass of dioritic composition in the southern half of Iron Duke. Sample 66-240, crossed polars. Feldspar, amphibole and quartz.

Fig. 43b. Thin section of chloritised amphibolite from a dyke in the vicinity of the magnetite-hematite-carbonate ore. Chlorite. Sample 78-224, crossed polars.

Thin sections (Fig.43) show the rock to be entirely chlorite with minor amounts of leucoxene, carbonate, zircon, magnetite and apatite (Whitehead and Burger, unpublished company reports). Two chlorites are sometimes present, differing slightly in strength of pleochroism and order of interference colour. Both occur as flaky, lath-like crystals which may be oriented at random or aligned parallel, forming a strong lineation. Many chlorite crystals have the form and general appearance of amphiboles in the unchloritised amphibolites and small patches with second order interference colours are sometimes present which may be remnant amphibole. Plagioclase ghosts, showing faint Carlsbad and Albite twinning are present in some sections, and occasionally the crystal outlines enclose a mass of fine chlorite crystals which have the same texture as sericite in unchloritised amphibolites. Leucoxene and ilmenite are distributed fairly evenly throughout the rock but carbonate, when present, is in cross-cutting veins and patches.

5. Hematite ore

The ore is granular blue hematite which varies in character from a hard, compact, massive rock (Fig.44) to a friable powdery mass that crumbles when touched. It is blue-black in outcrop, blue in tunnel faces and drill core and becomes red when mixed with clay, or with calcite in the deep northern orebody.

Six whole-rock analyses are given in Appendix I and two of the analyses are shown in Table 18. These show that the ore is essentially pure hematite with small amounts of Si, Mg and Ca in samples near to iron-formations, talcose rocks or magnetite-hematite-carbonate. It is low in trace elements except Zn with a maximum of 105 ppm, and Cu which shows erratic high values of up to 261 ppm in the layer of deep hematite ore below the magnetite-hematite-carbonate body. Most of the samples are drillhole samples, and it is difficult to establish whether the high zinc and copper values are related to features within the orebody or to basic intrusives. Trace element data are summarised in Fig.45.

In outcrops and in tunnel exposures, there is frequently a well developed fine scale banding, as shown in Fig.44, which is similar to that in the iron-formations. When a low magnification (x10) is used, the banding is seen to be due to varying pore space in different bands, the hematite being close packed and blocky in some bands and more open with a good deal of pore space in others. Small, well developed crystals of dark blue specular hematite sometimes project into the cavities.

Table 18 Whole-rock analyses of hematite ore from Iron Duke

A. Assays of drillcore by Chemical Laboratory, B.H.P., Whyalla

Per cent	42-105	42-315
SiO_2	1.8	9.2
Al_2O_3	0.4	0.8
Fe_2O_3	95.1	78.3
MgO	0.1	4.9
CaO	0.1	2.0
Na_2O	N.D.	N.D.
K_2O	N.D.	N.D.
TiO_2	0.1	0.1
MnO	0.1	0.3
S	N.D.	N.D.
P_2O_5	0.1	0.2
Ig. Loss	1.5	5.1
	99.3	100.9

B. Trace elements in hematite ore samples, XRF by author

	3178	71-995
Zn	13	105
Cu	3	140
Ni	2	47
Ba	35	21
Nb	0	0
Zr	0	0
Y	1	1
Sr	9	4
Rb	0	0

Fig. 44. Hematite ore sample showing well developed layering. Surface sample at 5000S. Scale in inches.

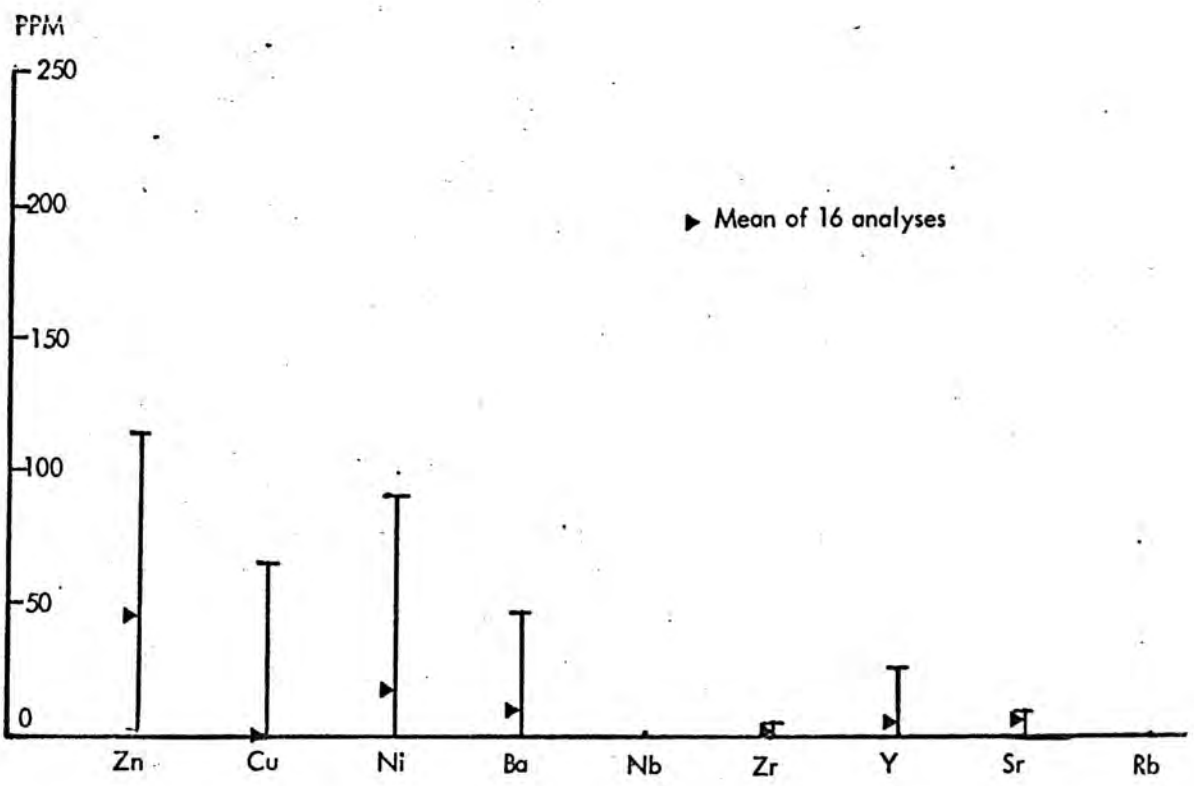

Fig. 45. Trace element data for hematite ore.

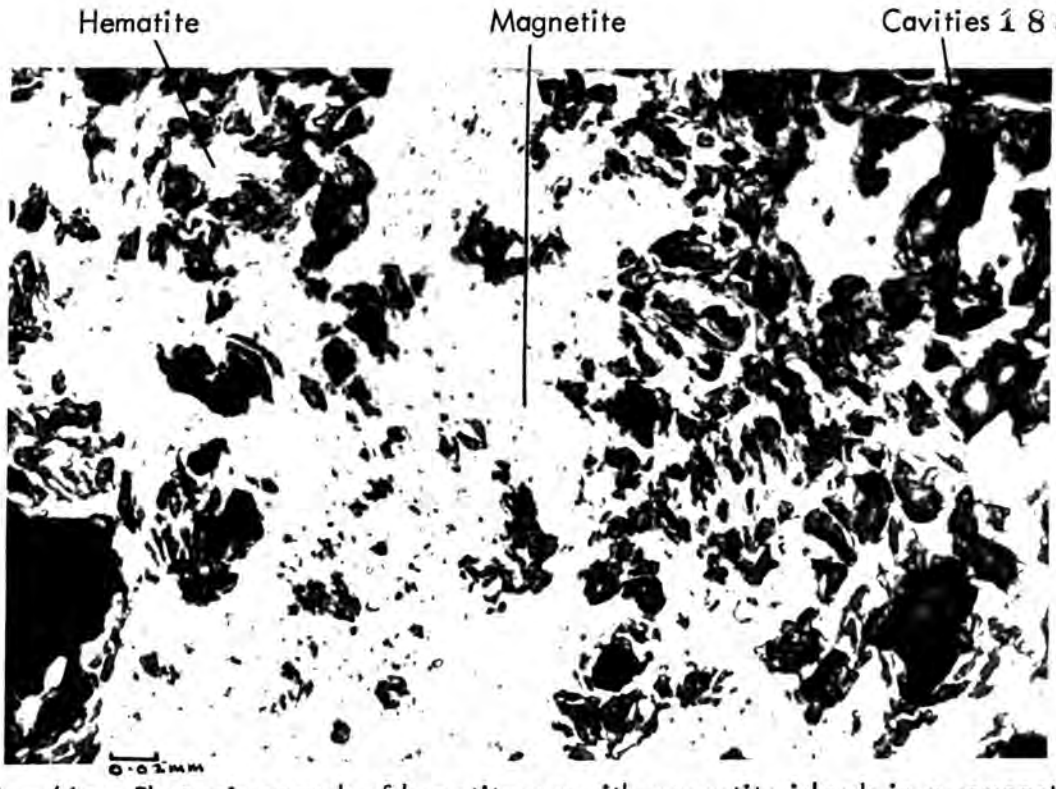

Fig. 46a. Photomicrograph of hematite ore with magnetite islands in a compact ore layer.
Sample no. H2, polars half crossed.

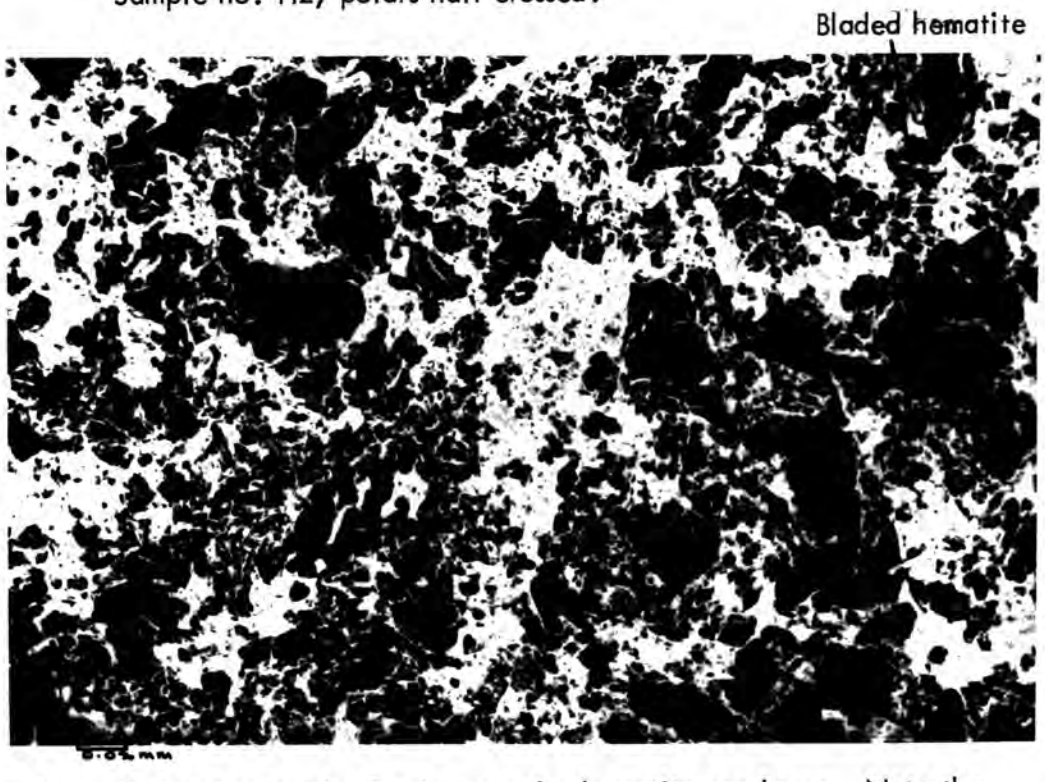

Fig. 46b. Photomicrograph of soft, granular hematite ore layer. Note the high percentage of open space and the small blades of hematite projecting into cavities.
Sample no. H2, polars half crossed.

Polished sections of typical ore show a fine grained interlocking mosaic of hematite grains with numerous, evenly dispersed cavities (Fig.46). Very fine grained bladed hematite is common and often forms a network that holds together the blockier grains. Under crossed polars, the grains are seen to consist of smaller, interlocked hematite crystals with irregular boundaries and in random orientation. Small islands of magnetite are common in the grain centres and the grains themselves often have a roughly cubic outline. Thus, a good deal of the ore appears to be formed from magnetite as reported by Edwards (1936).

In well banded samples, the bands show different micro-textures, more compact bands having a higher proportion of blocky grain forms and large evenly spaced cavities, whereas the softer, finer grained bands consist of very small hematite grains linked in a mesh with ubiquitous small cavities. Finer grained hematite is sometimes arranged in elongate outlines with the rough form of bladed crystals, similar in size and shape to the iron-formation amphiboles. The pore spaces are of varied shape and size but are often rounded and sometimes elongate. Small specularite crystals frequently project into the cavities and, less commonly, the corners of larger cubic grains also project into the cavities.

6. Schists of Death Adder Gully

The schists are fine grained compact rocks in outcrop which show a well marked schistosity on broken surfaces. They mark easily with a hammer, giving a white streak, and in thin section are seen to consist of quartz, biotite and chlorite together with lesser amounts of amphibole and garnet. Quartz lenticles are common and strike parallel to the schistosity.

The schists at the surface are similar in character to the argillaceous schists at Cook Gap to the north, described in Section I, although the Death Adder Gully schists contain rather more chlorite. Whole-rock analyses in Table 19 and Appendix I, show that the schists approximate in chemical composition to iron and magnesium rich shales and greywackes.

At depth, adjacent to the magnetite-hematite-carbonate body, there is a marked change of schist character with the chlorite content increasing and quartz-chlorite schist becoming the dominant rock type. Electron microprobe analyses of the chlorites show them to be iron-magnesium chlorites with a wide variety of iron-magnesium ratios. This is illustrated in Table 20, which shows analyses from a thin section (60-995) with two optically distinct chlorites, one being green and one brown. The brown chlorite is, in general, low in iron whereas the green chlorite has a high iron content, and the mineral composition is very similar to the chlorites in the Cook Gap schists described in Section I. It is unlikely that iron rich chlorites could have survived regional metamorphism to lower amphibolite facies grades and this, together with the lack of

Table 19. Chemical composition of schists in Death Adder Gully compared with average greywacke and lithic sandstone

Per cent	1. Average Greywacke	2. Lithic Sandstone	3. Death Adder Gully schist 4-85
SiO_2	66.7	66.1	63.0
Al_2O_3	13.5	8.1	10.0
Fe_2O_3	1.6	3.8)	12.1
FeO	3.5	1.4)	
MgO	2.1	2.4	6.5
CaO	2.5	6.2	0.1
Na_2O	2.9	0.9	N.D.
K_2O	2.0	1.3	N.D.
TiO_2	0.2	0.2	0.4
MnO	0.1	0.1	0.3
S	N.D.	N.D.	0.0
SO_3	0.3	N.D.	N.D.
P_2O_5	0.2	0.1	0.1
CO_2	1.2	5.0)	5.7 (lg. loss)
H_2O (Tot.)	3.0	4.3)	
	99.8	99.9	98.2

Notes: 1. Analyses 1 and 2 are mean compositions for those rock types, from F.H. Hatch and R.H. Rastall, "Petrology of the Sedimentary Rocks" 5th Edition, published 1971 by Thomas Murby & Co.

2. Analysis 3 is an assay of a chip channel sample over 5 feet of wall in Tunnel No. 4, Iron Duke.

Table 20. Electron microprobe analyses of chlorites in chloritised argillaceous schists from depth in Death Adder Gully

	Sample No. 60-995	
	Brown chlorite	Green chlorite
SiO_2	29.6	23.9
Al_2O_3	18.2	18.8
FeO	11.4	32.8
MgO	25.0	10.3
CaO	0.1	0.1
Na_3O	0.0	0.0
K_2O	0.0	0.0
TiO_2	0.0	0.1
MnO	1.6	0.8
Cr_2O_3	0.1	0.1
	86.0	87.0

Notes: 1. Fe expressed as FeO

2. Analyses by Dr. A. Peckett at author's request.

amphiboles and biotite, suggests that some subsequent chloritisation has taken place in the Death Adder Gully schists.

F. FLUID INCLUSIONS

In thin section, carbonates from the magnetite-hematite-carbonate body are frequently cloudy and, under high magnification, are seen to contain tiny inclusions some of which have bubbles moving in Brownian motion. These were first noted by Whitehead in unpublished company reports.

Fluid inclusion work requires sections or fragments sufficiently thick to ensure that all the fluid is retained on heating, and most of the carbonate proved too milky to be of use. However, some cleavage fragments, of coarsely crystalline vein material and from small euhedral crystals projecting into cavities, were sufficiently transparent for fluid inclusion work. Of 102 samples examined, 20 yielded results and the details are given in AppendixIV.

Fluid inclusions are of two main types (Roedder 1967); primary inclusions which result from small pockets of liquid becoming trapped within the crystal by differential growth and secondary inclusions which form when fluid penetrates fractures or cleavage planes in a pre-existing crystal and the fractures heal, leaving small pockets of liquid. The former are contemporary with the crystal but the latter may be formed during a subsequent period of hydrothermal activity. In the Iron Duke carbonates three types of inclusion can be distinguished:

(a) Suites of tiny (<0.01mm), generally ovoid inclusions arranged along inclined planes through the carbonate (Fig.47). They

are certainly controlled by fractures or cleavages and hence post-date the crystals but their homogenisation temperatures are similar to those of the larger, primary inclusions. They could have immediately followed crystallisation and still represent the one phase of hydrothermal activity, and are therefore called pseudosecondary inclusions (Roedder 1967).

(b) Larger (0·03mm - 0·06mm.) single inclusions, generally rhombic or square with sides parallel to the crystal faces when these can be seen (Fig.47). They tend to be isolated, often within clearer patches of carbonate and are considered to be primary, their shapes controlled by the growing crystal.

(c) Very large (>0·06mm) single inclusions, shaped identically to (b) but with unusually large bubbles which commonly fill up to one quarter of the visible inclusion area. They are also regarded as primary but are not used for temperature determinations as it is likely that necking has occurred, blocking off part of the inclusion and forcing the bubble into a relatively small volume. They give anomalously high temperatures as would be expected.

Many, but by no means all, of the inclusions contain a bubble which on average occupies about 2% to 5% of the total visible area. In the smaller inclusions the bubble is often in Brownian motion. Occasionally, larger inclusions may be divided by a faint straight or undulose line, suggesting the presence of two liquid phases. Small black specks, which remain unchanged on heating, frequently occur within the inclusions, but no

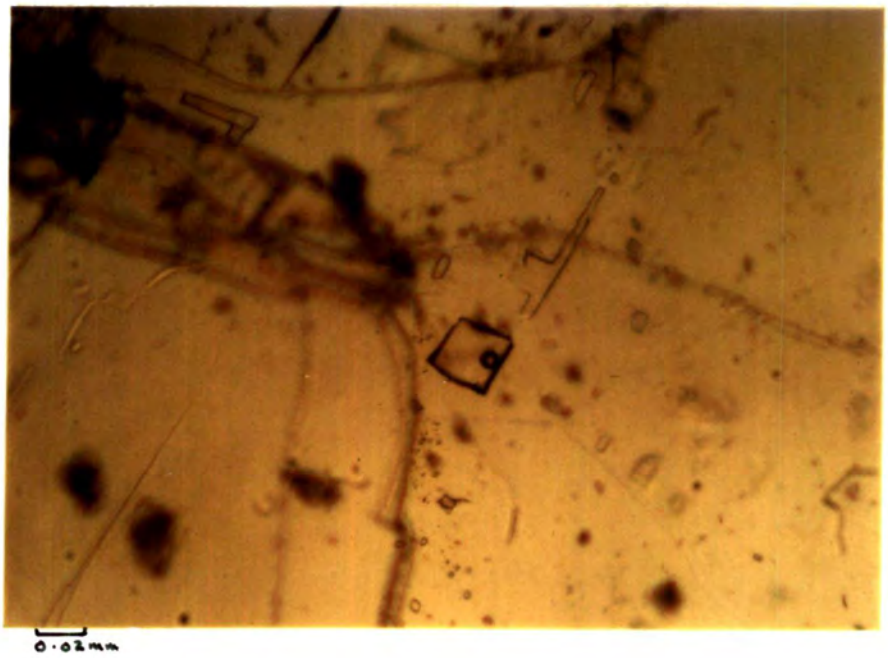

Fig. 47a. Primary fluid inclusion in ankerite.
Sample no. 86-686.

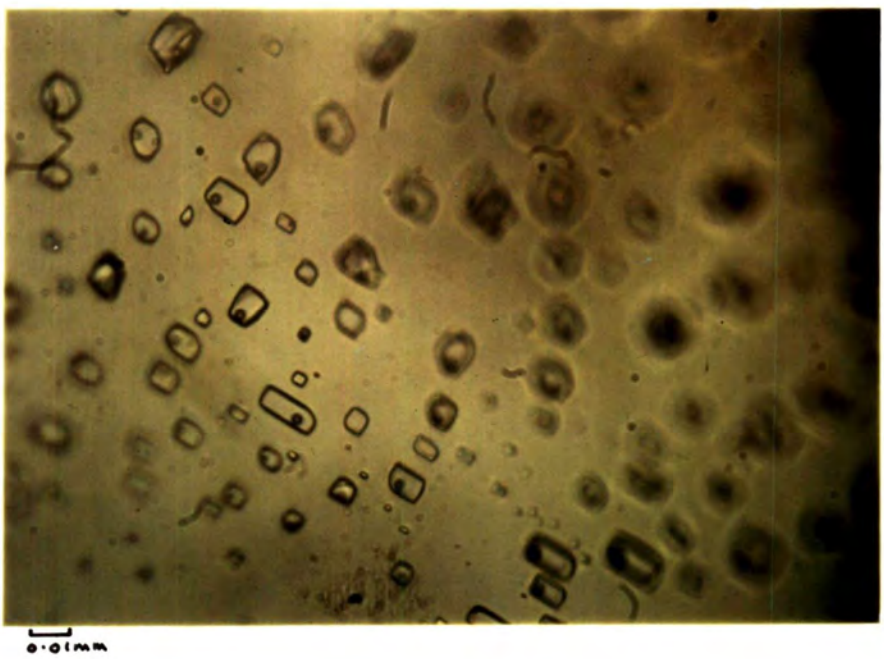

Fig. 47b. Suite of pseudosecondary inclusions in ankerite.
Sample no. 86-686.

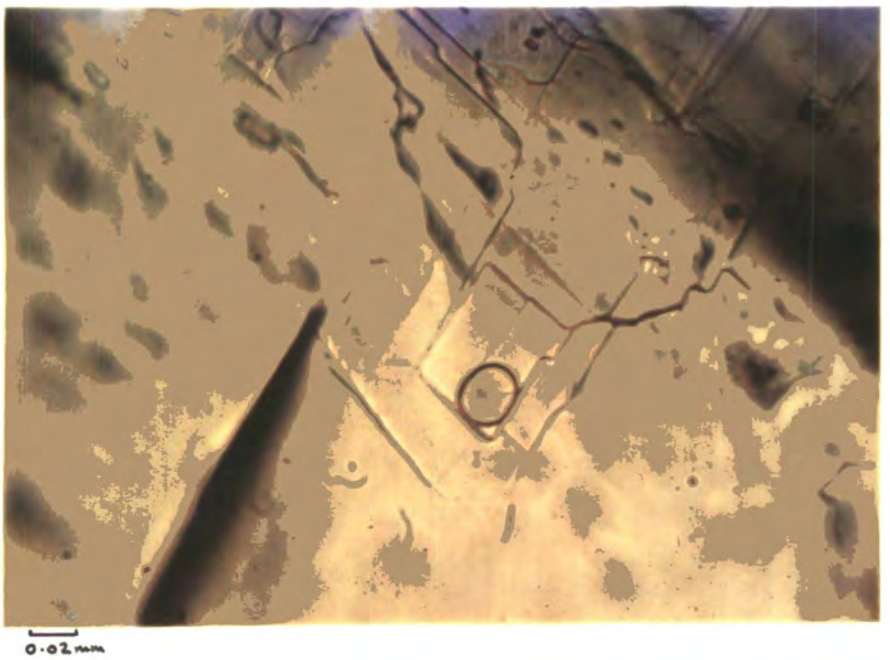

Fig. 47c. Primary inclusion with abnormally large bubble, probably due to necking. Sample no. 86-686.

crystalline substances were observed. The black specks may be opaque daughter minerals.

Temperature determinations were carried out using a Leitz microscope with a built-in heating stage as described in Appendix IV. The two most generally used methods of temperature determination are decrepitation and homogenisation (Roedder 1967, Yermakov 1950). A visual estimate of decrepitation was attempted by spreading a thin layer of crushed carbonate on the microscope heating stage and watching the sample for signs of movement whilst the temperature was raised. Movement of individual grains was occasionally violent but so rare as to provide no guide to the temperature of formation. The presence of considerable liquid within the crystals was shown by bubbling and flow from small cracks and fractures at the crystal surfaces. Audio-decrepitation was also attempted, using a sensitive microphone with the cover removed and a long, slender glass 'orchid' attached to the diaphragm. Crushed carbonate was placed in the wide end of the 'orchid' which was then fitted inside the heating stage. Rare explosions were detected but there was no indication of a general decrepitation temperature.

The homogenisation method is based on the principle that an inclusion completely filled with fluid at the temperature of formation will develop a bubble at lower temperatures due to the liquid contracting more rapidly than the surrounding crystalline material (Sorby 1858). On reheating, the bubble becomes smaller and disappears at a temperature defined as the homogenisation

temperature, which in some, but not all cases is the temperature of formation.

A bubble first forms in a liquid inclusion of given density when the pressure-temperature conditions fall to a certain point. Above this point, the inclusion will remain in liquid form to high temperatures provided sufficiently high pressures are maintained. The homogenisation method establishes the temperature of this point for a pressure of 1 atmosphere, but if the inclusion had formed under higher pressures it may have cooled from much higher temperatures before reaching the point at which a bubble could form. The homogenisation temperature is therefore a minimum temperature at which the inclusion was formed and a pressure correction is usually needed to obtain the true temperature of formation (Ingerson 1947, Yermakov 1950).

In addition to pressure and the correct choice of primary inclusions, Roedder (1967) cites three basic assumptions in using homogenisation temperatures:

(i) The fluid was a single, homogeneous phase.

(ii) The cavity did not change in volume after sealing.

(iii) Nothing is added to or lost from the inclusion after sealing.

Homogenisation temperatures for 203 primary inclusions from throughout the orebody are shown in Fig.48a. The dominant temperature is 120°C - 130°C but the curve is slightly asymmetric with a bulge in the region of 140°C - 160°C.

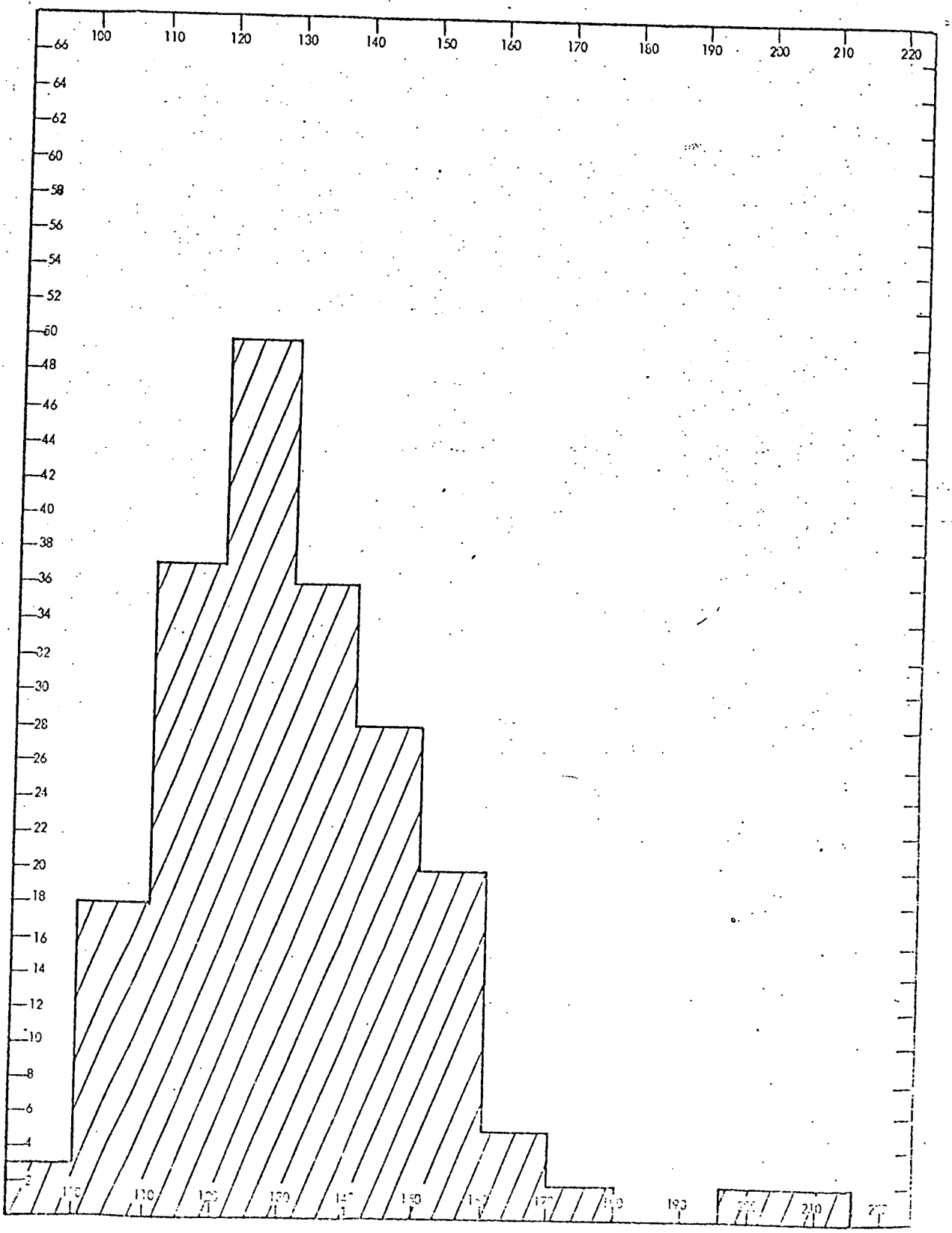

Fig. 48a. Homogenisation temperatures for 203 primary inclusions in magnetite-hematite-carbonate ore.

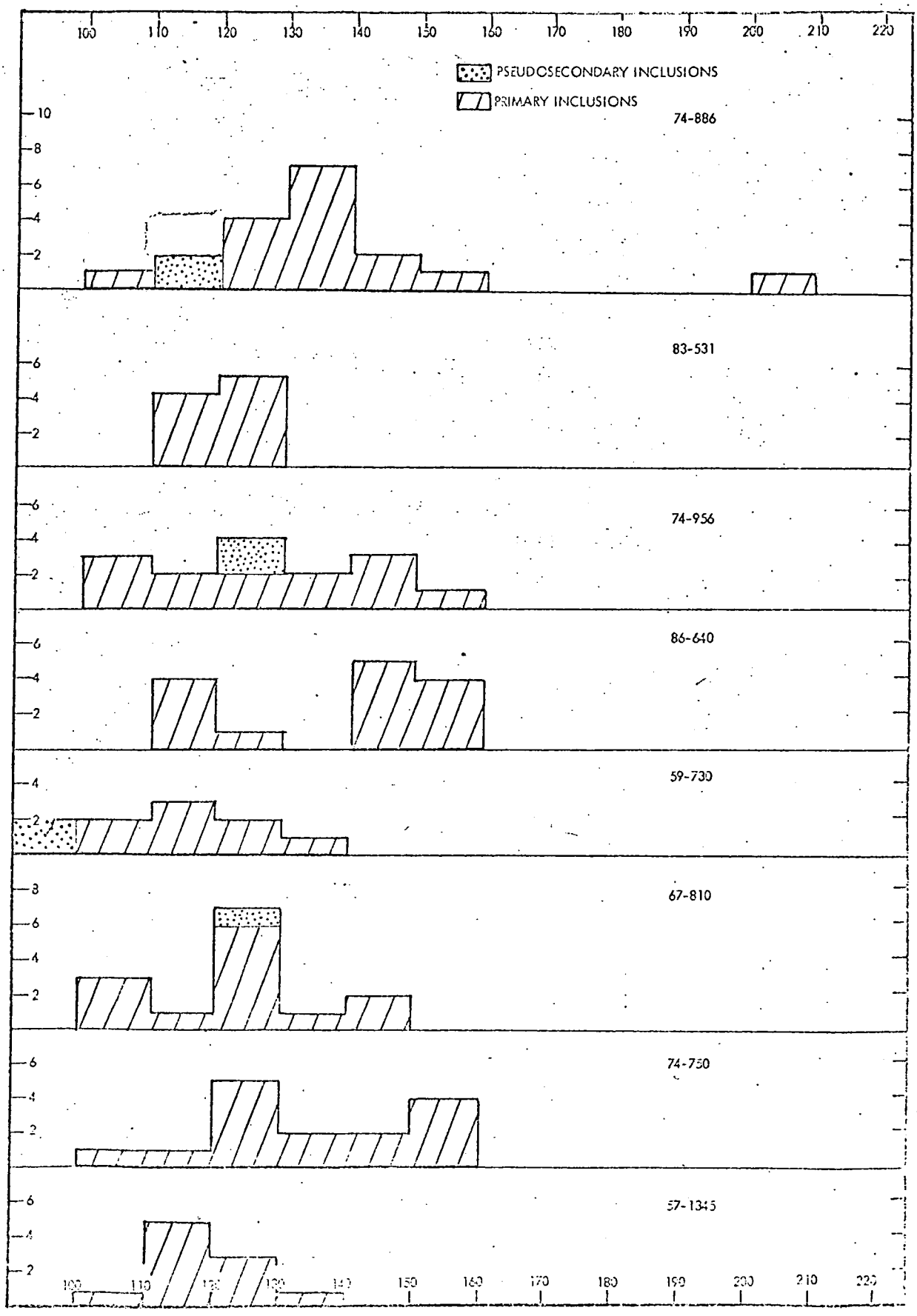

Fig. 48b. Fluid inclusion homogenisation temperatures for individual samples of magnetite-hematite-carbonate ore.

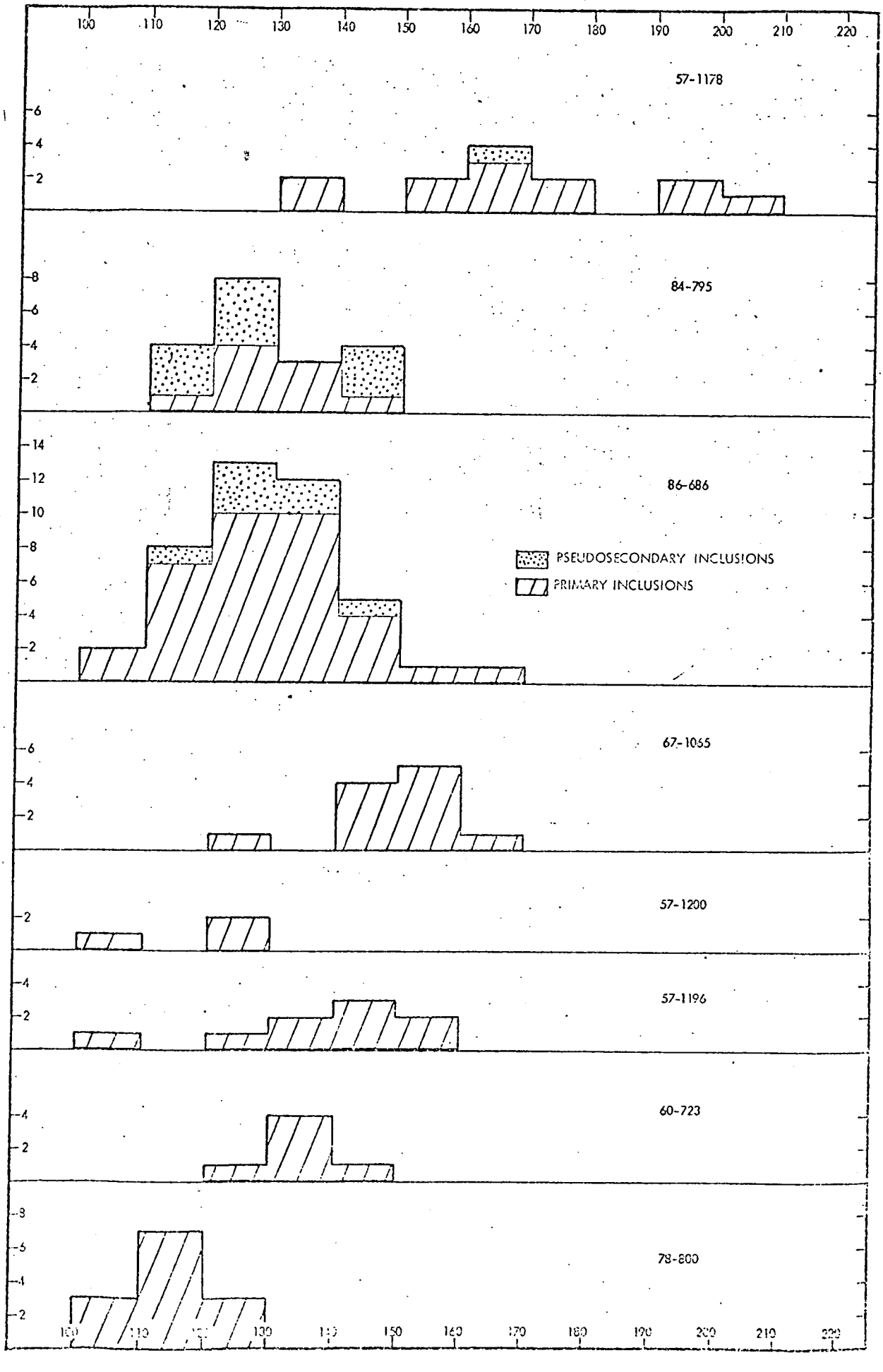

Fig. 48b. contd.

The individual results for 16 samples are shown in Fig.48b.

They group together as follows:

Table 21. Homogenisation temperatures for fluid inclusions

No. Samples	Temperature range
10	110°C - 140°C
3	140°C - 160°C
3	Two peaks, one in each of the above two temperature ranges.

Pseudosecondary inclusions gave broadly similar temperatures but less measurements were made and no definite groupings can be distinguished.

The primary inclusion homogenisation temperatures show that inclusions developed at two periods during the hydrothermal activity and at slightly different temperatures. Fig.49 is a generalised cross section of the orebody showing the approximate positions of the sixteen samples. The highest temperatures are recorded from the east and in the deep central part of the orebody. Lower temperatures are distributed throughout the whole orebody.

The chloritised basic dyke which cuts the orebody on the east side (Fig.49) is earlier than or contemporaneous with the hydrothermal activity as shown by the remnant igneous textures within the dyke. A sample from the contact (740750) shows two temperature peaks at 120°C - 130°C and 150°C - 160°C respectively. The dyke does not, therefore appear to have raised the temperatures locally to any great degree during the period that the inclusions were formed.

A limited number of freezing temperatures were determined

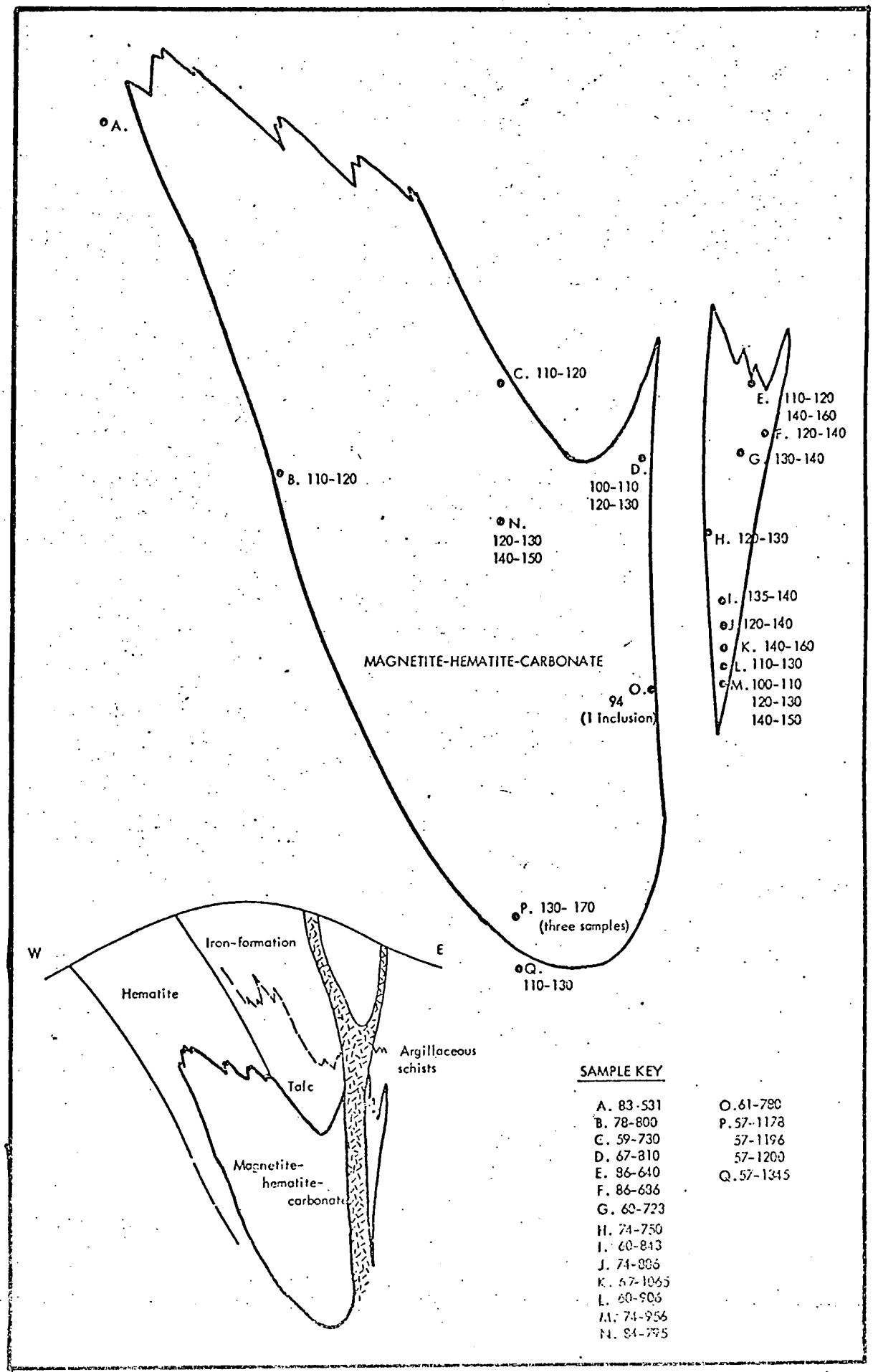

Fig. 49. Homogenisation temperatures of fluid inclusions in magnetite-hematite-carbonate ore and in carbonate veins below the main orebody. Scale for main diagram approximately 1 inch equals 160 feet.

using a freezing stage described in Appendix IV.

The freezing point of pure water is depressed by the addition of salts. Most deep natural hot waters and brines with NaCl as the main salt (Ellis 1967, Helgeson 1964). If NaCl is assumed to be the main salt present in a fluid inclusion, the depression of the freezing point can be correlated with known phase relationships in the NaCl-H_2O system and an estimate of the salt concentration can be made (Roedder 1962, 1963).

The inclusion is cooled until it is completely crystalline which usually means taking the temperature down to about -70°C. The temperature is then slowly raised until the crystals begin to melt and melting is maintained until only one crystal is left. The freezing temperature is defined as that temperature at which the last crystal melts under reversible equilibrium conditions (Roedder 1962). Equilibrium is checked by rapidly cooling the inclusion just before the last crystal disappears and the crystal should then begin to grow.

Freezing temperatures were determined on 31 inclusions in three samples (74-956, 86-686, 78-752). In one sample (78-956), the inclusions were in clear vein quartz and in the other two samples they were in vein carbonate. There was no difference in the results between quartz and carbonate.

The results may be summarised as follows:

Table 22. Freezing temperatures and indicated NaCl Contents

Number of inclusions	Freezing temperature °C	Indicated NaCl
26	-1° to -22°	18% to 21%
3	-12° to -14°	15% to 17%
2	-4° to -7°	7% to 8%

Inclusions with all three temperature ranges occurred within sample 86-686. This suggests that either the salt content was very variable in the fluid or that the inclusions represent several phases of hydrothermal activity with different salt contents in each.

Some inclusions did not completely freeze, part of the inclusion remaining liquid. This suggests the presence of liquid CO_2 which has a freezing point of -56.6°C and can remain unfrozen to temperatures well below that. However, it could also result from a metastable salt solution remaining liquid at low temperature.

From the freezing results, it is clear that the hydrothermal solutions were salt solutions but the proportion of different salts in solution remains unknown.

G. SUMMARY OF IRON DUKE GEOLOGY

The Iron Duke iron-formations are the lower of two major units which make up the Middleback Ranges. They are overlain by the argillaceous schists of Death Adder Gully and underlain by granitic gneisses and schists of the Gneiss Complex. The lower part of the Iron Duke iron-formation sequence contains a thick carbonate unit known as the basal carbonate.

The iron-formation sequence is folded into a tight synform which has a north-south striking axis pitching to the north at 10° to 20°, and an almost vertical, undulating axial plane. The east limb of the synform is intersected by a major north-south striking reverse fault which is inclined steeply to the west and has moved the iron-formations south and upwards relative to the schists of Death Adder Gully. Smaller scale faults with strikes in north-west and north east directions cut the iron-formations.

Hematite ore outcrops in the hinge area and west limb of the synform, passing northwards along strike in the west limb into iron-formations. The bulk of the ore is within 500 feet of the surface and passes down pitch and down dip into magnetite-hematite-carbonate and talcose rocks. A thin layer of ore extends down dip and pitch from the main orebody, along the base of the magnetite-hematite-carbonate body. The hematite ore is characterised by fine scale layering similar in appearance to that of the iron-formations, and the ore is frequently porous. It consists of equally sized hematite grains which sometimes show remnant magnetite patches and the spaces in porous ore are of similar size to the hematite grains.

The magnetite-hematite-carbonate occurs as a long cylindrical body in the hinge area and deeper parts of the synform west limb. Its shape may be broadly interpreted as a stratigraphic unit but in the centre of the synform the ore cuts across stratigraphic boundaries. The orebody has a steep eastern contact with schists of Death Adder Gully, the two being separated by the major high angle reverse fault. The ore consists of magnetite, hematite and carbonates in varied proportions and it is characterised by diffuse layering, brecciation and carbonate veining. Carbonate crystals within the ore are coarse grained and unoriented, producing typical metasomatic or hydrothermal textures. The bulk of the carbonate is an ankerite containing between about 5% and 15% $FeCO_3$ by weight, and this is the only carbonate present except at the base of the body where there is a thin calcite rich layer, and at the top of the body where intermixed ankerite and magnesiosiderite occur. The carbonate crystals are similar in composition in both the layered and vein structures, and this composition is almost identical to that of the underlying basal carbonate unit. The vein carbonate sometimes has small cavities into which project carbonate crystals showing inclusion zoning due to free growth. These show that hydrothermal solutions have moved through the magnetite-hematite-carbonate body, and studies of fluid inclusions in the carbonate crystals suggest that the solutions were brines at a minimum temperature of 120°C.

Talc rich zones occur immediately above and below the magnetite-hematite-carbonate body. The upper talc zone is thicker than the lower and passes gradually upwards into iron-formations.

It is characterised by green, iron-magnesium talc which occurs in crystals oriented parallel to the main fold axis, and by irregularly distributed quartz which, in thin section, has a bladed form. Hematite occurs in small, irregular spots and patches, whereas magnetite present in the rock is in small crystals confined to specific layers. The lower talc zone is thin, and consists of talc with lesser amounts of carbonate and considerable pyrite.

Iron-formations overly the hematite ore and the upper talc zone rocks and consist of fine grained quartz and iron oxides with lesser amounts of tremolite and grunerite-cummingtonite. They are identical to iron-formation units throughout the Middleback Ranges and are characterised by fine scale layering. In thin section, they have even, regular microtextures typical of regionally metamorphosed rocks.

The schists of Death Adder Gully consist of quartz, biotite and chlorite with lesser amounts of amphibole and garnet. At depth, adjacent to the magnetite-hematite-carbonate ore, they consist of quartz and chlorite, a good deal of the chlorite being rich in iron and therefore considered to be the result of chloritisation subsequent to metamorphism.

A large basic intrusive mass of dioritic composition penetrates the synform in the southern half of Iron Duke. Dykes extend northwards from this mass along the limbs of the synform, and where these dykes intersect the magnetite-hematite-carbonate and talc zones they are completely chloritised.

SECTION III: ORIGIN OF THE ORES

A. ORIGIN OF THE MAGNETITE-HEMATITE-CARBONATE ORE

1. Previous theories of ore genesis

Whitehead (1962 and company reports) proposed that the orebody formed by intense or prolonged carbonate metasomatism of siliceous iron-formations. The original rock type was a tremolite bearing iron-formation near the base of the sedimentary sequence, which was of variable thickness and in places contained layers or lenses of magnetite-ankerite. The unit was overlain by cummingtonite schists which were altered to spotted talc schists during the metasomatism. Solutions were circulated by the slow cooling of basic intrusives and the solution flow was controlled by folds, faults, fracture zones and impervious schist units. The solutions may have been heated meteoric waters guided to certain areas of the iron-formations by structures in overlying, younger sediments. In some company reports, Whitehead also drew attention to the possible association of hydrothermal activity with basic intrusives and with major shear structures.

Owen and Whitehead (1965) expressed the same basic theory, suggesting that the solutions were carbonic acid, the fluid movement was initiated by basic intrusives and the flow direction was controlled by structures.

Catley (1964) also considered that metasomatically introduced carbon dioxide penetrated amphibole rich iron-formations, converting the amphiboles to carbonate and talc. The silica released during this process was transferred to the

iron-formations above the ore, causing extensive silicification and reconstituting the rocks to produce the siliceous iron-formations in their present form. Carbon dioxide and water vapour were suggested as the metasomatic agents and the carbon dioxide was derived from the basal carbonate unit, or from within the iron-formation sequence, or from late igneous intrusives. The principle is the same as in Whitehead's theory in that most of the carbonate in the orebody is produced by carbonate metasomatism but the starting rock composition has emphasis on amphiboles.

Ashworth (1965) supported the concept of carbonate metasomatism and suggested that shearing in the basal carbonate unit may be the source of carbonate. This approach was later modified by Ashworth (1970, unpublished B.H.P. company report), with greater amphasis on the amount of original carbonate present in the iron-formation unit. The original rock type was considered to be a magnetite-carbonate unit with siliceous layers and the silica was removed from the unit during hydrothermal activity leaving magnetite-hematite-carbonate ore.

The processes envisaged in these concepts of ore-formation have not been described in detail in any publication or company report.

It is clear that hydrothermal solutions have been important in the formation of magnetite-hematite-carbonate ore. Points which are far less clear are, the composition of the original rock

2. Original rock types

(a) Magnetite-hematite-carbonate ore

The magnetite-hematite-carbonate ore is characterised by iron oxide layering which, although usually diffuse, is similar in scale and general appearance to layering in the iron-formation units. This suggests that the original rock type was a member of the iron rich sedimentary sequence, a conclusion supported by the stratigraphic position of the orebody within the lower part of the iron-formation sequence.

The combination of carbonates and iron oxides, which constitutes the orebody, is unusual for the Middleback Ranges and no thick sedimentary units of this composition are known in the area. Rock types at equivalent stratigraphic levels throughout the Middleback Ranges are normally siliceous iron-formations, often with considerable tremolite, and at Iron Duke the orebody appears to pass laterally into siliceous iron-formations. It is therefore considered probable that the original rock type contained some quartz and amphiboles which have been effectively replaced by carbonates during the hydrothermal process. This conclusion was reached by all previous authors and controversy centres on the proportion of carbonate originally present in the rock, rather than the quantity of siliceous minerals. Evidence on the presence of original carbonate is available from two sources; rock types laterally equivalent to the ore, and microtextures of layered ore fragments.

At Iron Duke, deep drilling in the northernmost part of the orebody suggests that the ore passes laterally into siliceous iron-formations with thick carbonate layers. Drilling in the west limb of the synform (DDH83) shows that the ore passes up dip into siliceous iron-formations with thin carbonate layers and the carbonate rich units contain some magnetite which is layered on a fine scale. Thus, carbonate layers are present in the Iron Duke iron-formation sequence at the stratigraphic level of the orebody and were almost certainly present in the original rock type.

The presence of original carbonate layers in the protore unit is also suggested by patches and fragments of finely banded ore which have regular, alternating layers of carbonate and iron oxides, similar in scale and appearance to the layered quartz and iron oxides of siliceous iron-formations. In thin section the carbonate has even, granular microtextures, as described in Section II, which are typically metamorphic rather than metasomatic microtextures. The carbonate is similar in chemical composition and in microtexture to carbonate units elsewhere in the Middleback Ranges which have not been affected by hydrothermal activity. Magnetite is usually the main iron oxide present in these layers and is sometimes altered along the crystal edges to hematite. The magnetite grains are similar in shape and distribution to those in unaltered iron-formation but are generally a little larger. These finely layered patches of ore were first recognised as original carbonate-iron oxide layers by Whitehead (1962 and B.H.P. company reports).

In several parts of the Middleback Ranges, drilling and surface exposures show that the lower iron-formation units are rich in tremolite due to the metamorphic reaction between quartz and Ca-Mg carbonates. Thicker carbonate layers, such as those described above in the iron-formations, are preserved essentially intact due to high CO_2 pressures within the layers. This indicates that the original sediments were rich in Ca-Mg carbonates in the lower part of the sequence and the carbonate proportion declined in the upper part of the succession. The protore unit occurs at an intermediate level, above the thick basal carbonate which represents dominantly carbonate sedimentation, and below the siliceous iron-formations which represent dominantly silica-iron sedimentation. It is therefore likely that the protore unit contained a considerable quantity of Ca-Mg carbonates, and that part of these reacted with quartz to form tremolite during metamorphism whilst the thicker carbonate layers remained unaltered.

It is concluded that the original rock type for the magnetite-hematite-carbonate ore was a layered iron-formation unit composed of 50% to 70% carbonate plus tremolite plus quartz, the remainder being iron oxides. There is no evidence available on the proportion of carbonate in the rock, but a maximum of 30% to 40% of the total rock would appear a reasonable estimate.

(b) Talc zone rocks

The upper talc zone occurs directly above the magnetite-hematite-carbonate ore and passes upwards gradually into siliceous

iron-formations. It consists of talc, quartz and iron oxides and some portions of the rock have a distinct layering similar in scale and appearance to the layering in unaltered siliceous iron-formations. The talc zone appears to extend up dip to the west and up pitch to the south into siliceous iron-formations although this lateral transition is somewhat obscured by the presence of hematite ore.

Whole-rock chemical analyses from the talc zone are similar to those of siliceous iron-formations, except for a marked increase in magnesia and a complete absence of calcium (Appendix I). Microtextures, which will be described in more detail later, show that both talc and quartz have replaced amphiboles and suggest that amphiboles were a major component in the original rock. Within the talc zone, the finely layered portions contain mainly magnetite rather than hematite, and appear to represent the original iron-formation layering with the magnetite having remained essentially in situ.

The evidence therefore suggests that the upper talc zone formed from amphibole rich iron-formations, and that magnetite present in the original rock has remained stable. However, considerable amounts of iron are held in the iron rich talc and the small patches and spots of specular hematite. This iron could result from the alteration of grunerite to talc, part being included in the talc minerals and part migrating to form the specular hematite. It is therefore concluded, in agreement with Whitehead, that the upper talc zone was rich in grunerite rather

than tremolite. On this basis, the original rock type is considered to have been an amphibole rich siliceous iron-formation with grunerite as the dominant amphibole. Thick bands of grunerite-quartz schist were intersected in a deep drillhole (DDH62) in iron-formations about half a mile north of Iron Duke, and this is the type of rock from which the upper talc zone could have formed.

There is no evidence on the original rock type of the lower talc zone. The zone occurs immediately below the orebody, is not more than about 50-100 feet thick in stratigraphic terms and is known from only one borehole (DDH57, Fig.20g). It consists of talc with some carbonate and pyrite, the latter two in irregular patches and veins. By analogy with the upper talc zone, the lower zone is assumed to be formed from amphibole schist, probably with less quartz than the upper zone, and containing considerable syngenetic pyrite.

3. Geochemistry of the hydrothermal solutions

(a) Direction of movement

A number of factors indicate that the fluids moved in a general upward direction and these are listed below and illustrated in Fig.50:

(i) The upper talc zone is much thicker than the lower.
(ii) Basic intrusives are completely chloritised within and above the orebody but not below.
(iii)Magnetite concentrations within the ore adjacent to intrusives and schists tend to be thicker at the lower contact.
(iv) In the transition zone between the orebody and the overlying talc zone, carbonate veins penetrate joints and fractures in the talcose rock and taper upwards.

The orebody and upper talc zone are both thickest and best developed in the deeper, northern part of the synform and become progressively thinner up pitch to the south. Their shape in three dimensions suggests that the fluid source was situated at depth to the north, and the fluids moved upwards and to the south along the axial region of the synform.

In several drillholes on the eastern side of the orebody, carbonate veining has increased with depth and is more prolific than in other parts of the ore. This slender evidence suggests that there may have been fluid penetration from depth along the eastern side of the orebody as well as from the north as suggested above.

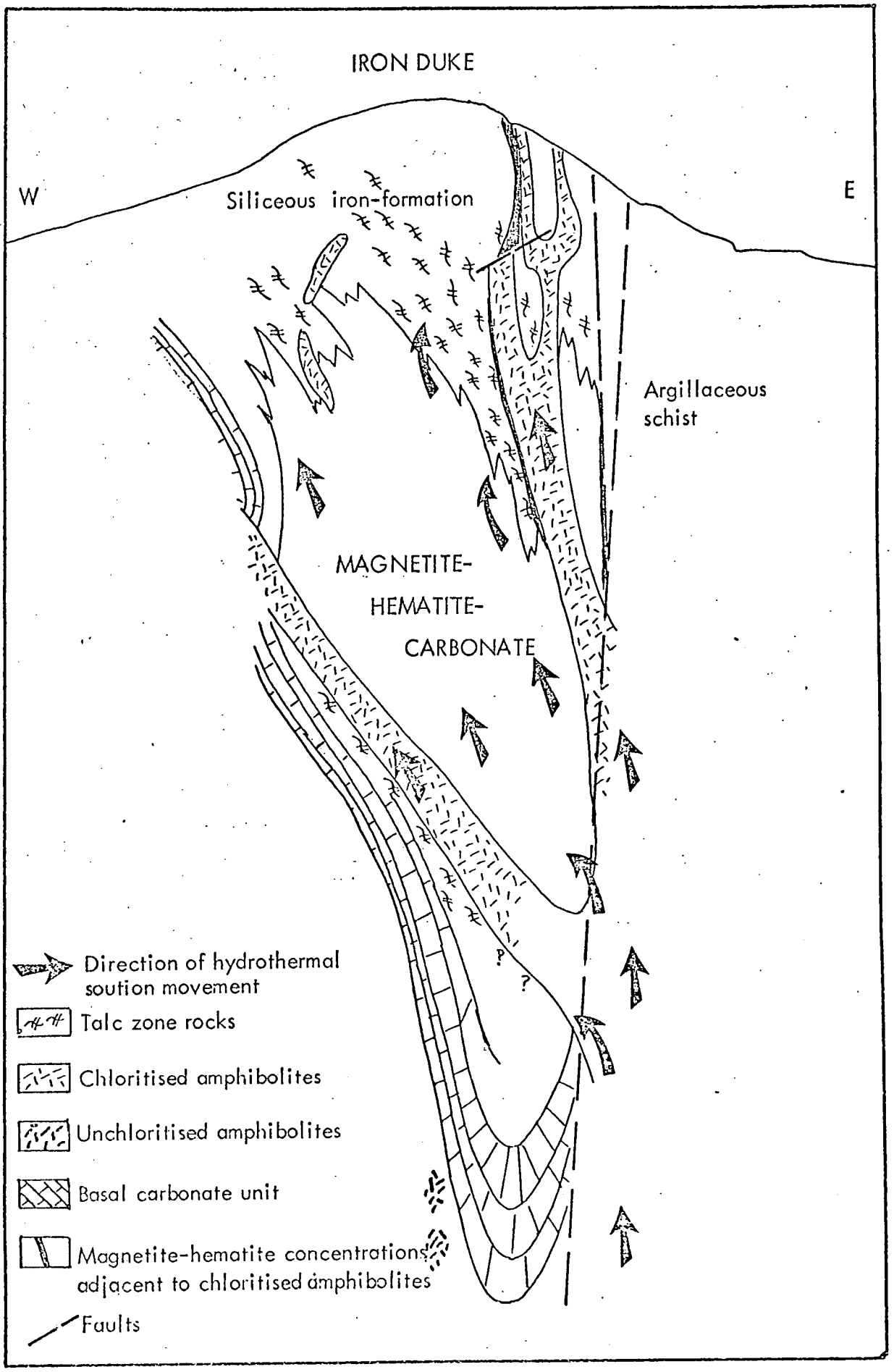

Fig. 50. Generalised cross section at 1000S to illustrate factors suggesting upward movement of hydrothermal solutions from depths to the east.

(b) Temperature and pressure

Homogenisation temperatures for fluid inclusions in the vein carbonate show that the minimum possible temperature of formation is in the order of 120°C to 130°C. A pressure correction would be needed to ascertain the true temperature of formation and the pressure is not known but an indication of the upper temperature limit is given by the recrystallisation of the ankerite, as discussed below.

Euhedral ankerite crystals often project into cavities in the vein carbonate. They grow from the ground mass carbonate and sometimes show a distinct zoning of light and dark bands parallel to the crystal faces, the dark bands being due to included matter and fluid. This zoning shows that the crystals grew from solution at different rates, the dark bands with inclusions representing periods of rapid growth. The crystals contain rather more iron than the groundmass carbonate, as described in Section II, but both conform to the general ankerite composition throughout the orebody. This indicates that the process was simply one of carbonate solution and redeposition, producing slight variations in the main components.

There is little information in the literature on ankerite solubility but a great deal on dolomite solubility and the low iron contents of the Iron Duke ankerite enable a direct comparison. Dolomite is soluble both congruently and incongruently, in the latter case calcite being formed (Krauskopf 1967). The process described above for the Iron Duke carbonate is congruent solution

and this is supported by the lack of calcite in the main part of the orebody. The way in which dolomite goes into solution is temperature dependent, congruent solution taking place between 60°C and 200°C and incongruent solution taking place below 60°C and above 200°C (Rosenburg and Holland 1964). This suggests an upper temperature limit in the order of 200°C for the vein carbonates although the experimental data in this region is rather uncertain.

The precise carbonate deposited from a chloride solution depends primarily upon the molar ratio of Ca^{++} and Mg^{++} in the fluid and the temperature at the time of carbonate deposition (Rosenburg et al. 1964, 1967, Lovering 1969) In the orebody vein carbonates, the solution appears to have dissolved ankerite in one place and redeposited it in another with only minor changes in composition, which suggests that the Ca^{++}/Mg^{++} ratio in the fluid was approximately the same as that of the carbonate mineral. Lovering (1969) plotted the molar Ca^{++}/Mg^{++} ratios for fluids in equilibrium with various carbonates against temperature and the graph is shown in Fig.51. The orebody vein carbonates have an atomic Ca/Mg ratio of approximately 1 which is equivalent to a solution molar ratio of about 1.7. On Lovering's graph this indicates a temperature in the order of 230°C to 280°C, dependent on the precise molar concentration of Ca^{++} and Mg^{++} in the solution.

These figures must be treated with caution as they are based on a number of assumptions including the congruent nature

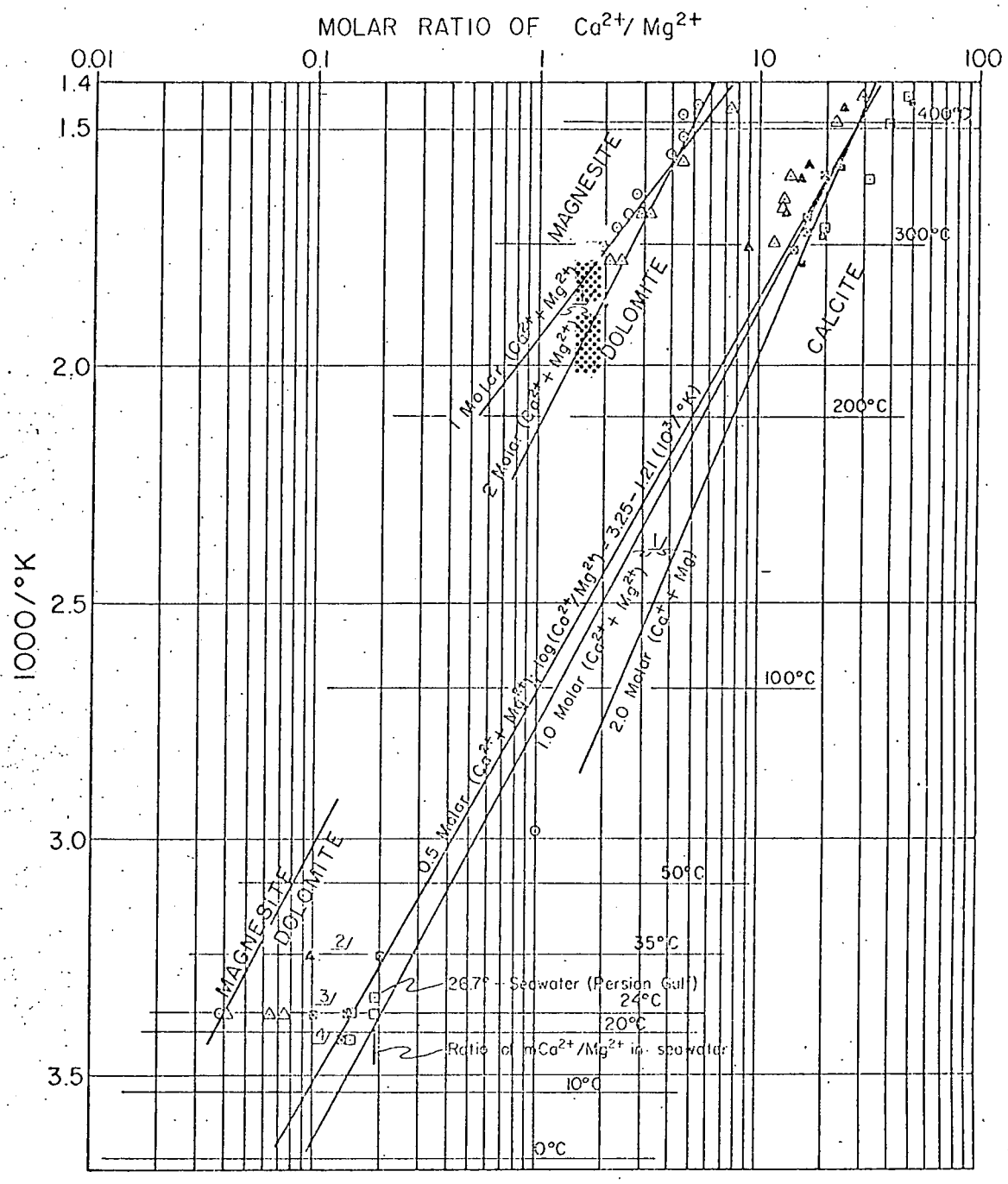

Fig. 51. Molar ratios of Ca^{2+}/Mg^{2+} chloride solutions precipitating, replacing or in equilibrium with calcite, dolomite and magnesite, 10° to 450°. Molar ratio of ankerite in the magnetite-carbonate-hematite ore shown by stippled area.
Diagram from Lovering, 1969.

of ankerite solution and the Ca^{++}/Mg^{++} ratio in the solution. Carbonates other than ankerite could have been formed at higher temperatures and been converted to ankerite as the temperatures fell. Despite these points, an upper limit of about 250°C appears reasonable for the hydrothermal activity and is a suitable temperature for the development of hydrothermal talc in the talc zone (French 1971).

An upper temperature limit of 250°C indicates a maximum pressure correction of 130°C for the fluid inclusion homogenisation temperatures. This, in turn suggests a pressure of 2-3 kb which is equivalent to a depth of about 7-11 km.

(c) Eh and pH

Within the carbonate rich bands the solutions must have been alkaline or the carbonate would have been removed. The equilibrium pH of an aqueous solution in contact with calcite at room temperature is between 8.4 and 9.9 dependent on the access of CO_2 to the solution (Garrels and Christ 1965). The CO_2 content of the Iron Duke solutions is not known but a pH of about 9 appears to be a reasonable estimate. The true pH would be somewhat less than 9 as pH values, including neutral, decrease with increasing temperature (Barnes and Ellis 1967). It is therefore more accurate to say that the pH of the hydrothermal solutions in contact with the carbonate minerals would be one or two units on the basic side of neutrality. A pH of this order conforms with data from hot waters and brines throughout the world (White, Hem and Waring 1963, Ellis 1967).

The presence of magnetite in the ore reflects an alkaline environment and also indicates reducing conditions as shown in Fig.51 (Garrels and Christ 1965). The partial oxidation of magnetite to hematite, which occurs frequently, suggests that the Eh values for the solutions were on the dividing line between magnetite and hematite in Fig.52a.

Siderite has a limited stability field and its presence at the top of the orebody, together with magnetite, suggests that in this part of the orebody the solutions had Eh-pH values on the dividing line between magnetite and siderite. The Eh-pH conditions indicated by the diagram may not be strictly applicable as the siderite contains considerable Mg and the stability field in the diagram is for pure siderite.

Pyrite is occasionally present within the ore and its stability field conforms to the Eh-pH values estimated above for the solutions.

The approximate position, in terms of Eh and pH, for the hydrothermal solutions is plotted on Fig.52a. The diagram is for 25°C and 1 atm pressure and the fields will change at higher pressure-temperature conditions and with different amounts of carbonate in solution. However, the ore mineralogy fits the diagram well and conforms to the interpretation of a basic solution in mildly oxidising to reducing conditions.

Variations in Eh-pH conditions are suggested by the presence of bladed magnetite in one sample (Fig.52b) and by

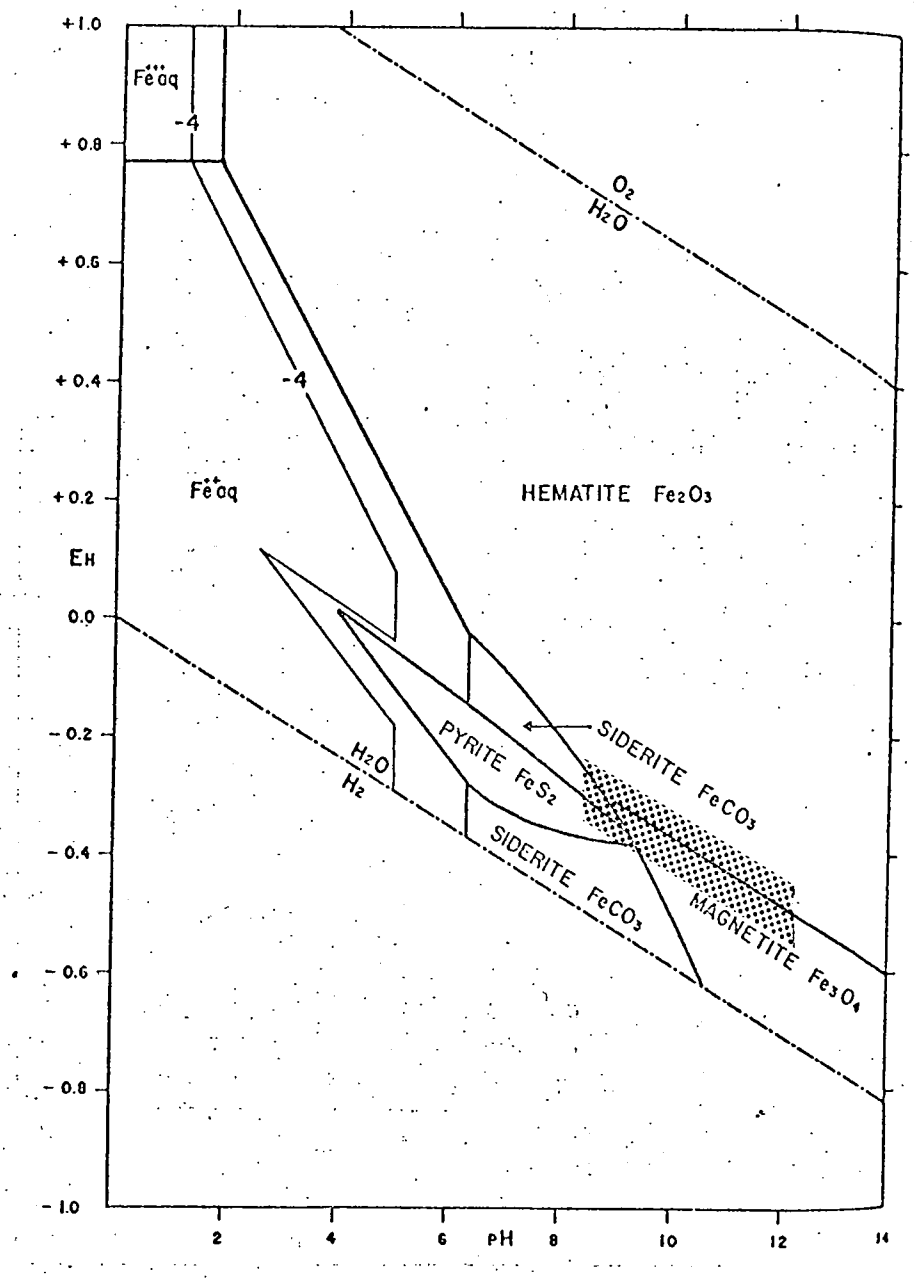

Fig. 52a. Stability relations of iron oxides, sulphides and carbonate in water at 25°C and 1 atmosphere total pressure. Total dissolved sulphur = 10^{-6}, total dissolved carbonate = 10^{0}, total dissolved iron 10^{-6} with contour at 10^{-4}. Estimated Eh-pH conditions of hydrothermal solutions in magnetite-hematite-carbonate ore shown by stippled area.
Diagram from garrels and Christ, 1967.

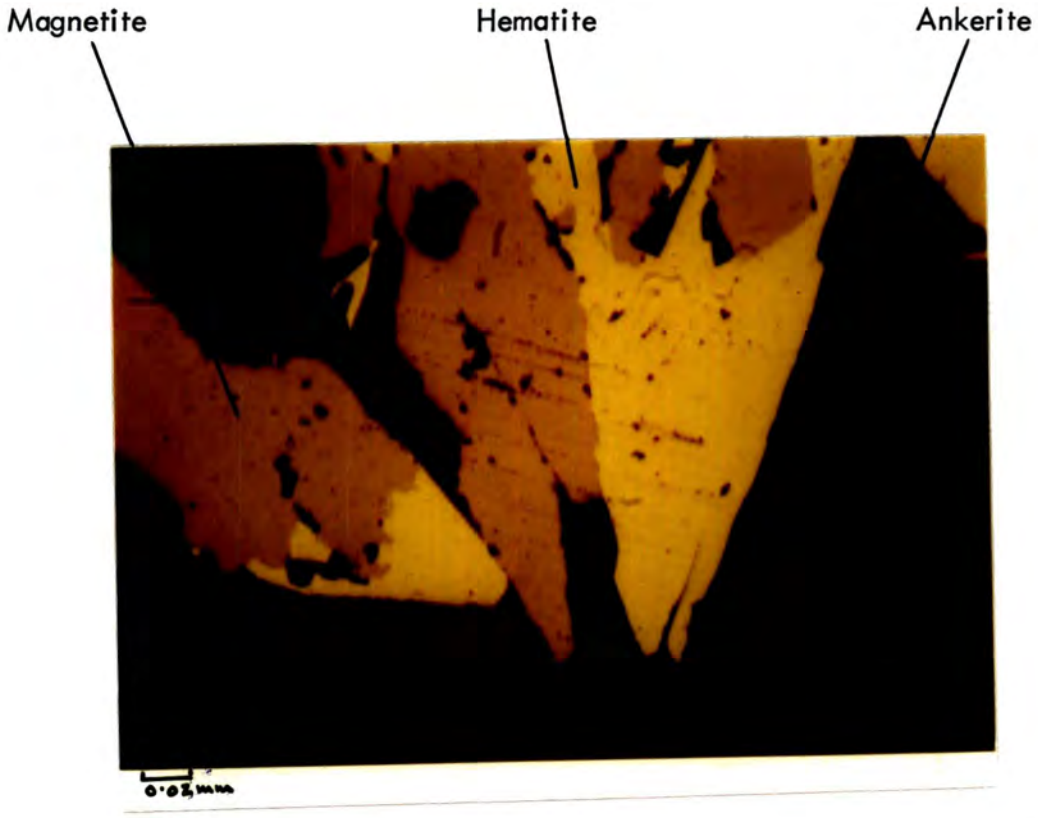

Fig. 52b. Bladed hematite and magnetite in vein ankerite. The iron oxide crystals have grown into the vein from a gragment of layered ankerite-magnetite-hematite.

concentrations of magnetite against chloritised intrusives and schists. The bladed magnetite projects from a fragment of banded ore into coarsely crystalline carbonate. Some of the blades are of hematite and in some hematite and magnetite are present together. A bladed form is highly unlikely for magnetite, which is cubic, and it must be replacing hematite. This is the reverse of the normal case in the orebody where magnetite is partially replaced by hematite, and suggests subtle variation in Eh-pH conditions. The magnetite concentrations at contacts with basic intrusives support this view. They contain no hematite and the solutions must have been rather higher in pH or lower in Eh than in the main part of the orebody.

In the talc zones, and in siliceous layers of the original rock, the pH would be lower than in the carbonate layers and probably approached the neutral point. Magnetite and hematite are both abundant in the talc zone, suggesting that the Eh conditions were similar to those within the orebody.

(d) Solution compositions

The freezing data for fluid inclusions in the orebody carbonates clearly indicates the presence of salts in solution. This conforms with data for deep natural waters in other parts of the world which are normally brines containing salts of sodium, calcium and magnesium (White, Hem and Waring 1963, Helgerson 1964). NaCl is the dominant salt in most natural brines and was probably present in considerable quantity in the Iron Duke solutions. The freezing data suggests an NaCl content which varied between 7% and

21%, if NaCl were the only salt present but it is probable that calcium and magnesium chlorides were also present, as the solutions were in contact with Ca-Mg carbonates. It can be reasonably concluded that the solutions were brines with a maximum possible salt content in the order of 21%.

Within the orebody, the solutions were in contact with carbonates and would be likely to contain bicarbonate. Roedder (1967), describes fluid inclusions in Iceland Spar and in two of the three quoted analyses bicarbonate exceeds Cl and Ca exceeds Na. Browne and Ellis (1970), describe chloride-bicarbonate solutions intersected in deep drillholes in the Ohaki-Broadlands hydrothermal area of New Zealand. By analogy with these examples, and because the orebody is rich in carbonate, it is assumed that the solutions were bicarbonate rich.

The solutions within the orebody are considered to have been salt solutions with sodium, calcium and magnesium salts in unknown proportions, together with considerable bicarbonate. They must also have carried some silica in solution and this is supported by the presence of late-stage quartz in some carbonate veins.

4. Mineral solubilities

Quartz and amorphous silica

Temperature has a strong effect on quartz solubility, there being a steady increase in solubility with increasing temperature as shown in Fig.53. Thus, at room temperature, the solubility of quartz in pure water is approximately 6 ppm whereas at 240°C the solubility is 440 ppm (Morey, Fourier and Rowe 1962). Above temperatures of about 350°C, pressure becomes important and there is a marked increase in solubility with increasing temperature at pressures over 1000 bars but a decrease in solubility at lower pressures (Kennedy 1950, Sharp 1965). The estimated positions of the Iron Duke solutions in terms of pressure and temperature are shown in Fig.53.

Solution pH is unimportant below 9 but there is a sudden increase in silica solubility above that level of alkalinity, as shown in Fig.53. Solution pH is influenced by the minerals with which the solutions are in contact and, as previously discussed, the pH would be different in the carbonate rich ore, the talc zones and the dykes. Estimated pH values for these three rock types are shown in Fig.53 and it is evident that in the carbonate rich ore the high pH would tend to increase silica solubility, whereas in the talc zones and intrusives the pH effects would be slight.

Dissolved salts have little affect on silica solubility but there is an increase proportional to the NaOH concentration in solution (Holland 1967). NaOH is not likely to be important at Iron Duke because any substantial amounts would probably have

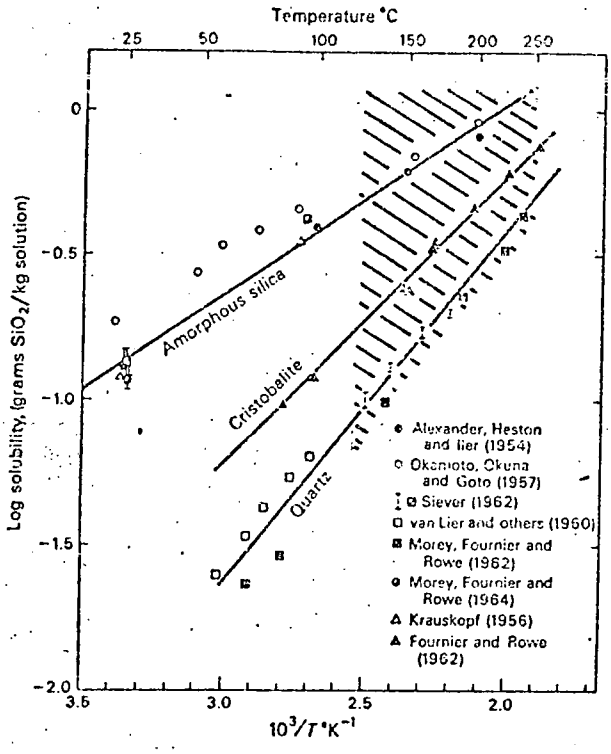

a. Solubility of quartz, cristobalite and amorphous silica in water between 25°C and 250°C.

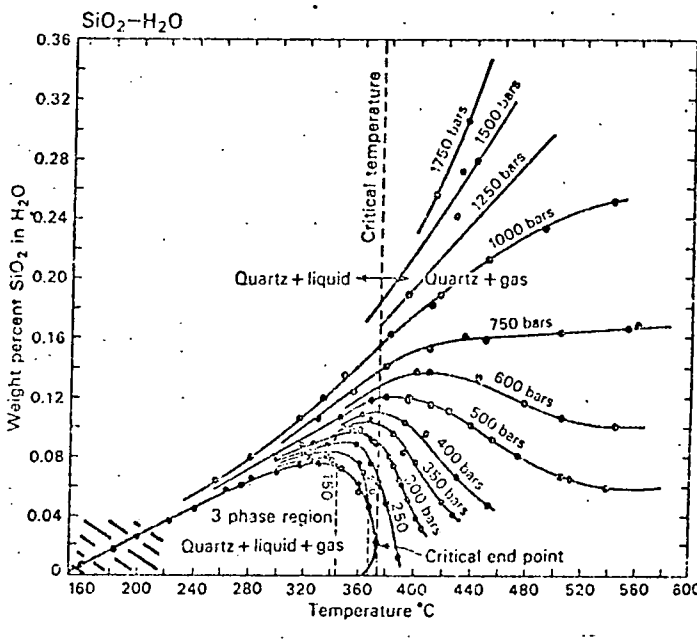

b. Solubility of quartz in water at temperatures up to 560°C and pressures up to 1750 bars.

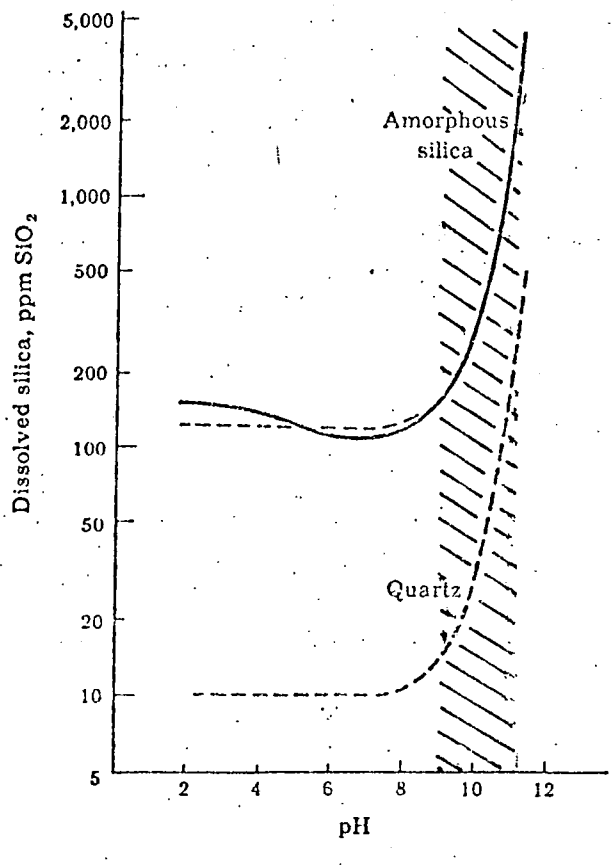

c. Solubility of silica in relation to pH at 25°C. For amorphous silica, solid line shows solubility determined experimentally, dashed line is calculated curve. For quartz, dashed line is calculated solubility.

Fig. 53. Solubility of quartz and amorphous silica in relation to temperature and pH.
a. and b. from Holland 1967.
c. from Krauskopf 1967. Used with permission of McGraw-Hill Book Cpy.
Shading indicates estimated position of Iron Duke hydrothermal solutions.

been detected by the freezing work on fluid inclusions. T.S. Lovering (1923) showed experimentally that bicarbonates can be effective solvents of silica at low temperatures and T.G. Lovering (1962) observed that some thermal spring waters with high concentrations of bicarbonate also contain relatively high amounts of silica. This association is not entirely substantiated by more extensive analysis of thermal waters (White, Hem and Waring 1963).

Complexing is unlikely to significantly affect silica solution and transport at Iron Duke, as the main possible complexing agents in most geological situations are sulphur and chlorine. Sulphur has very little affect on silica solubility (Crerar and Anderson 1971) and there is negligible sulphur within the ore or the overlying rocks. NaCl was probably present in the hydrothermal solutions but its presence produces only slight affects and tends to decrease rather than increase silica solubility (Holland 1967). Colloidal silica forms are also unlikely as colloids are not stable in electrolyte solutions such as brines (Barnes and Czamanske 1967).

Supersaturation can occur when dissolved silica is removed from the immediate vicinity of the quartz faces. This was demonstrated by Morey, Fournier and Rowe (1962) who obtained a supersaturated solution with 395 ppm silica at room temperature by rapidly rolling quartz fragments in a plastic bottle filled with pure water. The speed of rotation was of extreme importance and at low rates the solution contained the normal 6 ppm. At

Iron Duke, supersaturation is unlikely in the early stages of hydrothermal activity when the solutions were seeping through a tightly packed rock mass, but as cavities developed and solution movement became more pronounced it is possible that dissolved quartz was moved from interfaces and this may have increased the silica solubility.

The main factors likely to influence quartz and silica solubility at Iron Duke are temperature, solution pH and, to a much lesser extent, supersaturation.

Silicates

The effects of hydrothermal solutions on silicates are to alter or replace the mineral rather than direct removal in solution. These may involve hydration, dehydration, cation exchange and anion exchange (Meyer and Hemley 1967).

In the talc zone the amphiboles undergo cation exchange, and water plus a little silica is added to the structure. This may be expressed as follows:

$$\text{Tremolite} + SiO_2 + Fe^{++} + H_2O \longrightarrow \text{Talc} + Ca^{++}$$

$$\text{Grunerite} + SiO_2 + Mg^{++} + H_2O \longrightarrow \text{Talc} + Fe^{++}$$

The Fe^{++} is stabilised as iron oxide and the net result within an amphibole schist are gains in SiO_2, H_2O, Fe^{++} or Mg^{++} and a loss of Ca^{++}. The only major component removed in solution is

therefore calcium.

Within the orebody there is no evidence to show how pre-existing silicates were removed. Tremolite could be replaced directly by ankerite, as the main cations in both are Ca^{++} and Mg^{++} and the process would be one of anion exchange, with CO_3 replacing silica and water. Direct replacement of grunerite is more complex as the main cations in the amphibole are Fe^{++} and Mg^{++} so that Ca^{++} would have to be introduced to form an ankerite. It is likely, therefore, that the grunerite first changed to talc which was subsequently replaced by carbonate, whereas tremolite changed directly to carbonate.

Chloritisation of the intrusives is also a complex cation exchange process, together with a loss of silica and an addition of water. The major difference between the exchange process in the iron-formation amphiboles and that in the complex igneous silicates, is that the latter minerals contain considerable alumina resulting in chlorite rather than talc or carbonate.

The main result of silicate replacement in the orebody and alteration in the intrusives is a loss in silica. In this situation, with silica in solution derived from silicates, the solubility is likely to approach that of amorphous silica rather than quartz (Garrels and Christ 1965) and as shown in Fig.53, the solubility of amorphous silica is considerably higher than that of quartz.

Carbonates

There is extensive data on calcite solubility in the literature but much less concerning dolomite. The two solubilities are thought to be similar, with a much slower reaction rate on the part of dolomite (Holland 1967). For both carbonates, the causes of precipitation from solution are not fully understood.

Solution pH is a major factor influencing carbonate solubility and there is a marked increase in solubility in more acid solutions. This could explain the lack of carbonate in the talc zones and chloritised dykes where the solution pH was presumably lower than in the carbonate rich orebody.

Temperature can be an important influence in carbonate solution and precipitation, as the solubilities of calcite and dolomite decrease with increasing temperature (Holland 1967). As a result, these carbonates do not precipitate from cooling solutions and alternative precipitation mechanisms must be sought. The Iron Duke carbonates therefore cannot be attributed to precipitation as the hydrothermal solutions cooled.

Carbonate solubility increases with increasing amounts of CO_2 in solution, and any mechanism which removes CO_2 from solution will tend to cause carbonate precipitation. Mueller (1963) proposed that loss of CO_2 on boiling as solutions moved to lower temperature regions would cause carbonates to be precipitated. Sharp (1965) and Laffitte (1962) have suggested that rapid pressure changes in vein systems would also cause carbonates to be precipitated from hydrothermal solutions. These

concepts may be applicable to the truly vein carbonate at Iron Duke, but most of the ore consists of layered carbonate merging to vein carbonate of identical composition, suggesting that the carbonate has moved over very small distances where pressure differentials are likely to be small. One further factor affecting carbonate solution and precipitation is the presence of NaCl in solution, carbonate solubility increasing with increasing amounts of NaCl.

At Iron Duke, the process of carbonate solution and precipitation within the orebody was probably complex and depended upon the inter-relationships between solution pH, CO_2 content and NaCl content at any given point. Small fluctuations in these controls would arise as solution reactions with quartz and silicates took place and as new waves of solution entered the orebody, causing carbonate solution and precipitation from point to point.

Iron oxides

The information on iron oxide solubility is very limited in the pressure and temperature fields of hydrothermal solutions. At surface temperatures, iron is mainly soluble in acid solutions although some can be taken into solution up to a pH of about 9 under strongly reducing conditions (Garrels and Christ 1965, James 1966). Similar principles apply at higher temperatures, where experimental evidence shows that at 300°C to 500°C and 15 to 100 atmospheres acid salt solutions can contain up to about 300 ppm iron in reduced conditions but there is a rapid decrease to 5 ppm

or less in intermediate to alkaline solutions (Barnes 1967).

There is no evidence that components such as NaCl in solution affect the iron oxides solubilities. Bicarbonates may have some effect, as the only natural waters containing large quantities of iron in solution are certain bicarbonate or bicarbonate-sulphate groundwaters and some volcanic waters (James 1966).

At Iron Duke, most of the iron oxides present in the original rock appear to have remained essentially in situ, although some iron has moved in solution as shown by the presence of small magnetite veins. This is presumed to reflect slight variations in solution pH as the fluids moved through the orebody, causing local solution and precipitation.

5. Effects of the hydrothermal activity

(a) Magnetite-hematite-carbonate ore

The ore is characterised by structures, microtextures and bulk chemical compositions significantly different from members of the iron-formation units in other parts of the Middleback Ranges and these are clearly due to, or related to, the hydrothermal activity.

Brecciation, diffuse layering and carbonate veining occur throughout the orebody and are described in detail in Section II. These structures are characteristic of the ore and are not confined to any zone or specific part of the orebody, although carbonate veining tends to increase at depth on the east side.

The breccia and vein structures show clearly that there were openings and channelways within the orebody during the hydrothermal activity. The vein carbonate is typically coarsely crystalline and the veins frequently have small cavities with projecting euhedral crystals. This carbonate crystallised in an environment with planty of open space and the space must have been created subsequent to regional metamorphism, either by tectonic dislocation or by removal of components during the period of hydrothermal activity.

Some space within the orebody was certainly due to tectonic movement. This is illustrated, on a small scale, by

Fig. 54 which shows the plane of a low angle thrust in the talc zone just above the orebody. The thrust plane is marked by a breccia of ore fragments enclosed in typical vein carbonate and there is one small fragment of chlorite schist which is lithologically completely different from the surrounding rock types, and shows clearly that fragments have moved within the space created by the fault plane. It is clear, therefore, that there was tectonic movement during the hydrothermal activity and that some space was created by fracturing.

On the other hand, the breccia structures occur throughout the orebody and are not confined to any particular fracture system, nor do they increase near the major fault which bounds the ore on the east side. Furthermore, the breccias occur extensively through the ore but not in the iron-formations above and below the ore. The brecciation mechanism must have been operative throughout the entire orebody and yet restricted to the orebody and it is unlikely that this could be due to tectonism alone. One possible mechanism is that of repeated tectonic movement combined with the effects of chemical solution and high fluid pressures during the hydrothermal activity. In such a mechanism, space is created initially by the removal of components in solution and the brecciation represents adjustment structures caused by contemporaneous tectonic movement and the penetration of solutions under high pressures.

Diffusely banded material forms a high percentage of the total ore and is found throughout the orebody. In diffusely banded samples, the iron oxide layering is disturbed and irregular and,

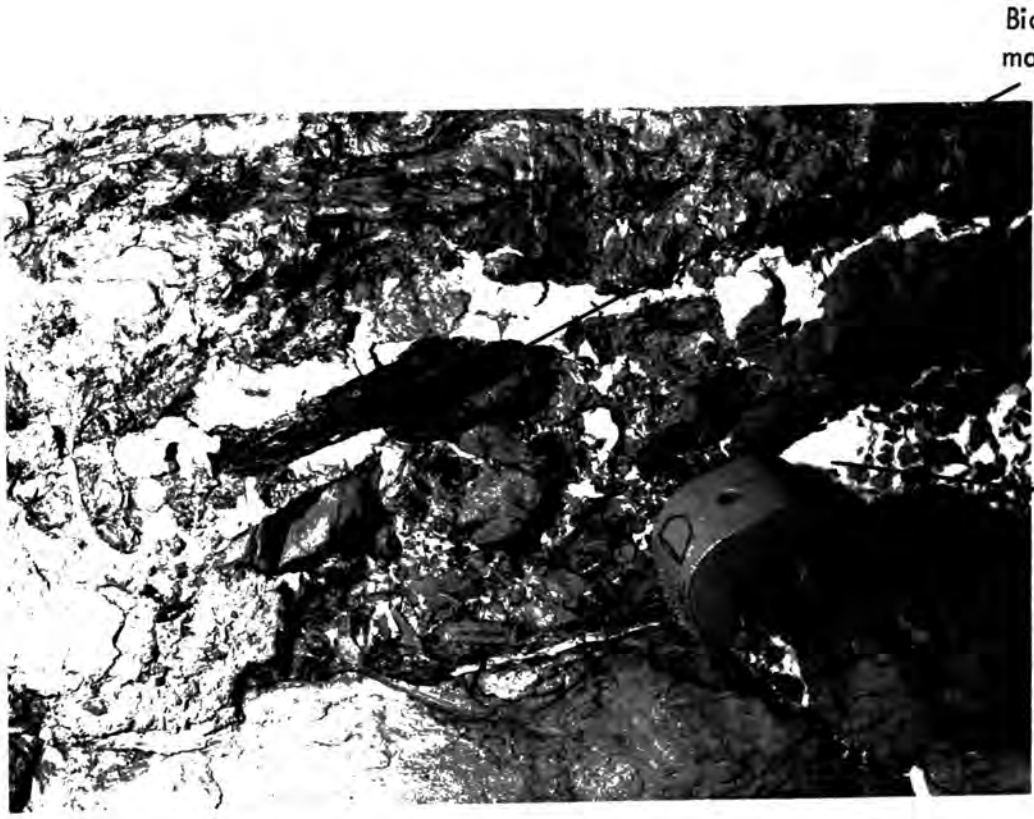

Fig. 54. Low angle thrust plane in chlorite-talc-magnetite rocks in Winze No. 4, south wall. Note the vein carbonate cementing breccia fragments and the single fragment of biotite-chlorite-magnetite schist.

in thin sections, the carbonate is seen to occur in large interlocking crystals which may cross the oxide layering (Fig.3b) and produce a coarse, unoriented microtexture quite different from those of unaltered iron-formations (Figs. 8a-f). This diffuse banding is restricted entirely to the orebody and is clearly a product of the ore forming processes.

There are two possible ways in which the diffuse layering may have developed; firstly by recrystallisation and redistribution of carbonate layers already present in the original rock, and secondly by metasomatic carbonate replacing quartz and amphiboles in siliceous iron-formation bands. The first method is suggested by the gradation of finely layered patches of ore into diffusely layered material (Figs. 25, 29). The magnetite layering gradually spreads over a wider area, the magnetite grains are partly but not wholly oxidised to hematite, and the carbonate crystals become larger, develope irregular shapes and have ragged edges. Electron microprobe analyses show that no significant chemical change accompanies the change of carbonate grain size and shape other than a slight tendency for the coarser material to be richer in iron (Section II and Appendix II). The second method, that of metasomatic replacement, was suggested by Whitehead (1962 and B.H.P. company reports) who records carbonate replacing quartz and talc in some samples. In the samples examined by the author, microtextures indicating carbonate replacement of quartz and talc were seen in samples from the top of the orebody near to the overlying talc zone. These samples have a diffuse layering which appears to be a remnant of the original fine iron-formation layering. It is

clear therefore, that both the recrystallisation and metasomatic replacement mechanisms can produce diffuse layering within the ore but there is no direct evidence to show which mechanism was dominant.

The simple mineralogy and geochemistry is a striking feature of the ore, and it is clear from the bulk chemical analyses shown in Section II and Appendix I that the ore consists of carbonates and oxides of three elements, iron, calcium and magnesium, all of which are characteristic of the iron-formation sequence. The bulk of the ore has a bulk chemical and mineralogical composition equivalent to that of the basal carbonate unit plus iron oxides, and this includes trace elements except for strontium which is a little higher in the ore. The hydrothermal solutions have not introduced any elements, such as sodium or potassium, which were not already available in the iron-formation sequence.

On the other hand, the original rock is assumed to have contained some quartz and amphiboles, yet the only trace of these remaining in the ore are the rare occurrences of small quartz crystals in carbonate veins. There are no remnant siliceous patches or remnant amphibole outlines. The hydrothermal process has thus been highly efficient in removing silica and substituting carbonate.

Any carbonate which was introduced was almost precisely the same composition as that already present in the original rock as shown by the similar analyses of layered and vein samples.

Furthermore, there was very little trace element concentration into the veins, the only detectable differences between vein and layered samples being:

(i) Vein carbonate tends to contain a little more MnO, Sr and Y than does banded ore.

(ii) Magnetite concentrations adjacent to chloritised intrusives contain up to 552 ppm Zn, but other trace elements are at levels similar to those throughout the rest of the ore.

There is, however, some carbonate zoning in the orebody on a broad scale. The bulk of the ore contains ankerite as the only carbonate and the ankerite does not vary greatly in chemical composition, as shown by electron microprobe and whole rock analyses (Appendices I and II). This shows that the proportions of calcium and magnesium in the hydrothermal solutions was also fairly constant, otherwise calcite and magnesite would occur within the main part of the orebody. At the top of the orebody, there is a thin layer of intermixed ankerite and magnesio-siderite, the latter occurring only as coarse crystals. The magnesio-siderite is the only carbonate in the ore which contains little or no calcium and it is considered, by the author, to form from ankerite at the upper margin of the orebody by the hydrothermal solutions selectively removing calcium from that region. At the base of the orebody there is a layer of calcite rich ore which is low in magnesia relative to the rest of the orebody and is rather higher in strontium. This calcite rich layer is difficult to explain in terms of the hydrothermal activity but is tentatively interpreted as an original calcite rich band in the sedimentary sequence.

(b) Talc zone rocks

The main effects of hydrothermal activity in the talc zone were the development of iron rich talc and the extensive redistribution of iron and silica. The precise nature of these changes was investigated by detailed study of four features, previously noted by Whitehead in company reports, and found only in talc zone rocks: replacement of amphiboles by talc, replacement of amphiboles by quartz, the occurrence of unusual, bladed quartz, and the development of specular hematite. The results are described below:

(i) Replacement of amphiboles by talc

In the transition zone between the upper talc zone and the iron-formations, individual amphibole crystals are altered along their edges to fibrous talc and may be completely replaced. The precise change of amphibole to talc was investigated in four samples (74-348, 59-679, 59-533, 62-1316).

All four samples contain bladed, well formed amphibole crystals identified optically by their strong second order interference colours and oblique extinction. These are altered at the edges to a finely fibrous mass and sometimes the alteration is more extensive with amphibole occurring as islands in fibrous material which has higher order interference colours (Fig.55). The amphibole patches and the surrounding talc were analysed by electron microprobe and the full results are given in Appendix II.

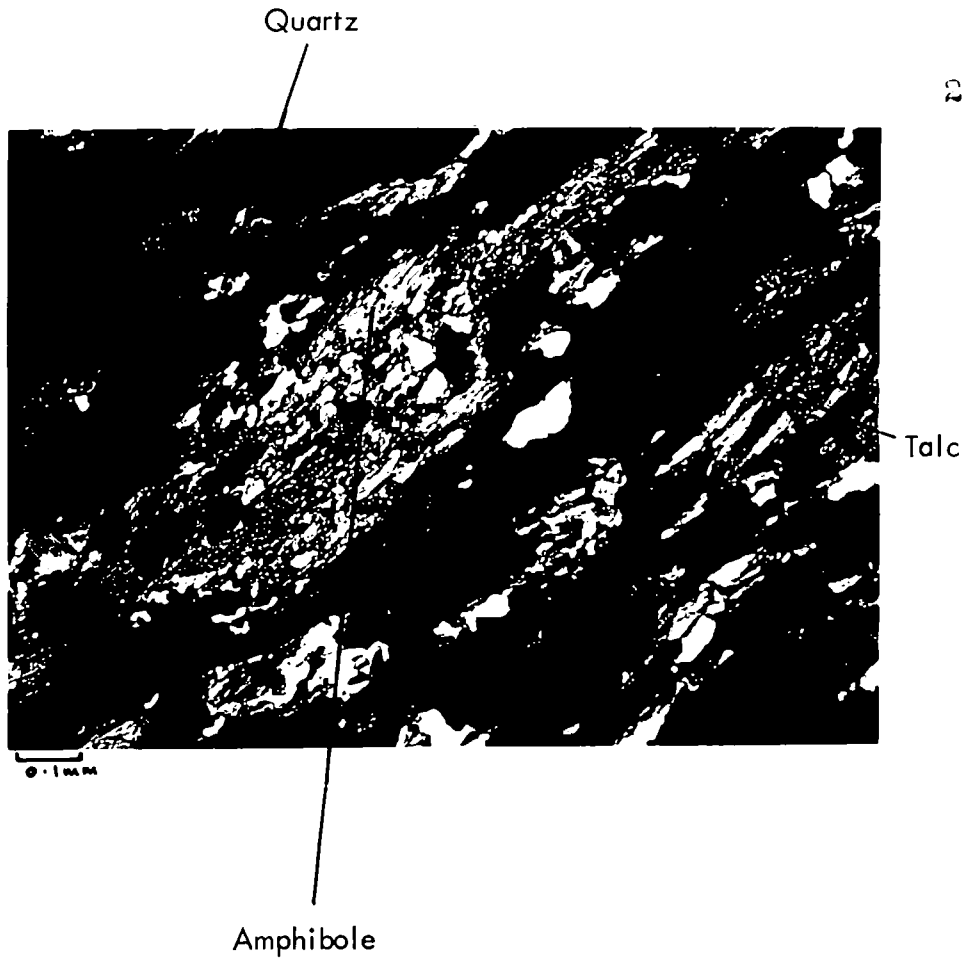

Fig. 55. Talc Zone - replacement of amphibole by talc in sample no. 59-533. Crossed polars.

Typical electron microprobe analyses are:

	CaO	MgO	FeO	SiO_2	Total
Amphibile remnant	0.2	21.2	10.4	58.9	93.0
Talc	0.1	23.6	10.7	59.2	93.3

In three of the samples, the analyses show no significant difference between the bladed and fibrous minerals and the compositions are similar to those of talc from within the main part of the zone. The talc is therefore pseudomorphing a pre-existing amphibole, with amphibole characteristics being retained in the remnant islands.

In the fourth sample (62-1316) the amphibole remnants are tremolite, identical in composition to that found in other parts of the Middleback Ranges. The surrounding fibrous talc is similar in composition to that found in the other three samples but it also contains granular, cloudy areas which give low total analyses and are probably carbonate.

The amphibole in the first three samples was probably grunerite. No carbonate was present and the amphibole had lost its chemical identity at an early stage of the replacement process before losing its crystal form and optical characteristics. This is in marked contrast to the tremolite of the fourth sample which retained its chemical identity until altered to a fibrous mass.

In all four samples the talc was of similar composition and conformed to the general talc composition within the main zone.

(ii) Replacement of amphibole by quartz

In the transition between the upper talc zone and the iron-formations, quartz occasionally clearly replaces amphibole. This was investigated by electron microprobe in one sample (78-443)

and the full results are given in Appendix I.

The amphiboles occur as bladed crystals with well developed cleavage along the crystal length and analyses show the amphibole to be grunerite. The crystals are partly replaced by quartz which takes the amphibole form (Fig.56). The quartz retains the amphibole cleavages and thin slivers of amphibole occur within the quartz along the cleavage lines. Where the replacement process is almost complete, an elongate quartz crystal with the shape of an amphibole, cleavages parallel to the long axis and oblique extinction, is the end product.

This replacement shows positively that silica has been mobile in the talc zone and is particularly important in the interpretation of bladed quartz in the main talc zone which is described below.

(iii) Within the upper talc zone, quartz occurs only in elongate, bladed forms as described in Section II. In talc schists these are narrow, elongate crystals but in siliceous bands and patches they are broad crystals with a well developed cleavage parallel to the long axis and oblique extinction (Fig.57).

The quartz crystals contain thin slivers of silicate minerals parallel to the cleavages. Electron microprobe reconnaissance showed that these are FeMg-silicates but the slivers were too narrow for accurate analysis. The quartz crystals are usually aligned parallel to the schistosity but individual

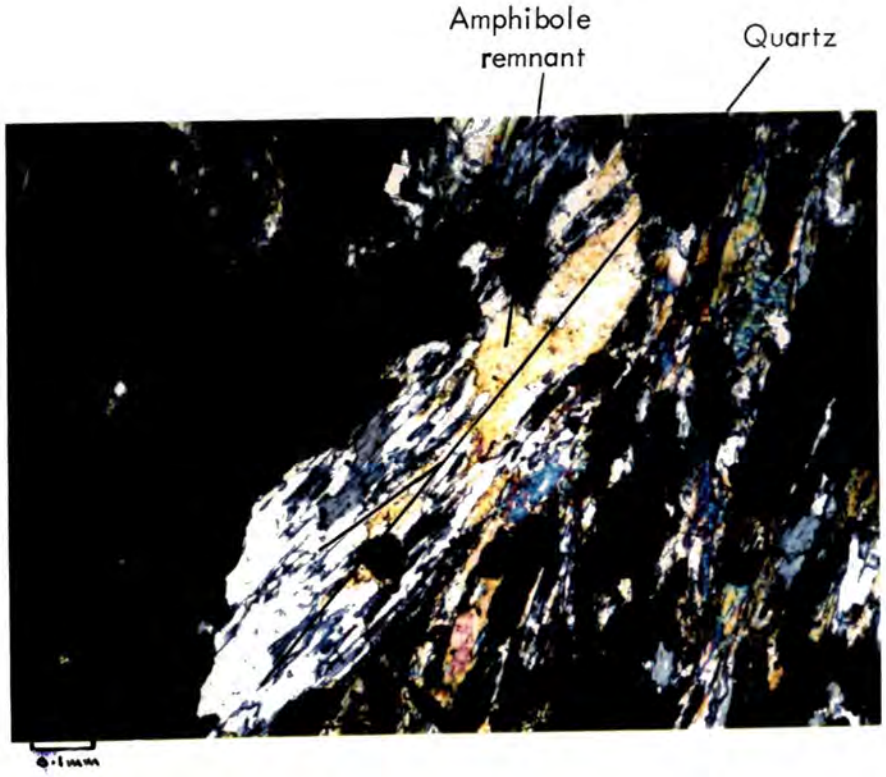

Fig. 56. Talc zone - replacement of amphibole by quartz in sample no. 74-348. Note that the quartz is taking the shape of the amphibole crystal. Electron microprobe analyses (Appendix II) establish that the amphibole in this sample is grunerite.
Crossed polars.

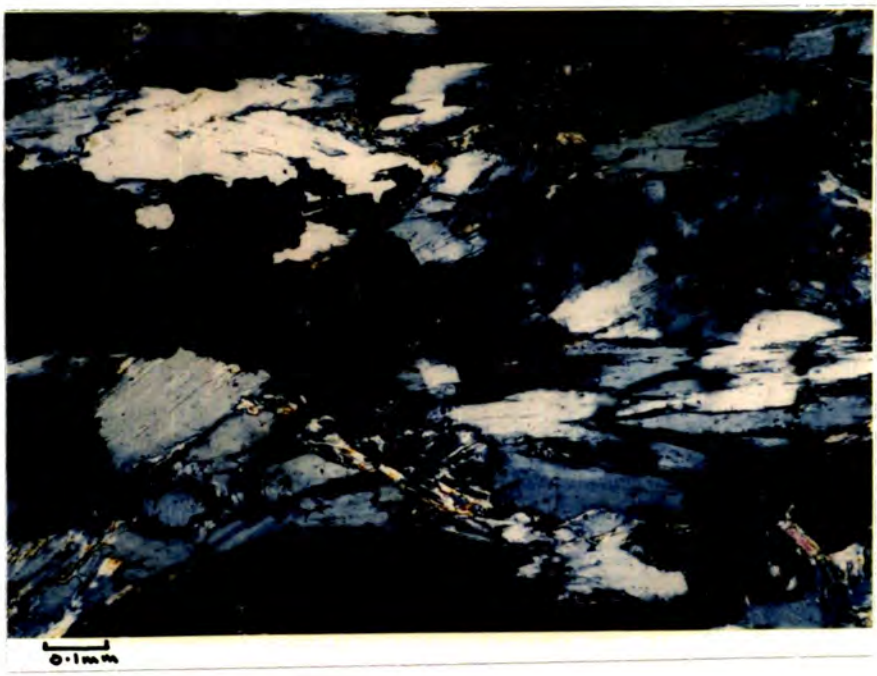

Fig. 57. Talc zone - bladed quartz with thin slivers of silicates giving the appearance of cleavages.
Sample 67-705, crossed polars.

crystals may be oblique to the main trend.

The crystal forms are identical to those of quartz which has replaced amphibole as described above and it is clear that the quartz crystallisation was controlled by pre-existing silicate mineralogy. This does not necessarily mean that all the quartz has replaced amphibole but that sufficient amphibole or talc was present during quartz growth to influence the crystal forms. Thus, any quartz which was present in the original rock type has recrystallised to a bladed form. This may be demonstrated in the iron-formations immediately above the talc zone, where fine talc fibres grow within fine grained quartz and the quartz grains begin to merge together and form elongate crystals parallel to the schistosity.

(iv) Specular hematite

Siliceous patches and bands in the talc zone are characterised by small spots of silvery, specular hematite, generally in the order of 1mm to 3mm across. These are dispersed throughout the rock and, in three dimensions, tend to have platelike forms with the long axes parallel to the schistosity. They are confined to rocks of the talc zone and are clearly products of the hydrothermal activity.

Magnetite rich bands are also present in the talc zone and their appearance suggests that they represent relict layering from the original iron-formation. The magnetite in the bands is

only partially oxidised to hematite, indicating that magnetite present in the original rock type remained essentially stable during hydrothermal activity.

The specular hematite is considered to represent iron which has been mobile in the talc zone and which has migrated to form spots. The iron was probably released from iron rich amphiboles during their alteration to talc and the parallel orientation of the spots suggests that hematite crystallisation was controlled by amphibole schistosity already present in the rock.

Amphibole replacement has probably been a major factor in the development of the talc zone. However, not all the talc is due to replacement of amphiboles, as very fine grained talc occurs interstitial to quartz grains in most samples from the iron-formations just above the talc zone and increases with increasing proximity to the main talc zone. This appears to have formed within the quartz as a direct result of the hydrothermal activity but the composition, so far as could be ascertained, is identical to talc which has formed directly from amphibole. There is no direct evidence to show which mechanism was dominant in the talc zone but most of the talc crystals are aligned parallel to the regional amphibole trend suggesting that crystallisation was controlled by pre-existing amphibole forms and that amphiboles formed a substantial portion of the original rock. A high percentage of quartz in the talc zone has the shape of amphibole crystals and contains thin slivers of silicates along parallel

cleavages, also suggesting that amphiboles formed a major component in the original rock type. The alteration of amphiboles was clearly accompanied by extensive redistribution of quartz already present in the rock and there was also movement of iron released during the amphibole alteration process. Iron oxides already present in the rock were partially oxidised but remained essentially in situ. These points conform to the suggestion, made earlier, that the original rock type of the upper talc zone was amphibole-quartz schist.

Whole rock analyses show that the talc zone rocks are broadly similar in composition to siliceous iron-formations (Section II and Appendix I). Magnesia and silica appear to be rather higher than in a comparable grunerite rich iron-formation but it is impossible to establish this firmly with the small core samples available for analysis. Trace element levels are uniformly low and are similar to those of unaltered iron-formations. One important feature is the complete absence of detectable calcium which is normally a minor component of iron-formation units. Some calcium must have been present in the original rock, as shown by tremolite remnants amongst the quartz and talc, but this has been virtually all removed during the hydrothermal process.

(c) Basic intrusives (amphibolites)

The main effect of the hydrothermal activity on the intrusives is to convert them completely to chlorite, as described in Section II. This occurs irrespective of whether the

intrusive is doleritic or a feldspar porphyry, which are the two types identified. The intrusives must pre-date the hydrothermal activity as they have remnant igneous textures and contain shadows of igneous minerals.

The replacement is volume for volume as can be established in Tunnel No.4, where a thick chloritised dyke retains an even grained igneous texture and chip-channel samples from the contact to the centre show a completely uniform composition (Table 23). In thin section, shadows of pre-existing plagioclase are sometimes seen.

Table 23. Analyses of chip-channel samples crossing the contact, and from the centre of a chloritised dyke, Tunnel No.4, 1000S. (Measurements in feet from Tunnel Portal)

	Fe	SiO_2	Al_2O_3	Ig.	CaO	MgO	Mn	S	TiO_2
Centre:									
375'-380'	17.7	30	16	11.1	0.05	14.0	0.75	0.08	1.1
Contact:									
420'-425'	16.5	33	15	10.0	0.05	14.0	0.75	0.08	1.0
425'-430'	19.4	29	15	10.0	0.1	13.0	0.65	0.07	1.1

All the chloritised intrusives have a similar mineral and chemical composition as shown in Fig.58 . This establishes that the alteration process was uniform irrespective of whether the intrusive was within the magnetite-hematite-carbonate or the talc zones.

Chloritisation has involved extensive chemical changes which can be estimated by comparison of altered and unaltered rocks.

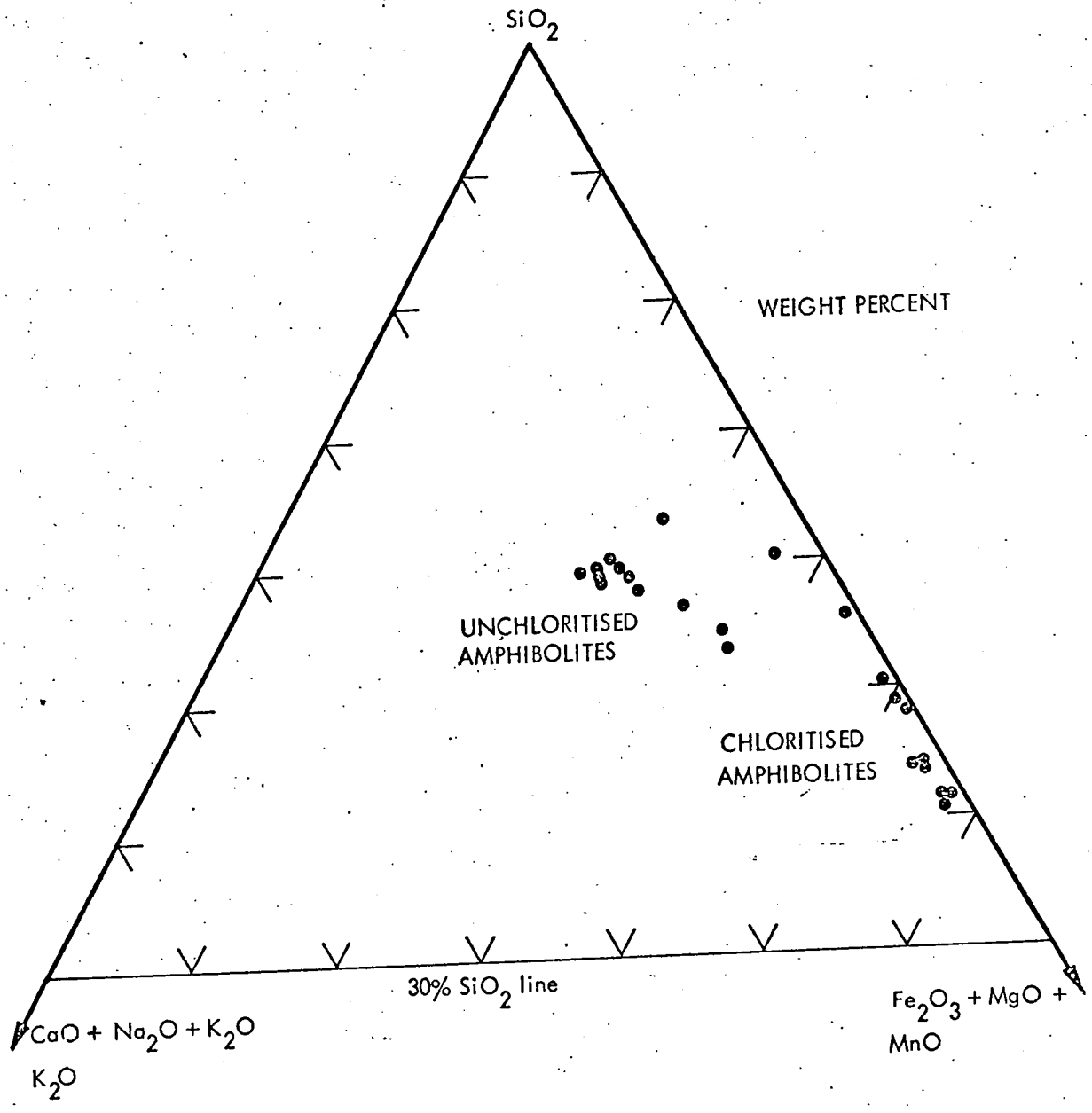

Fig. 58. Chemical compositions of unchloritised and chloritised amphibolites at Iron Duke.
Al_2O_3 is approximately the same for both groups and has not been included in the diagram.

Unaltered basic intrusives occur in the southern half of Iron Duke and, at depth, below the magnetite-hematite-carbonate orebody (Fig.50). These rocks are all similar in mineralogy and chemical composition. Some are partly chloritised and the chemical affect of chloritisation is to move the whole-rock composition towards that of the completely chloritised intrusives, as shown in Fig.59. The large basic mass in the southern half of Iron Duke shows this particularly well and it is from this mass that the chloritised dykes to the north are thought to extend. Remnant igneous micro-textures within the chloritised dykes are similar to those of the unaltered rocks except for one small body of chloritised feldspar porphyry which is different from any other igneous rocks in the area.

For these reasons, the original compositions of the chloritised intrusives are considered to be approximately the same as those of the unaltered basic intrusives and the chemical changes involved in chloritisation are shown in Table 24 and Fig.59.

The major losses and gains resulting from chloritisation are:

Substantial gains - Mg, Fe, H_2O, Zn

Substantial losses - Si, Ca, Na, Ba, Sr, Rb

The most striking feature of Table 24 is the scale on which the main components have moved. Over 40% of the total silica in the original rock and virtually all the calcium have been

Table 24. Chemical changes involved in chloritisation of amphibolites

Analyses by Chemical Laboratory, BHP, Whyalla

Per cent	Including water			Normalised on water free basin		
	Unchloritised 66-584	Chloritised 67-908	Changes involved in chloritisation Wt. per cent oxides	Unchloritised 66-584	Chloritised 67-908	Changes involved in chloritisation Wt. per cent oxides
SiO_2	51.2	29.6	- 21.6	51.1	32.4	- 18.7
Al_2O_3	13.4	13.7	+ 0.3	13.4	15.0	+ 1.6
Fe_2O_3	15.0	24.3	+ 9.3	15.0	26.6	+ 11.6
MgO	5.8	17.4	+ 11.6	5.8	19.0	+ 13.3
CaO	10.1	0.9	- 9.2	10.1	1.0	- 9.1
Na_2O	1.9	0.1	- 1.8	1.9	0.1	- 1.8
K_2O	0.6	0.0	- 0.6	0.6	0.0	- 0.6
TiO_2	1.4	2.9	- 1.5	1.4	3.2	+ 1.8
MnO	0.3	1.2	+ 0.9	0.3	1.3	+ 1.0
S	0.1	0.0	- 0.1	0.1	0.0	- 0.1
P_2O_5	0.3	1.2	+ 0.9	0.3	1.3	+ 1.0
Ig. Loss (H_2O)	0.9	9.4	+ 8.5			
	101.0	100.7		100.0	100.0	

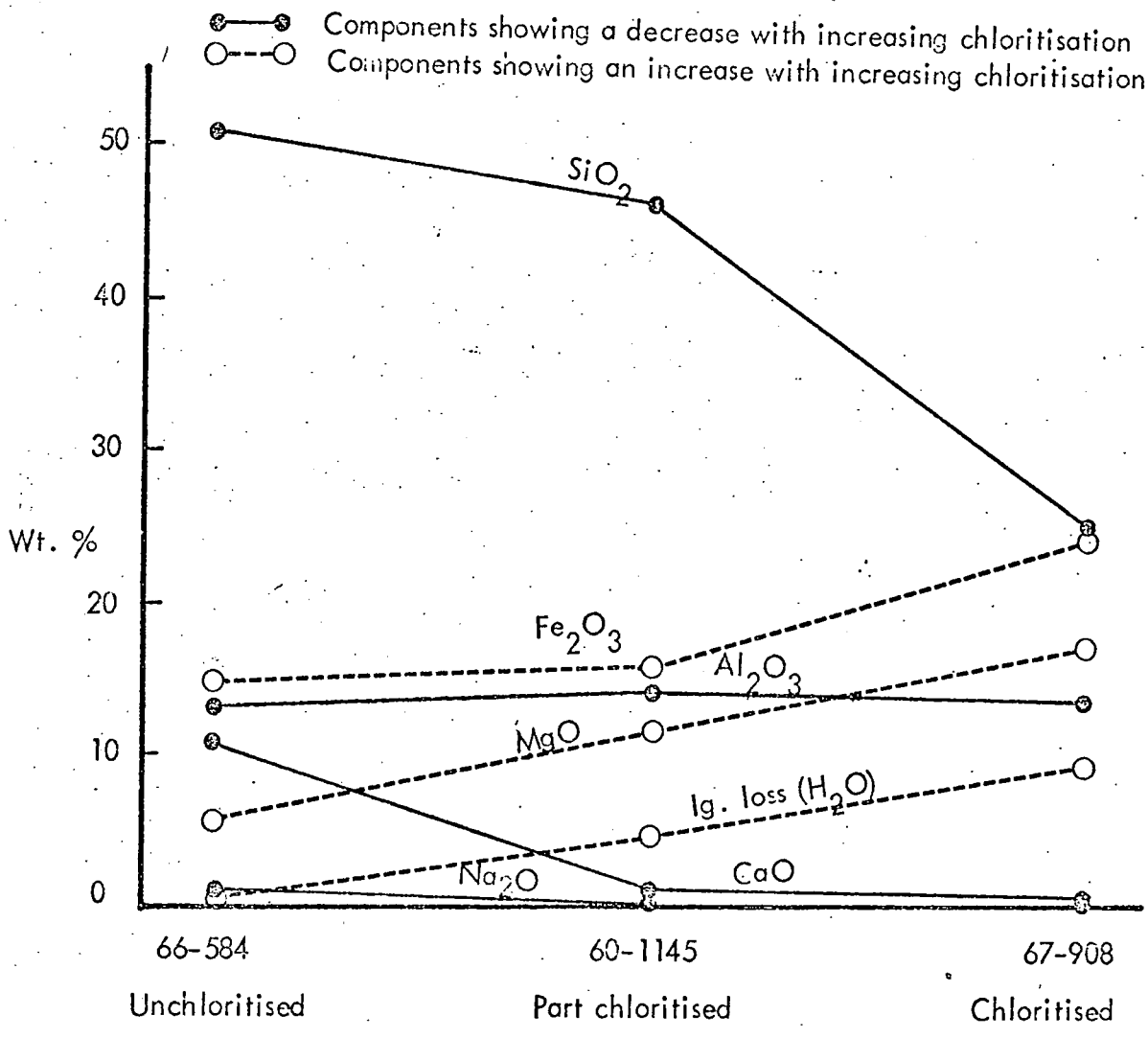

Fig. 59a. Changes in major element components during chloritisation, demonstrated by analyses of three amphibolite samples.

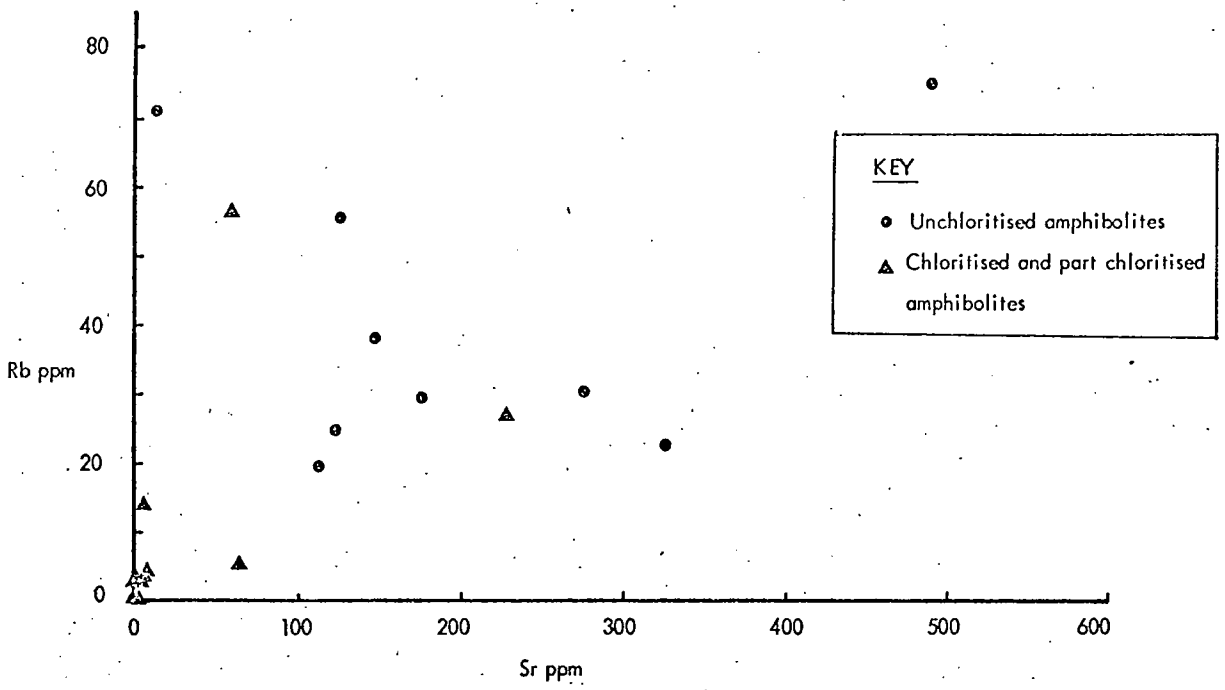

b. Sr and Rb values in chloritised and unchloritised amphibolites, values from Appendix I.
One sample of unchloritised amphibolite has unusually high Sr (798 ppm) and low Rb (2 ppm) and is not shown on the diagram.

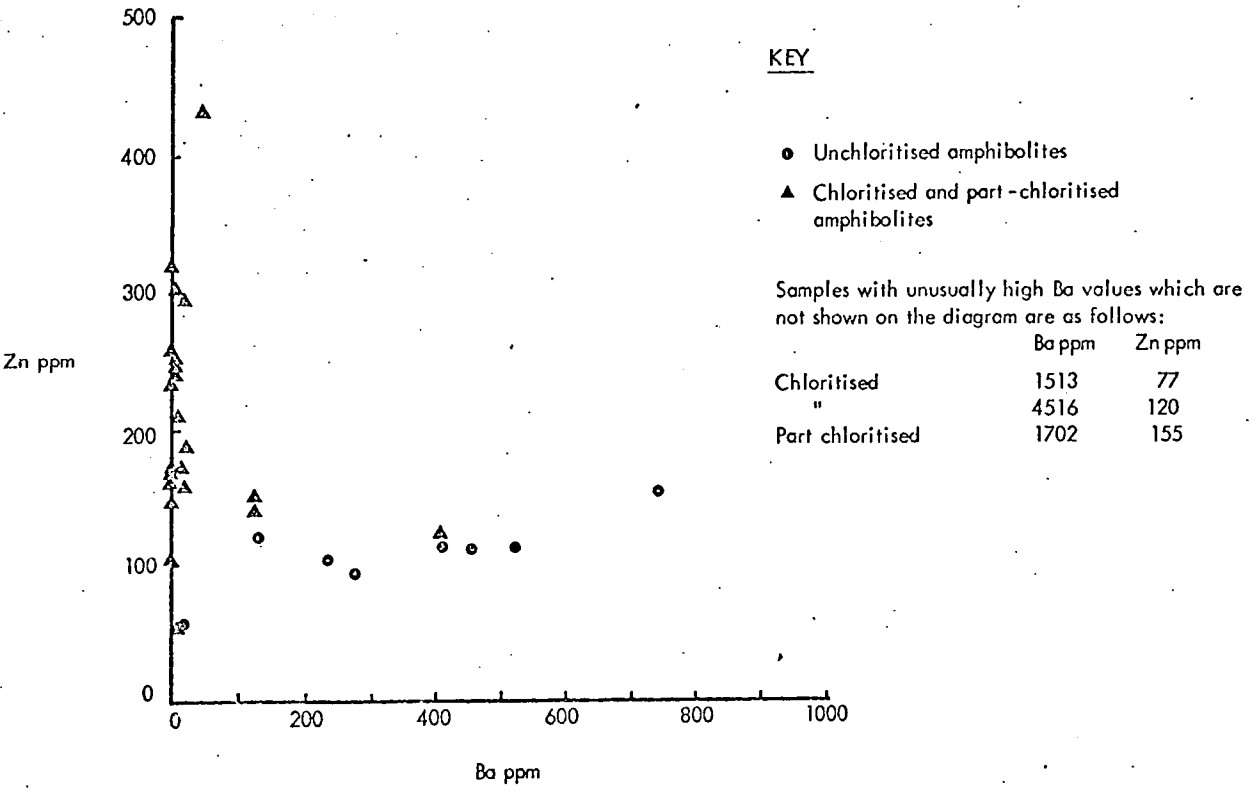

c. Ba and Zn values in chloritised and unchloritised amphibolites, values from Appendix I.

Fig. 59b. Changes in trace elements during chloritisation.

completely removed from the system. Iron and magnesium have been added, in rather lesser amounts and there has been a massive influx of water into the rock.

This process has been uniform throughout the region of hydrothermal activity, irrespective of whether the intrusive is in the ore or the talc zone. Furthermore, complete chloritisation extends well above the upper talc zone, affecting intrusives at high levels amongst unaltered iron-formation.

(d) Basal carbonate unit

Microtextures in the Iron Duke basal carbonate unit differ from those in carbonate units elsewhere in the Middleback Ranges. In the Iron Duke material, the carbonate crystals are larger, with somewhat ragged outlines and are often surrounded by fine grained granular carbonate as described in Section II. The larger crystals frequently contain fluid inclusions and sometimes appear to contain remnants of smaller crystals.

The facts described above suggest that the carbonate partially recrystallised during hydrothermal activity and it certainly appears that solutions, at least in small amounts, passed through the rock. The fine granular carbonate has the appearance of crushed material and the larger crystals tend to be elongate, with their long axes parallel which could result from recrystallisation under stress. These microtextures are interpreted, by the author, as products of recrystallisation due to fluid movement along grain boundaries and fractures during a period of tectonic disturbance.

The hydrothermal activity did not significantly change the composition of the rock. The basal carbonate unit at Iron Duke has the general composition of an ankerite and is similar in this respect to recorded analyses of carbonate units in other parts of the Middleback Ranges (Section II and Appendix I for analyses).

6. Mechanism of ore formation

The main effect of the hydrothermal solutions in the ore forming process was to remove silica from an iron-formation unit which contained layers of carbonate, amphiboles and some quartz. This silica removal could be achieved in two ways, firstly by the breakdown of silicate minerals releasing silica into solution, and secondly by metasomatic replacement of silicates by carbonates. The precise mechanism of silica removal at any particular point would depend upon the concentration of carbonate in solution; at carbonate-silicate interfaces metasomatic replacement would be particularly effective, whereas in silicate layers containing amphiboles and quartz there would be fluid-mineral reactions to form talc or direct removal of silica in solution. Both the replacement and removal mechanisms are considered to have been operative during the hydrothermal activity.

In either case, the silica released by the chemical reactions must have been held in solution and removed from the vicinity of the orebody. Within the orebody, silica removal would be facilitated by solution temperatures in the order of 200°C-300°C and a high pH due to the presence of carbonate, as discussed previously. These processes could take place only where the hydrothermal solutions were undersaturated in silica, which was evidently the case within the orebody but not in the surrounding talc zones, where the geochemical environment was more suited to silica precipitation than solution.

The process envisaged in ore formation is a gradual penetration of hot, carbonate rich solutions into an iron-formation unit containing layers rich in carbonates, amphiboles and quartz. Amphiboles and quartz were slowly replaced by carbonates, derived partly from the carbonate in solution and partly by redistribution of carbonates already present in the rock. The silica taken into solution was removed in a general upwards direction and the net result of the process was a silica loss, leaving small voids and cavities. Carbonate layers present in the original rock were gradually recrystallised and redistributed, producing diffusely layered structures. During this process, small amounts of carbonate were taken into solution and redeposited some distance away, resulting in a general upward movement of carbonate and leaving space behind. Carbonate introduced by the solutions crystallised with the carbonate already present in the original rock, merging with it and partly filling the cavities produced by silica loss and carbonate redistribution. The whole process is envisaged as one of gradual removal of silica, redistribution of carbonate and the creation of space which facilitated the movement of solutions.

In the first stages of ore formation, before the creation of space by the hydrothermal activity, the iron-formation protore unit must have been fine grained and tightly packed. Solution penetration during this phase is envisaged as being primarily by diffusion along crystal boundaries and through the crystal lattices. This concept of diffusion is supported by the facts that carbonate crystals in the layered ore fragments show signs of gradual

recrystallisation, the talc zone rocks show mineral changes such as amphiboles to talc, which must have resulted from diffusion, and the basic intrusives were converted in situ and completely to chlorite rock, which can only be explained by fluid or gaseous diffusion. The initial ore forming process is therefore regarded as one of carbonate metasomatism by diffusion carbonate rich fluids moving upwards into the iron-formations and carbonate minerals replacing the amphiboles and quartz. As fluid penetration became more extensive, the processes described above became more effective; silica was removed in solution, carbonates were redistributed and space was created within the orebody.

During subsequent stages of ore formation, the solutions moved freely through fractures and passageways in the orebody, as shown by the ubiquitous brecciation and vein carbonate. This space within the orebody is considered to result from repeated tectonic movement combined with high fluid pressures. Following the first stage of fluid diffusion, with its accompanying mineral changes, there was movement along the high angle reverse fault on the east side of Iron Duke. The movement had a strong lateral component, Iron Duke moving south relative to the schists of Death Adder Gully, and this resulted in shallow overthrusting to the south within the iron-formation sequence as shown by the small thrust previously described in Winze No.4. During the thrusting, the main body of siliceous iron-formations above the developing orebody acted as a rigid block, moving southwards and upwards over the ore below, a process facilitated by the lubricating effect of the

hydrothermal solutions. Fracturing developed in the protore unit, below the siliceous iron-formations, which was already partly reconstituted and had some space due to the action of the hydrothermal fluids. The fluids penetrated the fractures and this had two important effects; firstly the processes of silica removal and replacement were accelerated, and secondly high fluid pressures caused splintering and brecciation within the orebody. The talc zone immediately below the compact block of siliceous iron-formations became strongly folded and, to some extent, faulted. The whole process is considered to be one of continual fluid penetration and repeated tectonic movement over a long period of time resulting in a gradual expansion of the orebody through the iron-formation unit.

In the talc zone above the orebody, there is virtually no carbonate, and silica was precipitated from solution as shown by quartz replacing amphiboles and the widespread occurrence of bladed quartz. It is impossible, with available evidence, to establish firmly that silica was added to the original rock but the possibility is supported by the change from amphibole to talc, which involves the addition of silica, and by the presence of bladed quartz which has clearly crystallised during the hydrothermal activity. For these reasons, it is considered that silica taken into solution within the orebody was transferred upwards and stabilised in the talc zone as talc and quartz. There was also some movement of magnesia from the orebody to the talc zone but any calcium originally present in the talc zone was completely removed in solution.

The process envisaged in the upper talc zone formation is a steady movement of fluids from the orebody into overlying amphibole-quartz schists and iron-formations. Fluids immediately adjacent to the orebody were carbonate rich, and the amphiboles and quartz were replaced by carbonates. Further from the ore, the fluids were carbonate free but were rich in silica, calcium and magnesia derived from the breakdown of minerals within the orebody. Silica and magnesia were stabilised in quartz and talc, whereas calcium remained in solution and was removed from the system accompanied by any calcium originally present in the amphiboles. Fluid movement was by diffusion and the solutions moved upwards along the amphibole-quartz schist layer rather than into the overlying quartz rich iron-formation units.

The thin talc zone below the orebody consists primarily of talc with some carbonate, pyrite and minor quartz. It is believed to represent a thin amphibole rich schist with little original quartz, and the talc forming processes are considered to be similar to those in the upper zone except that the talc formed from amphiboles and quartz already present in the rock, and the fluids contained some carbonate. Pyrite, already present in the original rock, was taken into solution and precipitated a short distance away causing a general upward concentration.

In the basic intrusives, the fluids moved by diffusion through the whole rock, causing large scale chemical changes which involved removal of silica, calcium and alkalis, and addition of iron, magnesia and water. The alteration process affected all

basic intrusives within the orebody and talc zones, and extended upwards along basic dykes into the zone of unaltered iron-formations. The transfer of silica, calcium and alkalis is therefore assumed to have been upwards, away from the vicinity of the orebody, and these components were presumably stabilised in rocks at higher levels which have since been removed by erosion. The complete alteration of the basic dykes, in situ, shows that the hydrothermal fluids found penetration relatively easy and this could result from the intrusives being at higher temperatures than the surrounding rocks. Both the basic intrusives and the talc zones were siliceous environments, yet in the former silica was removed by the hydrothermal solutions and in the latter it was precipitated. This could also be due to higher temperatures in the basic intrusives, as silica solubility increases rapidly with increasing temperature.

Magnetite concentrations occur within the ore at contacts with chloritised basic intrusives and the faulted contact with argillaceous schists of Death Adder Gully, as described in Section II. They vary in thickness from a few inches to several feet, contain angular fragments of chloritised intrusives, and extend alongside the dykes into the siliceous iron-formations which overly the ore. The significance of these magnetite concentrations is not fully understood. It is clear that iron rich solutions have moved through open space alongside the intrusive dykes, and the angular dyke fragments can be explained as splintering due to high fluid pressures. However, within the orebody, the most striking feature of the concentrations is the lack of carbonate, in contrast with abundant carbonate throughout the rest of the ore. This suggests

that either the geochemical environment at dyke margins tended to keep carbonate in solution during the ore forming process, or that the solutions which precipitated magnetite were a separate, low carbonate phase predating or postdating the main oreforming solutions. Two possible alternative mechanisms to explain the magnetite concentrations are as follows:

(i) The dyke margins and faulted contacts with argillaceous schists provided ready access for migrating fluids and there was rapid movement along these channels, in advance of the main ore forming solutions. Carbonate tended to be stabilised in the main hydrothermal zone and the advance fluids were relatively lean in carbonate, with the result that iron was precipitated as iron oxide whereas the two other main components, calcium and magnesium, remained in solution.

(ii) The dykes were hotter than the surrounding rocks, causing rapid solution flow at their margins which prevented carbonate precipitation until the later stages of hydrothermal activity. During the later stages when most carbonate had been precipitated, the remaining solutions were carbonate deficient relative to the acidity of solutions adjacent to the dykes, with the result that carbonate was retained in solution, iron crystallised as magnetite and the remaining calcium and magnesium remained in solution.

7. Controls of ore formation

The shape of the orebody at Iron Duke conforms broadly to that of a lithological unit (Figs. 20a-g). This is not so apparent in the centre and east limb of the synform, where steeply dipping siliceous iron-formations pass down dip into the ore but, stratigraphy does appear to be a broad control in orebody shape and stratigraphic location. This is supported by the fact that the two other known occurrences of carbonate rich ore, at Iron Queen and Iron Baron, are both at the same stratigraphic level as the ore at Iron Duke. The stratigraphic control is considered to result partly from the mineralogy of existing rock types and partly from the presence of the underlying basal carbonate unit, as discussed below.

In the ore forming process described on previous pages, the initial stages of ore formation were controlled by the ability of the hydrothermal fluids to penetrate particular rock types by diffusion along grain boundaries and through crystal lattices. This diffusion mechanism resulted in extensive changes in rock composition and character, and the ease of fluid penetration would be strongly influenced by the mineralogy and chemistry of the original rock. The protore unit contained,by volume, 30% to 50% iron oxides and 50% to 70% intermixed carbonates, amphiboles and quartz, the amphibole being mainly tremolite. Above the protore unit were grunerite rich schists and iron-formations, and overlying these was the main sequence of quartz rich iron-formations. The fluids extensively penetrated the protore unit and the grunerite schists but made

relatively little penetration into the overlying quartz rich iron-formations. Within the protore unit, penetration into the carbonate rich layers was also restricted, as shown by the remnant finely layered portions within the ore. The amphiboles are therefore considered to be the main factor controlling fluid movement and their abundance in the protore unit and overlying amphibole schists allowed extensive fluid penetration in these units, whilst their relative paucity in the overlying massive iron-formations restricted penetration. As a result, the solutions moved up the limb and axial region of the synform within the amphibole rich units, rather than directly upwards into the massive, quartz rich, iron-formations. This conforms with Catley's (1963) proposal that amphiboles are a major control in the development of magnetite-hematite-carbonate ore, and with Whitehead's (1962) suggestion of a tremolite rich potential ore horizon.

The basal carbonate unit is critical to ore formation in several ways. Prior to contact with the carbonate, the solutions were moving through siliceous rocks, consisting of granite gneisses, metamorphosed sediments and the lower part of the iron-formation sequence. By analogy with deep, hot waters from many parts of the world, they would have a nearly neutral pH and probably contained considerable silica (White, Hem and Waring 1963, Helgeson 1963). On contact with the basalt carbonate, the pH would rise and fluid-carbonate reactions could take place to form calc-silicates such as resulting in a loss of silica from solution. A process of this type was described by Sawkins (1964) in the Providencia area of

North Central Mexico. At Iron Duke, unoriented diopside and tremolite occur within the basal carbonate unit and could be the product of such reactions. However, diopside and tremolite are higher temperature minerals than those found within the orebody, and if they are in fact products of the ore forming process, they must have formed at an early stage of the hydrothermal activity when temperatures were high and the amounts of fluid limited. The bulk of this silica removal probably took place at considerably greater depth down the pitch of the synform, in a region not yet penetrated by drilling. Having passed through the basal carbonate unit, the solutions would be alkaline, rich in carbonate and silica deficient, facilitating carbonate replacement and silica removal immediately above the carbonate unit. The ore forming process is therefore envisaged as commencing immediately above the basal carbonate unit and gradually spreading upwards away from it in units favourable to the replacement mechanisms. The process includes some movement of carbonate from the basal carbonate unit into the ore above. Carbonate compositions in the ore and basal carbonate support this possibility; the bulk of the ore carbonates, including both well banded and vein carbonates, have the same general composition as the basal carbonate. The presence of the basal carbonate is therefore essential, as it controls the solution geochemistry and provides a supply of carbonate to add to that already in the protore unit, thereby maintaining carbonate replacement in the orebody.

The final rock composition within the zone of hydrothermal alteration is controlled by the original rock chemistry, which is

therefore a major influence on the type of ore produced. In the protore unit, the abundant carbonate already present in the rock maintained a high carbonate content in the solutions, resulting in carbonate replacing amphiboles and quartz. Tremolite, being the dominant amphibole in the protore, facilitated the replacement process as the alteration to carbonate is relatively simple with ionic carbonate substituting for silica and calcium and magnesium remaining in the new mineral. In the talc zone, the original rocks were carbonate free, the solutions were lower in ionic carbonate, and the amphiboles altered to iron rich talc. Basic intrusives and the schists of Death Adder Gully adjacent to the orebody, developed chlorite due to the presence of aluminium in the original minerals. Thus, magnetite-hematite-carbonate would be prone to form in tremolite and carbonate rich units, whereas the ore development would be less extensive in units rich in quartz or grunerite. It is envisaged that different types of ore formed within the iron-formation wherever they were penetrated by hydrothermal solutions, and the precise type of ore depended upon the pre-existing mineralogy. In places where tremolite or carbonate was plentiful in the original rock, the orebody is likely to be extensive and consist of iron oxides and carbonates, as at Iron Duke. Alternatively, in places where quartz and grunerite predominated, the orebody will probably be small and contain remnant silica.

Folding had a strong effect on the shape and disposition of the Iron Duke orebody. So far as can be ascertained with present drilling information, the ore is thickest in the axial region of the

synform (Figs. 20a-g). This conclusion is based entirely on interpretation, as no drillhole has penetrated to the base of the ore in the east limb, but the thickest part of the orebody does coincide with the estimated position of the synform axial plane and the ore becomes thinner in the west limb. The thickening is considered to reflect two factors; original thickening of the units by flowage in the axial region of the fold, and relative ease of fluid penetration in this region. It is not clear whether the fluids became concentrated in the axial region due to it being a relatively low pressure zone or whether they moved mainly in response to mineral and chemical controls. In either case, the hydrothermal activity was most effective in the axial region of the synform and the fold dictates, to a large extent, the size and shape of the orebody.

Faulting is considered to be an important factor in the location and disposition of the ore. The eastern boundary of the orebody is defined by a high angle reverse fault which places the iron-formation units against the stratigraphically higher schists of Death Adder Gully. The precise age of this fault is not known, but there are magnetite concentrations within the ore adjacent to schist contacts, showing that at least part of the hydrothermal activity postdates major fault movement. On the other hand, interlocked slivers of ore and schist in drillholes, together with small scale faulting within the ore and talc zones of Tunnel No.4 and Winze No.4, suggest that some movement post dates the ore formation. On this basis, it is concluded that the fault has moved repeatedly,

probably over a long period of time and partly during the hydrothermal activity. The fault affects the ore forming process in two ways; firstly by placing a unit unfavourable to carbonate metasomatism, the Death Adder Gully schists, adjacent to the protore unit thereby defining the eastern limit of ore development, and secondly by localising the upward moving solutions along the fault zone. The latter is speculative and depends upon the interpretation of the solution source. In the proposed theory, the fault is regarded as part of a major north-south fracture zone extending for many miles and probably first developing in the waning stages of metamorphism. Fluids moved by diffusion into this relatively low pressure zone at great depth, and migrated slowly upwards, eventually penetrating the iron-formations. Movement was at least partly through the rock rather than along fractures, as shown by the chloritisation in Death Adder Gully schists adjacent to the fault and by similar localised chloritisation in the equivalent Cook Gap schists to the north, described in Sections I and II. In this concept, the presenceof the fault is essential to the ore forming process, as it dictates the initial flow of the hydrothermal solutions.

In the later stages of the hydrothermal activity, tectonic movement had a major effect on controlling the flow of solutions by creating fractures and channelways within the orebody. Prior to tectonic movement fluid migration must have been primarily by diffusion and the ore would be of limited extent. Tectonism had the effect of stimulating fluid movement and creating space, which

facilitated the ore forming process and resulted in a gradual expansion of the orebody.

8. Summary of magnetite-hematite-carbonate ore genesis

The full sequence of events leading to the formation of magnetite-hematite-carbonate and the talcose rocks is considered to be as follows:

(1) Sedimentation

The iron-formation sequence was deposited by chemical or biochemical precipitation of iron oxide, silica, carbonates and iron-magnesium silicates, together with thin clastic argillaceous units. The lowest part of the iron-formation sequence was rich in carbonate and included a thick carbonate unit, now known as the basal carbonate. Immediately above the basal carbonate was an interlayered unit, several hundred feet thick, of intermixed carbonate, quartz and iron oxides, possibly with smaller amounts of iron-magnesium silicates. Overlying this unit was an intermittent layer rich in iron-magnesium silicates or siderite together with quartz and lesser amounts of iron oxides, which reached a maximum thickness of about 100 feet. This passed upwards into the main sequence of silica-iron oxide rocks with minor amounts of carbonates and silicates.

(2) Folding and metamorphism

The iron-formations were strongly folded about north-south axes with crossfolding producing an en echelon fold pattern. At Iron Duke, the main fold was a tight, almost isoclinal in form and the carbonate and silicate units flowed into the hinge area.

Regional metamorphism reached lower amphibolite facies grades, with temperatures and pressures in the order of 450 °C and 2-6 kb. Water, and to a lesser extent carbon dioxide, migrated from the system but other components remained essentially in situ. Calcium-magnesium carbonates reacted with quartz to form tremolite, original iron-magnesium silicates reacted to form grunerite, as did siderite and quartz, and the argillaceous schist units developed biotite, hornblende, plagioclase and garnet. The result was a tightly packed, compact group of rocks characterised by even, fine grained textures, with the lower part of the sequence being particularly rich in tremolite and carbonate layers.

(3) Faulting, intrusions and initial fluid movement

During the waning stages of regional metamorphism, regional zones of dislocation developed, which were steeply dipping and had both lateral and vertical components of movement. At Iron Duke, one such zone was represented by a high angle reverse fault which moved the iron-formations southwards and upwards relative to overlying argillaceous schists.

Hydrothermal fluids migrated into the dislocation zones at depth, and moved upwards through fractures and by diffusion through the rocks. The fluid source is not known, but it is envisaged that the regional faults penetrated to great depths where they formed relatively low pressure zones into which fluids of metamorphic or igneous origin migrated.

Basic igneous masses were intruded during this period, one such mass penetrating the southern part of Iron Duke and dykes

extending from it along the limbs of the synform.

(4) Hydrothermal activity

Fluid migration continued upwards along the zones of dislocation, below the iron-formation sequence. These deep solutions probably had a pH approaching neutrality and a high silica content due to their contact with granitic rocks and metamorphosed clastic sediments. On reaching the iron-formations, the fluids continued their upward movement in the fault zone, passing through the lowest iron-formation units and into the basal carbonate unit. On contact with the basal carbonate, fluid-carbonate reactions took place forming calc-silicates and the fluid became silica deficient with a high pH. Having passed through the basal carbonate, the fluids entered the interlayered unit rich in carbonate and tremolite, and carbonate metasomatism began to take place with carbonate replacing quartz and tremolite. The fluids continued to move upwards along the fault zone but, at this stage, the iron-formation mineralogy became an important control. Penetration was most effective in amphibole rich layers, and was facilitated in the tremolite-carbonate rich unit by inherent carbonate enhancing the carbonate metasomatism. Penetration into the grunerite rich layer was effective but there was little solution movement into the overlying quartz rich iron-formations. As a result of these mineralogical controls, the fluids began to move upwards along the pitch of the synform, below the quartz rich iron-formations.

In the tremolite and carbonate rich protore unit, tremolite altered to ankerite and quartz was completely removed by the solutions. Carbonate layers already present in the rock were recrystallised and there was a general upward movement of carbonate through the body. Iron oxides already present in the rock remained essentially in situ but there was some movement of iron, probably released from grunerite during replacement by carbonate. Silica released during the replacement processes was transferred upwards in solution, together with lesser amounts of calcium and magnesium.

The overlying grunerite-quartz schists were extensively penetrated by the solutions which were now silica rich due to the reactions within the ore below. Grunerite, and any tremolite present, were altered to talc and were extensively replaced by quartz. The silica from the orebody was, therefore, effectively transferred to the talc zone above. In the talc zone below the ore, a similar process took place but with far less quartz and with some carbonate present. Iron sulphides, originally present as a layer at this stratigraphic level, were taken into solution and moved upwards over small distances in a similar manner to the carbonate movement within the ore.

The basic intrusives were, at this time, still cooling and were at rather higher temperatures than the surrounding rocks. The hydrothermal solutions moved into, and upwards along, the dykes causing uniform chloritisation and removing silica, calcium and alkalis whilst adding iron, magnesium and water. There was also

limited fluid penetration into the argillaceous schists of Death Adder Gully, where they were adjacent to the orebody, and the schists were locally chloritised.

This process extended over a long period of time, during which there was repeated movement on the major reverse fault on the east side of Iron Duke. The movement had a strong lateral component, with the iron-formations moving southwards relative to the schists of Death Adder Gully, and during the dislocation the siliceous iron-formations acted as a rigid block sliding south and upwards relative to the ore below. The movement was facilitated by the lubricating effect of the hydrothermal solutions and the steadily expanding upper talc zone. Within the orebody, some space had already been created by the mineral changes involving silica loss, and the tectonic movement combined with high fluid pressures to cause splintering and fracturing within the ore. With repeated tectonic movement and fluid penetration, the orebody gradually extended along the pitch of the synform below the main sequence of siliceous iron-formations. As the hydrothermal process drew to a close and temperatures fell, small amounts of quartz and pyrite were deposited from solution in the later carbonate veins within the ore.

B. ORIGIN OF THE HEMATITE ORE

1. General

Iron Duke is one of three major hematite ore bodies in the Middleback Ranges and there are numerous smaller bodies of similar type. All the ores have common features which must be taken into account in any theory of ore genesis. These are:

(1) The ore is blue, granular hematite varying from hard, blocky ore to friable, porous material which crumbles at a touch.

(2) All the major orebodies are at the same stratigraphic level near the base of the lower iron-formation unit.

(3) The orebodies occur in pitching synforms or steeply dipping fold limbs.

(4) All known orebodies outcrop and the bulk of the ore is within 800 feet of the present surface.

(5) All the orebodies pass laterally into iron-formations or into hidden magnetite-hematite-carbonate ore.

(6) Intrusives and schists within the ores are intensely weathered and consist predominantly of clay minerals.

Iron Monarch (Fig.1) is not included in the above description or the following discussion. The orebody has many of the common characteristics listed above but is unusual in containing a high proportion of hard hematite with considerable, irregularly distributed manganese. This orebody requires a separate, detailed study.

Numerous theories have been proposed for the origin of the hematite ores, as described briefly in Section I, but the three most important are, that the ore is sedimentary, that it is due to granitising fluids, and that it results from supergene leaching and enrichment. In the following pages, the evidence on ore genesis at Iron Duke will be outlined followed by a discussion of the main theories of ore genesis applicable to all the Middleback Range deposits, excepting Iron Monarch.

2. Evidence on the origin of Iron Duke hematite ore

The Iron Duke is typical of hematite ore bodies in the Middleback Ranges, in that it occurs in the hinge area and limb of a pitching synform, and is near the base of the iron-formation sequence just above the basal carbonate unit. It rests upon a large basic intrusive mass to the south, extending northwards down the pitch of the synform into magnetite-hematite-carbonate ore and along strike in the west limb into siliceous iron-formations (Section II, Figs. 18,20a-g).

The hematite ore frequently shows a distinct layering (Fig.6D) which closely resembles that of the iron-formations, and is due to thin layers of compact hematite separated by layers in which the hematite is more finely granular and there is more pore space. In outcrop and in tunnel exposures, the layering strikes north-south and dips inwards on either side of the synform axis in exactly the same way as the iron-formation layering. On the strike surfaces of layered fragments, well developed rodding is sometimes present which pitches north, parallel to the synform axis. These features show clearly that the layering pre-dated the folding and metamorphism. It must, therefore, be either original layering in an iron oxide sediment, or a relict layering from the pre-existing rock type.

Microtextures of layered ore samples were described in Section II and the most significant points are the large amount of pore space and the fine meshwork of bladed hematite, with tiny

Fig. 60a. Hematite ore, surface outcrop Iron Duke. Note the fine scale layering with individual layers having distinct characteristics. Scale in inches.

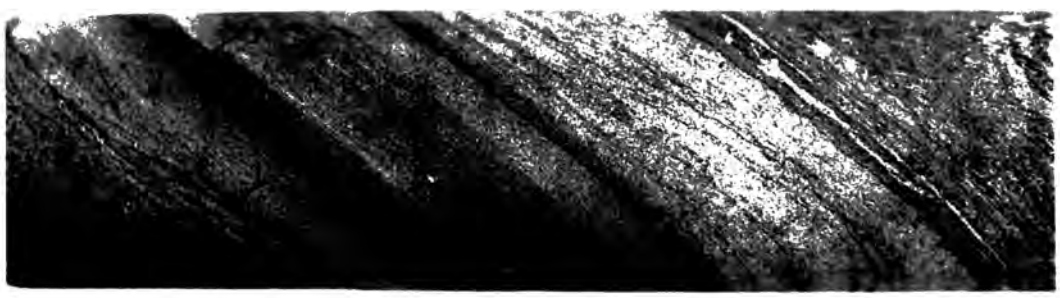

Fig. 60b. Iron-formation core from below the zone of oxidation. Scale in inches.

specularite crystals projecting into pore spaces, which binds together larger, blocky crystals. Neither the spaces nor the fine, unoriented meshwork could have survived regional metamorphism to lower amphibolite facies grades, and they must therefore have developed at some period subsequent to metamorphism. On this basis, it is concluded that a good deal of the ore was originally a fine grained, layered rock from which some components have been removed subsequent to regional metamorphism.

It is unlikely that the original rock type consisted of iron oxides alone, as suggested by Catley (1964). A good deal of the original rock was fine grained magnetite, as shown by cubic outlines and small remnant islands of magnetite in some hematite grains, and this has remained in situ forming the basic structure of the layering. The hematite grains are separated by spaces of similar dimensions to the grains themselves and, in Catley's concept, these spaces must have been originally filled by iron oxides. There is, however, no apparent reason for the selective removal of individual iron oxide grains whilst adjacent grains remained in situ, and this mechanism would have to operate throughout the entire orebody if the original rock type were iron ore. Furthermore, in layered ore samples, the cavity shapes in individual layers vary, producing different textures in each layer, as can be seen in Fig.60. This suggests that minerals of varied size and shape were present, and these have been removed, leaving hematite grains. Some patches of compact, massive hematite ore could be due to an inherently high iron content, but they could also result from later enrichment by iron oxides infilling the spaces in porous ore. Some movement

of iron has clearly taken place within the orebody, as shown by the fine grained specular hematite occurring within the cavities.

The most likely rock types from which the ore has formed are the siliceous iron-formations and the magnetite-hematite-carbonate. Field and drilling evidence shows that the hematite ore passes laterally into both these rock types, and also, to a lesser extent, into the talc zones surrounding the magnetite-hematite-carbonate body. The lateral transition to siliceous iron-formations can be seen, despite poor outcrop, on the west flanks of Iron Duke where bands of outcropping porous ore become progressively richer in silica and more compact to the north. A similar transition, to overlying siliceous iron-formations, takes place in Tunnel No.3, where there is a gradual change from porous ore to hard iron-formations, with the layering in the ore parallel to that in the iron-formation. These observed transitions suggest that at least some of the ore has formed by removal of quartz and amphiboles from siliceous iron-formations. This is supported by the general similarity of layering in the ore to that in the iron-formations. Each thin layer in the hematite ore has a texture caused by the shape and size of the cavities and of the hematite grains. These textures resemble the iron-formation textures described in Section I which result from various mineral combinations.

The transitions from hematite ore to the talc zones and magnetite-hematite-carbonate ore are known only by drilling. Analyses and lithological correlation of drillholes in the west limb of the synform show that the hematite ore passes down dip directly into

magnetite-hematite-carbonate and, to a lesser extent, into the upper and lower talc zones. The transition to the upper talc zone is irregular, and talc zone rocks are definitely present above the hematite ore in some places. In the transition to magnetite-hematite-carbonate, the hematite ore is similar to that nearer the surface, being blue, granular hematite with small cavities which sometimes contain carbonates. A narrow strip of hematite ore extends down dip and pitch from the main orebodies, forming a thin layer along the base of the magnetite-hematite-carbonate body (Figs.20a-g). This ore tends to be red, rather than blue, contains considerable pyrite and has numerous irregularly shaped cavities which produce a structure resembling the magnetite-hematite-carbonate breccias rather than the finely layered iron-formations. The basal carbonate unit occurs immediately below this layer and is saturated with red hematite dust along carbonate grain boundaries and cleavages. The ore layer passes laterally, down pitch, into the lower sulphide rich talc zone and the calcite rich layer at the base of the magnetite-hematite-carbonate body. The general impression is that the hematite has formed by removal of carbonates and silicates from the talc zone and the calcite rich layer.

The hematite ore does not appear to be a product of the hydrothermal activity that produced the magnetite-hematite-carbonate and talc zones. Hematite ore is best developed in the southern half of the area where the effects of hydrothermal activity are least, and is poorly developed in the north where the hydrothermal activity was intense. The only iron concentrations clearly produced by the hydrothermal activity are thin magnetite layers adjacent to intrusives

and schists, and most of the iron within the magnetite-hematite-carbonate body has remained stable or moved only small distances. Furthermore, the disposition of the hematite ore is such that it cannot be regarded as a halo around the hydrothermal activity which produced the magnetite-hematite-carbonate ore. Alternatively, the possibility must be considered that an earlier phase of hydrothermal activity produced porous magnetite-hematite ore by removing quartz and amphiboles from siliceous iron-formations, and that this ore was later penetrated by carbonate rich solutions which produced the magnetite-hematite-carbonate ore. This concept is regarded as unlikely, as it does not account for the complete lack of any sign of hydrothermal alteration associated with hematite ore in the southern part of Iron Duke, or the complete lack of carbonates and talc in the bulk of the hematite ore, despite its porosity which would allow extensive penetration by later solutions. Furthermore, small isolated hematite orebodies occur within the siliceous iron-formations and do not appear to be related to any form of hydrothermal activity. The upper talc zone is clearly a product of the hydrothermal activity which produced the magnetite-hematite-carbonate body, yet it occurs at the surface above the hematite ore in some places. This suggests that magnetite-hematite-carbonate was previously more extensive and that hematite ore has subsequently formed from it, by removal of the carbonates.

The hematite ore in the southern half of Iron Duke rests upon a large intrusive mass of dioritic composition. Precise relationships between the two rock types are difficult to ascertain because the top of the intrusive is intensely weathered. However,

the weathered portion of the intrusive is rich in fine grained hematite, apparently derived from the orebody above, and this shows that there has been some movement of iron subsequent to the igneous activity. In common with other hematite orebodies throughout the Middleback Ranges, schist bands and intrusive dykes within the Iron Duke ore are intensely weathered and consist primarily of clay minerals.

The general impression at Iron Duke, therefore, is that the hematite ore has developed from siliceous iron-formations, magnetite-hematite-carbonate ore and talcose rocks, by removal of quartz, silicates and carbonates. There is no evidence that this removal was effected by hydrothermal activity. On the other hand, there is considerable evidence of deep, intensive weathering which is confined to the vicinity of the ore, and which could have removed components from the original rocks. Intense weathering is shown by the high clay content of schists and intrusives within the ore, the hematite saturation in rocks immediately below the ore, and the change in character of hard siliceous iron-formations to soft powdery material adjacent to the ore.

3. Theories of hematite ore genesis

(a) Theory of sedimentation

Catley (1964) proposed a sedimentary origin for the Iron Duke hematite ore, suggesting that an iron oxide facies developed during deposition of the iron-formation sequence. This mechanism has been shown to be theoretically valid for ores within iron-formations in North America by James (1954, 1966) and Knowles and Gastil (1959). The iron-formations were deposited as chemically or biochemically precipitated iron oxides, silica, carbonates and iron-magnesium silicates. The precise composition of the sediment is largely a function of solution Eh and pH and, in certain geochemical environments it is possible for iron oxides to be precipitated essentially free from other components. The present iron ore bodies in the Middleback Ranges can therefore be regarded as primary concentrations formed during the sedimentation process.

As discussed in previous pages, the microtextures and pore space in Iron Duke ore could not have survived regional metamorphism to amphibolite facies grades and it is unlikely that the missing components were iron oxides. Furthermore, the theory does not explain the facts that all known hematite bodies in the Middleback Ranges occur in synforms or steeply dipping fold limbs, and that in all cases the bulk of the ore is relatively near the present land surface and passes downwards to other rock types at depth. For these reasons, the theory is regarded as untenable in the Middleback Ranges.

(b) Theory of granitisation

Miles (1954) proposed granitisation as the mechanism which concentrated iron into certain structural positions within the iron-formations. Miles considered that the iron-formations formed part of a thick, mildly metamorphosed sedimentary sequence which was strongly folded and subsequently penetrated by feldspathizing solutions. Great quantities of the original sediments were made over into gneisses and migmatites, particularly in the cores of regional antiforms where the fluids found penetration relatively easy (Fig.61). The main feldspathizing solutions were preceeded by waves of hydrothermal solutions which consisted mainly of heated waters, in part of supergene origin. These leached iron from the sediments and carried it forward as a basic front. On reaching the iron-formations, the advance fluids first leached silica and then began to concentrate the iron. If penetration continued, the iron-formations were completely made over into gneisses and migmatites. The Middleback Ranges are regarded as remnant keels of tight synclinal structures which were resistant to the granitising fluids. The ores occur in the stratigraphically lower iron-formation unit because it shielded the upper unit and was first exposed to the solutions, and they occur in synforms because these acted as structural traps in which the iron became concentrated. This process was supported in principle by Dorr (1964), who had independently invoked a similar mode of origin for hematite ores in Brazilian iron-formations, basing his conclusions on over one hundred man years work by a combined team of the United States

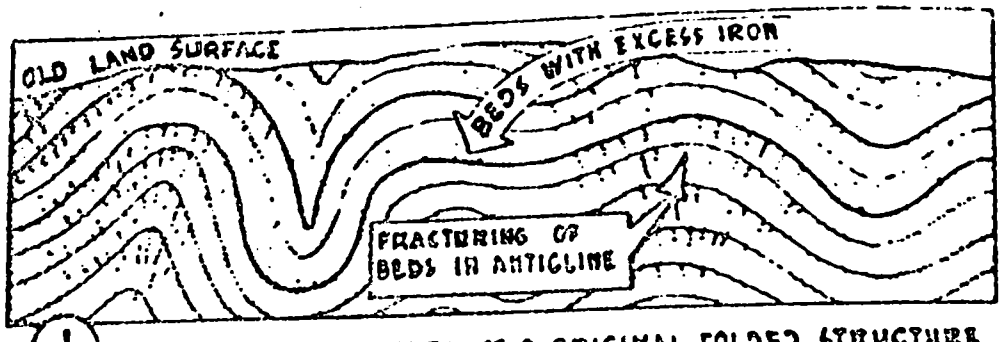

1 SHOWING OLD LAND SURFACE & ORIGINAL FOLDED STRUCTURE.

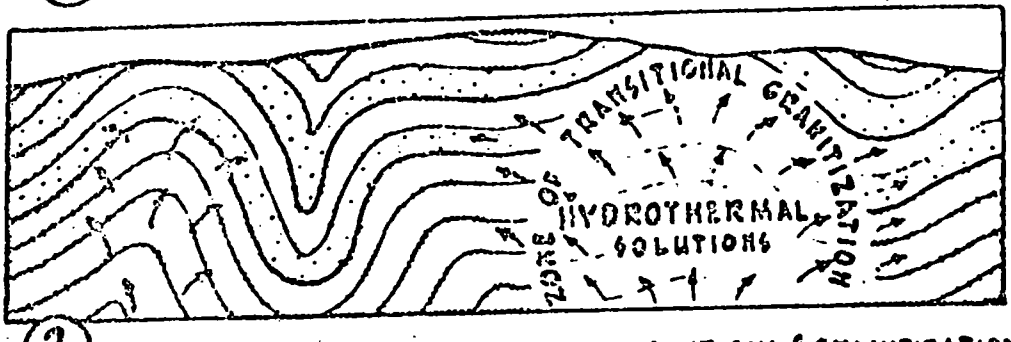

2. INTRODUCTION OF HYDROTHERMAL SOLUTIONS & GRANITIZATION

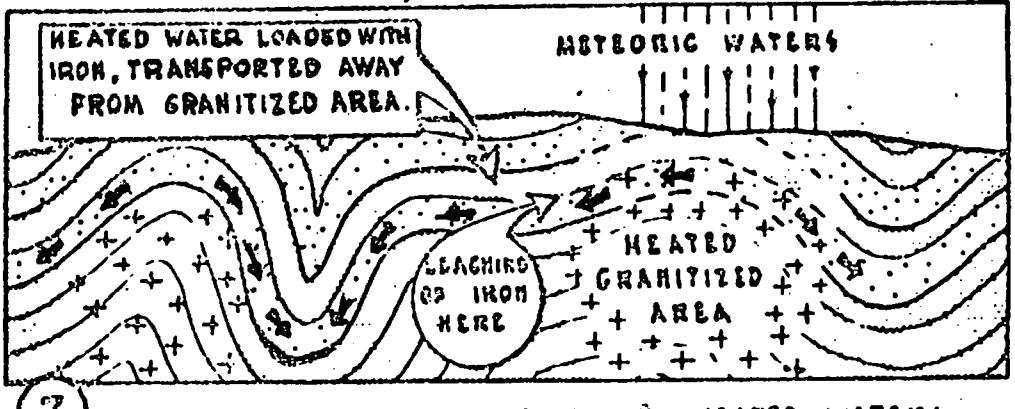

3 LEACHING AND MOVEMENT OF IRON BY HEATED WATERS.

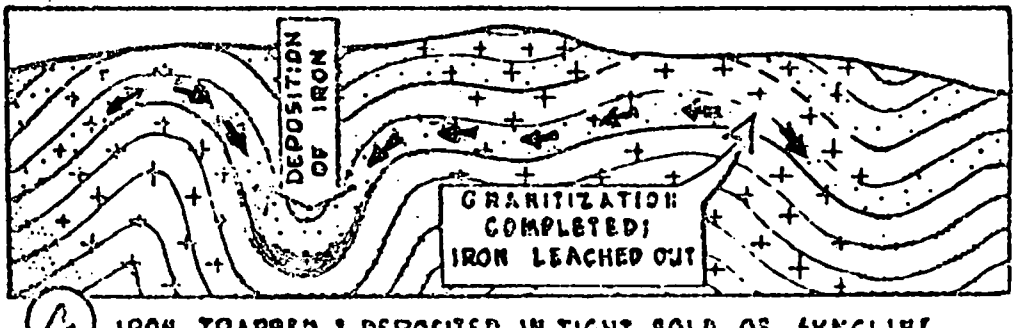

4. IRON TRAPPED & DEPOSITED IN TIGHT FOLD OF SYNCLINE.

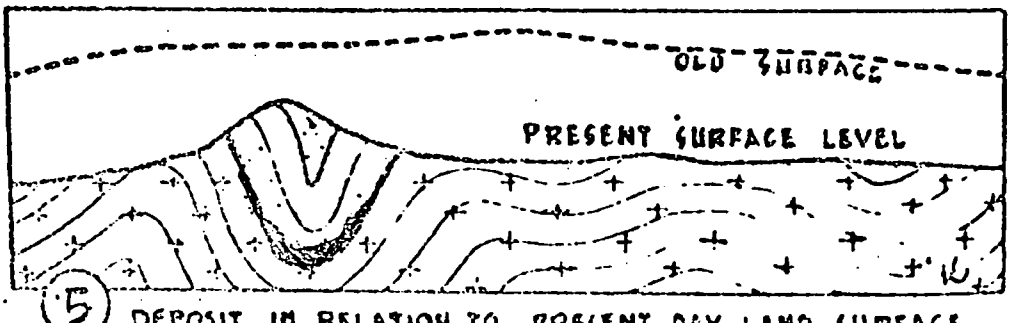

5 DEPOSIT IN RELATION TO PRESENT DAY LAND SURFACE.

Fig. 61 Concept of hematite ore formation by granitization, from Miles, 1954.

Geological Survey and the Departamento Nacional da Produca o Mineral of Brazil.

The theory explains the main characteristics of the orebodies, including the structural and stratigraphic controls. It is, however, regarded as untenable in the Middleback Ranges for the following reasons:

(i) There is no evidence of felspathisation in the Middleback Group rocks. The lowest units of the Middleback Group are argillaceous schists and thin iron-formations. These show no evidence of felspathisation or penetration by hydrothermal fluids, even when outcropping near to granitic rocks as at the south end of Iron Duke.

(ii) Iron formations in close proximity to the granitic rocks show no sign of iron enrichment or silica removal. This is particularly apparent on the east side of the South Middleback Range (Fig.62) where the lower iron-formation unit is thought to have been completely felspathised yet there is no sign of an iron rich front and the upper iron-formation contains no ore.

(iii) The hematite is low in elements which would be expected to accompany iron in a basic front. Basic fronts are generally envisaged as zones deficient in silica relative to the base content and are characteristically rich in Fe, Mg, Mn, Ti and P (Reynolds 1946, Mehnert 1964). A typical analysis of iron ore from Iron Baron is:

Fe	MgO	Mn	TiO_2	P
67.7	0.1	0.2	0.1	0.02

(Analysis by Chemical Laboratory, B.H.P., Whyalla).

The levels of Mn, Ti and P are comparable with, or less than, the levels in the iron-formations and the Mg level is considerably less in the ore.

There is also a marked lack of the basic silicates which are normally present in a basic front.

(iv) There is no evidence of iron concentrations within the gneisses, despite the fact that complete iron-formation units must have been made over into gneisses and migmatites. The only iron concentrations in the whole region are the orebodies of the Middleback Group which, in terms of the immense volumes being considered, are small, discrete bodies confined to a single stratigraphic level within the Middleback Group.

(c) Theory of supergene leaching and enrichment

The theory of supergene leaching and enrichment was first proposed by Rudd (1940) and subsequently supported, in general terms, by Whitehead (1962), Owen and Whitehead (1965), and in more detail by Ashworth (1965, 1970). The principle is simple; deep groundwaters penetrate the iron formations in favourable structural situations and remove gangue minerals, such as quartz and amphiboles, leaving hematite ore.

The theory explains the structural and stratigraphic positions of the orebodies, the intense weathering restricted to their vicinity, the microtextures in the ore, and the fact that in all known cases the bulk of the ore is within 800 feet of the present land surface. At Iron Duke, the theory also explains the

hematite saturation in rocks immediately below the ore, and the thin layer of hematite ore extending along the base of the magnetite-hematite-carbonate body. The theory of supergene leaching and enrichment is regarded, therefore, as the most applicable theory yet postulated for the hematite ores of the Middleback Ranges.

The mechanism of leaching and iron enrichment was described by Dorr (1964) and Macleod (1966). Rain water takes into solution small amounts of silica and carbonate and lesser amounts of iron. These are carried down to the water-table where silica and carbonate remain in solution but iron is precipitated in the ferric state forming a zone of iron enrichment. As the land surface is lowered, the water table correspondingly falls so that the iron enriched zone moves downward and leaching penetrates deeper. Gradual downward progression in this way produces hematite-goethite ore passing downwards to leached jaspilite. In the Hammersley Ranges, this type of ore is widespread and can be clearly related to a Tertiary weathering surface.

Ruckmick has demonstrated the feasibility of iron-ore formation by silica leaching in the Cerro Bolivar ores of South America, where groundwater contains a much greater proportion of silica than iron. Table 25 compares Ruckmick's analyses with a sample of ground-water from the Racecourse orebody, north of Iron Monarch.

Table 25 . Groundwater analyses from Cerro Bolivar and the Racecourse Area

	SiO_2 ppm	Fe ppm	Ph
Cerro Bolivar spring water	10.5	0.05	6.1
Cerro Bolivar bore water	15.0	0.1	7.2
Racecourse mine water	14.0	0.1	7.9

There are two main problems in applying this theory to the Middleback Range ores. One is the lack of hydrated iron oxides such as goethite which would be anticipated with weathering processes and the other is the reason for such deep, localised penetration of the groundwaters.

(i) Hydrated iron oxides

The lack of hydrated iron oxides was encountered by Macleod (1966) in the Hamersley Ranges where massive blue hematite extends to depths of over 800' below the surface. There is convincing evidence that this ore is due to supergene enrichment and Macleod suggested that the lack of hydrated iron oxides may be due to dehydration under load pressure.

Compaction does not appear to be applicable in the Middleback Ranges, where loose, powdery ore is erratically mixed with hard blocky ore to depths of several hundred feet below the surface. Furthermore, the fine hematite network in the ore and the remnant magnetite patches in the larger crystals suggest that the process was one of oxidation and hematite addition without the development of extensive goethite.

The phase change from goethite to hematite is not clearly understood. Limonite is the most common iron product of weathering but hematite forms at least locally in humid tropical areas (Krauskopf 1967). Berner (1969) showed by thermodynamic calculations that goethite is unstable relative to hematite and water in virtually all geological conditions and the maximum temperature at which goethite is likely to be stable is about 40°C.

This was somewhat qualified by Langmuir (1971) who showed that the goethite grain size is important, grains over 1 micron being stable relative to coarse grained hematite up to 80°C. The important point is that the stability of goethite is uncertain and that very fine grained goethite would certainly be metastable and would change to hematite, given sufficient time.

There is a little evidence suggesting that the ores were formed during the Pre-Cambrian. Pebbles of hematite are present in the Corunna conglomerate which is dated at approximately 1550 million years (Rudd 1940, Thomson 1969) and remnant magnetisation studies suggest that the ore is Upper Proterozoic in age (Chamalaun and Porath 1968, 1968a, Porath 1967). Chamalaun and Porath (1968) record contact effects in Iron Monarch hematite near to a cross cutting basic dyke on which they obtained a K-Ar age of 585 million years. It is also interesting to note that the palaeomagnetic results indicate an age of 1500 to 1600 million years for the large Hamersley Range deposits of north west Australia and the majority of palaeomagnetic poles from the West Australian iron ores are in broad agreement with those of the Middleback Ranges.

If the ores are pre-1550 million years in age, there is a strong possibility that hydrated iron oxides originally present would convert to hematite, and this process would be accelerated by any burial or slight compaction.

(ii) Groundwater penetration

The reason for the selective penetration of groundwater to depths of over 1000' below the surface is not clear. All the major orebodies are in synform structures and are underlain by schists or basic intrusives. This suggests structural traps with the solutions channelled by relatively impervious layers (Ashworth 1965).

Synform structures would act as solution traps as shown in Fig.62. A pitching synform offers a wide expanse of outcrop in the hinge area of the fold and the solutions are channelled inwards in contrast to a pitching antiform which offers the same width of outcrop but solutions are channelled outwards into the divergent fold limbs. The tighter the synform, the more intense is the channelling effect. However, the ores are not strictly confined to synforms and may occur in steeply dipping fold limbs, as at Iron Knight.

The underlying schists are impervious relative to the hematite ore but are more pervious than the iron-formations. In the initial stages of iron ore development, the schist layers would be more easily penetrated than the siliceous iron-formations and probably acted as seepage layers, facilitating ore formation. This process has been suggested by Macdonald and Grubb (1971) for shale bands within hematite ores of the Hamersley Ranges. In subsequent stages of ore formation, the hematite ore is more permeable than the schist and the latter will therefore channel

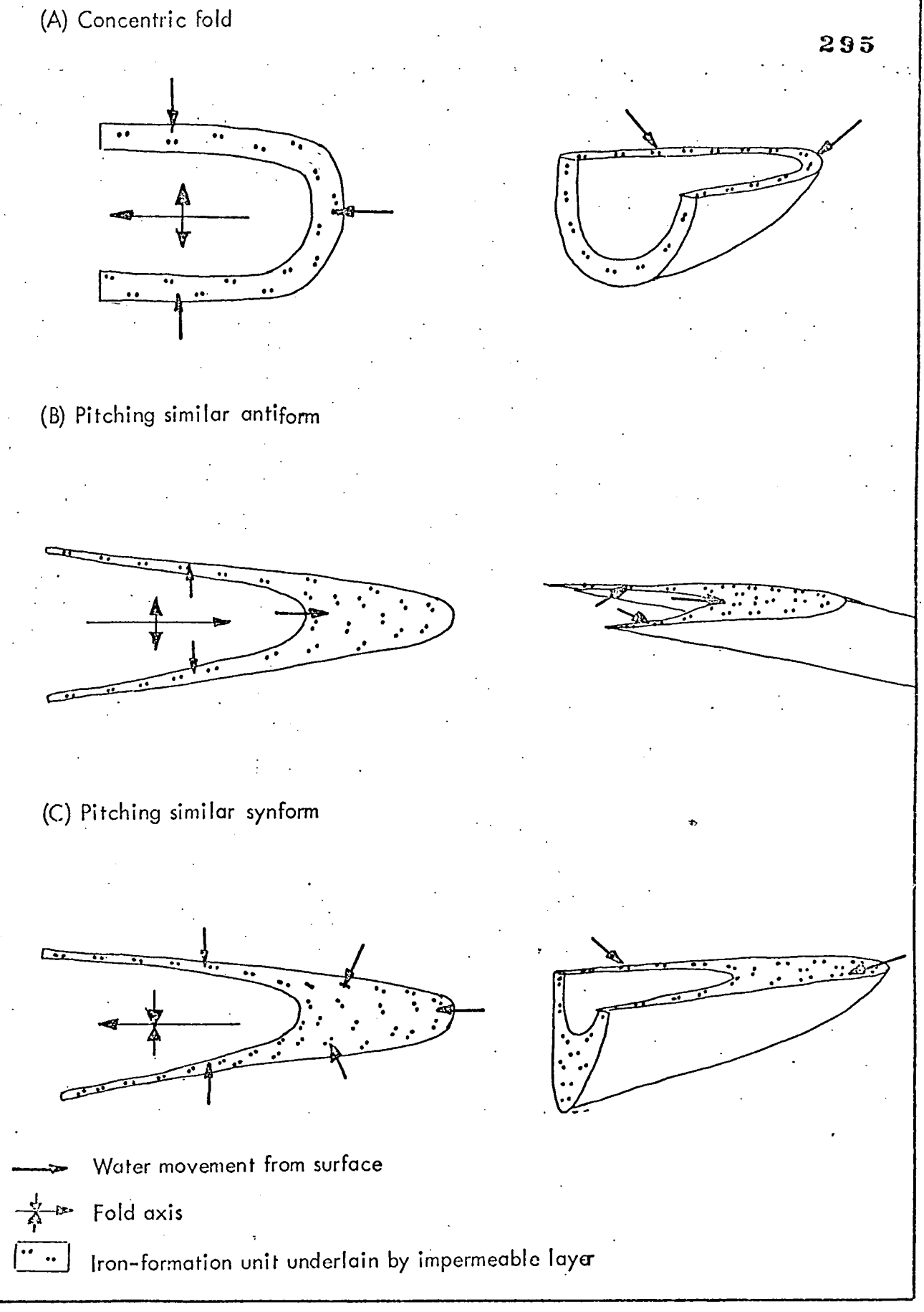

Fig. 62 Diagram to show the channelling effects of various fold structures on groundwater flow. Note the extensive outcrop area and strong channelling of groundwater into the nose of a pitching similar fold.

solutions into favourable structures. The ore forming process can be viewed as an initial slow seepage of groundwater along schist layers, removal of components from adjacent iron-formations leaving spaces, and a rapid flow of groundwater through the resultant porous ore.

Although schists and intrusives may have effectively stimulated ore development by facilitating fluid penetration, the ore bodies are too large to be governed entirely by this mechanism. All the major orebodies occur near the base of the lower iron-formation unit and there are no major bodies in the upper iron-formations, yet both iron-formation units are underlain by schists. This suggests that there is a mineralogical-chemical control which resulted in deep groundwater penetration at a particular stratigraphic level. Whitehead (1962) suggested that a tremolite bearing iron-formation near the base of the sequence should be regarded as a potential ore horizon, and Ashworth (1965) considered that this unit contained carbonate layers. Owen and Whitehead (1965) proposed that a 'softening up' of the unit by hydrothermal activity produced magnetite-hematite-carbonate which was later leached to form hematite ore.

At Iron Duke, the hematite ore is formed from iron-formations, magnetite-hematite-carbonate and talc zone rocks. Leaching is therefore not confined to a particular mineral or rock type and leached minerals include quartz, carbonates and silicates. The most important factor affecting fluid penetration

appears to be a single mineral, or a combination of minerals, which is easily leached. This may be illustrated by the thin layer of hematite ore which extends below the magnetite-hematite-carbonate at Iron Duke. The ore is confined to a narrow strip which coincides with the layer of calcite at the base of the magnetite-hematite-carbonate orebody. It increases in thickness in the hinge area of the synform. The ore is cavernous and contains remnant calcite which increases in quantity with increasing depth. The rocks above and below are unoxidised and the leaching solutions have penetrated down pitch and down dip picking out specifically the calcite layer and becoming progressively less effective with depth until the hematite passes into hematite-calcite-rock at a depth of about 1200' below the surface. The main controls in the formation of this orebody are the presence of calcite and the penetration of fluids along a favourable structure.

Carbonates can therefore play an important role in enabling deep fluid penetration, which supports Owen and Whitehead's suggestion that previous hydrothermal activity would facilitate hematite ore development. Furthermore, carbonate layers are sometimes present in iron-formations at the stratigraphic level of the hematite ore. However, a good deal of ore in all the deposits passes laterally into siliceous iron-formations which contain little or no carbonate. In these, fluid penetration was probably influenced by the presence of amphiboles in the rock. The amphiboles tend to weather easily, as shown by limonitised remnants in iron-formations at depths of 200 feet to 300 feet in some parts

of the Middleback Ranges, although in other places there are fresh amphiboles exposed at the surface. Amphibole schist layers could, therefore, contribute to ore formation by facilitating fluid penetration in a manner similar to the argillaceous schists. The essential difference is that the iron-formation amphiboles contain no alumina to stabilise silica as clay minerals and, on weathering, are converted to limonite or effectively removed, allowing further fluid access.

Both the hematite ores and the magnetite-hematite-carbonate bodies occur within the same stratigraphic unit, which at Iron Duke was rich in tremolite and carbonate before the ore forming processes took place. It is envisaged that the primary composition of this unit varied from place to place throughout the Middleback Ranges, and in some places the presence of carbonates and tremolite made the unit favourable to groundwater penetration and leaching. The hematite ores developed in these localities, some made favourable by the original mineral combinations, others by previous hydrothermal action on the rocks.

Once penetration was achieved, the solutions effectively removed large volumes of quartz, silicate and carbonate components. This process is easy to visualise above the level of the peneplain, but the major orebodies extend several hundred feet below this level and are themselves the deepest remnants of orebodies formed when the land surface was higher than the present day level. The removal of components from such depths is difficult to explain, but may be due to the upward diffusion of dissolved components combined with a periodic replenishment of colder, downward moving solutions.

4. Summary of hematite ore formation

The proposed sequence of events leading to the formation of hematite ore is as follows: (Fig. 63)

(1) Deposition of the iron-formation units. A unit near the base of the sequence, above the basal carbonate, contained variable amounts of carbonate intermixed with the quartz and iron oxides.

(2) Strong folding which produced pitching fold structures, and regional metamorphism to lower amphibolite facies grade. The carbonate rich unit near the base of the iron-formations became rich in tremolite but retained carbonate layers in places.

(3) Major faulting on a regional scale, and hydrothermal activity which formed magnetite-hematite-carbonate and talcose rocks in places throughout the Middleback Ranges. The hydrothermal effects were strongest in the carbonate and tremolite rich unit near the base of the sequence, and the rock types produced by the hydrothermal activity varied according to the precise mineral composition of the pre-existing rock.

(4) Uplift and peneplanation producing a topography similar to, but rather higher than, that of the present day.

(5) Intense weathering with silica and carbonate removal over the whole iron-formation area, causing a relative enrichment of iron at the surface. Deep groundwater penetration was confined

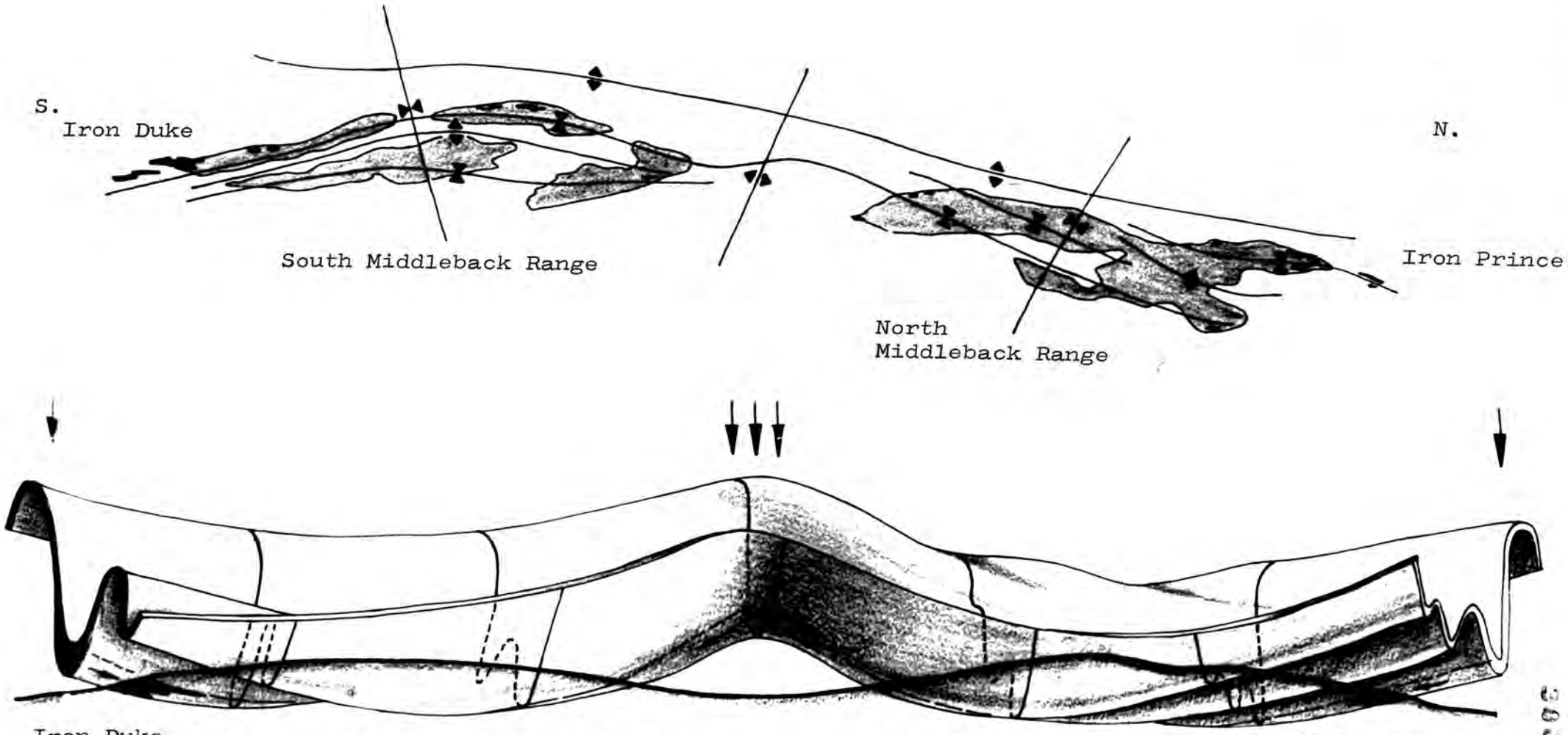

Fig.63. Diagram to illustrate the concept of hematite ore formation by supergene leaching and enrichment. Arrows indicate movement of rainwater and groundwater. Not to scale. Drawn by A. Vezis, BHP, Whyalla, from draft by author.

mainly to the tremolite and carbonate bearing unit near the base of the iron-formation sequence and to points at which hydrothermally altered rocks coincided with the water table. Favourable structures facilitated the leaching process by causing wide expanses of the favourable unit in hinge areas, and by channelling the solutions. Porous, limonite-hematite ore formed from the iron-formations and interlayered argillaceous schists, together with basic dykes, were converted to clay minerals. Argillaceous schists and basic masses immediately below the hematite ore acted as relatively impermeable layers, channelling the solutions in favourable structures. Iron was partially redistributed within the ore body, forming patches of hard blocky ore.

(6) Erosion over a long period of time to the present day topography Some faulting and intrusion of basic dykes took place during this period. The iron rich surface formed in the previous weathering phase was removed, to different levels throughout the area, so that in places the present surface rocks are quite fresh and in others weathering extends to several hundred feet. The deeper parts of the iron ore bodies remained and form the present hematite orebodies. During this period, limonite in the ore slowly converted to hematite.

CONCLUSIONS

1. The Middleback Range iron-formations have undergone regional metamorphism to lower amphibolite facies, at temperatures in the order of 450°C to 550°C and pressures between 2kb and 6kb. Within the iron-formations, the components remained essentially immobile, except for H_2O and CO_2, and individual layers behaved as closed chemical systems.

2. The metamorphosed iron-formations consist of fine-grained, even textured rocks with alternating layers of iron oxides, quartz, tremolite, grunerite and carbonate. The mineral layering reflects the original sedimentary layering.

3. The main period of metamorphism was followed by the development of major north-south zones of dislocation. Hydrothermal fluids penetrated these zones from depth and caused belts of retrograde metamorphism in argillaceous schist units within the iron-formation sequence.

4. At Iron Duke, hydrothermal fluids penetrated the lower part of the iron-formation sequence. The fluids were brines at temperatures and pressures in the order of 120° - 250°C and 2-3 kb. A unit near the base of the sequence consisted of interlayered iron oxides, carbonates, tremolite and quartz, and was particularly susceptible to fluid penetration due to the combined presence of carbonates and tremolite. The magnetite-hematite-carbonate orebody formed within this unit

by a complex process of carbonate metasomatism and direct removal of silica in solution. Grunerite rich iron-formations were partly silicified and converted to talcose and quartzose schists. Amphiboles were completely chloritised.

5. Fluid movement was partly by diffusion through crystal lattices, and along grain boundaries and cleavages. Extensive mineral changes and large scale transfer of components have resulted from this process.

6. Factors controlling the composition and disposition of the magnetite-hematite-carbonate ore include, the presence of a major reverse fault, the thick basal carbonate unit, and the tight synformal structure of Iron Duke. Magnetite-hematite-carbonate ore is likely to be found in other parts of the Middleback Ranges, where major zones of structural dislocation intersect thick development of the basal carbonate unit. The ore type will depend upon the mineralogy of the lower iron-formation units, whereas the structural setting will control the shape of the orebody.

7. Hematite orebodies in the Middleback Ranges were formed by deep groundwater penetration in favourable structural settings. Gangue minerals, such as quartz, amphiboles and carbonates were removed and part of the iron was redistributed. Ore controls, apart from structure, include the presence of favourably leached minerals such as amphiboles and carbonates, and the presence of underlying, relatively impermeable

argillaceous schist units and amphibolites. It is envisaged that all orebodies were connected with the Precambrian land surface.

8. A new carbonate mineral composition has been established, approximating to $Ca_{0.3}Mg_{0.4}Fe_{0.3}CO_3$. This composition suggests that there may be a solid solution series between points on the dolomite-ferrodolomite series and points on the magnesite-siderite series.

9. New natural talc compositions have been established, varying between $Mg_{2.8}Fe_{0.2}O_{10}(OH)_2$ and $Mg_{1.9}Fe_{1.1}O_{10}(OH)_2$. These compositions are on a solid solution series between talc and minnesotaite.

10. There is wide scope for further work on the Middleback Range iron ores and associated rock types. Projects which could be particularly useful regarding ore genesis are:
    (1) More detailed fluid inclusion work on inclusions in carbonates and quartz within the talc rocks, to ascertain precisely the fluid composition and the temperature of the hydrothermal activity.
    (2) Oxygen isotope studies of hematite-quartz in the hematite orebodies, magnetite-quartz in the iron-formations, and magnetite-hematite-carbonates-quartz in the carbonate rich orebody. The results would be valuable for comparison with data from iron-formations in other parts of the world, and may enable firm temperature estimates for the different rock types.

(3) A study of trace and minor elements within the hematite orebodies, particularly at Iron Monarch where the high manganese content is as yet unexplained.

(4) A structural study of the major faulting interpreted on the east side of the Iron Duke - Iron Duchess ridge. The use of petrofabrics and a texture goniometer may be the most useful line of approach.

(5) The process of mass transfer by diffusion, as illustrated by the Iron Duke chloritised amphibolites, warrents both laboratory and theoretical examination. Such a process has important implications in the formation of many hydrothermal ore deposits.

REFERENCES

The main references consulted during research are as follows:

ALBEE A.L. 1965 Distribution of Fe, Mg and Mn between garnet and biotite in natural mineral assemblages. Journ. Geol., vol.73, pps. 155-164.

ALEKSANDROV I.V.
ZMEENKOVA A.V. 1958 Evolution of rocks during progressive metamorphism as exemplified by the middle suite of the Krivoi Rog Series. Geokhim., No.1, pps.62-82.

ALEXANDER G.B.
HESTON W.M.
ILER R.K. 1954 The solubility of amorphous silica in water. Journ. Phys. Chem., vol.58, pps.453-455.

ASHWORTH K.L. 1965 Geology of Iron Duke, South Australia. The B.H.P. Technical Bulletin, vol.9, No.1, pps.23-30.

1971 Report on the geology of Iron Duke and the origin of iron ores in the Middleback Ranges, South Australia. Unpublished B.H.P. Cpy. Ltd. Report.

ATHERTON M.P. 1964 (1) The chemical significance of isograds. pps.169-202.
(2) The composition of garnets in regionally metamorphosed rocks. pps.281-290.
In: "Controls of Metamorphism", eds. Pitcher and Flynn, pub. Oliver and Boyd, London.

BANNO S. 1964 Petrologic studies on Sanbagawa crystalline schists in the Bessi-Ino district, central Sikoku, Japan. Journ. Fac. Sci. Univ. Tokyo, Sec.2, vol.15, pps.203-319.

BARNES H.L.
CZAMANSKE G.K. 1967 Solubilities and transport of ore minerals. In. "Geochemistry of Hydrothermal Ore Deposits", ed. H.L. Barnes, pub. Holt, Rinehart and Winston Inc., New York.

BAYLEY R.W. 1963 A preliminary report on the Pre-Cambrian iron deposits near Atlantic City, Wyoming. U.S.G.S. Survey Bull. 1142-C.

BENNINGTON K.O. 1956 Role of shearing stress and pressure in differentiation as illustrated by some mineral relations in the system $MgO-SiO_2-H_2O$. Journ. Geol., vol.64, pps.558-577.

BERGE J.W. 1971 Iron formation and supergene iron ores of the Goe Range Area, Liberia. Econ. Geol., vol.66, pps.947-960.

BERNER R.A. 1969 Goethite stability and the origin of red beds. Geochim. et Cosmochim. Acta, vol. 33, pps.267-273.

BLAKE R.L. 1965 Iron Phyllosilicates of the Cuyuna district, Minnesota. Am. Min., vol.50, pps.148-169.

BOND C. 1952 The deformation of banded ironstones in Southern Rhodesia. Econ. Geol., vol.47, No.8, pps.823-4.

BORCHERT H. 1960 Genesis of Marine Sedimentary Iron Ores. Inst. Min. Met. Bull., vol.69, Part 6, pps.261-279.

BOWEN N.L. 1940 Progressive metamorphism of siliceous limestone and dolomite. Journ. Geol., vol.48, pps.225-274.

BOSE M.K. 1958 Goethite - hematite relations - an ore microscope observation. Am. Min., vol. 43, pps.989-990.

BROWNE P.R.L.
ELLIS A.J. 1970 The Ohaki-Broadlands hydrothermal area, New Zealand: Mineralogy and related geochemistry. Am. Journ. Sci., vol.269, pps.97-131.

BURGER D. 1963 Notes on some carbonate minerals in the iron ore deposits of the Iron Duke area, South Middleback Range, South Australia. Proc. Aust. Inst. Min. Met., No.208, pps.55-80.

BUTLER P.Jr. 1969 Mineral compositions and equilibria in the metamorphosed Iron Formation of the Gagnon Region, Quebec, Canada. Journ. Pet., vol.10, Part.1, pps.56-101.

CAMPANA B. 1967 Stratigraphy - structural-palaeoclimatic controls of the newly discovered iron deposits of Western Australia. Minera Deposita, vol.1, No.1, pps.53-59.

CANNON R.T. 1963 Classification of amphibolites. Geol. Soc. Am. Bull., vol.74, pps.1087-1088.

CARVER R.E. 1965 Undulose extinction in fine-grained rocks. Journ. Sed. Pet., vol.35, No.4, pps.980-983.

CASTANA J.R.
GARRELS R.M. 1950 Experiments on the deposition of iron with special reference to the Clinton iron deposits. Econ. Geol., vol.45, No.8, pps.755-770.

CATLEY D. 1963 Some aspects of the Genesis of the Iron Duke orebody and associated rocks. Proc. Aust. Inst. Min. Met., vol.208, pps.81-123.

CHAKRABARTY K.L. 1963 Relationship of anthophyllite, cummingtonite and magnesio-cummingtonite in the metamorphosed Wabush iron-formation, Labrador. Can. Min., vol.7, Part 5.

CHAMALAUN F.H.
PORATH H. 1968 Palaeomagnetism of Australian hematite ore bodies Part I: The Middleback Ranges of South Australia. Roy. Astron. Soc. Geophys. Journ., vol.14,No.5,pps.451-462.

CHINNER G.A. 1960 Pelitic gneisses with varying Ferrous/Ferric Ratios from Glen Clova, Angus, Scotland. Journ. Pet., vol.1, Part 2, pps. 178-217.

COMPSTON W.
CRAWFORD A.R.
BOFINGER V.M. 1966 A radiometric estimate of the duration of Sedimentation in the Adelaide Geosyncline, South Australia. Journ. Geol. Soc. Aus., vol.13, pps.229-276.

COMPSTON W.
ARRIENS P.A. 1968 The Pre-Cambrian Geochronology of Australia. Can. Journ. Earth. Sciences, vol.5, pps.561-583.

COOPER J.R. 1957 Metamorphic and Volume losses in carbonate rocks near Johnson Camp, Cochise country, Arizona. Bull. Geol. Soc. Am., vol.68, p.577.

CRERAR D.A.
ANDERSON G.H. 1971 Solubility and solution reactions of quartz in dilute hydrothermal solutions. Chem. Geol., vol.8, No.2, pps.107-122.

CULLEN D.J. 1963 Tectonic implications of banded ironstone formations. Journ. Sed. Pet., vol.33, pps.387-392.

DAVIS S.N. 1964 Silica in streams and ground water. Am. Journ. Sc., vol.262, pps.870-891.

DEER W.A.
HOWIE R.A.
ZUSSMAN J. 1963 "Rock Forming Minerals", vols.1-5, Longmans, Publishers, London.

DEVORE G.W. 1955 The role of adsorption in the fractionation and distribution of elements. Journ. Geol., vol.63, pps.159-160.

DORR J. VAN N.II
BARBOSA A.L. de M 1963 Geology and ore deposits of the Itabira district, Minas Gerais, Brazil. Prof.Paper U.S.G.S.341-C.

DORR J. VAN N.II 1964 Supergene iron ores of Minas Gerais Brazil. Econ. Geol., vol.59, No.7, pps.1203-1240.

1965 Nature and origin of the high-grade hematite ores of Minas Gerais, Brazil. Econ. Geol., vol.60, pps.1-46.

DUNN J.A. 1935 The origin of iron ores in Singhbum, India. Econ. Geol., vol.30, pps.643-644.

1941 The origin of banded hematite ores in India. Econ. Geol., vol.36, pps.355-370.

EASTWOOD G.E.P. 1965 Replacement magnetite on Vancouver Island, British Columbia. Econ. Geol., vol.60, pps.124-148.

EDWARDS A.B. 1936 The iron ores of the Middleback Ranges, South Australia. Proc. Aust. Inst. Min. Met., New Series. No.102, pps.155-208.

1954 (1) Banded hematite quartzites from the Middleback Range - South Australia, pps. 206-213.
(2) Petrological study of rock from the Middleback Range and environs, pps.214-230.
(3) Manganiferous dolomites and related rocks from the Middleback Range - South Australia, pps.211-213.
In: "The Geology and Iron Ore Resources of the Middleback Range Area", Geol., Surv. South Aust. Bull., vol.33, by K.R. Miles.

ELLIS A.J. 1959 The solubility of calcite in CO_2 solutions. Am: Journ. Sc., vol.257, pps.354-365.

1963 The solubility of calcite in sodium chloride solutions at high temperatures. Am. Journ. Sc., vol.261, pps.259-267.

ELLIS A.J. 1967 The chemistry of some explored geothermal systems. In: "Geochemistry of Hydrothermal Ore Deposits", ed. H.L. Barnes, pub. Holt, Rinehart and Winston Inc., New York.

1968 Natural hydrothermal systems and experimental hot water/rock interaction: Reactions with NaCl solutions and trace element extraction. Geochim. et Cosmochim. Acta, vol.32, pps. 1356-1363.

1971 Magnesium ion concentrations in the presence of magnesium chlorite, calcite, CO_2 and quartz. Am. Journ. Sc., vol.271,pps.481-489.

ELLIS A.J.
GOLDING R.M. 1963 The solubility of carbon dioxide above 100°C in water and sodium chloride solutions. Am. Journ. Sc., vol.261, pps.47-60.

ENGEL A.E.J.
ENGEL C.E. 1960 Progressive metamorphism and granitisation of the major paragenesis, north west Adirondack Mountains, New York. Bull. Geol. Soc. Am., vol.71, pps.1-57.

1962 Hornblendes formed during progressive metamorphism of amphibolites, Northwest Adirondack Mountains, New York. Bull. Geol. Soc. Am., vol.73, pps.1499-1514.

ERNST W.G. 1968 "Amphiboles", pub. Springer-Verlag, New York.

FAUST G.T. 1949 Dedolomitisation and its relation to a possible derivation of a magnetite rich hydrothermal solution. Am. Min., vol.34, pps.780-823.

FENTON G.R. 1970 Iron Baron/Little Iron Baron deep drilling programme May 1969-June 1970. B.H.P. report, Whyalla.

FLASCHEN S.S.
OSBORN E.F. 1957 Studies of the system iron oxide-silica water at low oxygen partial pressure. Econ. Geol., vol.52, pps.923-943.

FORBES W.C. 1971 Iron content of Talc in the system $Mg_3 Si_4 O_{10}(OH)_2$ - $Fe_3 Si_4(OH)_2$. Journ. Geol., vol.79, No.1,pps.63-74.

FREDERICKSON A.F.
COX J.E. Jr. 1954 Mechanism of solution of quartz in pure water at elevated temperatures and pressures. Am. Min., vol.39, p.886.

FRENCH B.M. 1971 Stability relations of siderite ($FeCO_3$) in the system Fe-C-O. Am. Journ. Sc., vol.271, No.1, pps.37-78.

FRIEDMAN G.M. 1959 Identification of Carbonate Minerals by staining methods. Journ. Sed. Pet., vol. 29, No.1, pps.87-97.

FYFE W.S.
TURNER F.J.
VERHOOGEN J. 1958 Metamorphic reactions and metamorphic facies. Geol. Soc. Am. Mem.73.

GARRELS R.M.
THOMPSON M.E.
SIEVER R. 1960 Stability of some carbonates at 25° and 1 atmos. total pressure. Am. Journ. Sc. vol.258, pps.402-418.

GARRELS R.M.
CHRIST C.L. 1965 "Solutions, Minerals and Equilibria", pub. Harper and Row, New York.

GHOSE S. 1962 The nature of Mg^{2+} - Fe^{2+} distribution in some ferromagnesian silicate minerals. Am. Min., vol.47, pps.388-394.

GOODWIN A.M. 1956 Facies relations in the Gunflint iron formation. Econ. Geol., vol.51, pps. 565-595.

1962 Structure, stratigraphy and origin of iron formation, Michipicoten area, Algama District, Ontario. Bull. Geol. Soc. Am., vol.73, pps.561-568.

GREEN J.C. 1963 High level metamorphism of pelitic rocks in northern New Hampshire. Am. Min., vol.48, pps.991-1023.

GROSS G.A. 1965 Geology of iron deposits in Canada. Vols. II and III. Econ. Geol., Rep.No.22, Geol. Surv. Can.

GROSS W.H.
STRANGWAY D.W. 1961 Remnant magnetism and the origin of hard hematites in PreCambrian banded iron formation. Econ. Geol., vol.56, No.8, pps.1345-1362.

GRUNER J.W. 1930 Hydrothermal oxidation and leaching experiments their bearing on the origin of Lake Superior hematite-limonite ores. Econ. Geol., vol.25, pps.697-719 and 837.

1937 Hydrothermal leaching of iron ores of the Lake Superior type - modified theory. Econ. Geol., vol.32, pps.121-130.

GRUNER J.W. 1946 The mineralogy and geology of the taconites and iron ores of the Mesabi Range, Minnesota. Iron Range Resources and Rehabilitation Comm., St. Paul, Minnesota.

GUILD P.W. 1953 Iron Deposits of the Congonhas District, Minais Gerais. Econ. Geol., vol.48, No.8, pps.639-676.

GUNN P.J. 1967 Gravitational and magnetic interpretation of the Middleback Range area, South Australia. M.Sc. Thesis, University of Melbourne.

HARBORD N.H.
GOLDRING D.C. 1965 Formation of magnetite and haematite in iron ore sinters. J. Iron Steel Inst., vol.203, pps.349-360.

HARKER R.I.
TUTTLE O.F. 1955 The thermal dissociation of calcite, dolomite, and magnesite. Am. Journ. Sc., vol.253, pps.209-224.

HARRY W.T. 1950 Aluminium replacing silicon in some silicate lattices. Min. Mag., vol.29, pps.142-144.

HATCH F.H.
WELLS A.K.
WELLS M.K. 1961 "Petrology of the igneous rocks", 12th Edition, pub. Thomas Murby and Co., London.

HAYES A.O. 1915 Wabana iron ore of Newfoundland. Geol. Survey Can. Mem.78.

HAWLEY J.E.
ROBINSON S.C. 1948 The supposed oxidation of Fe_3O_4 by CO_2. Econ. Geol., vol.43, pps.603-609.

HELGESON H.C. 1964 "Complexing and Hydrothermal Ore Deposition", pub. Pergamon, New York.

HELGESON H.C.
GARRELS R.M.
MACKENZIE F.T.
1969 Evaluation of irreversible reactions in geochemical processes involving minerals and aqueous solutions - II. Applications. Geochim. et Cosmochim. Acta, vol.33, pps. 455-481.

HELLNER E.
SCHÜRMANN K.
1966 Stability of metamorphic amphiboles: the tremolite-ferroactinolite series. Journ. Geol., vol.74, pps.322-331.

HEM J.D.
1960 Chemical equilibrium diagrams for ground water systems. Int. Ass. Sc. Hydr., Bull. 19, pps.45-53.

HEY M.H.
1954 A new review of the Chlorites. Min. Mag., vol.30, pps.277-292.

HOLLAND H.D.
1959 Some applications of thermochemical data to problems of ore deposits: I stability relations among the oxides, sulphides, sulphates and carbonates of ore and gangue minerals. Econ. Geol., vol.54, pps.184-233.

1965 Some applications of thermochemical data to problems of ore deposits: II Mineral assemblages and composition of ore forming fluids. Econ. Geol., vol.60, pps.1101-1166.

1967 Gangue minerals in hydrothermal deposits. In: "Geochemistry of Hydrothermal ore Deposits" edited by H.L. Barnes, pub. Holt, Rinehart and Winston, New York.

HOLLAND J.G.
BRINDLE D.W.
1966 A self-consistent Mass absorption correction for silicate analysis by X-ray fluorescence. Spectrochim. Acta, vol.22, pps.2083-2093.

HOWIE R.A.
BRAODHURST F.M. 1958 X-ray data for dolomite and ankerite. Am. Min., vol.43, pps.1210-1214.

HUBER N.K. 1959 Some aspects of the Ironwood iron formation of Michigan and Wisconsin. Econ. Geol., vol.54, pps.82-118.

HUBER N.K.
GARRELS R.M. 1953 Relation of pH and oxidation potential to sedimentary iron mineral formation. Econ. Geol., vol.48, pps.337-357.

INGERSON E. 1947a Transportation and deposition of silica. Econ. Geol., vol.42, pps.560-562.

1947b Liquid inclusions in geologic thermometry. Am. Min., vol.47, pps.375-388.

JACK R.L. 1922 The iron ores of South Australia. Geol. Surv. South Aust. Bull. No.9.

JAMES H.L. 1951 Iron formation and associated rocks in the Iron River District, Michigan. Bull. Geol. Soc. Am., vol.62, pps.251-266.

1954 Sedimentary facies of iron formation. Econ. Geol., vol.49, pps.235-291.

1955 Zones of regional metamorphism in the Pre-Cambrian of northern Michigan. Bull. Geol. Soc. Am., vol.66, pps.1455-1488.

1958 Stratigraphy of Pre-Keweenan rocks in parts of northern Michigan. U.S.G.S. Prof. Paper 314-C.

JAMES H.L. 1960 Problems of stratigraphy and correlation of Pre-Cambrian rocks with particular reference to the Lake Superior region. Am. Journ. Sc., vol.258-A, pps.104-114.

1966 Chemistry of the iron-rich sedimentary rocks. U.S.G.S. Prof. Paper 440-W.

JAYARAMAN N. 1940 Alteration of tremolite to talc in the dolomite marbles of Yellandu Warangol district (Hyderabad, India). Proc. Ind. Acad. Sc. A, vol.12, p.65.

JOHNS R.K. 1961 Geology and Mineral Resources of Southern Eyre Peninsula. Geol. Survey South Aust. Bull.37.

JOHNS R.K.
SOLOMON M. 1952 The age of the Gawler Range Porphyry. Trans. R. Soc. S. Aus., 76 pps.41-44.

JONES M.T. 1968 The structural geology of the South Middleback Range. Honours B.Sc. Thesis, University of Adelaide.

JONES L.H.P.
HANDRECK K.A. 1963 Effects of iron and aluminium oxides on silica in solution in soils. Nature, vol.198, No.4883, pps.852-853.

JOPLIN G.A. 1964 "A Petrography of Australian Igneous Rocks", Angus and Robertson, Publishers, Sydney.

KALLIOKOSKI J. 1965 The metamorphosed iron ore of El Pao, Venezuela. Econ. Geol., vol.60, pps.100-116.

KENNEDY G.C. 1950 A portion of the system silica-water. Econ. Geol., vol.45, pps.629-653.

KERR P.F. 1955 Hydrothermal alteration and weathering Geol. Soc. Am. Spec. Paper 62, pps.525-544.

KING H.F. 1966 Estimation of ore reserves. 8th Comm. Min. and Met. Cong., vol.2, pps.296-300.

KLEIN C. 1966 Mineralogy and petrology of the metamorphosed Wabush iron formation, southwestern Labrador. Journ. Pet., vol.7, pps.246-305.

KNOPF A. 1929 The Mother Lode System of California. U.S.G.S. Prof. Paper 157.

KNOWLES D.M.
GASTIL R.G. 1959 Metamorphosed iron formations in South western Labrador. Can. Inst. Min. Met. Bull., pps.503-510.

KRAUSKOPF K.B. 1956 Dissolution and precipitation of silica at low temperatures. Geochim. et Cosmochim. Acta, vol.10, pps.1-26.

1967 "Introduction to Geochemistry", pub. McGraw-Hill Book Co., New York.

KRANCK S.H. 1961 A study of Phase Equilibria in a Metamorphosed Iron Formation. Journ. Pet., vol.2, Part 2, pps.137-184.

KRETZ R. 1959 Chemical study of Garnet, Biotite and Hornblende from gneisses of S.W. Quebec with emphasis on distribution of elements in coexisting minerals. Journ. Geol., vol.67, pps.371-402.

KULP J.L.
KENT P.
KERR P.P.
1951 Thermal study of the Ca-Mg-Fe Carbonate minerals. Am. Min., vol.36, pps.643-670.

LABERGE G.
1966 Altered pyroclastic rocks in iron formations in the Hamersley Range, Western Australia. Econ. Geol., vol.61, No.1, pps.147-161.

LAFFITTE P.
1962 Mechanism and duration of vein deposit formation. Econ. Geol., vol.57, pps. 587-594.

LANGMUIR D.
1971 Particle size effect on the reaction Goethite = Hematite + water. Am. Journ. Sc., vol.271, pps.147-156.

LAUDISE R.A.
BALLMAN A.A.
1961 The solubility of quartz under hydrothermal conditions. Journ. Phys. Chem., vol.65, pps. 1396-1400.

LEAKE B.E.
1963 Origin of amphibolites from North West Adirondacks, New York. Geol. Soc. Am. Bull., vol.74, pps.1193-1202.

1965 The relationship between composition of calciferous amphiboles and grade of metamorphism. In: "Controls of Metamorphism", eds. Pitcher and Flynn, pub. Oliver and Boyd, London.

LEGGO P.J.
COMPSTON W.
TRENDALL A.F.
1965 Radiometric Ages of some Pre-Cambrian rocks from the North west Division of Western Australia. Journ. Geol. Soc. Aust., vol.12, Part 2, pps.53-66.

LEPP H. 1963 Sedimentary iron formations. Econ. Geol., vol.58, No.4, pps.515-526.

LEPP H.
GOLDICH S.S. 1964 Origin of the Pre-Cambrian iron formations. Econ. Geol., vol.59, pps.1025-1060.

LOVERING T.G. 1962 The origin of jasperoid in limestone. Econ. Geol., vol.57, pps.861-887.

1923 The leaching of iron protores - solution and precipitation of silica in cold water. Econ. Geol., vol.18, pps.523-540.

LOVERING T.S. 1969 The origin of Hydrothermal and Low temperature Dolomite. Econ. Geol., vol.64, pps.743-754.

LYONS J.B.
MORSE S.A. 1970 Mg/Fe partitioning in garnet and biotite from some granitic, pelitic and calcic rocks. Am. Min., vol.55, pps.231-245.

MacDONALD
GRUBB 1971 Genetic implications of shales in the Brockman iron formation from Mount Tom Price and Wittenoom Gorge, Western Australia. Journ. Geol. Soc. Aust., vol.18, Part 1, pps.81-86.

MACLEOD W.N. 1966 The Geology and iron deposits of the Hamersley Range area, Western Australia. Geol. Surv. West Aust. Bull.117.

McNAMARA M.J. 1965 The lower greenschist facies in the Scottish Highlands. Geol. Foren. Stock. Forh., vol.87, pps.347-389.

MEHNERT K.R. 1968 "Migmatites and the origin of granitic rocks"., pub. Elsevier Publishing Company, Amsterdam.

MEYER C.
HEMLEY J.J. 1967 Wall rock alteration. In: "Geochemistry of hydrothermal ore deposits", ed. H.L. Barnes, pub. Holt, Rinehart and Winston Inc., New York.

MILES K.R. 1941 Magnetite-hematite relations in the banded iron formations of Western Australia. Proc. Aust. Inst. Min. Met., vol.124, pps.193-200.

1942 The blue asbestos bearing banded iron formation of the Hamersley Ranges, W. Australia. Geol. Surv. West. Aust. Bull. 100.

1943 Grunerite in Western Australia. Amer. Min., vol.28, pps.25-38.

1946 Metamorphism of jasper bars in Western Australia. Quart. Journ. Geol. Soc., vol.102, pps.115-155.

1952a Tertiary Faulting in North-western Eyre Peninsular, South Australia. Trans. Roy. Soc. S. Aust., vol.75(1), pps.89-96.

1952b The iron ore resources of South Australia. 19th Int. Geol. Congress, Algeria, La Genese des gites de Fer (abstract).

1954 The Geology and Iron ore resources of the Middleback Range area. Geol. Surv. South Aust. Bull.33.

MILLER J.P. 1952 A portion of the system calcium carbonate - CO_2 - water, with geological implications. Am. Journ. Sc., vol.250, pps.161-203.

MIYASHIRO A. 1953 Calcium poor garnet in relation to metamorphism. Geochim. et Cosmochim. Acta, vol.4, pps.179-208.

MOORE E.S. 1946 Origin of iron deposits of the "Lake Superior" type. New York Acad. Sc. Trans., Series 2, vol.9, No.2, pps.43-51.

MOREY G.W. 1956 Action of hot water on some carbonates. Bull. Geol. Soc. Am., vol.67, pps.1721-1722.

MOREY G.W.
FOURNIER R.O.
ROWE J.J. 1962 The solubility of quartz in water in the temperature interval from 25°C to 300°C. Geochim. et Cosmochim. Acta, vol.26, pps. 1029-1043.

1964 The solubility of amorphous silica at 25°C. Journ. Geophys. Res., vol.69, pps. 1995-2002.

MUELLER R.F. 1960 Compositional characteristics and equilibrium relations on mineral assemblages of a metamorphosed iron formation. Am. Journ. Sc., vol.258, pps.449-497.

MÜLLER G.
SCHNEIDER A. 1971 Chemistry and Genesis of Garnets in Metamorphic Rocks. Contr. Min. Pet., vol.31, pps.178-200.

NANDI K. 1967 Garnets as indices of progressive regional metamorphism. Min. Mag., vol.36, pps.89-93.

NORRISH K.
HUTTON J.T. 1969 An accurate X-ray spectrographic method for the analysis of a wide range of geological samples. Geochim. et Cosmochim. Acta, vol.33, pps.431-453.

O'CONNOR T.L.
GREENBERG S.A. 1958 The kinetics for the solution of silica in water. Journ. Phys. Chem., vol.62, pps.1195-1198.

OLLIER C. 1969 "Weathering", pub. Oliver and Boyd, Edinburgh.

O'ROURKE J.E. 1961 Palaeozoic banded iron formation. Econ. Geol., vol.56, pps.331-361.

OWEN H.B. 1964 The Geology of the Iron Monarch Orebody. Proc. Aust. Inst. Min. Met., vol.208, pps.152-153.

OWEN H.B.
WHITEHEAD S. 1965 Middleback Range Iron Ore Deposits in "Geology of the Australian Ore Deposits", 8th Comm. Min. Met. Cong., pps.301-308.

PARK C.F.Jr. 1959 Origin of hard hematite in itabirite. Econ. Geol., vol.54, pps.573-587.

PERCIVAL F.G. 1954 Nature and occurrence of iron ore deposits. In: "Survey of world iron ore resources", United Nations, New York, pps.45-76.

1967 Textures of Brockman Iron formation jaspilite, Western Australia. Econ. Geol., vol.62, No.3, pps.431-432.

PORATH H. 1967 Palaeomagnetism and the age of Australian hematite ore bodies. Earth and Plan. Sci. Letts., vol.2, No.5, pps.409-414.

PORATH H.
CHAMALAUN F.H. 1968 Palaeomagnetism of Australian Hematite ore bodies: II Western Australia. Roy. Ast. Soc. Geophys. Journ., vol.15, No.3, pps. 253-264.

QUIRKE T.R.Jr. 1961 Geology of the Temiscamie iron formation, Lake Albanel iron range, Mistassini territory, Quebec, Canada. Econ. Geol., vol.56, pps.299-320.

RANSOM D.M. 1971 Host control of recrystallized quartz grains. Min. Mag., vol.38, pps.83-88.

ROEDDER E. 1962 Studies of fluid inclusions I: Low temperature application of a dual-purpose freezing and heating stage. Econ. Geol., vol.57, pps.1045-1061.

1963 Studies of fluid inclusions II: Freezing data and their interpretation. Econ. Geol., vol.58, pps.167-211.

1967 Fluid inclusions as samples of ore fluids. In: "Geochemistry of hydrothermal ore deposits", ed. H.L. Barnes, pub. Holt, Rinehart and Winston Inc., New York.

1971 Fluid-inclusion evidence on the Environment of Formation of Mineral Deposits of the Southern Appalachian Valley. Econ. Geol., vol.66, pps.777-791.

REYNOLDS D.L. 1946 The sequence of chemical changes leading to granitization. Geol. Soc. Lond. Quart. Journ., vol.102, pps.389-446.

ROSENBERG P.E.
BURT D.M.
HOLLAND H.D.
1967 Calcite-dolomite-magnesite stability relations in solutions: the effect of ionic strength. Geochim. et Cosmochim. Acta, vol.31, pps.291-396.

ROSENBERG P.E.
HOLLAND H.D.
1964 Calcite-dolomite-magnesite stability relations in solutions of elevated temperatures. Science, vol.145, pps. 700-701.

RUCKMICK J.C.
1963 The iron ores of Cerro Bolivar,Venezuela. Econ. Geol., vol.58, No.2, pps.218-237.

RUDD E.A.
1940 The Geology and ore reserves of the Middleback Ranges, South Aust. Unpublished B.H.P. Cpy. Ltd. Report.

RUDD E.A.
MILES K.R.
1953 Iron ores of the Middleback Ranges, S.A. In: "Geology of Aust. ore deposits", 5th Emp. Min. Met. Cong., vol.1, pps.449-463.

SAKAMOTO T.
1950 The origin of the Pre-Cambrian banded iron ores. Am. Journ. Sc., vol.248, pps.449-474.

SAWKINS F.J.
1964 Lead-zinc ore deposition in the light of fluid inclusion studies, Providencia Mine, Zacatecas, Mexico. Econ. Geol., vol.59, pps.883-919.

SAXENA S.K.
1968 Distribution of elements between coexisting minerals and the nature of solid solutions in garnet. Am. Min., vol.53, pps.994-1014.

SHARP W.E.
1965 The deposition of hydrothermal quartz and calcite. Econ. Geol., vol.60, pps.1635-1644.

SCHMIDT R.G. 1963 Geology and ore deposits of the Cuyuna north Range, Minnesota. U.S.G.S. Prof. Paper 407.

SHIDO F. 1958 Plutonic and metamorphic rocks of the Nakoso and Iritono districts in the Central Abukuma Plateau. Journ. Fac. Sci. Univ. Tokyo, Sec.2, vol.11, pps.131-

SHUNZO Y. 1966 Decomposition of siderite to magnetite at lower oxygen fugacities: a thermo-chemical interpretation and geological implications. Econ. Geol., vol.61, pps.768-776.

SIEVER R. 1962 Silica solubility 0° - 200°C and the diagenesis of siliceous beds. Journ. Geol., vol.70, No.2, pps.127-150.

SMALE D. 1966 The Petrology and age relations of rocks in the Moonabie Range, South Australia. Trans. Roy. Soc. S. Aust., vol.90, pps.154-165.

SMYTHE J.A.
DUNHAM K.C. 1947 Ankerites and chalybites from the northern Pennine orefield and the north-east coalfield. Min. Mag., vol.28, pps.53-74.

SORBY H.C. 1858 On the microscopic structure of crystals, indicating the origin of minerals and rocks. Geol. Soc. London Quart. Journ., vol.14, Part 1, pps.453-500.

SPENCER
PERCIVAL 1952 The structure and origin of the banded hematite jaspers of Singhbum, India. Econ. Geol., vol.47,pps.365-383.

SPRY A. 1969 "Metamorphic Textures". Pub. Pergamon Press, London.

STAM J.C. 1963 Geology, petrology and iron deposits of the Guiana Shield, Venezuela. Econ. Geol., vol.58, pps.70-83.

STRAUSS C.A. 1963a The iron ore deposits in the Thabazimbi area, Transvaal. In: "The ore deposits of Southern Africa", Geol. Soc. of S. Af., vol.II, pps.383-392.

1963b The iron ore deposits in the Sishen area, Cape Province. In: "The ore deposits of Southern Africa", Geol. Soc. of S. Af., vol.II, pps.393-403.

STURT B.A. 1962 The composition of garnet from pelitic schists in relation to the grade of regional metamorphism. Journ. Pet., vol.3, pps. 181-191.

SWEATMAN T.R.
LONG J.V.P. 1969 Quantitative Electron-Probe Microanalysis of Rock-forming minerals. Jounr. Pet., vol.10, Part 2, pps.332-379.

TAKENOUCHI S.
KENNEDY G.C. 1965 The solubility of carbon dioxide in NaCl solutions at high temperatures and pressures. Am. Journ. Sc., vol.263, pps.445-454.

TALBOT J.L.
HOBBS B.E. 1968 The relationship of metamorphic differentiation to other structural features at three localities. Journ. Geol., vol.76, pps.581-587.

TAYLOR C.P. 1964 Geophysical exploration for iron ore in the Middleback Range area. Proc. Aust. Inst. Min. Met., No.209, pps.19-41.

TAYLOR G.H. 1954 Petrography of some rocks from the Middleback Range area. In: "The Geology and Iron Ore Resources of the Middleback Range Area", Geol. Surv. S. Aust. Bull.33, pps.231-247.

TENNANT C.B. 1957 X-ray determination of the dolomite - calcite ratio of a carbonate rock. Am. Min., vol.42, pps.23-29.

THOMSON B.P. 1966 The lower boundary of the Adelaide system and older basement relationships in South Australia. Journ. Geol. Soc. Aus., vol.13, Part 1, pps.203-227.

1969 Pre-Cambrian Crystalline Basement in "Handbook of South Australia Geology", ed. L.W. Parkin, pub. Geol. Surv. S. Aust.

TILLEY C.E. 1920a The metamorphism of the Pre-Cambrian Dolomites of Southern Eyre Peninsular, South Australia. Geol. Mag., vol.57, (10), pps.449-462.

1920b The metamorphism of the Pre-Cambrian Dolomites of southern Eyre Peninsular, Trans. Roy. Soc. Aust., vol.4, pps.143-144.

1921a Pre-Cambrian Para-Genesis of southern Eyre Peninsular. Geol. Mag., vol.58, (6), pps.251-259.

1921b The Graphite rocks of Sleaford Bay, South Australia. Econ. Geol., vol.16 (3), pps.184-198.

TILLEY C.E. 1921c The Granite-Gneisses of Southern Eyre Peninsular (South Australia) and their associated amphibolites. Quart. Journ. Geol. Soc., vol.77, pps.75-134.

TRENDALL A.F. 1968 Precambrian Banded Iron Formation deposition. Bull. Geol. Soc. Am., vol.79, pps.1527-1544.

TRENDALL A.F. BLOCKLEY J.G. 1970 The Iron Formations of the Precambrian Hamersley Group, Western Australia with special reference to the associated Crocidolite. Geol. Surv. West. Aust. Bull.119.

TURNER F.J. 1948 Mineralogical and structural evaluation of the metamorphic rocks. Geol. Soc. Am. Mem. 30, pps.299-304.

1968 "Metamorphic Petrology". Pub. McGraw-Hill Book Company, New York.

TYLER S.A. 1948 Itabirite of Minas Gerais, Brazil. Journ. Sed. Pet., vol.118, No.2,pps.86-87.

1949 Development of Lake Superior soft iron ores from metamorphosed iron formations. Bull. Geol. Soc. Am., vol.60, pps.1101-1124.

WAARD D. de 1959 Anorthite content of plagioclase in basic and pelitic crystalline schists as related to metamorphic zoning in the Usu Massif, Timor. Am. Journ. Sc., vol.257, pps.553-562.

WALKER T.R. 1960 Carbonate replacement of detrital crystalline silicate minerals as a source of authigenic silica in sedimentary rocks. Bull. Geol. Soc. Am., vol.71, pps.145-152.

WALKER T.R. 1967 Formation of red beds in ancient and modern deserts. Geol. Soc. Am. Bull., vol.78, pps.353-

WARD L.K. 1949 The genesis of the Iron Ores of the Middleback Range, South Australia. Proc. Aust. Inst. Min. Met., New Series 152-3, pps.229-240.

WARNE S.St.J. 1962 A quick field or laboratory staining scheme for the differentiation of major carbonate minerals. Journ. Sed. Pet., vol.32, No.1, pps.29-38.

WEEKS W.F. 1956a A thermo-chemical study of equilibrium relations during metamorphism of siliceous carbonate rocks. Journ. Geol., vol.64, pps.245-270.

1956b Heats of formation of metamorphic minerals in the system CaO-MgO-SiO_2 H_2O and their petrological significances. Journ. Geol., vol.64, pps.456-472.

WEYE P.K. 1959 Change in solubility of calcium carbonate with temperature and CO_2 content. Geochim. et Cosmochim. Acta, vol.17, pps. 214-225.

WHITE D.E.
BRANNOCK W.W.
MURATA K.J. 1956 Silica in hot spring waters. Geochim. et Cosmochim. Acta, vol.10, pps.27-59.

WHITE D.E.
HEM J.D.
WARING G.A. 1963 Chemical composition of sub-surface waters. U.S.G.S. Prof. Paper 440-F.

WHITEHEAD S. 1959-1961 Unpublished B.H.P. Cpy. Ltd. reports on Iron Duke diamond drillholes: 47, 57, 60, 59, and Iron Duchess diamond drillholes 62 and 63.

1962 The iron formations of the Middleback Ranges, South Australia. B.H.P. Technical Bull., No.13, pps.11-16.

WHITTEN G.F. 1966 The geology of some South Australian iron deposits. M.Sc. Thesis, University of Adelaide.

WHITTLE A.W.G. 1954 Petrology, in "The Geology and Iron Ore Resources of the Middleback Range Area", Geol. Surv. S. Aust. Bull.33, pps.186-198.

WIENERT F. 1933 Formation of Martite and other iron oxides in sideritic ore of the Marquette District, Michigan. Econ. Geol., vol.28, pps.68-74.

WILKINS R.W.T. 1970 Iron-magnesium distribution in the tremolite-actinolite series. Am. Min., vol.55, pps.1993-

WINKLER H.G.F. 1967 "Petrogenesis of Metamorphic rocks". Pub. Springer-Verlag, Berlin.

WOOD J.A.Jr. 1958 The solubility of quartz in water at high temperatures and pressures. Am. Journ. Sc., vol.256, pps.40-47.

WYLLIE P.J.
TUTTLE O.F. 1959 Melting of calcite in the presence of water. Am. Min., vol.44, pps.453-459.

WYLLIE P.J. 1965 Melting relationships in the system $CaO-MgO-CO_2-H_2O$ with petrologic applications. Journ. Pet., vol.6, pps.101-123.

YERMAKOV N.P. 1965 Ed. "Research on the Nature of Mineral-forming Solutions". Pub. Pergamon Press, 1965.

ZEN E. 1960 Metamorphism of Lower Palaeozoic rocks in the vicinity of the Taconic Range in west-central Vermont. Am. Min., vol.45, pps.129-175.

APPENDIX I - WHOLE ROCK ANALYSES

Whole-rock analyses used in the text and listed in the following pages include XRF analyses carried out by the author in Durham, together with quantitative analyses and drill core assays carried out by the Chemical Laboratory, B.H.P., Whyalla. Occasionally published analyses from sources such as Miles (1954) are used to illustrate particular points.

The XRF analyses were carried out using pressed powder briquettes with a Phillips PW 1212 x-ray fluorescence spectrometer. Most of the samples consisted of small portions of drill core, and these were split lengthwise before crushing. The samples were ground to a fine powder using a jaw crusher and disc mill, and the powders were then briquetted.

For major elements, twenty quantitative analyses of Iron Duke rock types carried out by the Chemical Laboratory, B.H.P., Whyalla were used, together with one basic igneous rock standard sample available within the Geology Department at Durham. The samples analysed by XRF include a wide variety of rock types and not more than five standard analyses could be used for any particular group of samples. Mass absorption corrections were applied using the method of Holland and Brindle (1966), but for some rock types the raw count data was closer to the standard analyses than the corrected results. For some rock types, therefore, the analyses are based on the raw count data, whilst for others mass absorption corrections have been applied. Notes on the precise technique used and on the analytical precision and accuracy are included immediately before the analyses for each major rock type.

For trace element calibration, a series of synthetic glass standards available in the Geology Department was used for the basic igneous rocks and Schists, and four groups of synthetic standards were made from "Specpure" chemicals (Johnson, Matthey & Co.) for the iron rich rock types. The major element compositions of the latter standards were; $CaCO_3$, 50% Fe_2O_3 - 50% SiO_2, 70% Fe_2O_3 - 30% $CaCO_3$, Fe_2O_3,

and these base mixes were spiked with "Specpure" trace element compounds. Corrections were applied for K interference on Nb, Zr and Y. Comments on trace element calibration are included in the notes prior to each group of analyses.

The quantitative analyses by the Chemical Laboratories, B.H.P., Whyalla, were carried out by a combination of wet chemical and spectrographic methods, as follows :

Emission spectrograph :	SiO_2 (20%), Al_2O_3, P, CaO (10%), MgO (10%), Mn, TiO_2
Wet chemical :	Fe, SiO_2 (20%), CaO (10%), MgO (10%), S.
Atomic absorption :	Na, K

Drill core assays employ the same techniques but with less checking and precision. In all the B.H.P. analyses, elemental values were determined for Fe, Mn and P, and these were recalculated as oxides by the author.

Two water determinations were carried out on chloritised amphibolites, using a Riley Furnace.

B. - Iron-formations - XRF analyses

Major elements

The chemical compositions of the iron-formations are very similar to those of the talc zone rocks, and it was originally intended to combine quantitative analyses from both groups as XRF standards. However, it became clear that the two rock types react differently to XRF analysis. For example, the following two samples have similar iron contents, yet the iron-formation sample shows a considerably higher XRF count :

62-606 (iron-formation)	Fe_2O_3	SiO_2	MgO
Per cent	40.0	55.1	3.8
P - 1/b	343,175	99,910	19,946
77-275 (talc zone)			
Per cent	42.0	47.2	8.6
P - 1/b	290,908	111,776	120,442

This variation between the two rock groups is further illustrated in Fig. ~~IA,~~ 1-1a and it is evident that each group requires a separate calibration curve, based upon samples of its own rock types. As a result, only five quantitative analyses could be used for iron-formation calibration, and this number is insufficient to give more than approximate rock compositions because the silica, iron and magnesia contents in the iron-formations are very variable. Iron-formation XRF analyses shown in the following pages have totals between 94.5% and 106.5%, and in most cases magnesium is well outside the standard calibration range. The analyses should therefore be regarded only as a general indication of rock composition.

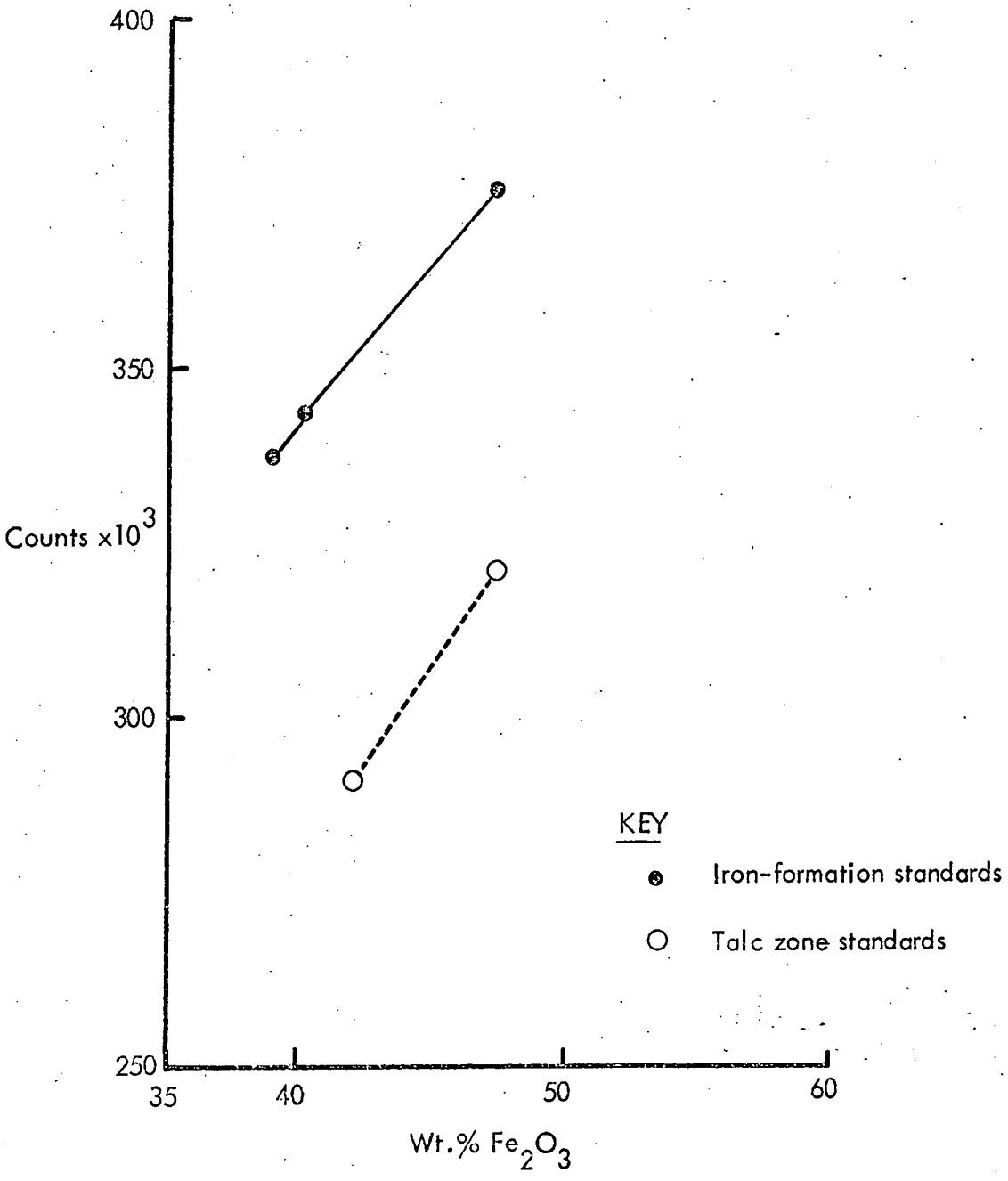

Fig. I-11a. XRF counts for Fe on iron-formation and talc zone standard samples. Trend lines point towards counts for hematite and magnetite ore samples which are outside diagram on upper right.

B. - Iron-formations - XRF analyses - continued

XRF results for the iron-formation standard samples are shown in Table I-1, and it is evident that in general the analyses based on uncorrected counts are closer to the quantitative analyses than are the analyses based on mass absorption corrected counts and normalised in the manner described by Holland and Brindle (1967). There is also a major unexplained error in the computer calculation for normalised values of sample 62-606. The raw count analyses were therefore used throughout.

The XRF major element analyses of iron-formations were carried out primarily as a guide for trace element determinations, as the iron content has an important effect on a number of trace elements. However, the results as described above show two important points :

(1) It is essential to use a large number of standards, the minimum probably being about ten covering a wide range of each element, for even semi-quantitative analysis of iron-formations.

(2) The mineralogy of the standards must be similar to that of the iron-formation. The cause of the analysis variation between iron-formations and talc zone rocks is not immediately evident, but the two rock groups differ in mineralogy rather than geochemistry. The iron-formations contain fine-grained quartz, magnetite and amphiboles, whereas the talc zone rocks contain coarse grained quartz, magnetite-hematite and talc. The most significant differences are therefore the presence of talc rather than amphibole, and the general coarser grain size of the talc zone rocks. It is possible that talc orientation during pellet preparation has the effect of shielding iron oxide grains, thereby reducing the overall iron count and increasing the silica and magnesia. However, the cause of the observed variation requires further investigation.

Table I-1 - Iron-formation standard sample calibration

Quantitative analyses by Chemical Laboratory, B.H.P., Whyalla.

XRF (1) are analyses based on uncorrected counts.

XRF (2) are analyses based on counts corrected for mass absorption and normalised.

	SiO_2	Al_2O_3	Fe_2O_3	MgO	CaO	Na_2O	K_2O	TiO_2	MnO	S	P_2O_5	Ig.Loss	Total
H2													
Quantitative	1.00	0.90	96.80	0.10	0.10	0.08	0.04	0.05	0.10	0.04	0.09	0.8	100.10
XRF (1)	1.69	0.91	92.72	0.00	0.24	0.00	0.02	0.05	0.10	0.10	0.13	N.D.	95.96
XRF (2)	2.24	0.96	96.12	0.00	0.24	0.01	0.02	0.06	0.11	0.11	0.13	N.D.	100.00
3431													
Quantitative	1.30	0.30	92.40	0.30	1.30	0.05	0.02	0.05	0.10	0.01	0.14	4.6	100.57
XRF (1)	0.56	0.26	96.15	0.37	1.29	0.00	0.00	0.05	0.10	0.10	0.12	N.D.	99.01
XRF (2)	0.68	0.22	97.12	0.50	1.17	0.01	0.02	0.04	0.08	0.08	0.10	N.D.	100.00
62808													
Quantitative	46.10	0.10	47.20	3.20	0.30	0.01	0.01	0.05	0.30	0.07	0.05	+0.3	97.09
XRF (1)	51.42	0.14	47.76	3.70	0.17	0.00	0.02	0.05	0.30	0.00	0.05	N.D.	103.62
XRF (2)	46.72	0.10	49.31	3.39	0.12	0.01	0.02	0.04	0.24	0.00	0.05	N.D.	100.00
62606													
Quantitative	55.10	0.10	40.00	3.80	0.30	0.03	0.01	0.05	0.30	0.05	0.14	0.2	100.08
XRF (1)	52.67	0.13	40.13	3.84	0.29	0.00	0.02	0.05	0.30	0.00	0.12	N.D.	97.54
XRF (2)	88.28	1.38	0.00	5.81	1.72	0.11	0.01	0.56	1.67	0.00	0.46	N.D.	100.00
62988													
Quantitative	54.40	0.20	39.20	4.90	0.30	0.03	0.01	0.05	0.30	1.02	0.28	+0.8	99.89
XRF (1)	51.57	0.16	38.85	4.44	0.32	0.00	0.01	0.05	0.30	1.00	0.28	N.D.	96.97
XRF (2)	Not determined for this sample												

Table I-2 - Calibration ranges for iron-formation Major element analyses (XRF)

Element	Percentage range
SiO_2	1.00 to 55.10
Al_2O_3	0.10 to 0.90
Fe_2O_3	39.20 to 96.80
MgO	0.10 to 4.90
CaO	0.10 to 1.30
Na_2O	0.01 to 0.08
K_2O	0.01 to 0.04
TiO_2	0.05 to 0.05
MnO	0.10 to 0.30
S	0.01 to 1.02
P_2O_5	0.05 to 0.28

B. - Iron-formations - XRF analyses - continued

Trace elements

Synthetic standards consisting of 50% Fe_2O_3 and 50% SiO_2 were used. In the trace element ranges required for iron-formations, calibration of standards was good for Zn, Cu, Ba, Y, Sr, and Rb, as shown in Table I-3 below. Ni and Zr determinations varied by fixed amounts from the standard values, and for each rock determination 3 was subtracted from the Ni determinations below 30 ppm and 4 from Zr determinations below 10 ppm. No Nb values were available for this set of standards, so an approximate Nb level was determined for the rock samples using an assumed curve mid-way between the Nb values for the lunar and 70% Fe_2O_3 - 30% $CaCO_3$ standards. Note the poor correlation for Cu below 8 ppm.

Table I-3 - Trace element calibration for 50% Fe_2O_3 - 50% SiO_2 standards

ppm	Zn	Cu	Ni	Ba	Zr	Y	Sr	Rb
31	31	34	33	32	32	31	90	43
16	10	14	20(17)	14	18	13	16	10
8	7	7	11(8)	3	10	3	8	3
4	5	17	7(4)	N.D.	8(4)	0	3	1
0	4	8	3(0)	N.D.	N.D.	N.D.	N.D.	N.D.

( ) Values after manual correction

Nominal detection limits calculated from accumulated background values are :

	Zn	Cu	Ni	Ba	Zr	Y	Sr	Rb
ppm	1	5	3	11	3	3	3	2

The iron-formation samples selected for trace element analysis all contain between 40% and 60% Fe_2O_3, thereby conforming broadly to the synthetic standard composition.

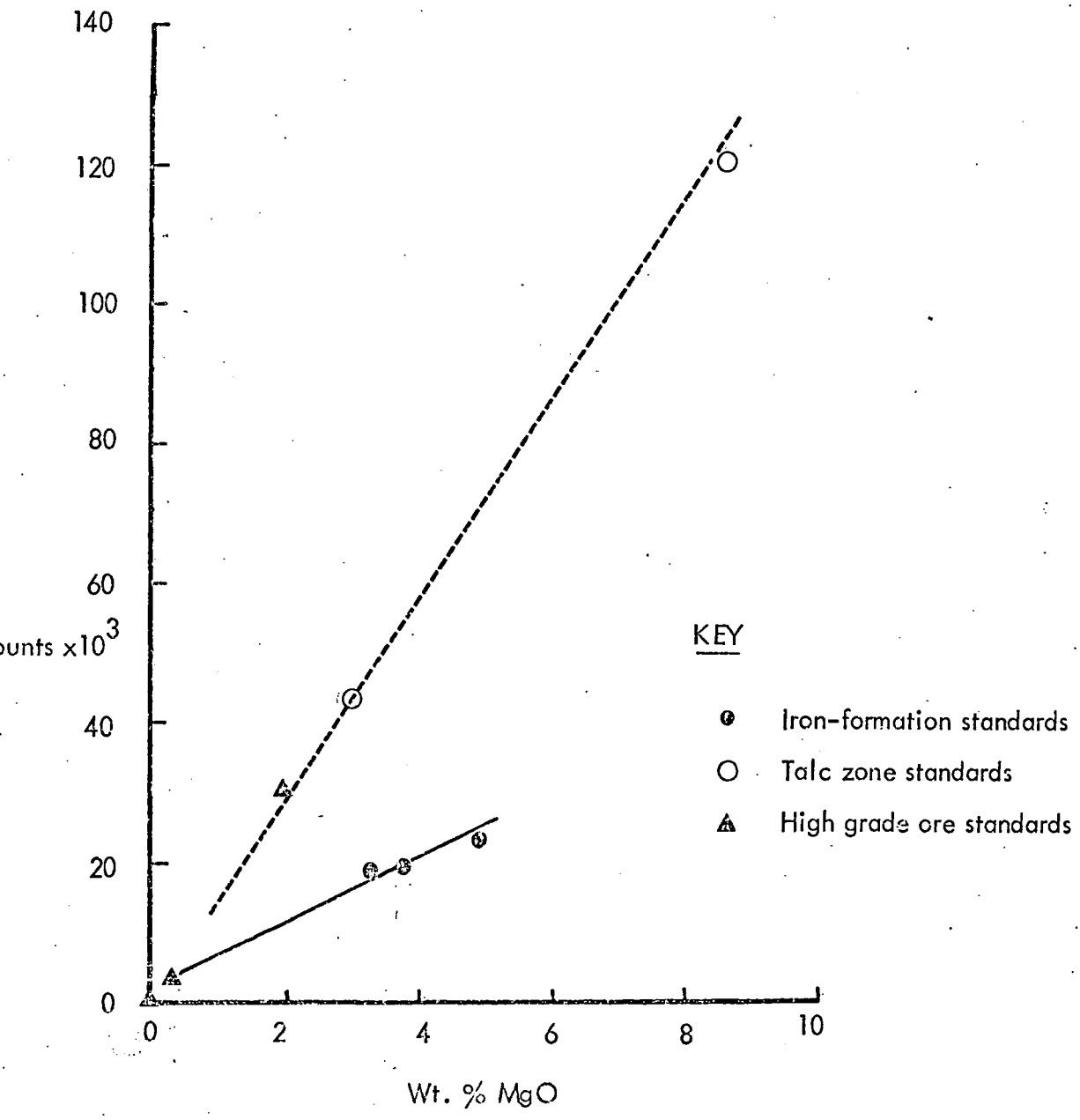

Fig. I-1b. XRF counts for Mg on iron-formation, talc zone and high grade ore standards.

Whole-rock analyses - Middleback Ranges

Iron-formations - major element analyses by Chemical Laboratory, B.H.P., Whyalla. Trace elements, XRF by author.

Per cent	62-808	62-606	62-988
SiO_2	46.1	55.1	54.4
Al_2O_3	0.1	0.1	0.2
Fe_2O_3	47.2	40.0	39.2
MgO	3.2	3.8	4.9
CaO	0.3	0.3	0.3
Na_2O	0.0	0.0	0.0
K_2O	0.0	0.0	0.0
TiO_2	0.1	0.1	0.1
MnO	0.3	0.3	0.3
S	0.1	0.1	1.0
P_2O_5	0.1	0.1	0.3
Ig. Loss	+0.3	0.2	+0.8
	97.2	100.1	100.1
ppm			
Zn	23	29	
Cu	2	0	
Ni	6	6	
Ba	0	0	
Nb			
Zr	0	1	
Y	0	0	
Sr	0	0	
Rb	0	0	

Note: 1. Fe expressed as Fe_2O_3

2. Nb is in the order of 1ppm to 4ppm

Whole-rock analyses - Middleback Ranges

Iron-formations and chip-channel samples.

Assays of drill core and chip-channel samples by Chemical Laboratory, B.H.P., Whyalla.

Per cent	T3 265	T3 370	57- 2426
SiO_2	56.0	31.0	49.0
Al_2O_3	0.5	1.4	0.5
Fe_2O_3	41.5	58.6	45.3
MgO	0.1	3.6	2.5
CaO	0.1	0.1	2.8
Na_2O	N.D.	N.D.	N.D.
K_2O	N.D.	N.D.	N.D.
TiO_2	0.0	0.0	0.2
MnO	0.1	0.3	0.2
S	0.0	0.0	0.0
P_2O_5	0.1	0.0	0.1
Ig.Loss	1.5	3.4	0.1
	99.9	98.4	100.7

Whole-rock analyses - Middleback Ranges

Iron-formation analyses of Middleback Range rocks from Miles (1954), and of overseas iron-formations from James (1966).

Per cent	1	2	3	4
SiO_2	20.56	46.94	37.54	51.52
Al_2O_3	0.37	0.00	0.80	0.08
Fe_2O_3	73.10	51.00	50.41	35.37
FeO	4.49	1.41	10.17	10.24
MgO	0.10	0.00	0.19	0.20
CaO	0.27	Tr	Tr	0.02
Na_2O	N.D.	0.00	0.03	N.D.
K_2O	N.D.	0.00		
TiO_2	0.0	0.0	Tr	N.D.
MnO	0.03	0.02	0.0	N.D.
S	N.D.	0.00	0.58	N.D.
P_2O_5	N.D.	0.39	N.D.	0.06
H_2O	1.66	0.68	0.28	1.48
CO_2	0.00	N.D.	0.23	1.06
	100.58	100.44	100.23	100.03

Analyses 1 and 2, Middleback Ranges (Miles 1954).

Analysis 3, hematite-magnetite iron-formation, Krivoi Rog series, Ukraine, U.S.S.R. (James 1966).

Analysis 4, magnetite-chert, Biwabik iron-formation, Mesabi District, Minnesota, U.S.A. (James 1966).

Whole-rock analyses - Middleback Ranges

Iron-formations - XRF determinations.

G = grunerite present, T = tremolite present, S = pyrite present.

* = major element more than 10% beyond calibration range.

Per cent	62-733G	62-623G	62-1073G	62-1015G	62-1078T
SiO_2	39.5	42.2	43.6	44.3	39.5
Al_2O_3	0.2	0.2	0.2	0.2	0.2
Fe_2O_3	46.4	46.0	45.9	44.9	49.5
MgO	7.5*	6.2	5.5*	6.2*	10.9*
CaO	0.5	0.4	0.3	0.3	0.3
Na_2O	0.0	0.0	0.0	0.0	0.0
K_2O	0.1	0.0	0.0	0.0	0000
TiO_2	0.1	0.1	0.1	0.1	0.1
MnO	0.5*	0.3	0.4	0.3	0.4
S	0.2	0.0	0.1	0.1	0.4
P_2O_5	0.1	0.3	0.1	0.1	0.2
	95.1	95.7	96.2	96.5	101.4
ppm					
Zn	15	10	16	24	21
Cu	9	6	14	7	14
Ni	17	9	15	17	18
Ba	0	0	0	0	0
Nb					
Zr	0	2	6	0	1
Y	1	2	0	1	0
Sr	0	0	1	0	2
Rb	0	0	0	0	0

Note: 1. Nb is in the order of 1ppm to 4ppm

Whole-rock analyses - Middleback Ranges

Iron-formations - XRF determinations - continued

Per cent	62-943TS	62-592	70-916	74-387	57-2049
SiO_2	38.1	53.7	58.2	42.6	71.2*
Al_2O_3	0.3	0.1	0.2	0.2	0.2
Fe_2O_3	48.7	46.8	36.7	50.6	16.5*
MgO	7.1*	5.0	3.9	7.0*	7.6*
CaO	0.4	0.3	0.7	0.4	3.6*
Na_2O	0.0	0.0	0.0	0.0	0.0
K_2O	0.0	0.0	0.0	0.0	0.0
TiO_2	0.1	0.1	0.1	0.1	0.1
MnO	0.3	0.2	0.2	0.4	0.2
S	1.2*	0.0	0.1	0.0	0.2
P_2O_5	0.2	0.4*	0.8*	0.5*	0.4
	96.4	106.6	100.9	101.8	100.0
ppm					
Zn	11	10	12	15	N.D.
Cu	26	8	6	7	N.D.
Ni	13	1	9	29	N.D.
Ba	0	0	0	0	N.D.
Nb					N.D.
Zr	00	0	0	1	N.D.
Y	0	4	5	2	N.D.
Sr	2	3	1	2	N.D.
Rb	0	0	0	0	N.D.

Note: 1. Nb is in the order of 1ppm to 4ppm

Whole-rock analyses - Middleback Ranges

Iron-formations - XRF determinations - continued.

Per cent	J7
SiO_2	67.0*
Al_2O_3	0.2
Fe_2O_3	38.5
MgO	0.0
CaO	0.2
Na_2O	0.0
K_2O	0.0
TiO_2	0.1
MnO	0.1
S	0.1
P_2O_5	0.0
	106.2
ppm	
Zn	6
Cu	0
Ni	5
Ba	2
Nb	
Zr	1
Y	0
Sr	5
Rb	0

Note: 1. Nb is in the order of 1ppm to 4ppm

C. - Magnetite-hematite-carbonate ore and basal carbonate unit - XRF analyses.

Major elements

Six standards were used, all being quantitative analyses by the Chemical Laboratory, B.H.P., Whyalla. The standard calibrations are shown in Table I-3, and the uncorrected count analyses are considered preferable to the corrected, normalised analyses. There is considerable variation in the accuracy of the XRF analyses relative to the quantitative analyses, and the XRF data should be regarded as showing the general levels of elements present rather than as precise determinations. The analyses are intended as a broad guide to the ore composition and are necessary as a control for trace element determinations.

Trace elements

Two sets of synthetic standards were used for the magnetite-hematite-carbonate ore. One of $CaCO_3$ and the other 70% Fe_2O_3 - 30% $CaCO_3$. Calibration of these standards is shown in Table I-4. In the 70% Fe_2O_3 - 30% $CaCO_3$ standards, there is poor correlation between the known element values and the XRF values for Ba 0-250 ppm and Zr below 30 ppm. The values of these elements for the rock samples have therefore been indicated in general terms, such as 16 ppm.

The iron content of each rock sample was used as a guide for the choice of standard, over 30%. Fe_2O_3 samples being calibrated against 70% Fe_2O_3 - 30% $CaCO_3$ standards and under 30% Fe_2O_3 samples being calibrated against $CaCO_3$ standards. The accuracy of trace element determinations for any particular sample depends to a large extent on the similarity of the sample major element composition to that of the standard particularly with respect to the iron content. Thus, trace element determinations for samples of virtually pure carbonate with low iron contents are regarded as quantitative, as they are calibrated against $CaCO_3$ standards which contain no iron. Similarly, samples with

C. - Magnetite-hematite-carbonate ore and basal carbonate unit - XRF analyses - continued.

about 70% Fe_2O_3 are calibrated against 70% Fe_2O_3 - 30% $CaCO_3$ standards and the trace element determinations are regarded as quantitative. However, many samples have an intermediate iron content with 20% - 50% Fe_2O_3, and for these the trace elements are regarded as semi-quantitative or as general indications of the element level. For example, sample 47-1065 contains 29.5% Fe_2O_3 and shows the following trace element levels when calibrated against the two sets of standards:

	Zn	Cu	Ni	Ba	Nb	Zr	Y	Sr	Rb
$CaCO_3$ Stds	13	N.D.	3	0	0	3	23	12	5
70% Fe_2O_3 - 30% $CaCO_3$ Stds	17	N.D.	8	30	N.D.	16	19	19	3

Samples of magnetite within the hematite-magnetite-carbonate ore were calibrated against synthetic hematite standards, which are discussed under the section on XRF analysis of hematite ore.

Table I-4 - Magnetite-hematite-carbonate standard samples calibration

Quantitative analyses by Chemical Laboratory, B.H.P., Whyalla.

XRF (1) are analyses based on uncorrected counts.

XRF (2) are analyses based on counts corrected for mass absorption and normalised.

	SiO_2	Al_2O_3	Fe_2O_3	MgO	CaO	Na_2O	K_2O	TiO_2	MnO	S	P_2O_5	Ig.Loss	Total
60732													
Quantitative	0.70	0.30	87.90	2.90	4.80	0.20	0.11	0.05	0.30	0.07	1.10	2.90	101.33
XRF (1)	1.16	0.31	86.92	2.36	4.67	0.00	0.07	0.05	0.00	0.04	1.11	3.30	99.99
XRF (2)	1.41	0.33	85.89	2.92	4.75	0.05	0.09	0.05	0.01	0.05	1.14	3.30	100.00
57712													
Quantitative	0.50	0.30	83.60	4.20	5.80	0.16	0.07	0.05	0.30	0.03	0.09	6.10	101.20
XRF (1)	0.63	0.26	85.07	3.83	5.58	0.00	0.08	0.05	0.25	0.03	0.07	4.10	99.95
XRF (2)	0.74	0.27	81.71	5.03	5.73	0.05	0.07	0.05	0.23	0.03	0.11	5.98	100.00
86734													
Quantitative	1.30	0.20	56.20	8.60	13.70	0.22	0.11	0.05	0.40	0.04	10.32	19.20	100.34
XRF (1)	1.11	0.22	58.59	11.67	14.47	0.00	0.08	0.05	0.50	0.03	0.27	13.10	100.09
XRF (2)	1.03	0.17	59.65	12.48	14.52	0.03	0.05	0.04	0.45	0.03	0.24	11.31	100.00
60842													
Quantitative	0.30	0.20	46.20	10.40	17.50	0.19	0.08	0.05	2.10	0.02	0.28	23.90	101.22
XRF (1)	0.37	0.24	40.33	10.93	18.04	0.00	0.08	0.05	2.43	0.03	0.27	23.20	95.96
XRF (2)	0.37	0.23	43.88	11.18	18.51	0.04	0.07	0.05	2.42	0.03	0.24	22.97	100.00
571140													
Quantitative	0.90	0.30	37.50	9.40	19.30	0.16	0.06	0.05	4.40	0.07	0.14	27.70	100.38
XRF (1)	0.55	0.23	37.55	8.63	19.92	0.00	0.07	0.05	4.15	0.08	0.18	28.60	100.00
XRF (2)	0.51	0.21	39.57	8.25	19.37	0.04	0.08	0.05	4.01	0.07	0.16	27.67	100.00
67823													
Quantitative	2.10	0.20	15.70	18.70	21.10	0.07	0.02	0.05	0.80	0.02	0.05	40.60	99.41
XRF (1)	1.98	0.24	18.64	16.77	19.92	0.00	0.08	0.05	0.98	0.04	0.09	41.20	99.99
XRF (2)	2.11	0.54	0.00	11.89	19.81	0.11	0.17	0.12	1.33	0.07	0.06	63.80	100.00

Table I-5 - Calibration ranges for magnetite-hematite-carbonate ore and basal carbonate unit.

Element	Percentage range
SiO_2	0.30 to 2.10
Al_2O_3	0.20 to 0.30
Fe_2O_3	15.70 to 87.90
MgO	2.90 to 18.70
CaO	4.80 to 21.10
Na_2O	0.07 to 0.22
K_2O	0.02 to 0.11
TiO_2	0.05 to 0.05
MnO	0.30 to 4.40
S	0.02 to 0.07
P_2O_5	0.05 to 1.10

Table I-6 - Trace element calibration for $CaCO_3$ and 70% Fe_2O_3 - 30% $CaCO_3$ standards.

$CaCO_3$

ppm	Zn	Cu	Ni	Ba	Nb	Zr	Y	Sr	Rb
250	262	N.D.	254	220	247	238	239	257	234
125	125	N.D.	126	119	127	120	119	125	134
63	63	N.D.	64	60	58	65	58	61	62
31	26	N.D.	34	32	29	30	29	30	27
16	13	N.D.	12	13	15	19	19	16	13
8	N.D.	N.D.	N.D.	N.D.	N.D.	9	9	N.D.	N.D.
4	N.D.	N.D.	N.D.	N.D.	N.D.	5	6	N.D.	N.D.
0	0	N.D.	0	0	0	2	4	0	3
Nominal detection limits from accumulated background values:									
	3		2	8	3	3	3	3	2

70% Fe_2O_3 - 30% $CaCO_3$

	Zn	Cu	Ni	Ba	Nb	Zr	Y	Sr	Rb
250	249	N.D.	235	243	N.D.	246	248	251	236
125	121	N.D.	114	106	N.D.	134	126	127	147
63	63	N.D.	63	57	N.D.	65	65	66	40
31	29	N.D.	35	30	N.D.	31	30	31	35
16	12	N.D.	23	9	N.D.	11	16	14	14
8	7	N.D.	9	2	N.D.	1	8	6	8
4	0	N.D.	5	N.D.	N.D.	1	2	N.D.	N.D.
0	0	N.D.	0	0	N.D.	0	0	6	0
Nominal detection limits from accumulated background values:									
	3		4	9		3	3	3	5

Whole-rock analyses - Iron Duke

Magnetite-hematite-carbonate ore.

Major element analyses by Chemical Laboratory, B.H.P., Whyalla.

Trace elements, XRF by author.

Per cent	86-734	60-842	57-1140	67-823
SiO_2	1.3	0.3	0.9	2.1
Al_2O_3	0.2	0.2	0.3	0.2
Fe_2O_3	56.2	46.2	37.5	15.7
MgO	8.6	10.4	9.4	18.7
CaO	13.7	17.5	19.7	21.1
Na_2O	0.2	0.2	0.2	0.1
K_2O	0.1	0.1	0.1	0.0
TiO_2	0.1	0.1	0.1	0.1
MnO	0.4	2.1	4.4	0.8
S	0.0	0.0	0.1	0.0
P_2O_5	0.3	0.3	0.1	0.1
Ig. Loss	19.2	23.9	27.7	40.6
	100.3	101.3	100.5	99.5
ppm				
Zn	12	4	5	2
Cu	N.D.	N.D.	N.D.	N.D.
Ni	5	8	12	0
Ba	< 30	< 30	< 30	0
Nb	N.D.	N.D.	N.D.	0
Zr	< 16	< 16	< 16	2
Y	1	15	14	20
Sr	7	6	14	29
Rb	0	1	0	4

Note: 1. Fe expressed as Fe_2O_3

Whole-rock analyses - Iron Duke

Magnetite-hematite-carbonate-typical ore samples.

Assays of drill core by Chemical Laboratory, B.H.P., Whyalla.

Per Cent	57-547	57-975	59-971	60-804
SiO_2	2.3	1.2	1.0	0.2
Al_2O_3	0.9	0.1	0.2	0.2
Fe_2O_3	61.0	56.9	39.2	56.9
MgO	6.7	8.0	11.4	5.0
CaO	10.0	13.6	20.4	18.2
Na_2O	N.D.	N.D.	N.D.	N.D.
K_2O	N.D.	N.D.	N.D.	N.D.
TiO_2	0.0	0.0	0.1	0.0
MnO	0.8	0.6	1.2	1.9
S	0.6	0.0	0.0	0.0
P_2O_5	0.3	0.0	0.0	0.2
Ig. Loss	15.6	19.2	27.6	18.4
	98.2	99.6	101.1	101.0

Whole-rock analyses - Iron Duke

Magnetite-hematite-carbonate ore - typical ore with ankerite as the main carbonate.

XRF analyses - see preceding notes.

*Major element over 10% outside calibration range.

Per cent	59-1099	57-765	59-919	47-717	78-770
SiO_2	0.5	0.6	0.3	0.9	0.2
Al_2O_3	0.2	0.2	0.2	0.3	0.2
Fe_2O_3	50.5	20.7	26.8	39.0	24.9
MgO	7.5	14.8	13.5	13.2	15.1
CaO	14.7	22.8*	20.5	18.5	22.5
Na_2O	0.0	0.0	0.0	0.0	0.0
K_2O	0.1	0.1	0.1	0.1	0.1
TiO_2	0.1	0.1	0.1	0.1	0.1
MnO	2.4	1.0	1.0	0.8	1.0
S	0.0	0.0	0.0	0.0	0.0
P_2O_5	0.2	0.2	0.1	0.1	0.2
Diff.	23.8	39.5	37.4	27.0	35.7
	100.0	100.0	100.0	100.0	100.0
ppm					
Zn	32	23	23	18	2
Cu	0	N.D.	N.D.	0	N.D.
Ni	12	1	1	28	7
Ba	<30	0	0	<30	0
Nb	N.D.	0	0	N.D.	0
Zr	<16	2	3	<16	4
Y	10	8	28	9	25
Sr	7	6	12	19	5
Rb	1	4	4	2	5

Note: 1. Fe expressed as Fe_2O_3

Whole-rock analyses - Iron Duke

Magnetite-hematite-carbonate ore - typical ore with ankerite as the main carbonate - continued.

Per cent	59-749	61-883	74-929	74-953
SiO_2	0.4	0.4	0.3	1.6
Al_2O_3	0.2	0.2	0.2	0.2
Fe_2O_3	35.7	45.2	62.8	54.1
MgO	12.6	11.2	8.4	9.4
CaO	19.1	17.5	12.6	14.4
Na_2O	0.0	0.0	0.0	0.0
K_2O	0.1	0.1	0.1	0.1
TiO_2	0.1	0.1	0.1	0.1
MnO	0.6	0.7	0.5	1.0
S	0.0	0.0	0.0	0.0
P_2O_5	0.2	0.3	0.3	0.2
Diff.	31.0	24.3	14.7	18.9
	100.0	100.0	100.0	100.0
ppm				
Zn	0	2	3	0
Cu	0	0	0	0
Ni	10	8	6	7
Ba	<30	< 30	< 30	< 30
Nb	N.D.	N.D.	N.D.	N.D.
Zr	<16	< 16	< 16	< 16
Y	10	7	8	19
Sr	8	7	8	12
Rb	0	0	0	2

Note: 1. Fe expressed as Fe_2O_3

Whole-rock analyses - **Iron Duke**

Magnetite-hematite-carbonate - typical ore from the lower part of the orebody, containing intermixed ankerite and calcite or calcite as the only carbonate.

XRF analyses - see preceding notes.

*Major element over 10% outside calibration range.

Per cent	59-919	74-956	47-1065	57-1205	84-1250
SiO_2	0.1	0.3	0.8	0.9	0.4
Al_2O_3	0.2	0.2	0.2	0.2	0.2
Fe_2O_3	30.4	27.5	29.5	25.3	68.9
MgO	9.8	10.9	8.8	0.0*	0.0*
CaO	21.4*	22.0*	19.3	32.0*	15.8
Na_2O	0.0	0.0	0.0	0.0	0.0
K_2O	0.1	0.1	0.1	0.1	0.1
TiO_2	0.1	0.1	0.1	0.1	0.1
MnO	3.8	1.5	2.7	0.6	0.7
S	0.0	0.0	0.0	0.0	0.1
P_2O_5	0.1	0.2	0.2	0.3	0.1
Diff.	34.0	37.2	38.3	40.5	13.7
	100.0	100.0	100.0	100.0	100.0
ppm					
Zn	0	90	13	0	106
Cu	N.D.	N.D.	N.D.	N.D.	N.D.
Ni	12	0	3	9	9
Ba	<30	0	0	30	< 30
Nb	N.D.	0	0	0	N.D.
Zr	< 16	3	3	6	< 16
Y	23	24	23	12	6
Sr	18	9	12	204	32
Rb	0	4	5	3	0

Note: 1. Fe expressed as Fe_2O_3

Whole-rock analyses - Iron Duke

Magnetite-hematite-carbonate - typical ore from the lower part of the orebody - continued.

Per cent	60-892
SiO_2	0.2
Al_2O_3	0.2
Fe_2O_3	19.8
MgO	0.0*
CaO	34.9
Na_2O	0.0
K_2O	0.1
TiO_2	0.1
MnO	2.7
S	0.0
P_2O_5	0.7
Diff.	41.3
	100.0
ppm	
Zn	1
Cu	N.D.
Ni	3
Ba	0
Nb	0
Zr	7
Y	9
Sr	208
Rb	2

Note: 1. Fe expressed as Fe_2O_3

Whole-rock analyses - Iron Duke

Magnetite-hematite-carbonate - layered ore.

XRF analyses - see preceding notes.

*Major element over 10% outside calibration range.

Per cent	59-791	84-928	84-870	57-979	57-900
SiO_2	0.3	0.6	0.4	1.3	0.7
Al_2O_3	0.2	0.2	0.2	0.2	0.2
Fe_2O_3	47.9	64.8	63.7	48.1	55.0
MgO	12.1	8.9	8.2	12.4	12.0
CaO	17.1	11.9	12.0	17.1	15.8
Na_2O	0.0	0.0	0.0	0.0	0.0
K_2O	0.1	0.0	0.1	0.1	0.1
TiO_2	0.1	0.1	0.1	0.1	0.1
MnO	0.6	0.7	0.6	0.8	0.8
S	0.0	0.0	0.0	0.0	0.0
P_2O_5	0.2	0.3	0.2	0.3	0.2
Diff.	21.4	12.4	14.5	19.6	15.1
	100.0	100.0	100.0	100.0	100.0
ppm					
Zn	0	16	79	1	13
Cu	N.D.	N.D.	N.D.	N.D.	N.D.
Ni	7	14	7	3	4
Ba	<30	<30	<30	<30	<30
Nb	N.D.	N.D.	N.D.	N.D.	N.D.
Zr	<16	<16	<16	<16	<16
Y	4	22	2	24	11
Sr	5	2	5	7	2
Rb	0	4	0	3	0

Note: 1. Fe expressed as Fe_2O_3

Whole-rock analyses - Iron Duke

Magnetite-hematite-carbonate - layered ore - continued.

Per cent	60-885	60-382
SiO_2	0.2	0.4
Al_2O_3	0.2	0.2
Fe_2O_3	36.8	25.8
MgO	0.0*	0.0*
CaO	29.1	32.1
Na_2O	0.0	0.0
K_2O	0.1	0.1
TiO_2	0.1	0.1
MnO	2.0	2.4
S	0.0	0.0
P_2O_5	0.5	0.4
Diff.	31.0	38.5
	100.0	100.0
ppm		
Zn	0	0
Cu	N.D.	N.D.
Ni	9	0
Ba	< 30	0
Nb	N.D.	0
Zr	< 16	4
Y	3	14
Sr	153	192
Rb	0	2

Note: 1. Fe expressed as Fe_2O_3

Whole-rock analyses - Iron Duke

Magnetite-hematite-carbonate - vein carbonates with minor iron oxides.

XRF analyses - see preceding notes.

*Major element over 10% outside calibration range.

Per cent	60-805	59-809	67-1104	74-981	74-666
SiO_2	0.2	0.8	0.7	0.8	0.3
Al_2O_3	0.2	0.2	0.3	0.2	0.2
Fe_2O_3	24.1	12.9*	9.0*	18.4	34.0
MgO	13.0	15.7	11.7	11.9	12.8
CaO	21.9*	24.4*	25.1*	21.4*	15.7
Na_2O	0.0	0.0	0.0	0.0	0.0
K_2O	0.1	0.1	0.1	0.1	0.1
TiO_2	0.1	0.1	0.1	0.1	0.1
MnO	2.1	1.1	4.4	2.2	1.7
S	0.0	0.0	0.0	0.0	0.0
P_2O_5	0.2	0.1	0.1	0.1	0.0
Diff.	38.1	44.6	48.5	44.8	35.1
	100.0	100.0	100.0	100.0	100.0
ppm					
Zn	2	3	10	1	0
Cu	N.D.	N.D.	N.D.	N.D.	N.D.
Ni	3	9	8	0	5
Ba	0	0	0	0	<30
Nb	0	0	1	0	N.D.
Zr	4	3	23	3	<16
Y	15	10	23	22	120
Sr	4	8	14	20	28
Rb	4	2	5	3	0

Note: 1. Fe expressed as Fe_2O_3

Whole-rock analyses - Iron Duke

Magnetite-hematite-carbonate - vein carbonates with minor iron oxides - continued.

Per cent	67-810	59-730	61-939	74-912	84-876
SiO_2	0.2	1.2	0.8	0.1	1.1
Al_2O_3	0.2	0.2	0.3	0.2	0.2
Fe_2O_3	7.0*	37.3	5.4*	12.7	3.3*
MgO	16.6	7.2	14.8	10.6	16.8
CaO	25.6*	17.0	26.1*	26.1*	25.9*
Na_2O	0.0	0.0	0.0	0.0	0.0
K_2O	0.1	0.1	0.1	0.1	0.1
TiO_2	0.1	0.1	0.1	0.1	0.1
MnO	0.7	2.8	1.9	1.7	1.2
S	0.0	0.0	0.0	0.0	0.0
P_2O_5	0.1	0.0	0.1	0.1	0.1
Diff.	49.4	34.1	50.4	48.3	51.2
	100.0	100.0	100.0	100.0	100.0
ppm					
Zn	0	3	14	0	0
Cu	N.D.	N.D.	N.D.	N.D.	N.D.
Ni	3	8	5	3	3
Ba	0	<30	0	0	0
Nb	0	N.D.	0	0	0
Zr	4	<16	4	3	1
Y	10	0	31	14	11
Sr	56	20	21	20	0
Rb	3	0	4	4	4

Note: 1. Fe expressed as Fe_2O_3

Whole-rock analyses - Iron Duke

Magnetite-hematite-carbonate ore - intermixed siderite and ankerite.

XRF analyses - see preceding notes.

*Major element over 10% outside calibration range.

Per cent	60-637	74-657
SiO_2	5.4*	1.9
Al_2O_3	0.2	0.2
Fe_2O_3	82.6	70.3
MgO	7.7	14.8
CaO	1.7*	1.0*
Na_2O	0.0	0.0
K_2O	0.1	0.1
TiO_2	0.1	0.1
MnO	1.1	1.9
S	0.0	0.0
P_2O_5	0.4	0.0
Diff.	0.7	9.7
	100.0	100.0
ppm		
Zn	2	1
Cu	N.D.	N.D.
Ni	3	5
Ba	<30	<30
Nb	N.D.	N.D.
Zr	<16	58
Y	10	22
Sr	6	2
Rb	0	0

Note: 1. Fe expressed as Fe_2O_3

Whole-rock analyses - Iron Duke

Trace elements in magnetite concentrations at the contacts of magnetite-hematite-carbonate ore and chloritised amphibolites.

XRF analyses.

ppm	60-753	67-M	57-869	T-4	59-1033
Zn	36	522	153	12	21
Cu	0	0	0	26	0
Ni	9	0	26	0	0
Ba	2	0	0	0	5
Nb	0	0	0	0	0
Zr	3	0	24	0	0
Y	2	3	5	9	3
Sr	5	4	5	6	9
Rb	0	0	0	0	0

Whole-rock analyses - Iron Duke

Basal carbonate

XRF analyses - see preceding notes.

Per cent	47-1084	59-1352	83-543	57-1645	83-575
SiO_2	0.1	0.4	0.4	1.5	0.6
Al_2O_3	0.2	0.2	0.2	0.3	0.2
Fe_2O_3	6.5	6.7	8.6	9.4	9.1
MgO	13.8	12.8	12.8	11.2	12.0
CaO	27.7	26.1	26.7	26.7	27.3
Na_2O	0.0	0.0	0.0	0.0	0.0
K_2O	0.1	0.1	0.1	0.1	0.1
TiO_2	0.1	0.1	0.1	0.1	0.1
MnO	1.0	1.1	0.8	1.0	0.7
S	0.0	0.0	0.0	0.1	0.0
P_2O_5	0.1	0.1	0.2	0.1	0.2
Diff.	50.4	52.4	50.1	49.5	49.7
	100.0	100.0	100.0	100.0	100.0
ppm					
Zn	15	1	6	11	0
Cu	N.D.	N.D.	N.D.	N.D.	N.D.
Ni	8	3	4	14	3
Ba	0	0	0	0	0
Nb	0	0	0	0	0
Zr	2	3	3	8	15
Y	2	11	6	6	12
Sr	14	18	10	37	10
Rb	4	3	4	2	3

Note: 1. Fe expressed as Fe_2O_3

Whole-rock analyses - Iron Duke

Basal carbonate - continued.

Per cent	83-689	59-1435	47-1197	47-1041
SiO_2	0.3	0.1	0.1	1.0
Al_2O_3	0.2	0.2	0.2	0.2
Fe_2O_3	2.7	4.0	5.4	7.5
MgO	16.0	15.0	14.6	13.7
CaO	27.9	27.7	27.4	26.3
Na_2O	0.0	0.0	0.0	0.0
K_2O	0.1	0.1	0.1	0.1
TiO_2	0.1	0.1	0.1	0.1
MnO	0.7	0.8	0.9	1.0
S	0.0	0.0	0.0	0.0
P_2O_5	0.2	0.2	0.2	0.1
Diff.	51.8	51.8	51.0	50.0
	100.0	100.0	100.0	100.0
ppm				
Zn	8	5	11	3
Cu	N.D.	N.D.	N.D.	N.D.
Ni	11	4	5	14
Ba	0	0	0	1
Nb	0	0	0	0
Zr	3	2	3	3
Y	6	5	4	7
Sr	14	8	10	25
Rb	2	3	5	3

Note: 1. Fe expressed as Fe_2O_3

C. - Talc zone rocks - XRF analyses

Major elements

Five standards were used, all being analyses of talc zone rocks and hematite or magnetite ore carried out by the Chemical Laboratory, B.H.P., Whyalla. The discussion concerning iron-formation analyses applies also to talc zone analyses, and the XRF major element determinations shown in the following pages can be regarded only as broad indications of the rock compositions.

The results for standards calibration are shown in Table I-7, and uncorrected counts were used for rock analyses because they are in general more accurate for Fe_2O_3 and MgO than the corrected, normalised analyses, although SiO_2 values are erratic.

Trace elements

The synthetic 50% Fe_2O_3 - 50% SiO_2 standards were used, and comments made in relation to the iron-formations are also applicable to the talc zone analyses.

Table I-7 - Talc zone standard sample calibration

Quantitative analyses by Chemical Laboratory, B.H.P., Whyalla.

XRF (1) are analyses based on uncorrected counts.

XRF (2) are analyses based on counts corrected for mass absorption and normalised.

	SiO_2	Al_2O_3	Fe_2O_3	MgO	CaO	Na_2O	K_2O	TiO_2	MnO	S	P_2O_5	Ig.Loss	Total
H2													
Quantitative	1.00	0.90	96.80	0.10	0.10	0.08	0.04	0.05	0.10	0.04	0.09	0.80*	100.10
XRF (1)	1.05	0.91	92.03	0.00	0.14	0.00	0.03	0.05	0.11	0.04	0.12	N.D.	94.48
XRF (2)	1.16	0.96	97.31	0.00	0.17	0.01	0.04	0.05	0.12	0.04	0.14	N.D.	100.00
3431													
Quantitative	1.30	0.30	92.40	0.30	1.30	0.05	0.02	0.05	0.10	0.01	0.14	4.6*	100.60
XRF (1)	1.15	0.24	94.68	0.15	1.30	0.00	0.03	0.05	0.10	0.03	0.11	N.D.	96.86
XRF (2)	Not determined												
T4													
Quantitative	33.60	0.20	85.60	1.80	0.30	0.11	0.04	0.05	0.30	0.05	0.32	8.4*	100.80
XRF (1)	6.30	0.17	88.14	2.09	0.29	0.00	0.02	0.05	0.30	0.04	0.32	N.D.	97.72
XRF (2)	Not determined												
77-275													
Quantitative	47.20	0.10	42.00	8.60	0.10	0.01	0.01	0.05	0.10	0.02	0.09	0.7*	99.00
XRF (1)	46.81	0.13	41.71	8.51	0.08	0.00	0.02	0.05	0.09	0.03	0.08	N.D.	97.51
XRF (2)	43.29	0.10	48.40	7.88	0.08	0.00	0.02	0.04	0.07	0.03	0.08	N.D.	100.00
59-387													
Quantitative	47.70*	0.10	47.30	3.00	0.10	0.01	0.01	0.05	0.10	0.05	0.14	+0.4*	98.52
XRF (1)	57.20	0.15	47.54	3.06	0.09	0.00	0.02	0.05	0.09	0.03	0.15	N.D.	108.43
XRF (2)	47.77	0.10	49.07	2.69	0.09	0.00	0.02	0.03	0.07	0.02	0.14	N.D.	100.00

* Not used in calibration curves

Table I-8 - Calibration ranges for talc zone rock samples

Element	Percentage range
SiO_2	0.00 to 47.20
Al_2O_3	0.10 to 0.90
Fe_2O_3	42.00 to 96.80
MgO	0.10 to 8.60
CaO	0.10 to 1.30
Na_2O	0.01 to 0.11
K_2O	0.01 to 0.04
TiO_2	0.05 to 0.05
MnO	0.10 to 0.30
S	0.01 to 0.05
P_2O_5	0.09 to 0.32

Whole-rock analyses - Iron Duke

Talc zone rocks -

Major element analyses by Chemical Laboratory, B.H.P., Whyalla.

Trace elements, XRF by author.

Per cent	59-387	77-275
SiO_2	47.7	47.2
Al_2O_3	0.1	0.1
Fe_2O_3	47.3	42.0
MgO	3.0	8.6
CaO	0.1	0.1
Na_2O	0.0	0.0
K_2O	0.0	0.0
TiO_2	0.1	0.1
MnO	0.1	0.1
S	0.0	0.0
P_2O_5	0.1	0.1
Ig. Loss	+0.4	0.7
	98.1	99.0
ppm		
Zn	5	5
Cu	0	0
Ni	7	8
Ba	0	0
Nb		
Zr	1	4
Y	0	0
Sr	0	1
Rb	0	0

Note: 1. Fe expressed as Fe_2O_3

2. Nb is in the order of 1ppm to 4ppm

Whole-rock analyses - Iron Duke

Talc zone rocks.

XRF analyses - see preceding notes.

*Element over 10% outside calibration range.

Per cent	59-633	77-995	77-326	57-402	57-261
SiO_2	52.9*	24.5	48.5	32.7	48.4
Al_2O_3	0.1	0.2	0.1	0.1	0.1
Fe_2O_3	38.7	69.9	44.2	60.3	44.0
MgO	8.8	5.3	8.1	6.0	6.0
CaO	0.1	2.6*	0.1	0.2	0.1
Na_2O	0.0	0.0	0.0	0.0	1.1
K_2O	0.0	0.0	0.1	0.0	0.0
TiO_2	0.1	0.1	0.1	0.1	0.0
MnO	0.1	0.4	0.1	0.1	0.1
S	0.0	0.0	0.0	0.1	0.0
P_2O_5	0.1	0.2	0.2	0.1	0.1
Diff.	0.0	0.0	0.0	0.3	0.1
	100.9	103.2	101.5	99.7	99.9
ppm					
Zn	18	N.D.	7	17	12
Cu	0	N.D.	0	8	0
Ni	6	N.D.	5	16	23
Ba	0	N.D.	0	0	0
Nb		N.D.			
Zr	1	N.D.	0	3	7
Y	0	N.D.	1	2	5
Sr	0	N.D.	1	1	3
Rb	0	N.D.	0	0	0

Note: 1. Fe expressed as Fe_2O_3

2. Nb is in the order of 1ppm to 4ppm

Whole-rock analyses - Iron Duke

Talc zone rocks - XRF trace elements.

ppm	57-465	59-533	57-458
Zn	21	11	14
Cu	0	0	0
Ni	40	7	7
Ba	0	0	0
Nb			
Zr	4	0	0
Y	0	0	2
Sr	0	2	2
Rb	0	0	0

Nb is in the order of 1ppm to 4ppm

D. - Amphibolites and argillaceous schists - XRF analyses.

Major elements

Five standard analyses were used for the amphibolite determinations, including four quantitative analyses by the Chemical Laboratory, B.H.P., Whyalla and one basic igneous rock analysis (BR) from the Geology Department in Durham. There is reasonably good correlation between the corrected, normalised XRF results and the standard analyses, as shown in Table I-9, but the XRF results are regarded as semi-quantitative because of the small number of standards.

The Whyalla quantitative analyses of chloritised intrusives have Ignition Loss values of between 9% and 10%. Similarly, the low totals of XRF element determinations suggest the presence of 10% or more volatiles in the chloritised amphibolites. Water determinations were carried out on two samples and showed that, in those samples, the volatile component was water. However, a number of the XRF totals are in the order of 81% to 85%, suggesting a volatile component of 15% to 19%. In these samples, there may be small amounts of carbonate or there may be volatiles present which were not detected by the analysis. Their analyses are shown in the following pages but are not used in calculations.

Trace elements

Synthetic glass standards, used in the Geology Department at Durham for Lunar work, were used for trace element determinations of the amphibolites. Note the poor correlation for Ba below 80 ppm and Zr below 40 ppm.

Table I-9 - Amphibolite standard sample calibration

Four quantitative analyses by Chemical Laboratory, B.H.P., Whyalla.
One quantitative analysis (BR) by Geology Department, Durham.
XRF (1) are analyses based on uncorrected counts.
XRF (2) are analyses based on counts corrected for mass absorption and normalised.

	SiO_2	Al_2O_3	Fe_2O_3	MgO	CaO	Na_2O	K_2O	TiO_2	MnO	S	P_2O_5	Ig.Loss	Total
66584													
Quantitative	51.20	13.40	15.00	5.80	10.10	1.86	0.60	1.40	0.30	0.14	0.28	0.90	100.98
XRF (1)	52.43	13.28	14.32	7.73	8.91	1.61	0.67	1.11	0.25	0.09	0.45	0.90	101.76
XRF (2)	51.22	11.33	15.05	6.84	10.83	1.65	0.71	1.26	0.27	0.09	0.46	0.99	100.00
BR													
Quantitative	38.60	10.40	12.41	12.60	13.80	3.05	1.45	2.70	0.21	0.04	1.03	2.60	98.89
XRF (1)	39.56	11.10	11.98	12.51	12.58	3.17	1.42	2.58	0.19	0.07	1.17	2.60	98.93
XRF (2)	39.27	10.53	12.23	12.08	14.04	3.21	1.42	3.07	0.22	0.06	1.19	2.68	100.00
601109													
Quantitative	34.00	16.00	17.30	19.50	0.20	0.08	0.04	0.65	0.50	0.03	0.32	9.60	98.22
XRF (1)	29.44	16.52	19.33	21.53	0.70	0.18	0.03	0.74	0.64	0.10	0.38	9.60	99.17
XRF (2)	32.46	17.31	17.24	21.20	0.26	0.18	0.03	0.65	0.55	0.10	0.38	9.66	100.00
67908													
Quantitative	29.60	13.70	24.30	17.40	0.90	0.11	0.04	2.90	1.20	0.06	1.24	9.40	100.85
XRF (1)	27.84	12.36	22.64	15.86	1.20	0.16	0.02	3.03	1.26	0.10	0.58	9.40	94.46
XRF (2)	30.45	13.90	23.28	17.26	0.84	0.16	0.02	2.56	1.21	0.10	0.62	9.59	100.00
A													
Quantitative	15.40	7.20	17.20	16.50	14.10	0.11	0.06	0.65	1.30	0.17	0.14	28.70	101.53
XRF (1)	19.52	7.44	17.93	14.17	15.71	0.09	0.05	0.84	1.18	0.09	0.43	28.70	106.14
XRF (2)	16.05	8.11	18.17	14.52	13.40	0.07	0.04	0.82	1.22	0.08	0.38	27.13	100.00

Table I-10 - Calibration ranges for amphibolite major element analyses (XRF)

Element	Percentage range
SiO_2	15.40 to 51.20
Al_2O_3	7.20 to 16.00
Fe_2O_3	12.41 to 24.30
MgO	5.80 to 19.50
CaO	0.20 to 14.10
Na_2O	0.08 to 3.05
K_2O	0.04 to 1.45
TiO_2	0.65 to 2.90
MnO	0.21 to 1.30
S	0.03 to 0.17
P_2O_5	0.14 to 1.24

Table I-11 - Trace element calibration for synthetic glass standards.

Values in ppm

Ba True	Ba XRF	Nb True	Nb XRF	Zr True	Zr XRF
5000	4613	250	232	626	611
2500	2395	127	125	317	323
1252	792	63	58	162	164
626	615	32	31	81	79
323	309	16	16	41	41
182	156	8	10	20	38
81	84	4	3	0	0
40	28	2	3		
20	28	0	1		
0	0				

Y True	Y XRF	Sr True	Sr XRF	Rb True	Rb XRF
250	251	506	529	1000	984
125	122	257	256	500	520
63	63	132	137	251	243
32	33	69	70	126	129
0	0	38	37	63	63
		22	18	32	33
		14	13	16	15
		0	3	8	9
				0	0

Zn True	Zn XRF	Cu True	Cu XRF	Ni True	Ni XRF
1000	948	1000	962	1000	977
500	501	500	501	500	501
125	122	125	117	125	121
63	61	63	60	63	64
32	34	32	37	32	34
8	8	8	7	8	7
4	4	4	5	4	4
0	2	0	8	0	2

Nominal detection limits calculated from accumulated background values:

	Zn	Cu	Ni	Ba	Nb	Zr	Y	Sr	Rb
ppm	2	3	2	7	2	2	2	2	2

Whole-rock analyses - Iron Duke

Amphibolites - major element analyses by Chemical Laboratory, B.H.P., Whyalla.

Trace elements, XRF by author.

	Unchloritised	Chloritised	
Per cent	66-584	60-1109	67-908
SiO_2	51.2	34.0	29.6
Al_2O_3	13.4	16.0	13.7
Fe_2O_3	15.0	17.3	24.3
MgO	5.8	19.5	17.4
CaO	10.1	0.2	0.9
Na_2O	1.9	0.1	0.1
K_2O	0.6	0.0	0.0
TiO_2	1.4	0.7	2.9
MnO	0.3	0.5	1.2
S	0.1	0.0	0.0
P_2O_5	0.3	0.3	1.2
Ig. Loss	0.9	9.6	9.4
	100.0	98.2	100.7
ppm			
Zn	113	172	239
Cu	82	0	70
Ni	56	74	78
Ba	409	12	9
Nb	3	11	6
Zr	90	323	174
Y	29	32	27
Sr	115	0	4
Rb	20	0	0

Note: 1. Fe expressed as Fe_2O_3

2. Water determinations on 60-1109 and 67-908 by the author gave 10.4% and 11.1% respectively.

Whole-rock analyses - Iron Duke

Amphibolites - unchloritised.

XRF analyses - see preceding notes.

Per cent	74-324	66-584	66-C	57-2325	57-2368
SiO_2	55.0	51.6	50.7	51.8	51.0
Al_2O_3	11.1	11.4	11.1	10.7	11.0
Fe_2O_3	13.4	15.3	16.4	12.0	14.6
MgO	9.9	6.9	6.2	8.5	7.2
CaO	8.2	10.2	9.7	10.9	9.9
Na_2O	0.1	1.7	1.7	1.5	2.6
K_2O	0.1	0.7	0.8	2.6	1.6
TiO_2	1.3	1.3	1.9	0.9	1.2
MnO	0.3	0.3	0.3	0.2	0.3
S	0.1	0.1	0.1	0.1	0.1
P_2O_5	0.4	0.5	0.5	0.6	0.4
Diff.	0.1	0.0	0.6	0.2	0.1
	100.0	100.0	100.0	100.0	100.0
ppm					
Zn	58	113	113	77	112
Cu	0	82	50	0	709
Ni	35	556	37	126	48
Ba	19	409	525	1513	463
Nb	3	3	4	2	1
Zr	81	90	118	93	78
Y	27	29	37	19	22
Sr	708	115	124	493	124
Rb	2	20	25	76	56

Note: 1. Fe expressed as Fe_2O_3

Whole-rock analyses - Iron Duke

Amphibolites - unchloritised - continued.

Per cent	57-2300	82-715
SiO_2	51.5	51.5
Al_2O_3	10.9	11.8
Fe_2O_3	13.8	14.0
MgO	7.5	7.0
CaO	11.3	11.1
Na_2O	2.3	2.0
K_2O	0.8	0.7
TiO_2	1.1	1.2
MnO	0.3	0.3
S	0.1	0.1
P_2O_5	0.5	0.5
Diff.	0.0	0.0
	100.0	100.0
ppm		
Zn	93	121
Cu	8	123
Ni	46	50
Ba	277	134
Nb	2	2
Zr	78	79
Y	21	25
Sr	328	177
Rb	23	30

Note: 1. Fe expressed as Fe_2O_3

Whole-rock analyses - Iron Duke

Amphibolites - partly chloritised and chloritised.

XRF analyses - see preceding notes.

Per cent	57-2144	60-1145	66-555	57-2103	57-2311
SiO_2	49.2	46.5	45.8	40.7	41.4
Al_2O_3	12.0	14.4	11.8	13.4	13.6
Fe_2O_3	14.8	16.0	16.2	14.9	17.1
MgO	8.6	11.7	9.4	11.9	9.7
CaO	9.2	1.1	7.3	6.1	5.6
Na_2O	1.9	0.2	1.4	0.1	1.1
K_2O	0.9	1.3	0.8	1.6	0.8
TiO_2	1.2	2.7	1.3	1.1	1.1
MnO	0.3	0.5	0.4	1.3	0.3
S	0.1	0.1	0.1	0.1	0.1
P_2O_5	0.4	0.6	0.5	0.4	0.5
Diff.	1.4	4.9	5.0	8.4	8.7
	100.1	100.0	100.0	100.0	100.0
ppm					
Zn	104	154	155	120	123
Cu	6	4	48	134	0
Ni	54	144	57	56	86
Ba	236	742	1702	4516	404
Nb	0	17	2	0	4
Zr	79	205	90	79	101
Y	24	27	28	21	24
Sr	277	16	148	58	223
Rb	31	72	39	56	27

Note: 1. Fe expressed as Fe_2O_3

Whole-rock analyses - Iron Duke

Amphibolites - chloritised.

XRF analyses - continued

Per cent	66-530	66-456	71-1044	67-124	74-707
SiO_2	42.7	37.1	30.5	30.7	31.2
Al_2O_3	12.7	12.6	14.1	14.9	14.1
Fe_2O_3	16.6	17.5	19.7	18.7	19.8
MgO	15.9	18.3	18.2	18.4	17.8
CaO	0.4	0.3	0.9	0.6	0.7
Na_2O	0.1	0.2	0.2	0.2	0.2
K_2O	0.2	0.0	0.0	0.0	0.1
TiO_2	1.5	1.3	2.5	2.5	2.1
MnO	0.6	0.6	1.0	1.0	0.6
S	0.1	0.1	0.1	0.1	0.1
P_2O_5	0.4	0.4	0.7	0.5	0.6
Diff.	8.8	11.6	12.1	12.4	12.7
	100.0	100.0	100.0	100.0	100.0
ppm					
Zn	139	149	169	210	164
Cu	0	12	2	31	0
Ni	50	53	81	175	69
Ba	125	126	3	9	20
Nb	4	2	8	18	6
Zr	108	102	182	238	170
Y	29	33	31	36	26
Sr	6	2	3	3	3
Rb	14	0	0	0	2

Note: 1. Fe expressed as Fe_2O_3

Whole-rock analyses - Iron Duke

Amphibolites - chloritised.

XRF analyses - continued

Per cent	83-767	61-590	71-324	71-553	59-1153
SiO_2	35.5	29.2	30.1	29.1	29.4
Al_2O_3	12.7	12.2	13.7	14.3	12.7
Fe_2O_3	17.7	23.0	22.2	21.6	21.9
MgO	18.7	16.4	15.5	16.0	16.0
CaO	0.3	0.6	0.3	0.3	0.1
Na_2O	0.2	0.2	0.2	0.1	0.2
K_2O	0.0	0.0	0.0	0.0	0.0
TiO_2	1.1	2.3	1.1	1.0	1.8
MnO	0.5	0.6	1.0	1.5	1.6
S	0.1	0.1	0.1	0.1	0.1
P_2O_5	0.4	0.5	0.4	0.4	0.3
Diff.	12.8	14.9	15.4	15.6	15.9
	100.0	100.0	100.0	100.0	100.0
ppm					
Zn	104	188	247	322	303
Cu	0	69	86	0	36
Ni	46	73	50	63	352
Ba	0	22	9	1	7
Nb	2	3	2	2	13
Zr	81	124	85	88	248
Y	71	21	58	17	15
Sr	0	5	1	0	3
Rb	0	3	0	0	1

Note: 1. Fe expressed as Fe_2O_3

Whole-rock analyses - Iron Duke

Amphibolites - chloritised.

XRF analyses - continued

Per cent	59-970	59-1093	60-956	59-992	78-359
SiO_2	28.4	27.2	28.0	26.5	29.5
Al_2O_3	14.3	13.8	15.3	12.4	12.7
Fe_2O_3	21.7	22.4	21.5	22.3	22.6
MgO	16.0	15.8	16.7	15.2	15.7
CaO	0.3	0.5	0.2	2.7	0.3
Na_2O	0.1	0.2	0.1	0.1	0.2
K_2O	0.0	0.1	0.0	0.1	0.0
TiO_2	1.2	2.1	0.4	1.7	1.2
MnO	1.6	1.2	1.2	1.3	0.6
S	0.1	0.1	0.1	0.1	0.1
P_2O_5	0.4	0.5	0.4	1.1	0.4
Diff.	15.9	16.1	16.4	16.5	16.7
	100.0	100.0	100.0	100.0	100.0
ppm					
Zn	259	296	540	429	148
Cu	43	18	0	0	80
Ni	53	22	32	471	48
Ba	2	24	0	47	2
Nb	4	33	7	19	0
Zr	93	146	156	435	82
Y	21	15	36	65	8
Sr	00	8	0	63	2
Rb	0	4	0	5	0

Note: 1. Fe expressed as Fe_2O_3

Whole-rock analyses - Iron Duke

Amphibolites - chloritised.

XRF analyses - continued

Per cent	78-788	67-848	74-750	59-966	78-135
SiO_2	27.8	28.1	27.5	28.7	30.1
Al_2O_3	12.6	12.9	12.6	12.1	8.1
Fe_2O_3	24.1	23.6	26.0	20.0	28.2
MgO	14.3	14.3	12.6	17.7	12.2
CaO	0.9	0.2	0.3	0.7	0.5
Na_2O	0.2	0.1	0.2	0.2	0.3
K_2O	0.0	0.0	0.0	0.0	0.1
TiO_2	1.9	1.1	1.2	0.7	1.3
MnO	0.8	1.2	0.8	1.1	0.2
S	0.1	0.1	0.1	0.0	0.1
P_2O_5	0.6	0.4	0.4	0.4	0.5
Diff.	16.7	18.0	18.3	18.4	18.4
	100.0	100.0	100.0	100.0	100.0
ppm					
Zn	233	171	252	174	61
Cu	0	0	0	34	101
Ni	60	57	47	56	48
Ba	0	2	6	3	12
Nb	5	4	6	3	10
Zr	153	91	113	70	106
Y	25	7	13	12	23
Sr	1	0	2	4	2
Rb	0	0	0	0	2

Note: 1. Fe expressed as Fe_2O_3

Whole-rock analyses - Iron Duke

Argillaceous Schists of Death Adder Gully.

Assays of chip-channel samples near surface in Tunnel No. 4.

Per cent	4-80	4-85
SiO_2	67.0	63.0
Al_2O_3	10.0	10.0
Fe_2O_3	8.6	12.1
MgO	7.0	6.5
CaO	0.1	0.1
Na_2O	N.D.	N.D.
K_2O	N.D.	N.D.
TiO_2	0.4	0.4
MnO	0.3	0.3
S	0.0	0.0
P_2O_5	0.1	0.1
Ig. Loss	5.1	5.7
	98.6	98.2

Notes; 1. Fe expressed as Fe_2O_3

2. Analysis and assays by Chemical Laboratory, B.H.P., Whyalla.

Whole-rock analyses - Iron Duke

Argillaceous schists of Death Adder Gully.

Trace elements, XRF by author.

ppm	60-995	60-1042	T-4
Zn	284	427	52
Cu	0	0	0
Ni	24	36	21
Ba	0	39	100
Nb	4	7	5
Zr	96	164	122
Y	12	23	11
Sr	0	0	3
Rb	0	1	38

60-995
60-1042 - Samples of drillcore from depth in the zone of chloritisation.

T-4 - Surface sample of quartz-chlorite-biolite schist.

Hematite ore

No major element analyses were carried out by XRF. Trace element determinations were calibrated using Fe_2O_3 standards.

Table I-12 - Trace elements calibration for synthetic Fe_2O_3 standards

ppm	Zn	Cu	Ni	Ba	Nb	Zr	Y	Sr	Rb
1000	957	780	819	988	N.D.	990	961	N.D.	855
500	507	588	492	514	507	497	502	487	367
250	N.D.	N.D.	N.D.	N.D.	N.D.	287	246	N.D.	N.D.
125	347	172	146	112	125	121	123	126	119
63	60	111	66	60	60	61	60	64	62
31	35	32	29	38	30	26	37	35	44
16	17	15	11	17	10	9	14	13	17
8	4	7	9	2	5	3	8	9	5
4	2	20	1	N.D.	N.D.	0	1	N.D.	N.D.
Nominal detection limits calculated from accumulated background values	4	15	4	13	4	3	3	4	4

Note the generally poor copper correlation, the low Zr below 63 ppm and Nb below 30 ppm, and the erratic Zn value for the 125 ppm standard.

Whole-rock analyses - Iron Duke

Hematite ore - surface samples

Major element analyses by Chemical Laboratory, B.H.P., Whyalla.

Trace elements, XRF by author.

Per cent	H2	3431
SiO_2	1.0	1.3
Al_2O_3	0.9	0.3
Fe_2O_3	96.8	92.4
MgO	0.1	0.3
CaO	0.1	1.3
Na_2O	0.1	0.1
K_2O	0.0	0.0
TiO_2	0.1	0.1
MnO	0.1	0.1
S	0.0	0.0
P_2O_5	0.1	0.1
Ig.Loss	0.8	4.6
	100.1	100.6

ppm	
Zn	56
Cu	32 64
Ni	0
Ba	0
Nb	0
Zr	0
Y	1
Sr	9
Rb	0

Whole-rock analyses - Iron Duke

Hematite ore from the main orebody in the west limb of the synform.

Assays of drill core by Chemical Laboratory, B.H.P., Whyalla.

Per Cent	42-75	42-105	42-275	42-315
SiO_2	10.0	1.8	3.8	9.2
Al_2O_3	2.7	0.4	0.3	0.8
Fe_2O_3	80.8	95.1	94.1	78.3
MgO	0.1	0.1	0.9	4.9
CaO	0.1	0.1	0.1	2.0
Na_2O	N.D.	N.D.	N.D.	N.D.
K_2O	N.D.	N.D.	N.D.	N.D.
TiO_2	0.4	0.1	0.1	0.1
MnO	0.1	0.1	0.1	0.3
S	N.D.	N.D.	N.D.	N.D.
P_2O_5	0.2	0.1	0.0	0.2
Ig. Loss	5.3	1.5	1.0	5.1
	99.7	99.3	100.4	100.9

Whole-rock analyses - Iron Duke

Hematite ore from below the magnetite-hematite-carbonate body.

Assays of drill core by Chemical Laboratory, B.H.P., Whyalla.

Per Cent	47-738	59-1154
SiO_2	1.4	4.0
Al_2O_3	0.8	1.9
Fe_2O_3	94.4	83.9
MgO	0.7	2.8
CaO	1.1	2.5
Na_2O	N.D.	N.D.
K_2O	N.D.	N.D.
TiO_2	0.6	0.1
MnO	0.2	0.6
S	0.0	0.1
P_2O_5	0.1	0.1
Ig. Loss	1.3	4.0
	100.6	100.0

Whole-rock analyses - Iron Duke

Trace elements in hematite ore

XRF analyses

ppm	3178	47-453	66-100	66-117	66-325
Zn	13	12	33	17	27
Cu	3	19	61	68	197
Ni	2	0	0	0	0
Ba	35	0	0	0	0
Nb	0	0	0	0	0
Zr	0	0	0	0	0
Y	1	4	2	2	5
Sr	9	11	7	3	8
Rb	0	0	0	0	0

3178 - surface sample

47-453 - drillcore in transition of hematite ore to magnetite-hematite-carbonate.

66-100, 66-117, 66-325 - Hematite ore near to amphibolite.

Whole-rock analyses - Iron Duke

Trace elements in hematite ore, with small amounts of carbonate, from the hematite orebody at the base of the magnetite-hematite-carbonate.

ppm	59-1123	47-744	59-1077	47-800	59-1109
Zn	8	12	2	101	20
Cu	0	0	0	54	261
Ni	15	0	0	53	16
Ba	8	48	8	9	7
Nb	0	0	1	0	0
Zr	0	0	0	0	0
Y	9	1	0	11	10
Sr	9	3	5	9	7
Rb	0	0	0	0	0

ppm	71-995	47-853	59-1214	59-1146	84-1228
Zn	105	81	74	33	114
Cu	140	0	63	93	14
Ni	47	34	92	49	0
Ba	21	0	177	2	0
Nb	0	0	0	0	0
Zr	0	4	2	8	4
Y	7	27	13	9	4
Sr	4	7	9	2	1
Rb	0	0	0	0	2

APPENDIX II - MINERAL ANALYSES

Techniques

Mineral analyses were carried out on polished-thin sections using a Cambridge "Geoscan" electron probe microanalyser. A counting rate of 10 seconds was used for all analyses except the trace elements in iron oxides, when the rate was 30 seconds. Standards consisted of analysed metals and minerals, and the results were corrected in the manner described by Sweatman and Long (1969).

For carbonate analyses, the beam was defocussed to a diameter of 15 - 20 microns to prevent volatilization. Despite this, some of the carbonate totals are low and no additional elements were detected in spectrometer scans, which suggests that some volatilization has occurred, possibly of very small near surface fluid inclusions.

No rock samples of Cook Gap Schist were available and the analyses were carried out using thin sections with the cover slip removed. The sections were too thin to polish effectively, and the irregular surface tends to cause variation in the analyses. The Cook Gap Schist mineral analyses are therefore regarded as semi-quantitative.

Electron microprobe analyses - Middleback Ranges

Carbonates in iron-formation units.

Element totals recalculated as carbonates.

	$CaCO_3$	$MgCO_3$	$FeCO_3$	$MnCO_3$	Total
83-575					
Equigranular carbonate layer amongst siliceous iron-formation:					
Carbonate Crystal (1)	51.1	34.5	13.9	0.6	100.1
Carbonate Crystal (2)	51.2	35.0	13.8	0.9	100.9
Carbonate Crystal (3)	50.5	32.9	16.1	1.2	100.7
62-1316					
Calcite Crystal in Amphibole rich layer	99.0	0.0	0.1	N.D.	99.11

Electron microprobe analyses - Middleback Ranges

Amphiboles in iron-formations.

	63	63	62-1050	62-1050	62-1050
Oxide weight percentage					
SiO_2	49.2	49.0	51.9	53.8	52.6
Al_2O_3	0.0	0.0	N.D.	N.D.	N.D.
FeO	40.9	41.4	34.1	33.9	33.9
MgO	5.9	5.6	10.9	11.0	11.1
CaO	0.2	0.3	0.3	0.2	0.2
Na_2O	0.0	0.2	N.D.	N.D.	N.D.
TiO_2	0.0	0.0	N.D.	N.D.	N.D.
MnO	0.6	0.6	N.D.	N.D.	N.D.
	96.8	97.1	97.2	98.9	97.8
Atomic proportions on the basis of 23 oxygens.					
Si	7.96	7.94	8.02	8.11	8.05
Al	0.00	0.00	--	--	--
Fe2	5.34	5.61	4.41	4.27	4.34
Mg	1.42	1.35	2.51	2.47	2.53
Ca	0.04	0.05	0.05	0.03	0.03
Na	0.00	0.06	--	--	--
Ti	0.00	0.00	--	--	--
Mn	0.08	0.08	--	--	--

Electron microprobe analyses - Middleback Ranges

Amphiboles - continued

	62-1050	62-1050	62-1050	59-426	59-426
Oxide weight percentage					
SiO_2	51.2	51.8	51.9	50.5	49.7
Al_2O_3	N.D.	N.D.	N.D.	0.3	0.3
FeO	35.0	34.2	34.4	34.0	35.7
MgO	11.0	10.9	11.6	10.6	10.1
CaO	0.2	0.2	0.2	0.4	0.3
Na_2O	N.D.	N.D.	N.D.	N.D.	N.D.
TiO_2	N.D.	N.D.	N.D.	N.D.	N.D.
MnO	N.D.	N.D.	N.D.	0.7	0.6
	97.4	97.1	98.1	96.5	96.7
Atomic proportions on the basis of 23 oxygens.					
Si	7.94	8.01	7.95	7.91	7.85
Al	--	--	--	0.06	0.06
Fe2	4.54	4.42	4.41	4.46	4.71
Mg	2.54	2.51	2.65	2.48	2.38
Ca	0.03	0.03	0.03	0.07	0.05
Na	--	--	--	--	--
Ti	--	--	--	--	--
Mn	--	--	--	0.09	0.08

Electron microprobe analyses - Middleback Ranges

Amphiboles - continued

	59-426	57-2081	57-2081	57-2081	78-443
Oxide weight percentage					
SiO_2	51.6	53.3	52.9	53.7	52.8
Al_2O_3	0.4	0.2	0.3	0.2	N.D.
FeO	35.5	28.4	31.4	31.1	30.0
MgO	9.5	12.4	11.7	12.1	12.4
CaO	0.3	1.3	0.7	0.8	0.1
Na_2O	N.D.	N.D.	N.D.	N.D.	N.D.
TiO_2	N.D.	N.D.	N.D.	N.D.	N.D.
MnO	0.4	0.7	1.5	1.0	N.D.
	97.7	96.3	98.5	98.9	95.3
Atomic proportions on the basis of 23 oxygens.					
Si	7.99	8.11	8.00	8.04	8.13
Al	0.07	0.04	0.05	0.04	--
Fe2	4.60	3.61	3.97	3.90	3.87
Mg	2.19	2.81	2.64	2.70	2.85
Ca	0.05	0.21	0.11	0.13	0.02
Na	--	--	--	--	--
Ti	--	--	--	--	--
Mn	0.05	0.09	0.19	0.13	--

Electron microprobe analyses - Middleback Ranges

Amphiboles - continued

	78-443	74-387	74-387	74-387	74-387
Oxide weight percentage					
SiO_2	54.4	50.7	50.3	51.2	51.3
Al_2O_3	N.D.	N.D.	N.D.	N.D.	N.D.
FeO	29.8	37.1	37.0	36.9	36.9
MgO	12.6	8.3	8.3	8.6	8.6
CaO	0.1	0.3	0.3	0.3	0.2
Na_2O	N.D.	N.D.	N.D.	N.D.	N.D.
TiO_2	N.D.	N.D.	N.D.	N.D.	N.D.
MnO	N.D.	N.D.	N.D.	N.D.	N.D.
	96.9	96.4	95.9	97.0	97.0
Atomic proportions on the basis of 23 oxygens.					
Si	8.20	8.03	8.02	8.04	8.05
Al	--	--	--	--	--
Fe2	3.76	4.92	4.93	4.85	8.84
Mg	2.83	1.96	1.97	2.01	2.01
Ca	0.02	0.05	0.05	0.05	0.03
Na	--	--	--	--	--
Ti	--	--	--	--	--
Mn	--	--	--	--	--

Electron microprobe analyses - Middleback Ranges

Amphiboles - continued

	74-387	1707	1707	1707	77-1185
Oxide weight percentage					
SiO_2	51.5	56.3	56.7	57.8	57.8
Al_2O_3	N.D.	N.D.	N.D.	N.D.	N.D.
FeO	37.2	7.2	6.9	7.6	6.2
MgO	8.5	19.9	20.4	20.0	21.0
CaO	0.2	12.8	13.2	13.4	12.6
Na_2O	N.D.	N.D.	N.D.	N.D.	N.D.
TiO_2	N.D.	N.D.	N.D.	N.D.	N.D.
MnO	N.D.	N.D.	N.D.	N.D.	N.D.
	97.4	96.2	97.2	98.8	97.4
Atomic proportions on the basis of 23 oxygens.					
Si	8.06	7.99	7.96	8.0	8.04
Al	--	--	--	--	--
Fe2	4.87	0.86	0.81	0.88	0.72
Mg	1.98	4.21	4.27	4.13	4.35
Ca	0.03	1.95	1.99	1.99	1.85
Na	--	--	--	--	--
Ti	--	--	--	--	--
Mn	--	--	--	--	--

Electron microprobe analyses - Middleback Ranges

Amphiboles - continued

	77-1185	77-1185	2052	2052	2052
Oxide weight percentage					
SiO_2	57.8	57.3	57.1	55.7	58.3
Al_2O_3	N.D.	N.D.	N.D.	N.D.	N.D.
FeO	7.0	6.1	6.8	6.0	6.0
MgO	20.7	21.2	20.1	20.8	21.7
CaO	11.6	12.2	13.2	12.7	13.3
Na_2O	N.D.	N.D.	N.D.	N.D.	N.D.
TiO_2	N.D.	N.D.	N.D.	N.D.	N.D.
MnO	N.D.	N.D.	N.D.	N.D.	N.D.
	97.1	96.8	97.2	95.2	99.3
Atomic proportions on the basis of 23 oxygens.					
Si	8.07	8.02	8.01	7.95	7.97
Al	--	--	--	--	--
Fe2	0.82	0.71	0.80	0.72	0.69
Mg	4.31	4.42	4.20	4.43	4.42
Ca	1.74	1.83	1.98	1.94	1.95
Na	--	--	--	--	--
Ti	--	--	--	--	--
Mn	--	--	--	--	--

Electron microprobe analyses - Middleback Ranges

Amphiboles - continued

	59-679	59-679	57-2081	1627
Oxide weight percentage				
SiO_2	58.1	58.7	55.0	53.9
Al_2O_3	N.D.	N.D.	0.2	0.7
FeO	4.2	4.7	16.6	13.9
MgO	22.9	21.1	13.9	15.0
CaO	12.5	11.2	12.5	11.4
Na_2O	N.D.	N.D.	N.D.	0.3
TiO_2	N.D.	N.D.	N.D.	N.D.
MnO	N.D.	N.D.	N.D.	0.3
	97.7	95.7	98.2	95.5
Atomic proportions on the basis of 23 oxygens.				
Si	7.99	8.19	7.99	7.96
Al	--	--	0.03	0.12
Fe2	0.48	0.55	2.02	1.72
Mg	4.69	4.39	3.01	3.30
Ca	1.84	1.68	1.95	1.80
Na	--	--	--	0.09
Ti	--	--	--	--
Mn	--	--	--	0.04

Electron microprobe analyses - Middleback Ranges.

Biotites from Cook Gap Schist

Cover slips removed from thin sections - analyses semi-quantitative.

	1958	5-157
Oxide weight percentage		
SiO_2	30.7	34.5
Al_2O_3	21.9	17.1
FeO	21.2	22.1
MgO	8.8	8.4
CaO	0.2	0.4
Na_2O	0.0	0.1
K_2O	8.4	8.2
TiO_2	0.5	1.6
MnO	0.0	0.1
	91.7	92.5

Atomic proportion on the basis of 23 oxygens.		
Si	5.14	5.73
Al	4.33	3.35
Fe2	2.97	3.07
Mg	2.20	2.08
Ca	0.04	0.07
Na	0.00	0.03
K	1.80	1.74
Ti	0.06	0.20
Mn	0.00	0.01

Electron microprobe analyses - Middleback Ranges

Amphibole from Cook Gap Schist.

Cover slip removed from thin section - analyses semi-quantitative.

	5-157
Oxide weight percentage	
SiO_2	42.9
Al_2O_3	16.7
FeO	19.5
MgO	6.8
CaO	11.4
Na_2O	3.0
K_2O	0.3
TiO_2	0.3
MnO	0.5
	101.4

Atomic proportion on the basis of 23 oxygens.

Si	6.25
Al	2.87
Fe2	2.37
Mg	1.48
Ca	1.78
Na	0.85
K	0.06
Ti	0.03
Mn	0.06

Electron microprobe analyses - Middleback Ranges

Feldspars from Cook Gap Schist.

Cover slip removed from thin section - analyses semi-quantitative.

	1961	1961
Oxide weight percentage		
SiO_2	56.1	56.5
Al_2O_3	25.3	25.3
FeO	0.1	0.0
MgO	0.2	0.2
CaO	6.5	6.5
Na_2O	7.3	6.9
K_2O	0.9	1.3
TiO_2	0.0	0.0
MnO	0.0	0.0
	96.4	96.7
Atomic proportions on the basis of 28 oxygens.		
Si	10.44	10.48
Al	5.55	5.53
Fe2	0.02	0.00
Mg	0.06	0.06
Ca	1.30	1.29
Na	2.64	2.48
K	0.21	0.31
Ti	0.00	0.00
Mn	0.00	0.00
End member compositions.		
AB	63.57	60.81
AN	31.27	31.65
OR	5.16	7.54

Electron microprobe analyses - Middleback Ranges

Chlorite from Cook Gap Schist.

Cover slip removed from thin section - analysis semi-quantitative.

	5-1952
Oxide weight percentage	
SiO_2	24.8
Al_2O_3	20.6
FeO	31.9
MgO	9.2
CaO	0.1
Na_2O	0.1
K_2O	2.1
TiO_2	0.3
MnO	0.1
	89.2

Atomic proportion on the basis of 28 oxygens.

Si	5.40
Al	5.29
Fe2	5.81
Mg	2.99
Ca	0.02
Na	0.04
K	0.58
Ti	0.05
Mn	0.02

Electron microprobe analyses - Iron Duke

Chlorites in chloritised argillaceous schists of Death Adder Gully. Section 60-995 with cover slip removed.

	Brown chlorite	Green chlorite
SiO_2	29.6	23.9
Al_2O_3	18.2	18.8
FeO	11.4	32.8
MgO	25.0	10.3
CaO	0.1	0.1
Na_2O	0.0	0.0
K_2O	0.0	0.1
TiO_2	0.0	0.1
MnO	1.6	0.8
Cr_2O_3	0.1	0.1
	86.0	87.0

Reconnaissance through the thin section shows a wide range of Fe:Mg ratios.

Analyses by Dr. A. Peckett, Geology Department, University of Durham, rounded to first decimal place by the author.

Electron microprobe analyses - Middleback Ranges

Garnets in Cook Gap Schist.

Cover slips removed from thin sections - analyses semi-quantitative.

	G1 1961	G2 1961	G3 5-157	G4 5-1952	G5 5-1952
Oxide weight percentage					
SiO_2	36.1	35.8	35.5	35.5	36.5
Al_2O_3	21.6	22.0	20.2	21.7	21.6
FeO	26.1	26.0	25.5	36.8	36.5
MgO	1.4	1.4	1.5	1.0	1.3
CaO	2.9	3.1	5.2	1.4	2.8
Na_2O	0.1	0.2	0.3	0.0	0.0
K_2O	0.1	0.0	0.0	0.0	0.0
TiO_2	0.1	0.0	0.1	0.1	0.1
MnO	10.2	11.6	9.7	2.2	1.7
	98.6	100.1	98.0	98.7	100.5
Atomic proportions on the basis of 24 oxygens.					
Si	5.92	5.82	5.90	5.87	5.90
Al	4.18	4.22	3.96	4.23	4.12
Fe2	3.58	3.53	3.54	5.09	4.94
Mg	0.35	0.34	0.37	0.25	0.31
Ca	0.51	0.54	0.93	0.25	0.49
Na	0.40	0.06	0.10	0.00	0.00
K	0.02	0.00	0.00	0.00	0.00
Ti	0.01	0.00	0.12	0.01	0.12
Mn	1.42	1.60	1.37	0.31	0.23

End member compositions.

	Almandine(Fe)	Spessartite(Mn)	Grossularite(Ca)	Pyrope(Mg)
G1	61.1	24.2	8.7	6.0
G2	58.7	26.6	9.0	5.7
G3	57.0	22.1	15.0	6.0
G4	86.4	5.3	4.2	4.2
G5	82.7	3.9	8.1	5.3

Electron microprobe analyses - Iron Duke

Carbonates in samples of typical magnetite-hematite-carbonate ore. All samples have both layered and vein structures.

Element analyses calculated as carbonates.

	$CaCO_3$	$MgCO_3$	$FeCO_3$	$MnCO_3$	Total
85-665					
Vein crystal, clear	50.8	31.3	13.3	2.0	97.4
Vein crystal, cloudy	51.5	38.2	6.5	2.0	98.2
Crystals in iron oxide rich layer	50.9	37.6	7.9	2.3	98.7
Crystals in iron oxide rich layer	51.7	37.1	8.9	2.8	100.5
60-643					
Crystal in iron oxide rich layer	49.2	34.9	15.8	1.0	100.9
57-900					
Crystal in iron oxide rich layer	50.1	35.8	10.1	1.1	97.1
Crystal in iron oxide rich layer	51.0	36.5	8.7	1.7	97.9
Crystal in iron oxide rich layer	52.6	36.0	6.1	2.4	97.1
Vein Carbonate adjacent to above crystals	51.3	35.9	7.9	2.5	97.6

Electron microprobe analyses - Iron Duke

Carbonates in samples of typical magnetite-hematite-carbonate ore - continued.

	$CaCO_3$	$MgCO_3$	$FeCO_3$	$MnCO_3$	Total
57-1239					
Crystal in iron oxide rich layer	90.2	0.1	3.8	3.7	97.7
Vein carbonate	92.1	0.1	0.3	4.6	97.1
Sequence from carbonate in layered portion of sample to vein carbonate:					
Carbonate in iron oxide rich layer	93.2	0.0	0.5	5.1	97.5
Carbonate at edge of iron oxide rich layer	92.1	0.0	0.1	5.3	97.5
Vein carbonate	94.7	0.0	0.3	2.6	97.6
Interstitial carbonate	92.4	0.0	0.3	4.2	96.9
Adjacent vein carbonate	92.5	0.3	0.4	3.7	96.9
Sequence from interstitial to vein carbonate:					
Interstitial	93.2	0.0	0.5	5.1	98.8
Edge of interstitial	92.1	0.0	0.1	5.3	97.5
Vein carbonate	94.7	0.0	0.3	2.6	97.6

Electron microprobe analyses - Iron Duke

Carbonates in samples of typical magnetite-hematite-carbonate ore - continued.

	$CaCO_3$	$MgCO_3$	$FeCO_3$	$MnCO_3$	Total
61-780					
Typical large vein crystal	52.5	39.8	5.0	0.9	98.2
Large vein crystal adjacent to cavity	51.2	33.5	11.3	1.7	97.7
Clear vein crystal	51.1	34.1	11.5	1.8	98.5
Slightly cloudy vein crystal	51.7	33.7	11.1	2.1	98.6
Very cloudy vein crystal	50.6	29.5	13.9	3.4	97.4
Small interstitial crystal	49.6	39.2	11.8	0.8	101.4
Small interstitial crystal	51.3	39.7	5.3	0.8	97.1

Electron microprobe analyses - Iron Duke

Carbonates in well layered samples of magnetite-hematite-carbonate ore.

Element analyses recalculated as carbonates.

85-810	$CaCO_3$	$MgCO_3$	$FeCO_3$	$MnCO_3$	Total
Crystal in iron oxide rich layer	54.8	38.9	3.7	0.8	98.2
Crystal in iron oxide rich layer	56.8	37.9	4.6	0.8	100.1
Crystal in iron oxide rich layer	55.0	39.8	4.1	1.9	100.8
2					
Equigranular carbonate	51.3	41.3	5.3	1.6	99.5

Electron microprobe analyses - Iron Duke

Carbonates in veins within the magnetite-hematite-carbonate ore.

Element analyses recalculated as carbonates.

	$CaCO_3$	$MgCO_3$	$FeCO_3$	$MnCO_3$	Total
67-1039					
Clear crystal, good cleavage	51.0	32.7	12.5	1.7	97.9
Cloudy crystal, good cleavage	48.0	34.2	15.0	1.8	99.0
Carbonate crystal within magnetite vein:					
Clear rim	51.4	31.7	14.6	1.8	99.5
Cloudy interior	49.8	31.2	15.5	1.6	98.1
1					
Clear crystal	51.0	31.5	13.8	2.0	98.3
Cloudy crystal	50.3	30.5	13.9	2.4	97.1
59-900					
Cloudy crystal	51.9	37.5	6.0	2.0	97.4
78-800					
Cloudy crystal	50.2	34.0	11.4	1.3	96.9

Electron microprobe analyses - Iron Duke

Intermixed ankerites and siderites within the magnetite-hematite-carbonate ore.

Element analyses recalculated as carbonates.

	$CaCO_3$	$MgCO_3$	$FeCO_3$	$MnCO_3$	Total
60-643					
Ankerite	43.1	30.4	23.1	3.1	99.7
Ankerite	49.2	34.9	15.8	1.0	100.9
Ankerite	51.1	35.1	8.9	1.2	96.3
Ankerite crystal:					
Outer rim	46.5	28.8	20.9	1.7	97.9
Centre	50.3	28.4	17.8	1.7	98.2
Magnesio-siderite	1.5	43.5	50.9	3.7	98.6
Magnesio-siderite	0.4	40.8	53.4	4.2	98.8
Magnesio-siderite	0.4	38.4	55.7	4.6	99.1
Magnesio-siderite	0.3	40.6	52.3	5.3	98.5
Magnesio-siderite	0.1	41.3	54.8	3.2	99.4
Zoned crystal of magnesio-siderite and ankerite;					
Clear outer rim	0.6	38.3	57.5	3.5	99.9
Mottled intermediate zone	31.0	31.9	32.0	2.9	97.8
Mottled intermediate zone	51.0	38.0	7.0	0.9	96.9
Centre	50.6	37.3	7.3	1.0	96.2
74-811					
Ankerite	51.2	30.7	15.5	1.4	98.8
Crystal of dominant carbonate in the sample	35.2	31.1	30.7	1.7	98.7

Electron microprobe analyses - Iron Duke

Trace elements in magnetite grains within different types of magnetite-hematite-carbonate ore.

		Si	Mn	Mg	Ti
Banded magnetite-ankerite (83-575)		0.36	0.04	0.18	0.16
	same grain	0.12	0.00	0.10	0.13
		0.12	0.00	0.05	0.10
	smaller grains	0.07	0.00	0.10	0.13
		0.07	0.00	0.18	0.27
Typical ore (74-579)	Banded portion	0.05	0.00	0.00	0.03
		0.26	0.06	0.00	0.00
		0.07	0.06	0.00	0.00
	vein portion	0.19	0.26	0.00	0.00
		0.19	0.18	0.00	0.00
Vein magnetite (67-1029)		0.19	0.18	0.00	0.03
		0.19	0.20	0.00	0.03
		0.19	2.12	0.00	0.10
Synthetic hematite (standard)		0.07	0.31	0.00	0.03
		0.20	0.20	0.00	0.03

Electron microprobe analyses - Iron Duke

Carbonates in the Basal Carbonate unit.

Element analyses recalculated as carbonates.

47-1041	$CaCO_3$	$MgCO_3$	$FeCo_3$	$MnCO_3$	Total
Typical large crystal	52.6	33.5	12.5	1.1	99.7
Typical large crystal	52.5	33.5	12.8	1.7	100.7
Small interstitial crystals	52.1	33.1	12.2	1.8	99.2
Small interstitial crystals	53.0	32.9	12.0	2.3	100.2

Sequence from a typical large, clear carbonate crystal to the surrounding granular, fine-grained, cloudy matrix;

Large crystal centre	53.2	32.9	12.9	1.6	100.6
Large crystal rim	51.4	32.3	13.3	2.2	99.2
Fine-grained matrix	52.1	32.1	11.4	3.3	98.9

Electron microprobe analyses - Iron Duke

Diopside in Basal Carbonate unit.

SA1

Oxide	weight percentage
SiO_2	52.8
Al_2O_3	0.3
FeO	7.6
MgO	13.1
CaO	24.1
Na_2O	0.4
K_2O	N.D.
TiO_2	0.1
MnO	0.8
	99.2

Atomic proportions on the basis of 6 oxygens.

Si	2.0
Al	0.0
Fe2	0.3
Mg	0.8
Ca	1.0
Na	0.0
K	-
Ti	0.0
Mn	0.0

Electron microprobe analyses - Iron Duke

Talcs in samples from the talc zone.

	2159	2159	2159	77-275	77-275
Oxide weight percentage					
SiO_2	61.0	60.1	63.1	57.2	57.4
Al_2O_3	0.2	0.2	0.2	0.2	0.1
FeO	10.5	13.0	12.0	14.3	14.1
MgO	24.1	23.0	23.1	20.7	20.4
CaO	0.0	0.0	0.1	0.1	0.1
Na_2O	0.1	0.3	0.1	0.0	0.0
TiO_2	0.0	0.0	0.0	0.0	0.0
MnO	0.0	0.0	0.0	0.0	0.0
	95.9	96.6	98.6	92.5	92.1
Atomic proportions on the basis of 22 oxygens.					
Si	8.03	7.96	8.11	7.98	8.03
Al	0.03	0.03	0.03	0.03	0.02
Fe2	1.16	1.44	1.29	1.67	1.65
Mg	4.73	4.54	4.42	4.30	4.25
Ca	0.00	0.00	0.01	0.02	0.02
Na	0.03	0.08	0.03	0.00	0.00
Ti	0.00	0.00	0.00	0.00	0.00
Mn	0.00	0.00	0.00	0.00	0.00

Electron microprobe analyses - Iron Duke

Talcs - continued

	77-275	77-275	74-453	74-453	74-453
Oxide weight percentage					
SiO_2	58.1	57.7	57.7	58.5	57.9
Al_2O_3	N.D.	0.2	N.D.	N.D.	N.D.
FeO	11.4	10.7	17.9	17.7	18.3
MgO	23.0	22.7	19.3	19.2	18.6
CaO	0.1	0.0	0.0	0.0	0.0
Na_2O	0.0	0.0	N.D.	N.D.	N.D.
TiO_2	N.D.	0.0	N.D.	N.D.	N.D.
MnO	0.1	0.0	N.D.	N.D.	N.D.
	92.7	91.3	94.9	95.4	94.8
Atomic proportions on the basis of 22 oxygens.					
Si	7.98	8.01	7.97	8.02	8.02
Al	--	0.03	--	--	--
Fe2	1.31	1.24	2.07	2.03	2.12
Mg	4.71	4.69	3.98	3.92	3.84
Ca	0.02	0.00	0.00	0.00	0.00
Na	0.00	0.00	--	--	--
Ti	--	0.00	--	--	--
Mn	0.01	0.00	--	--	--

Electron microprobe analyses - Iron Duke

Talcs - continued

	74-453	74-453	59-633	59-633	59-633
Oxide weight percentage					
SiO_2	57.5	56.0	60.5	61.8	58.9
Al_2O_3	N.D.	N.D.	N.D.	N.D.	N.D.
FeO	17.1	16.6	8.4	3.1	8.2
MgO	19.1	19.9	25.1	28.7	25.7
CaO	0.2	0.0	0.0	0.1	0.0
Na_2O	N.D.	N.D.	N.D.	N.D.	N.D.
TiO_2	N.D.	N.D.	N.D.	N.D.	N.D.
MnO	N.D.	N.D.	N.D.	N.D.	N.D.
	93.9	92.5	94.0	93.7	92.8
Atomic proportions on the basis of 22 oxygens.					
Si	8.01	7.92	8.04	8.04	7.95
Al	--	--	--	--	--
Fe2	1.99	1.96	0.93	0.34	0.93
Mg	3.96	4.19	4.97	5.56	5.17
Ca	0.03	0.00	0.00	0.01	0.00
Na	--	--	--	--	--
Ti	--	--	--	--	--
Mn	--	--	--	--	--

Electron microprobe analyses - Iron Duke

Talcs - continued

	83-670	83-670	74-453	74-453	74-453
Oxide weight percentage					
SiO_2	58.5	58.5	56.4	56.2	55.2
Al_2O_3	N.D.	N.D.	N.D.	N.D.	N.D.
FeO	12.3	11.8	18.1	17.9	18.0
MgO	22.5	22.6	18.8	18.8	19.1
CaO	0.0	0.0	0.0	0.0	0.0
Na_2O	N.D.	N.D.	N.D.	N.D.	N.D.
TiO_2	N.D.	N.D.	N.D.	N.D.	N.D.
MnO	0.0	0.0	N.D.	N.D.	N.D.
	93.3	92.9	93.3	92.9	92.3
Atomic proportions on the basis of 22 oxygens.					
Si	8.00	8.01	7.95	7.95	7.89
Al	--	--	--	--	--
Fe2	1.41	1.35	2.14	2.12	2.15
Mg	4.59	4.61	3.95	3.97	4.07
Ca	0.00	0.00	0.00	0.00	0.00
Na	--	--	--	--	--
Ti	--	--	--	--	--
Mn	0.00	0.00	--	--	--

Electron microprobe analyses - Iron Duke

Talcs - continued

	74-453	74-453	74-453	59-633
Oxide weight percentage				
SiO_2	59.5	56.4	57.4	60.3
Al_2O_3	N.D.	N.D.	N.D.	N.D.
FeO	16.1	18.4	16.8	9.1
MgO	18.2	18.2	20.0	25.2
CaO	0.0	0.1	0.0	0.1
Na_2O	N.D.	N.D.	N.D.	N.D.
TiO_2	N.D.	N.D.	N.D.	N.D.
MnO	N.D.	N.D.	N.D.	N.D.
	93.8	93.1	94.2	94.7
Atomic proportions on the basis of 22 oxygens.				
Si	8.20	7.98	7.96	8.00
Al	--	--	--	--
Fe2	1.86	2.18	1.95	1.01
Mg	3.74	3.84	4.13	4.98
Ca	0.00	0.02	0.00	0.01
Na	--	--	--	--
Ti	--	--	--	--
Mn	--	--	--	--

Electron microprobe analyses - Iron Duke

Replacement of amphiboles by talc and quartz.

In the following descriptions, the term amphibole applies to crystals which optically appear to be amphiboles but in some cases the analyses have low totals, suggesting partial or complete conversion to talc.

	CaO	MgO	FeO	SiO_2	Total
1. Alteration to talc					
74-348					
Amphibole crystal	0.0	18.8	17.7	57.7	94.2
Amphibole crystal	0.1	19.4	17.2	57.8	94.5
Fibrous area adjacent to well formed crystal	0.1	21.4	14.0	57.8	93.3
Typical amphibole in centre of talc	0.1	19.6	16.1	56.4	92.2
Talc	0.0	20.6	15.0	57.6	93.2
Amphibole	0.1	18.5	17.6	57.4	93.6
59-679					
Amphibole	12.8	22.3	4.1	62.3	101.5
Amphibole	12.6	22.5	3.6	62.5	101.2
Talc border of above amphibole	1.9	24.2	8.4	58.8	93.3
Amphibole	12.5	22.9	4.2	58.1	97.7
Fibrous amphibole talc	11.2	21.1	4.7	58.7	95.7
Fawn granular patch-carbonate quartz	18.3	19.2	4.6	36.3	78.4

Electron microprobe analyses - Iron Duke

Replacement of amphiboles by talc and quartz - continued.

	CaO	MgO	FeO	SiO_2	Total
59-533					
Amphibole	0.1	23.7	10.8	57.2	91.8
Talc rim	0.1	23.8	11.1	56.2	91.2
Amphibole	0.1	23.7	10.6	59.4	93.8
Amphibole	0.1	23.8	11.3	58.3	93.5
Amphibole	0.2	21.2	11.7	60.5	93.6
Fibrous talc	0.1	23.6	10.4	58.9	93.0
Fibrous talc	0.1	23.3	10.7	59.2	93.3
62-1316					
Amphibole	13.2	20.1	6.8	57.1	97.2
Fibrous edge of amphibole crystal	5.7	14.8	11.2	67.7	99.4
Fibrous talc with quartz	0.9	22.3	8.0	66.2	97.4

2. Alteration to quartz

78-443					
Amphibole slivers in quartz	0.1	13.7	36.3	50.8	100.9
Amphibole remnant	0.1	12.6	29.8	54.4	96.9
Amphibole remnant	0.1	10.1	33.8	54.3	98.3

APPENDIX III - STAINING, AND X-RAY DIFFRACTION DATA

1. Staining

84 carbonate rich samples were stained to determine the types of carbonate present. The samples were predominantly of magnetite-hematite-carbonate ore, from throughout the orebody, with a lesser number from the basal carbonate unit.

Staining was carried out in the manner described by Warne (1962). Carbonate rich samples were cut using a diamond saw and the flat face was etched in dilute HCl for several minutes, washed in distilled water and left to dry. The sample was then placed in Alizarin Red S and allowed to react for about five minutes. Calcite becomes stained a bright, deep red after this period, but ankerite and siderite are uncoloured. Samples of carbonates other than calcite were then washed in distilled water, dried, and placed in a bath containing equal volumes of Alizarin Red S and 30% sodium hydroxide solution. After heating the solution for about five minutes, the ankerite becomes stained a distinct red-mauve and the siderite is dark brown. Quartz remains completely unstained during the process.

2. X-ray diffraction

A Phillips x-ray diffraction unit at the South Australian Institute of Technology was used for rapid identification of carbonates in the magnetite-hematite-carbonate ore and basal carbonate unit. Debye-Scherrer cameras with 57.3mm radii were employed, using rolled spindles of finely ground mineral and Co radiation with an Fe filter. The films were measured by a calibrated scale and no precise calculations were attempted. Forty two carbonate samples from stained specimens were x-rayed, of which thirty one had similar diffraction patterns with d-spacings conforming in position with those of the A.S.T.M. dolomite and ankerite cards but with intensities between the A.S.T.M. values for those minerals. This carbonate was termed Type B

for convenient reference and its x-ray diffraction data is shown in Table IV - 1. An analysis of hand-picked Type B material from DDH 57-749, shows it to be an intermediate ankerite :

SiO_2	Al_2O_3	Fe_2O_3	MgO	CaO	MnO	S	P_2O_5	Ig.Loss	Total
0.1	0.1	9.7	15.7	28.4	1.2	0.0	0.0	44.4	99.6

Twenty of the thirty one Type B samples fitted precisely the three main line positions shown in Table IV - 1, and the other eleven samples had d-spacings slightly higher or lower than those shown in the table. Samples other than Type B included three of siderite, four of calcite, and four were mixtures of Type B and siderite or calcite. The location of all the samples is listed in Table IV - 2.

In Durham, a Phillips PW 1130/10 x-ray diffraction unit was used, with 114.95mm diameter Debye-Scherrer cameras and finely powdered samples mounted on glass spindles. Co radiation and an Fe filter was used for all samples. The films were measured on a Hilger and Watts scale with vernier attachment. D- spacings and cell parameters were calculated in the manner described by Hall (1971).

The results for one sample of magnesio-siderite were supplied to A.S.T.M. for inclusion in the mineral index file.

Table IV-1 - X-ray diffraction data for carbonate Type B.

Carbonate Type B

Data compiled from nine samples

Degrees 2θ		d (A°)	Rel. Intensity
27.9		3.71	W (M)
35.9		2.90	VS
38.8		2.69	W
41.2		2.54	W
43.5		2.42	WM
47.9		2.21	M (S)
51.2		2.07	VW
52.4		2.03	M (W)
57.6		1.86	VW (W)
59.5 (double)		1.80	M (S)
69.3	Approx.	1.57	VW
70.5	"	1.55	W
74.6	"	1.48	W
76.4	"	1.45	VW
79.6	"	1.40	W
83.5	"	1.34	W

Intensity code :

VS = Very strong
S = Strong
M = Moderate
W = Weak
VW = Very weak

Table IV-2 - Location of x-ray diffraction samples

Type B

DDH 57 - 560
- 724
- 748
- 749 (A,B,C)
- 795
- 582
- 1003
- 1042
- 1215
- 1720

DDH 78 - 675
- 800
- 818
- 878
- 937

DDH 61 - 823
- 902
- 949 (A,B)

DDH 59 - 727
- 831
- 900
- 1148

DDH 67 - 432

DDH 47 - 1182

DDH 71 - 695

DDH 85 - 493
- 676
- 817

Siderite

DDH 74 - 492
- 542
- 840

Calcite

DDH 57 - 1215
- 1343

DDH 47 - 1091

DDH 60 - 901

Mixed carbonates

DDH 57 - 582
- 724

DDH 85 - 472'6"

DDH 86 - 455

APPENDIX IV - FLUID INCLUSION DATA

Homogenisation work was carried out using a Leitz heating stage microscope fitted with UM 20/0.33 and 32/0.60 objectives, and a 10 x ocular. The specimens were placed adjacent to a cromel-alumel thermocouple and the temperatures were recorded on a Phillips Chart recorder. Temperature calibration was effected by observing organic compounds of known melting point sealed in capillary tubes, and placed in approximately the same position as the samples. Small flakes of carbonate from the faces of well developed crystals were used mainly, together with one sample of mixed carbonate and quartz which was prepared as a thin doubly polished wafer between 0.1mm and 0.5mm in thickness. The inclusions were examined at a heating rate of $10^{o}C$ to $15^{o}C$ per minute, which was decreased as the bubble reduced in size. The temperature at which the bubble disappeared was recorded, or estimated in cases where the bubble became lost to view in shadow during the final stages of contraction. Duplicate runs were made frequently and all inclusions were examined for leakage on cooling.

Freezing work was carried out using the same microscope and a stage designed and made by Smith (thesis in preparation) which utilized nitrogen passed through liquid nitrogen. The sample was placed within a small chamber, adjacent to the thermocouple, and low temperature nitrogen was introduced to the chamber, resulting in a temperature in the order of $-50^{o}C$. Most of the inclusions froze completely after a period of up to one hour at this temperature. The temperature was then raised gradually by reducing the flow of nitrogen, and the point at which the last crystal melted was recorded. In each case, the last crystal was immediately reformed by decreasing the temperature, to establish that the process was reversible. Calibration was effected by using inorganic standards of known freezing points.

In the early stages of the work, an attempt was made to ascertain the homogenisation temperatures using decrepitation techniques. Samples of crushed carbonate were placed upon the heating stage and examined as the temperature was raised. Fluid could be seen emerging at some carbonate crystal faces, and occasionally there was isolated movement as a grain fractured, but there was no general sample decrepitation.

Homogenisation data

Individual fluid inclusion homogenisation temperatures, in carbonate fragments.

All samples are ankerite unless stated otherwise.

P = Primary
PS = Pseudo secondary

86-686

P °C	143	148	120	128	136
	136-143	129	138-143	133	112
	112	129	136	138	104
	102	155	138	138	126
	124	119	126-136	136-140	133
	116-121	167	121	119	116
	116	145	121	121	121
PS °C	119	129	138	126-136	126
	116-121	145			

67-1065

P °C	121	160	143	150	158
	160	140-148	145	152	160
	164				

74-956

P °C	114	121-128	153	141	133
	138	143	129	141	109
	114	102	107		
PS °C	128	126			

83-531

P °C	124	114-124	124-129	119	112
	126	119	124	116	

Homogenisation data - continued

74-886

P °C	126	139	102	208	114-126
	114-126	145	133	121	126-131
	136	129-133	150	160	138
	136				
PS °C	112	114			

57-1345 (Calcite)

P °C	119	119	109-114	104	119
	124	121	126	116	133

74-750 (Siderite at contact with chloritised amphibolite)

P °C	102	143-148	155	155	121
	121	133	131	121	126
	116	126	153	153	143-148

67-810

P °C	131	141	116-121	116-121	116-121
	121	126	109	129	104
	142-145	109	119	104	
PS °C	114-121				

59-730

P °C	104	119	119	114	102
	121	136	121-124		
PS °C	90	90-94			

86-640

P °C	102-119	109-119	119	109-119	148
	143-148	148-150	121	155	153
	150	153-155	153-158	143	

Homogenisation data - continued

84-795

P °C	128	126-131	131	145	138
	112	121	126	126	
PS °C	148	119	119	150	116
	114-124(4)	148			

57-1178 (Calcite)

P °C	138	160	172	192	206
	184-199	131	175	162	170-175
	162	164	160		
PS °C	167				

74-563 (Siderite)

P °C	143	129			
PS °C	143-150				

60-723

P °C	143	130-138	130-138	138	133-138
	126				

60-843

P °C	135-140(3)				

57-1200 (Calcite)

P °C	107	126	126		

57-1196 (Calcite)

P °C	133	107	139	152	141
	128	149	143	143-155	

Homogenisation data - continued

78-800

P °C	111-116	123	116	116-123	117
	102	128	114	110	116
	100-102	120	120		

61-780

P °C	94		

60-906

P °C	114	100-125	110-180

Freezing data

Melting points for the last crystals in inclusions within individual samples are :

Sample	No. inclusions	Freezing temperature °C
78-956 (Quartz)	1	-12°
	3	-16°
78-752 (Ankerite)	4	-20° to -18°
	1	-4°
86-686 (Ankerite)	2	-22°
	5	-19° to -18°
	12	-16°
	2	-14° to -13°
	1	-7° (2nd phase in inclusion with two phases, one with freezing point of 18°)
	31	

In sample 74-956 (ankerite), there are two main types of fluid inclusions:

(1) Relatively large, angular inclusions with boundaries approximately parallel to the crystal edges and generally isolated from other inclusions. These freeze completely on cooling and the last crystal melts at about -11°C.

(2) Small, rounded or crescent shaped inclusions which often appear to consist of two phases, in some cases two liquid phases and in others one liquid phase and one of small crystals. They tend to occur in lines or grouped together in suites. On cooling, the liquid phases only partially freezes and the crystals disappear at -20°C to -16°C.